Lanthanide-Based Luminescent Hybrid Materials

Koen Binnemans*

Katholieke Universiteit Leuven, Department of Chemistry, Celestijnenlaan 200F, bus 2404, B-3001 Leuven, Belgium

Received February 5, 2007

Contents

1. Introduction

The photoluminescence properties of rare-earth (lanthanide) compounds have been fascinating researchers for decades.[1−14] An attractive feature of luminescent lanthanide compounds is their line-like emission, which results in a high color purity of the emitted light. The emission color depends on the lanthanide ion but is largely independent of the environment of a given lanthanide ion. Most of the studies on these compounds have been limited to either inorganic compounds (lanthanide phosphors) or molecular lanthanide compounds (for instance, the β-diketonate complexes). For about one decade, there has been a strong interest in *lanthanide-based organic−inorganic hybrid materials*. In these materials, a molecular lanthanide complex is embedded in an inorganic host matrix (like the sol−gel-derived materials), or alternatively, an inorganic lanthanide compound (like a polyoxometalate complex or a lanthanide-doped nanoparticle) is embedded in an organic polymer matrix. Of course, the distinction between these classes is not well-defined, as illustrated by the organically modified xerogels. The study of luminescent lanthanide compounds in hybrid materials is not only of fundamental interest, because these materials have also a high potential for different applications (optical amplifiers, optical waveguides, OLEDs, etc.). In general, these hybrid materials have superior mechanical properties and have a better processability than the pure molecular lanthanide complexes. Moreover, embedding a lanthanide complex in a hybrid matrix is also beneficial for its thermal stability and luminescence output.

Koen Binnemans was born in Geel, Belgium, in 1970. He obtained his M.Sc. degree (1992) and Ph.D. degree (1996) in Chemistry at the Catholic University of Leuven, under the supervision of Prof. C. Görller-Walrand. In the period 1999−2005, he was a postdoctoral fellow of the Fund for Scientific Research Flanders (Belgium). He did postdoctoral work with Prof. Jacques Lucas (Rennes, France) and Prof. Duncan W. Bruce (Exeter, U.K.). In 2000, he received the first ERES Junior Award (ERES, European Rare-Earth and Actinide Society). From 2002 until 2005, he was (part-time) associate professor. Presently, he is professor of chemistry at the Catholic University of Leuven. His current research interests are metal-containing liquid crystals (metallomesogens), lanthanide-mediated organic reactions, lanthanide spectroscopy, luminescent molecular materials, and ionic liquids.

* Fax: +32 16 32 79 92. E-mail: Koen.Binnemans@chem.kuleuven.be.

10.1021/cr8003983 CCC: $71.50
Published on Web 08/04/2009

Table 1. Electronic Structure of the Trivalent Lanthanide Ions

element	symbol	atomic number (Z)	configuration Ln^{3+}	ground state Ln^{3+}
lanthanum	La	57	[Xe]	$^1S_0$
cerium	Ce	58	[Xe]$4f^1$	$^2F_{5/2}$
praseodymium	Pr	59	[Xe]$4f^2$	$^3H_4$
neodymium	Nd	60	[Xe]$4f^3$	$^4I_{9/2}$
promethium	*Pm*	61	[Xe]$4f^4$	$^5I_4$
samarium	Sm	62	[Xe]$4f^5$	$^6H_{5/2}$
europium	Eu	63	[Xe]$4f^6$	$^7F_0$
gadolinium	Gd	64	[Xe]$4f^7$	$^8S_{7/2}$
terbium	Tb	65	[Xe]$4f^8$	$^7F_6$
dysprosium	Dy	66	[Xe]$4f^9$	$^6H_{15/2}$
holmium	Ho	67	[Xe]$4f^{10}$	$^5I_8$
erbium	Er	68	[Xe]$4f^{11}$	$^4I_{15/2}$
thulium	Tm	69	[Xe]$4f^{12}$	$^3H_6$
ytterbium	Yb	70	[Xe]$4f^{13}$	$^2F_{7/2}$
lutetium	Lu	71	[Xe]$4f^{14}$	$^1S_0$

The aim of this review is to give an overview of the different types of lanthanide-based hybrid materials and to compare their respective advantages and disadvantages. The literature has been covered until March 2009. Both the preparation of these materials and their luminescence properties will be discussed. The device construction and the physics behind these devices will not be covered in detail. The definition of hybrid material is interpreted rather broadly in this review, so lanthanide-ion-doped inorganic sol−gel glasses and polymers doped with organic lanthanide complexes also are discussed. Because the literature on lanthanide-doped nanoparticles is explosively growing, a selection of the work most relevant to materials chemistry has been made.

For specialized information on the different classes of hybrid materials and their applications, the reader is referred to the available books[15,16] and reviews.[17−35] A special reference is made to recent reviews on lanthanide-containing hybrid materials.[36−38]

2. Luminescence of Lanthanide Complexes

2.1. Principles of Lanthanide Luminescence

The trivalent ions of the lanthanide series are characterized by a gradual filling of the 4f orbitals, from $4f^0$ (for La^{3+}) to $4f^{14}$ (for Lu^{3+}) (Table 1). One of the most interesting features of these ions is their photoluminescence. Several lanthanide ions show luminescence in the visible or near-infrared spectral regions upon irradiation with ultraviolet radiation. The color of the emitted light depends on the lanthanide ion. For instance, Eu^{3+} emits red light, Tb^{3+} green light, Sm^{3+} orange light, and Tm^{3+} blue light. Yb^{3+}, Nd^{3+}, and Er^{3+} are well-known for their near-infrared luminescence, but other lanthanide ions (Pr^{3+}, Sm^{3+}, Dy^{3+}, Ho^{3+}, and Tm^{3+}) also show transitions in the near-infrared region. Gd^{3+} emits in the ultraviolet region, but its luminescence can only be observed in the absence of organic ligands with low-lying singlet and triplet levels. When the light emission by lanthanide ions is discussed, one often uses the term "luminescence", rather than the terms "fluorescence" or "phosphorescence". The reason is that the terms fluorescence and phosphorescence are used to describe light emission by organic molecules and that these terms incorporate information on the emission mechanism: *fluorescence* is singlet-to-singlet emission (i.e., a spin-allowed transition) and *phosphorescence* is triplet-to-singlet emission (i.e., a spin-forbidden transition). In the case of the lanthanides, the emission is due to transitions inside the 4f shell, thus intraconfigurational f−f transitions. Because the partially filled 4f shell is well shielded from its environment by the closed $5s^2$ and $5p^6$ shells, the ligands in the first and second coordination sphere perturb the electronic configurations of the trivalent lanthanide ions only to a very limited extent. This shielding is responsible for the specific properties of lanthanide luminescence, more particularly for the narrow-band emission and for the long lifetimes of the excited states. Ce^{3+} is a special case because this ion emits intense broadband emission due to allowed f−d transitions. The position of the emission maximum strongly depends on the ligand environment of the Ce^{3+} ion. Depending on the method of excitation, different types of luminescence are defined, for example, *photoluminescence* (emission after excitation by irradiation with electromagnetic radiation), *electroluminescence* (emission by recombination of electrons and holes under the influence of an electric field), *chemiluminescence* (nonthermal production of light by a chemical reaction), or *triboluminescence* (emission observed by applying mechanical stress to crystals or by fracture of crystals).

Although photoluminescence of lanthanide ions can be an efficient process, all lanthanide ions suffer from weak light absorption. Because the molar absorption coefficients ε of most of the transitions in the absorption spectra of the trivalent lanthanide ions are smaller than 10 L mol^{-1} cm^{-1}, only a very limited amount of radiation is absorbed by direct excitation in the 4f levels. Since the luminescence intensity is not only proportional to the luminescence quantum yield but also to the amount of light absorbed, weak light absorption results in weak luminescence. However, the problem of weak light absorption can be overcome by the so-called *antenna effect* (or *sensitization*). Weissman discovered that intense metal-centered luminescence can be observed for lanthanide complexes with organic ligands upon excitation in an absorption band of the organic ligand.[39] Because of the intense absorption bands of organic chromophores, much more light can be absorbed by the organic ligands than by the lanthanide ion itself. Subsequently, the excitation energy is transferred from the organic ligands to the lanthanide ion by intramolecular energy transfer. In his seminal paper, Weissman described this phenomenon for the europium(III) complexes of salicylaldehyde, benzoylacetone, dibenzoylmethane, and *meta*-nitrobenzoylacetone. It took about 20 years before the importance of Weissman's work was fully appreciated, although Sevchenko and Trofimov showed that his experiments could be reproduced.[40] However, since the mechanisms of the energy transfer from the organic ligand to the lanthanide ion were investigated in the early 1960s and since it was realized that the lanthanide β-diketonate complexes have potential as the active component in chelate lasers, intense research activity has been going on in the field of luminescent materials based on molecular lanthanide complexes.

The commonly accepted mechanism of energy transfer from the organic ligands to the lanthanide ion is that proposed by Crosby and Whan (Figure 1).[41−43] Upon irradiation with ultraviolet radiation, the organic ligands of the lanthanide complex are excited to a vibrational level of the first excited singlet state ($S_1 \leftarrow S_0$). The molecule undergoes fast *internal conversion* to lower vibrational levels of the S_1 state, for instance, through interaction with solvent molecules. The excited singlet state can be deactived radiatively to the ground state (*molecular fluorescence*, $S_1 \rightarrow S_0$) or can

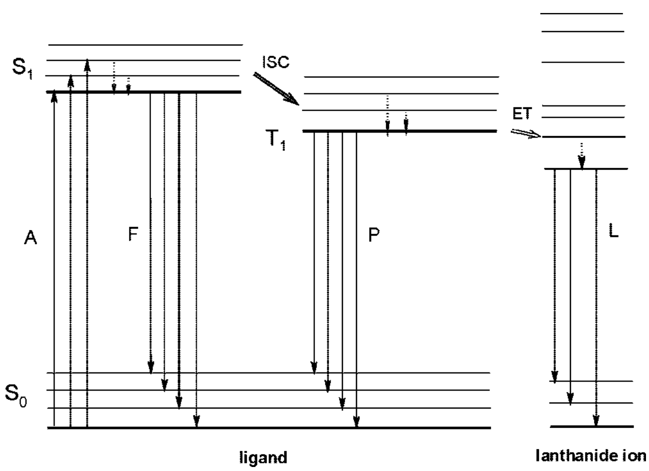

Figure 1. Schematic representation of photophysical processes in lanthanide(III) complexes (antenna effect). Abbreviations: A = absorption; F = fluorescence; P = phosphorescence; L = lanthanide-centered luminescence; ISC = intersystem crossing; ET = energy transfer; S = singlet; T = triplet. Full vertical lines indicate radiative transitions; dotted vertical lines indicate nonradiative transitions.

undergo nonradiative *intersystem crossing* from the singlet state S_1 to the triplet state T_1. The triplet state T_1 can be deactivated radiatively to the ground state, S_0, by the spin-forbidden transition $T_1 \rightarrow S_0$. This results in *molecular phosphorescence*. Alternatively, the complex may undergo a nonradiative transition from the triplet state to an excited state of the lanthanide ion. After this indirect excitation by energy transfer, the lanthanide ion may undergo a radiative transition to a lower 4f state by characteristic line-like photoluminescence or may be deactivated by nonradiative processes. According to Whan and Crosby the main cause of nonradiative deactivation of the lanthanide ion is vibronic coupling with the ligand and solvent molecules.[41] Although Kleinerman proposed a mechanism of direct transfer of energy from the excited singlet state S_1 to the energy levels of the lanthanide ion, this mechanism is now considered not to be of great importance.[44] Indeed this process is often not efficient due to the short lifetime of the singlet excited state. Excitation of the lanthanide ion via the singlet state is known for Tb^{3+}[45] and for Eu^{3+}.[46] Direct excitation from a singlet state to the 4f levels of a Nd^{3+} ion was demonstrated by van Veggel and co-workers for dansyl- and lissamine-functionalized neodymium(III) complexes.[47] Direct light in the triplet level followed by energy transfer to the lanthanide ion is a less observed and less studied phenomenon.[48] Luminescence by the lanthanide ion is only possible from certain levels, which are termed *resonance levels*. The main resonance levels are $^4G_{5/2}$ for Sm^{3+} (17 800 cm^{-1}), $^5D_0$ for Eu^{3+} (17 250 cm^{-1}), $^5D_4$ for Tb^{3+} (20 430 cm^{-1}), and $^4F_{9/2}$ for Dy^{3+} (20 960 cm^{-1}). If the lanthanide ion is excited to a nonemitting level, either directly by excitation in the 4f levels or indirectly by energy transfer, the excitation energy is dissipated via nonradiative processes until a resonance level is reached. Radiative transitions become then competitive with the nonradiative processes, and metal-centered emission can be observed. Line emission by a lanthanide ion is only possible if nonradiative deactivation, molecular fluorescence, and phosphorescence can be minimized. In order to populate a resonance level of a lanthanide ion, it is necessary that the lowest triplet state of the complex is located at an energy nearly equal or above the resonance level of the lanthanide ion, not below. When the energy levels of the organic ligands are below that of the resonance level of the lanthanide ion, molecular fluorescence or phosphorescence of the ligand is observed, or no light emission at all is observed. The luminescence observed for a specific lanthanide complex is therefore a sensitive function of the lowest triplet level of the complex relative to a resonance level of the lanthanide ion. Because the position of the triplet level depends on the type of ligand, it is therefore possible to control the luminescence intensity observed for a given lanthanide ion by variation of the ligand.[49] The position of the triplet level is also temperature dependent, so the luminescence caused by indirect excitation through organic ligands is much more temperature sensitive than luminescence caused by direct excitation of the 4f levels. Sato and Wada investigated the relationship between the efficiency of the intermolecular energy transfer from the triplet state to the lanthanide ion and the energy difference between the triplet state and resonance levels of the lanthanide ions.[50] The authors determined the energy of the triplet states by measuring the phosphorescence spectra of gadolinium(III) β-diketonate complexes at 77 K in a glass-forming EPA solution (5 parts diethyl ether, 5 parts 3-methylpentane, and 5 parts ethanol by volume). Because the 4f levels of Gd^{3+} are located above the triplet levels, no metal-centered emission can be observed for Gd^{3+}. Moreover, the presence of a heavy paramagnetic ion enhances the intersystem crossing from the singlet to the triplet state because of mixing of the triplet and singlet states (*paramagnetic effect*).[51,52] By the spin–orbit coupling interaction, the triplet state acquires a partially singlet character and the selection rules are relaxed. By the presence of the Gd^{3+} ion, the decay time of the triplet state is reduced.[53] Cryogenic temperatures are often necessary to observe phosphorescence, because otherwise the triplet state is deactived by nonradiative processes. Also fluorescence competes with phosphorescence. At 77 K, the solvent quenching of the triplet state is negligible. The triplet levels are always located at a lower energy than the singlet levels. Although energy transfer to the lanthanide ion takes place from the lowest triplet level T_1, it is sometimes possible to observe in the phosphorescence higher lying triplet states such as T_2 as well. The efficiency of the energy transfer is proportional to the overlap between the phosphorescence spectrum of the ligand and the absorption spectrum of the lanthanide ion. The overlap decreases as the triplet state energy increases. A close match between the energy of the triplet state and the energy of the receiving 4f level of the lanthanide ion is not desirable either, because energy back transfer of the lanthanide ion to the triplet state can occur. For instance, Latva et al. observed that energy back transfer from the excited Tb^{3+} ion to the ligand occurs when the energy difference between the $^5D_4$ level of Tb^{3+} and the lowest triplet state of the ligand is less than 1850 cm^{-1}.[54] Because of the energy transfer of the organic ligands to the lanthanide ion, the fluorescence and phosphorescence of the ligands is quenched.[55,56] When the energy transfer is not very efficient, it is possible to observe some remaining ligand emission in combination with the lanthanide-centered emission.

Another possibility to sensitize lanthanide luminescence is via *charge-transfer states*.[57−60] This is especially the case for trivalent lanthanide ions that can easily be reduced to the divalent state (redox-sensitive lanthanide ions) like Sm^{3+}, Eu^{3+}, and Yb^{3+}, where light can be absorbed by an intense ligand-to-metal charge transfer state (LMCT state) from which the excitation energy can be transferred to the 4f levels of the lanthanide ion. This process only works well if the LMCT state lies at high-enough energy. For instance, for Eu^{3+}, sensitization through a LMCT state is efficient if the LMCT lies above 40 000 cm^{-1}. Low-lying LMCT states will partially or totally quench the luminescence.[61] In the case of Eu^{3+}, metal-centered luminescence is totally quenched if the energy of the LMCT is less than 25 000 cm^{-1}. Also strongly absorbing chromophores containing d-block metals can be used for sensitizing lanthanide luminescence.[62−68] Because these chromophores absorb in general at longer wavelengths than the most often used organic chromophores (typically in the visible spectral region), *d-block chromophores* are especially useful for sensitizing the near-infrared luminescence of lanthanide ions like Nd^{3+}, Er^{3+}, and Yb^{3+}.

The *luminescence quantum yield* Φ is an important parameter for evaluation of the efficiency of the emission process in luminescent materials. The quantum yield is defined as the ratio of the number of emitted photons to the number of absorbed photons per time unit:[69]

$$\Phi = \frac{\text{number of emitted photons}}{\text{number of absorbed photons}} \quad (1)$$

For luminescent lanthanide complexes, the *overall luminescence quantum yield*, Φ_{tot}, upon excitation of the ligands is determined by the efficiency of sensitization or energy transfer (η_{sens}) and by the quantum yield of the lanthanide luminescence step (Φ_{Ln}):[70]

$$\Phi_{tot} = \eta_{sens}\Phi_{Ln} \quad (2)$$

Φ_{Ln} is called the *intrinsic luminescence quantum yield*, and it is the quantum yield determined by direct excitation in the 4f levels of the Ln^{3+} ion. The intrinsic quantum yield, Φ_{Ln}, is directly related to the rate constants for radiative deactivation (k_r) and nonradiative deactivation (k_{nr}), by the relationship

$$\Phi_{tot} = \frac{k_r}{(k_r + k_{nr})} \quad (3)$$

Φ_{Ln} expresses how well the radiative processes compete with nonradiative processes. The factor k_r is temperature-independent. Processes that contribute to k_{nr} are energy back transfer to the ligands, energy transfer quenching (important for Eu^{3+}), and matrix vibrations. Especially, OH and NH vibrations are effective in quenching lanthanide luminescence. Haas and Stein investigated the different pathways for radiative and radiationless deactivation of excited states of lanthanide ions, and they point especially to the role of high-energy vibrations in the radiationless deactivation processes.[71,72] The nonradiative rate constant contains contributions from a temperature-independent term, which accounts for the deactivation to the ground state, and a temperature-dependent term, which can play a role when upper-lying short-lived excited states are thermally accessible.[73] The nonradiative processes influence the *observed luminescence lifetime*, τ_{obs}, whereas they do not influence the *radiative lifetime*, τ_R (= $1/k_r$). The *radiative lifetime* is the lifetime of an excited state in the absence of nonradiative transitions. Although sometimes the term "natural lifetime" is used instead of "radiative lifetime", the former term should be abandoned. The intrinsic quantum yield can be determined using the equation

$$\Phi_{Ln} = \frac{\tau_{obs}}{\tau_{rad}} \quad (4)$$

The observed lifetime, τ_{obs}, can be derived from intensity decay curves. However, it is not easy to experimentally determine the radiative lifetime, τ_R. Many authors consider this quantity to be a constant value for a given lanthanide ion. However, this is an incorrect assumption. Equally wrong is the assumption that τ_R can be obtained by measurement of τ_{obs} after cooling the sample to a sufficiently low temperature (77 K or lower). The best approach to obtain τ_R is by calculation of this value with the aid of the experimentally derived Judd−Ofelt intensity parameters, Ω_λ ($\lambda = 2, 4, 6$). These parameters can be derived from optical absorption spectra of the lanthanide complex.[74] The Judd−Ofelt parametrization scheme works remarkably well for ions like Nd^{3+}, Er^{3+}, and Ho^{3+} but is more difficult to apply for Pr^{3+}. The fact that the Judd−Ofelt theory does not produce well the intensities of Pr^{3+} spectra has been the subject of much debate.[75−78] A special case is Eu^{3+}, where the τ_R can be determined without knowledge of the intensity parameters using the Einstein coefficient for spontaneous emission *A* of the magnetic dipole transition $^5D_0 \rightarrow {}^7F_1$, the refractive index *n*, and the ratio of the total integrated intensity to the integrated intensity of the $^5D_0 \rightarrow {}^7F_1$ transition.[70]

The overall quantum yield, Φ_{tot}, can be experimentally measured, but the determination of reliable values is not an easy task. The measurement of *absolute quantum yields* is critical and requires special equipment because it is necessary to know the amount of excited light received by the sample. These measurements are done by the use of scattering agents and an integrating sphere to calibrate the system. For routine work, one is often satisfied with the determination of *relative quantum yields*. In this case, the quantum yield of the unknown is compared with that of a reference sample:

$$\Phi_X = \left(\frac{A_R}{A_X}\right)\left(\frac{E_X}{E_R}\right)\left(\frac{n_X}{n_R}\right)^2\Phi_R \quad (5)$$

where Φ is the luminescence quantum yield, *A* is the absorbance at the excitation wavenumber, *E* is the area under the corrected emission curve (expressed in number of photons), and *n* is the refractive index of the solvents used. The subscripts R and X refer to the reference and the unknown, respectively. The ideal absorbance values for luminescence measurements lie between 0.05 and 0.04. When the absorbance is above 0.05, the emission intensity can no longer be assumed proportional to the concentration of the analyte (no linear relationship between the emission intensity and the concentration). Only when the sample and the reference have the same absorbance at the excitation wavelength, absorbance up to 0.5 can be tolerated. When the absorbance is too low, the impurities from the medium may become important with respect to the amount of analyte. Moreover, at low concentrations the dissociation of the complex in solution can be a problem, especially when the formation constants are not very high. It is advisible to use the same excitation wavelength for measuring the luminescence of the standard and the unknown. One should not choose the excitation wavelength on the edge of an excitation band, because upon excitation on the edge, a slight change in wavelength will induce a large change in the amount of light absorbed. When the same solvent is used for both the reference and the unknown, the factor $(n_X/n_R)^2$ will be equal to unity. For lanthanide complexes, the quantum yield depends on the excited state of the ligand or metal ion, because sensitization of the lanthanide ion can go through several energy migration paths, the efficiency of which depends on the particular levels involved. For integration of the emission spectra, the spectra have to be expressed as a function of the wavenumber (cm^{-1}) and not as a function of the wavelength. Of course, the luminescence quantum yield has to be determined by the use of corrected emission spectra. Finding a suitable reference (standard) is often a serious problem, especially when one wants to perform measurements on luminescent materials that emit in the near-infrared region. The reference compound has to emit in the same region as the lanthanide ion of interest does. Most of the fluorescence standards are organic compounds that show broadband emission, whereas the lanthanide ions exhibit line-like emission. For determination of the luminescence quantum yield of europium(III) complexes, cresyl violet (Φ = 54% in methanol) or rhodamine 101 (Φ = 100% in ethanol) can be used as standards.[79] For terbium(III) complexes, quinine sulfate (Φ = 54.6% in 0.5 M aqueous H_2SO_4) and 9,10-diphenylanthracene (Φ = 90% in cyclohexane) can be used.[79] Another standard for lanthanide complexes emitting in the visible region is $[Ru(bipy)_3]Cl_2$ (λ_{ex} = 400 nm, Φ = 2.8% in water).[80] Bünzli and co-workers proposed the use of europium(III) and terbium(III) tris(dipicolinate) complexes as secondary standards for luminescence quantum yield determination.[81]

For solid samples, standard phosphors can be used.[82−85] The relevant expression is

$$\Phi_X = \left(\frac{1 - R_R}{1 - R_X}\right)\left(\frac{\phi_X}{\phi_R}\right)\Phi_R \tag{6}$$

where R is the amount of reflected excitation radiation and ϕ is the integrated photon flux (photons s^{-1}). Commercial phosphors that can be used as standard for luminescence quantum yields are Y_2O_3/3% Eu^{3+} (YOX-U719 Philips, Φ = 99%) for europium(III) emission and $GdMgB_5O_{10}$/Tb^{3+},Ce^{3+} (CBT-U734 Philips, Φ = 95%) for terbium(III).[86] A solid standard that is easily obtainable is sodium salicylate, which has a broadband emission with a maximum at 450 nm and a luminescence quantum yield of 60% at room temperature.[83] One of the few examples of direct determination of absolute quantum yield of lanthanide complexes is the work of Gudmundsen et al.[87] These authors determined the absolute quantum efficiency of the europium(III) 2-thenoyltrifluoroacetonate complex $[Eu(tta)_3]$ in acetone by a calorimetric method. By this technique, the temperature rise of the samples due to nonradiative deactivation is measured. The quantum efficiency in acetone at 25 °C was determined as 0.56 ± 0.08. Only the $^5D_0 \rightarrow {}^7F_2$ transition was considered, because the authors argue that this transition accounts for more than 95% of the total emission of the complex. For the determination of the luminescence quantum yields, it is not necessary to record emission spectra at high resolution.[72] The errors on the experimentally determined luminescence quantum yields can be quite high (up to 30%), so one has to be careful with drawing conclusions when quantum yields of different systems are compared. The luminescence quantum efficiency of the europium(III) β-diketonate complex $[Eu(nta)_3(dmso)_2)]$ (0.75) is one of the highest observed for solid europium(III) complexes.[88]

Whereas the luminescence quantum yield gives an idea of the luminescence quenching in the whole system, the luminescence decay time indicates the extent of quenching at the emitting ion site only. Bhaumik studied the temperature variation of the luminescence quantum yield and the decay times of various europium(III) β-diketonate complexes in various solvents.[89] Although the luminescence decay times of the complexes were quite different from one another at room temperature, the values for the different complexes were very much the same at 77 K (ca. 450 μs). This indicates that the rate of quenching at the Eu^{3+} site approached a constant value at this temperature. Fluorine substitution in the ligand resulted in a decrease of the quenching and thus in an increase of the decay time at room temperature (up to a factor 2). Although the decay times of the europium(III) complexes were similar at 77 K, this was not the case for the corresponding luminescence quantum yields. This gives an indication of the fact that quenching occurs not only at the lanthanide ion site but in the ligand as well. The luminescence quantum yields of the fluorinated complexes were found to be higher than those of the nonfluorinated complexes. During a time-resolved study of the spectroscopic properties of tris and tetrakis complexes of europium(III) with dibenzoylmethane ligands in glass-forming solvents, Watson et al. observed that the $^5D_0$ emission intensity rose exponentially from an apparent initial intensity to a maximum within several microseconds and decayed exponentially on a much longer (millisecond) time scale.[90] The emission of the $^5D_1$ level was found to decay on a microsecond time scale, and the rise time of the $^5D_0$ emission was virtually identical with the decay time of the $^5D_1$ emission. It is an interesting phenomenon that the lifetime of the tris complexes is shorter than that of the tetrakis complexes at 77 K, but the reverse is true at room temperature.

The reader who is interested in more theoretical aspects of lanthanide spectroscopy is referred to the specialized literature. The classic works in this field are the books of Dieke,[91] Wybourne,[92] Judd,[93] and Hüfner,[94] although it must be admitted that they are not easy to understand for readers without a strong background in mathematics. Several other books[95−97] and reviews[14,74,98,99] are available. The classic work for the assignment of the energy levels of the trivalent ions is the "blue book" of Carnall and co-workers, but this internal report of the Argonne National Laboratory had unfortunately only a limited circulation.[100] Therefore, the series of papers of Carnall on the energy level structure of trivalent lanthanide ions in aqueous solution is suggested as an alternative for the "blue book".[101−104] The two papers of Judd and Ofelt on the theory of intensities of lanthanide spectra are citation classics (Judd−Ofelt theory),[105,106] but the well-known Ω_λ intensity parameters were introduced by Axe.[107] Carnall applied Judd−Ofelt theory to the lanthanide ions in aqueous solution.[108,109] Several other reviews on intensities of f−f transitions have been published.[74,110−113]

2.2. Lanthanide β-Diketonates

Lanthanide β-diketonates are complexes of β-diketone ligands (1,3-diketones) with lanthanide ions. These complexes are the most popular and the most intensively investigated luminescent lanthanide coordination compounds. Their popularity is partially because many different β-diketones are commercially available and the synthesis of the corresponding lanthanide complexes is relatively easy but also because of their excellent luminescence properties. Unfortunately, they suffer from a poor photostability upon UV irradiation. An extensive review on lanthanide β-dike-

Table 2. Overview of β-diketones used as ligands in lanthanide complexes

abbreviation	name	synonym
Hacac	acetylacetone	2,4-pentanedione
Hbtfac	benzoyltrifluoroacetone	
Hbzac	benzoylacetone	1-phenyl-1,3-butanedione
Hdnm	dinaphthoylmethane	
Hfacam	3-(trifluoroacetyl)-*d*-camphor	
Hfod	6,6,7,7,8,8,8-heptafluoro-2,2-dimethyl-3,5-octanedione	
Hhfac	hexafluoroacetylacetone	1,1,1,5,5,5-hexafluoro-2,4-pentanedione
Hntac	2-naphthoyltrifluoroacetone	4,4,4-trifluoro-1-(2-naphtyl)-1,3-butanedione
Hptp	1-phenyl-3-(2-thienyl)-1,3-propanedione	
Htfac	trifluoroacetylacetone	1,1,1-trifluoro-2,4-pentanedione
Hthd (Hdpm)	2,2,6,6-tetramethyl-3,5-heptanedione	dipivaloylmethane
Htta	2-thenoyltrifluoroacetone	4,4,4-trifluoro-1-(2-thienyl)-1,3-butanedione

tonate complexes has been written by Binnemans.[114] In several reviews on luminescent lanthanide compounds, the β-diketonate complexes are described.[115−118] Because of their frequent use in lanthanide-based luminescent hybrid materials, some of the general properties of the lanthanide β-diketonate complexes will be discussed in this section.

Three main types of lanthanide(III) β-diketonate complexes have to be considered: *tris complexes*, *Lewis base adducts of the tris complexes* (ternary lanthanide β-diketonates), and *tetrakis complexes*. The neutral tris complexes or tris(β-diketonates) have three β-diketonate ligands for each lanthanide(III) ion, and they can be represented by the general formula [Ln(β-diketonate)$_3$]. Because the coordination sphere of the lanthanide ion is unsaturated in these six-coordinate complexes, the lanthanide ion can expand its coordination sphere by oligomer formation (with bridging β-diketonate ligands) but also by adduct formation with Lewis bases, such as water, 1,10-phenanthroline (phen), 2,2′-bipyridine (bipy), or tri-*n*-octylphosphine oxide (topo). It is also possible to arrange four β-diketonate ligands around a single lanthanide(III) ion, and in this way, tetrakis complexes or tetrakis(β-diketonates) with the general formula [Ln(β-diketonate)$_4$]$^-$ are formed. These complexes are anionic, and electric neutrality is achieved by a countercation. The cation can be an alkali metal ion (Li^+, Na^+, K^+, Cs^+, Rb^+), but more often it is a protonated organic base (pyridiniumH$^+$, piperidiniumH$^+$, isoquinoliniumH$^+$, etc.) or a quaternary ammonium ion (Et_4N^+, But_4N^+, Hex_4N^+, etc.). A list of the most often used β-diketones is given in Table 2 and in Chart 1. A difference is made between the β-diketone and the corresponding β-diketonate ligand that is obtained by deprotonation of the β-diketone (i.e., the conjugate base of the β-diketone). For instance, Hacac stands for acetylacetone, and acac is the acetylacetonate ligand. Lewis bases found in lanthanide β-diketonate complexes are shown in Chart 2. In two often-cited papers that were published in the same issue of the *Journal of the American Chemical Society*, Melby et al.[119] and Bauer et al.[120] give experimental procedures for the synthesis of the adducts of the tris and tetrakis complexes. These procedures are still the standard procedures for the synthesis of the lanthanide β-diketonates.

Most europium(III) β-diketonate complexes show an intense luminescence, but many β-diketonates are not good ligands to sensitize the luminescence of terbium(III) ions. The reason is that the triplet level of many β-diketonate ligands with aromatic substituents is below that of the resonance level $^5D_4$ of Tb^{3+}. Terbium(III) β-diketonate complexes often show weak or no luminescence at room temperature, although sometimes stronger luminescence is observed at liquid nitrogen temperature. Besides europium(III) and terbium(III) complexes, visible photoluminescence can be expected for the β-diketonate complexes of samarium(III) and dysprosium(III).[121] Weak visible or near-infrared emission is possible for the complexes of praseodymium(III), neodymium(III), holmium(III), erbium(III), thulium(III), and ytterbium(III). It has already been mentioned that no metal-centered photoluminescence can be observed for gadolinium(III) complexes because of the high energy of the 4f levels. Because La^{3+} has an empty 4f shell and Lu^{3+} a filled 4f shell, no metal-centered luminescence can be observed for the complexes of these ions. Serafin and co-workers investigated the influence of different substituents on the β-diketonate ligands on the intramolecular energy transfer.[122,49] They determined the position of the first excited singlet S_1 by measuring the absorption spectra of the complexes. The authors found that the position of S_1 does not affect directly the energy transfer from the β-diketonate ligand to the lanthanide ion. On the other hand, the intersystem crossing (singlet-to-triplet transition) depends on the substituents. When the energy transfer from the ligand to the lanthanide ion is inefficient, the metal-centered luminescence is weak and at the same time an emission band due to the molecular phosphorescence is observed. One can say that in these cases, the triplet state is only partially quenched by the lanthanide ion. When the lanthanide luminescence is absent, the intensity of the phosphorescence band can approach that of the corresponding gadolinium(III) complex. The efficiency of the energy transfer from the organic ligand to the lanthanide ion is proportional to the overlap between the ligand phosphorescence spectrum and the absorption spectrum of the lanthanide(III) ion.[123]

Although the europium(III) β-diketonate complexes often show an intense luminescence, the luminescence intensities are strongly dependent on the type of β-diketone and on the type of complex. Moreover, it is very often difficult to compare the luminescence output of different samples. The luminescence intensity is related not only to the quantum yield of luminescence but also to the amount of absorbed radiation. For this reason, the luminescence of solid samples will also depend on the position of the sample in the light beam that is used for excitation. The luminescence intensity of lanthanide chelates that are excited in the ligand bands is much more dependent on the temperature than the luminescence that is observed upon direct excitation in the f−f levels. It is possible to find some regularities in the luminescence output of europium(III) β-diketonates. The weakest luminescence is observed for the tris complexes. Lewis base adducts give higher intensities, and the tetrakis β-diketonate complexes gives the highest luminescence intensity. The complexes of aliphatic β-diketones (acetylacetone, trifluoroacetylacetone, or hexafluoroacetylacetone) give weakly luminescent europium(III) complexes because of the large

Chart 1. Structures of β-Diketone Ligands for Lanthanide Complexes[a]

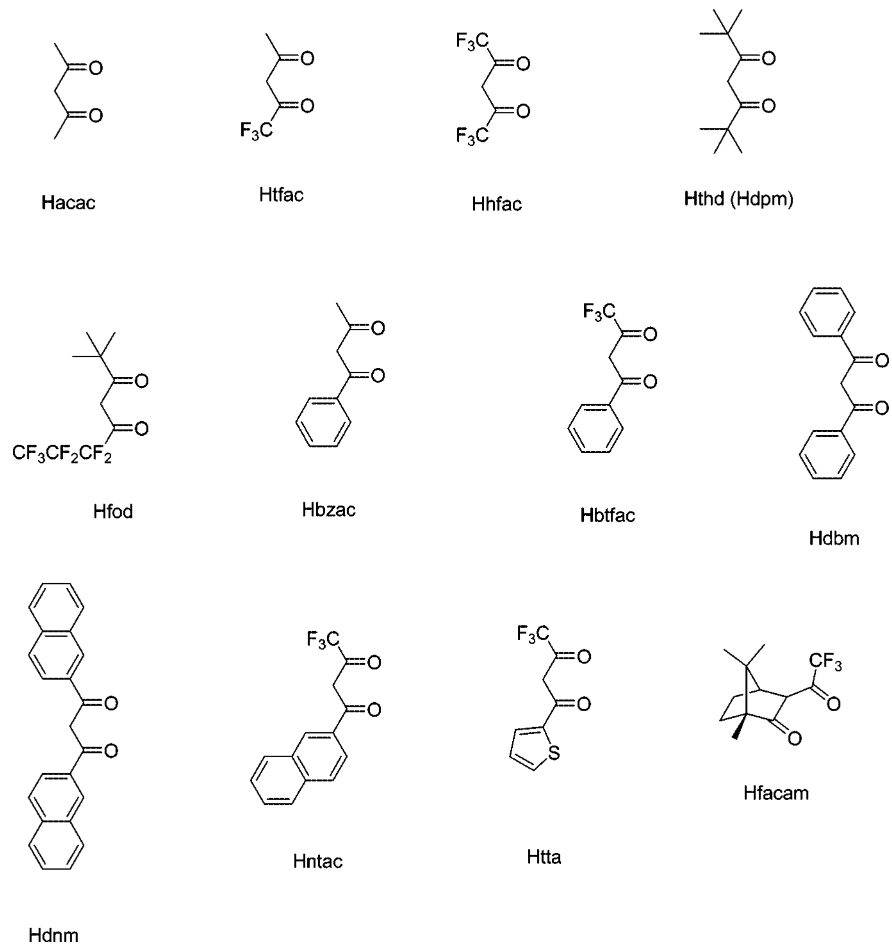

[a] The molecules are in the keto form. The abbreviations are explained in Table 1.

Chart 2. Structures of Lewis Bases Used in Lanthanide β-Diketonate Complexes

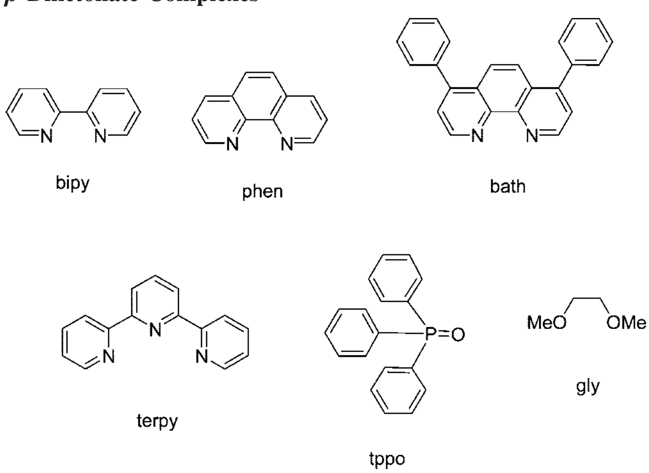

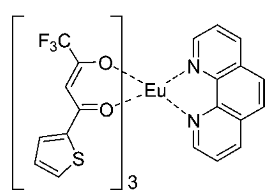

Figure 2. Structure of the luminescent europium(III) β-diketonate complex $[Eu(tta)_3(phen)]$.

energy gap between the resonance levels of the Eu^{3+} ion and the triplet state of the ligand, which makes energy transfer to the europium(III) ion less efficient.[49] Combinations of aromatic and aliphatic substituents on the β-diketones (benzoylacetone, benzoyltrifluoroacetone, 2-thenoyltrifluoroacetone) give europium(III) complexes with a more intense luminescence. In these systems, the energy transfer from the ligand to the lanthanide ion is more efficient. The increase in luminescence intensity in such systems is also attributed to the increased anisotropy around the europium(III) ion.[49] Among the Lewis base adducts, a complex that is well-known for its good luminescence properties is $[Eu(tta)_3(phen)]$, where tta is the conjugated base of 2-thenoyltrifluoroacetone (Htta) and phen represents 1,10-phenanthroline (Figures 2 and 3). Among the terbium(III) β-diketonate complexes, strong luminescence is observed for the tris complexes of acetylacetone, di-*p*-fluorodibenzoylmethane, and trifluoroacetylacetone.[49] The highest luminescence intensity is observed for terbium(III) complexes of acetylacetone.[124] In order to obtain luminescent terbium(III) β-diketonate complexes with aromatic substituents, complexes of 1-indoleacetylacetone and 3-indoleacetylacetone were prepared.[125,126] The reason for this choice was that the triplet level of the indole group is at a higher energy than the energy of the triplet level of a phenyl group. Yang et al. stated that the presence of a rigid planar structure in the complex causes a higher intensity of the sensitized luminescence because such structure allows a better energy transfer.[124] The fact that a stronger luminescence is observed for $[Eu(tta)_3(phen)]$ than for $[Eu(tta)_3(bipy)]$ is in agreement with this rule. The luminescence of europium(III) complexes

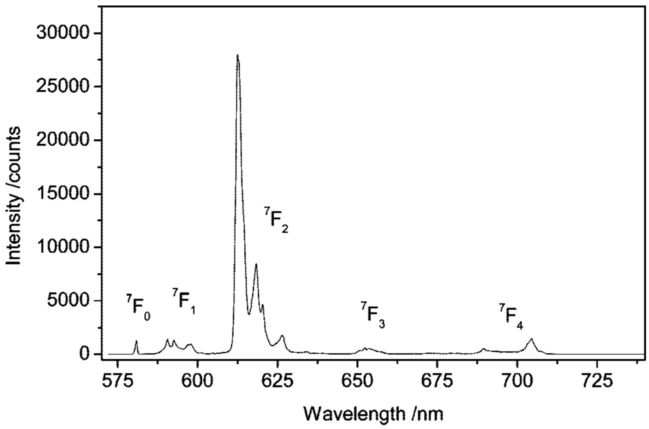

Figure 3. Luminescence spectrum at 77 K of [Eu(tta)$_3$(phen)] in a KBr pellet. The excitation wavelength was 396 nm. All the transitions start from the $^5D_0$ state.

can be quenched by a low-lying ligand-to-metal charge-transfer state (LMCT state).[127,128] Such a LMCT state can deactivate the excited singlet or triplet states of the ligand.

3. Sol−Gel Hybrid Materials

3.1. Inorganic Sol−Gel Systems

Lanthanide-doped oxide glasses like phosphate, borate, or silicate glasses have been intensively studied because they are promising materials for high-power lasers[13,129−131] and optical amplifiers.[132] However, the preparation of silicate glasses with high lanthanide concentrations is problematic due to the low solubility of lanthanide oxides in these glass matrices and to the resulting phase separation.[133] Silicate glasses with doping concentrations higher than 0.5 mol % of lanthanide ions can be prepared via the sol−gel process, although obtaining a uniform distribution of the lanthanide ions is not an easy task.[134−137] Lanthanide concentrations higher than 20 mol % have been reported for these lanthanide-doped sol−gel glasses.[138]

The *sol−gel process* is a chemical synthesis technique that is used for the preparation of gels, glasses, and ceramic powders.[139−143] An attractive feature of the process is that it enables preparation of glasses at far lower temperatures than those of the conventional melt processes. Not only does this allow avoidance of the problems of phase separation and crystallization that are often observed for high-temperature melt processes, but it is also possible to encapsulate organic compounds or metal complexes in the sol−gel glass.[144−148] It is often observed that encapsulation in sol−gel glasses increases the photostability of organic luminophores.[149,150] The sol−gel process can be used to prepare bulk samples (monoliths) as well as thin films and fibers. The gels can easily be formed in different shapes. The starting products for the preparation of silicate sol−gel glasses are tetraorthosilicates or tetraalkoxysilanes, $Si(OR)_4$, like tetraethylorthosilicate (TEOS, $Si(OC_2H_5)_4$), which is mixed with water and a mutual solvent to form a homogeneous solution. This solvent is typically the same alcohol as generated by the hydrolysis reaction of tetrahydrofuran. Another often used alkoxide precursor is tetramethylorthosilicate (TMOS, $Si(OCH_3)_4$). Hydrolysis of TEOS is slower than that of TMOS because of the retarding effect of the bulkier ethoxy groups. Partial hydrolysis of the alkoxide leads to the formation of silanol groups, Si−OH, with the release of alcohol. Instead of complete hydrolysis to silicic acid, condensation reactions take place in solution. These condensation reactions result in the formation of Si−O−Si siloxane bonds and lead to the production of alcohol or water. A simplified reaction scheme for the hydrolysis and condensation of a tetraalkoxysilane $Si(OR)_4$ is

Hydrolysis:
$$Si(OR)_4 + nH_2O \rightarrow Si(OR)_{4-n}(OH)_n + nROH \quad (7)$$

Condensation:
$$(RO)_3Si{-}OR + HO{-}Si(OR)_3 \rightarrow (RO)_3Si{-}O{-}Si(OR)_3 + ROH \quad (8)$$

or

$$(RO)_3Si{-}OH + HO{-}Si(OR)_3 \rightarrow (RO)_3Si{-}O{-}Si(OR)_3 + H_2O \quad (9)$$

Besides the type of alkoxide used for the hydrolysis, important reaction parameters are $r = H_2O(mol)/Si(mol)$, solvent, catalyst, pH, temperature, and pressure. Water is used as a reagent in the hydrolysis reaction, but it is also a byproduct of the condensation reaction. A molar ratio $r = 2$ is sufficient for a complete reaction. Under most conditions however, the hydrolysis of the alkoxide is incomplete and the condensation reactions proceed simultaneously. In this case, complete hydrolysis is achieved only when $r > 10$. Alkoxysilanes and water are immiscible. Therefore a solvent in which both components are soluble, such as an alcohol, is used. The hydrolysis can be acid- or base-catalyzed. A typical acidic catalyst is hydrochloric acid, while typical basic catalysts are sodium hydroxide, potassium hydroxide, or ammonium hydroxide. Also a nucleophile like the fluoride ion can be used as the catalyst. The acid- and base-catalyzed hydrolysis of a tetraalkoxysilane are shown in Scheme 1. The acid-catalyzed hydrolysis involves the protonation of the alkoxide group, followed by nucleophilic attack by a water molecule to form a pentacoordinated intermediate, followed by the elimination of an alcohol molecule. The base-catalyzed hydrolysis involves the nucleophilic attack on the silicon atom by the hydroxide anion to form a negatively charged pentacoordinated intermediate, followed by the elimination of an alkoxide anion.

Oligomers and polymers are formed by the condensation reaction, and this leads to the formation of colloidal particles in the solution. The term *sol* is used for the suspension of colloidal particles that is formed by the hydrolysis of the tetraorthosilicate precursor and the initial phases of the condensation reaction. When the colloidal particles undergo additional polymerization reactions, an interconnecting network is formed. The viscosity of the solution increases during this gelation process, and a *gel* is obtained. Whereas the sol is a fluid, the gel has a rigid three-dimensional structure with an interstitial liquid phase. At the *gel point*, when the last bond that completes the three-dimensional network is formed, a sudden increase in the viscosity of the solution is observed. The *sol−gel transformation* can be monitored by different spectroscopic methods. After gelation, the gels are kept for some time in a sealed vessel so that no evaporation of solvent can take place. This is the *aging process*, during which the condensation reactions continue and further cross-links in the network are formed. The aging process is followed by the *drying process*, which involves removal of the liquid phase from the interconnected porous network. If the liquid

Scheme 1. Acid- and Base-Catalyzed Hydrolysis of a Tetraalkoxysilane, $Si(OR)_4$

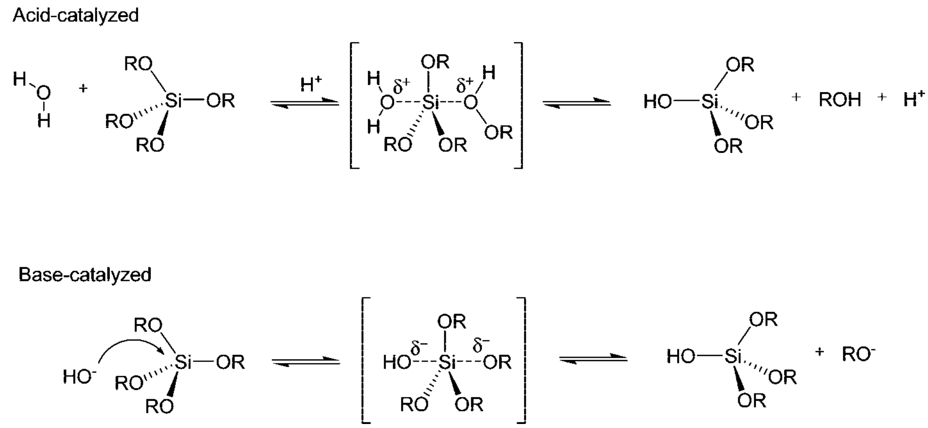

phase is removed by conventional drying, a *xerogel* is obtained. The drying step can be performed at room temperature or at elevated temperatures (<200 °C). During the drying process, the gel shrinks. Additional cross-links can be formed when the network collapses and unreacted −OH and −OR groups come into contact. Not all of the liquid phase will be removed during the drying process, and a considerable amount of liquid is retained in the pores. The final volume of the xerogel is only about 1/8th of the original volume. It should be noted that it is often difficult to obtain high-quality monolithic xerogels, because the xerogel tends to crack during the drying process.[151] The surface tension of the remaining liquid in the pores stresses the silica network, and these stress forces can cause severe cracking. Cracking can be avoided or limited by drying very slowly, often over a period of several months. An alternative approach is the addition of a *drying control chemical additive* (DCCA) like *N*,*N*-dimethylformamide (DMF) to the precursor solution.[152] Thomas et al. applied a particulate silica filler material to ensure crack-free drying of the gel.[153] They also added propylene oxide to reduce the gelation time. The xerogel can be transformed to a compact silicate glass by heating to high temperatures up to 1100 °C, which is still well below the melting point of silica.[154] Several processes take place as the temperature increases: elimination of residual water and organic components, relaxation of the gel structure, and finally densification by viscous sintering. When the liquid phase is removed from the gel by supercritical drying in an autoclave, an *aerogel* is formed. During supercritical drying, the gel is heated above the critical temperature and pressure of the liquid phase. Aerogels have very low densities and are good thermal insulators, but they are not often used as host for spectroscopically active metal ions or organic molecules.[155] The aerogel can also be further densified to a silica glass. To get thin films, the silica gel is spin-coated or dip-coated prior to gelation on a suitable substrate (e.g., a microscope glass slide or a quartz disk). In the *spin coating* process, an excess amount of a sol solution is placed on the substrate, which is then rotated at high speed (typically between 1000 and 10000 rpm) to spread the fluid by centrifugal force. Rotation is continued while the fluid spins off the edges of the substrate, until the desired thickness of the film is achieved. Because the solvent is usually volatile, it simultaneously evaporates. The thickness of the film depends on the spinning rate, the concentration and viscosity of the solution, and the solvent. In the *dip coating* process, a substrate is immersed in the sol and then slowly withdrawn at a constant rate.

Three general methods can be used to incorporate or immobilize luminescent complexes into sol−gel glasses: (1) *impregnation*; (2) *doping*; (3) *chemical immobilization*.[156] To impregnate a complex into the sol−gel glass, the silica matrix is immersed for some time in a solution that contains a fairly high concentration of the luminescent complex. During the period of immersion, the complex will diffuse into the channels or pores of the silica glass. To dope the complex in the sol−gel glass, the complex is added to the silica sol prior to gelation. During gelation, the complex is trapped in the pores and channels of the silica host. It is also possible to dope the complex in the silica matrix by adding a metal salt and ligand to the silica gel, whereby the complex itself is formed *in situ* in the gel or in the xerogel (often during a heat treatment). Chemical immobilization of the complex is achieved by addition of organosilicon compounds with coordinating groups to the sol−gel precursor solution, so that organically modified silicates (*ormosils*, see below) are obtained. The most often used method for incorporation of the luminescent complexes into the silica matrix is the doping method.

The first lanthanide-doped sol−gel silica glasses were samples prepared by dissolving inorganic lanthanide salts like hydrated europium(III) chloride or europium(III) nitrate in the sol. In a seminal paper, Levy et al. used the Eu^{3+} ion as a sensitive luminescent probe to monitor the transformation of a gel into a glass.[157] The authors noticed a gradual increase of the total intensity of the luminescence spectrum and a relative increase in the intensity of the hypersensitive transition $^5D_0 \rightarrow {}^7F_2$ as a function of time and as a function of increase in temperature of dehydration of the gel. The authors concluded that the environment of the Eu^{3+} ion in the final sol−gel glass resembled that of Eu^{3+} in oxide glasses. Reisfeld and co-workers compared the intensity ratios $I(^5D_0 \rightarrow {}^7F_2)/I(^5D_0 \rightarrow {}^7F_1)$ for many different glass systems, including sol−gel glasses.[158] A distinct increase in the ratio as a function of increasing temperature is observed. Campostrini et al. performed a detailed spectroscopic study of Eu^{3+}-doped silica sol−gel glasses.[159] By comparing the luminescence spectra recorded at different temperatures, they were able to follow the changes in the matrix from a wet gel to a compact silica glass. Parameters that were considered are the luminescence decay of the $^5D_0$ state, the line width of the emission bands, and the crystal-field fine structure. These authors considered the changes in the luminescence spectra at lower temperatures (25−250 °C) to investigate the gel-to-xerogel transition in these Eu^{3+}-doped systems.[160] Luminescence studies revealed that the xerogel-to-glass transition is a continuous process.[161−165] During the initial dehydration steps, two different environments could be observed for the Eu^{3+} ion, a liquid-like and a dry environment.[161] In samples heated to temperatures below 250 °C, the hydroxyl groups present in the matrix can efficiently quench the luminescence by nonradiative relaxation. In samples heated to temperatures above 250 °C, clustering of Eu^{3+} ions and quenching by energy transfer is observed. This clustering is also evident from more efficient energy migration between Eu^{3+} ions after the gel-to-glass transition.[166] The clustering of lanthanide ions during heat treatment was observed by Jia and co-workers for silica glasses codoped with yttrium(III) oxide.[167] The problems associated with hydroxyl quenching and clustering of lanthanide ions will be discussed in detail below. High-resolution spectroscopic studies at low temperatures were used to get an idea about the energy distribution of the different Eu^{3+} sites.[168,169] Studies on the densification process of silica glasses by Eu^{3+} luminescence measurements have been complemented by Raman studies.[170] Lochhead and Bray investigated the influence of the counteranion (nitrate, chloride, or perchlorate) on the spectroscopic behavior of europium(III) salts in sol−gel glasses.[171] They measured the energy of the $^5D_0 \leftarrow {}^7F_0$ transition in the excitation spectra to determine whether the counterion was in the first or in the second coordination sphere. Inner sphere complexes with the counterions were observed for the nitrate and chloride salts (strongest effect for nitrate ions) but not for the perchlorate salt. However, upon thermal treatment of the xerogels, the counterion effects were removed. The formation of a crystalline phase in silica sol−gel glasses containing high concentrations of $Ca(NO_3)_2$ could be monitored by Eu^{3+} luminescence thanks to the appearance of crystal-field fine structure in the luminescence spectra during crystallization.[172] The luminescence properties of Eu^{3+} in a sol−gel-derived glass have been compared with those of Eu^{3+} in a melted glass.[173] The sol−gel glass gave a more efficient luminescence due to a strong absorption band around 250 nm. This band is most likely due to Eu^{2+} present in the sol−gel glass. The environment of Eu^{3+} in sol−gel-derived silica glasses has been studied by EXAFS.[174] A luminescence study of titania (TiO_2) thin films prepared by the sol−gel process revealed that the luminescence decay time of the $^5D_0$ state of Eu^{3+} increased upon heat treatment to 400 °C, but samples heated to 500 °C showed a shorter luminescence decay time.[175] This difference was attributed to differences in the crystalline structure of TiO_2. The transformations sol → gel → glass have been studied for Eu^{3+}-doped SnO_2 gels.[176] It is also possible to monitor the changes in the sol−gel matrix during the dehydration of the gel upon formation of the xerogel by recording the absorption spectra rather than the luminescence spectra. The intensity and fine structure of the hypersensitive transitions were found to change during dehydration and further heat treatment of the samples.[177−179] A useful ion for studies by UV−vis absorption spectroscopy is Nd^{3+}, because of the presence of the hypersensitive transition $^4G_{5/2} \leftarrow {}^4I_{9/2}$ around 585 nm in the absorption spectrum.

Although most studies on structural changes in sol−gel glasses have used Eu^{3+} as a luminescent structural probe, some authors have considered other lanthanide ions as luminescent probe for the glass structure. Pucker et al. reported on a combined Raman and luminescence spectroscopy study with Tb^{3+} as luminescent probe.[180] A less conventional luminescent probe for the gelation and drying of sol−gel glasses is Ce^{3+}, because of the broadband emission of this ion (Figure 4).[181] It should be noted that Ce^{3+} is partially oxidized to Ce^{4+} in the drying gels at 100 °C.[182] Above 200 °C, total oxidation of Ce^{3+} to Ce^{4+} takes place. Valence changes of lanthanide ions in sol−gel glasses during heat treatment have also been observed for Eu^{3+}-doped glasses. Heat treatment of Eu^{3+}-doped sol−gel glasses can lead to partial reduction of Eu^{3+} to Eu^{2+}.[173] However, the strongest effects were observed for sol−gel glasses codoped with alumina.[183−185] This reduction can be an advantage, because the light energy absorbed by the intense UV absorption band of Eu^{2+} can be transferred to Eu^{3+} leading to a higher luminescence efficiency.[173,184] Eu^{3+} ions bound to 15-crown-5 in silica glass can be photoreduced by irradiation with UV radiation ($\lambda = 320$ nm).[186] The proposed mechanism for the photoreduction is that the Eu^{3+} ion is first photoexcited to a charge-transfer state and the excited Eu^{3+} ion receives an electron from the unshared electron pairs of the oxygen atom of the neighboring silanol groups so that Eu^{3+} is reduced to Eu^{2+}. The divalent oxidation state of europium is stabilized by the 15-crown-5 ligand. It was observed that the reduction continues after the irradiation with UV radiation had stopped. The explanation for this phenomenon is that the oxygen-associated hole centers formed by UV radiation slowly release their electrons so that Eu^{3+} can be reduced in the absence of any UV light. The rapid photoreduction of Eu^{3+} to Eu^{2+} gives excellent *persistent spectral hole burning* (PSHB) properties to this glass, and these holes are stable at room temperature.[187] Additional studies confirmed the stabilizing effect of 15-crown-5 and related compounds on the stability of Eu^{2+} in sol−gel glasses.[188] Zaitoun et al. observed that during the sol−gel process, a large concentration of structural defects are formed in the polymeric oxo-bridged silica network and that these defects generate a large amount of electron−hole (e^-−h^+) carriers.[189,190] Eu^{3+} ion present in the gel can harvest these e^-−h^+ pairs, resulting in a reduction of Eu^{3+} to Eu^{2+}. The Eu^{2+} ions are stabilized at the cation vacancies by forming Eu^{2+}−hole complexes. In Figure 5, the emission spectrum of an aqueous solution of Eu^{3+} is compared with that of a Eu^{3+}-doped sol at the gelation point. In the latter case, simultaneous emission by Eu^{2+} and Eu^{3+} is clearly visible. The reduction is inhibited in the presence of EDTA, because of the strong stabilizing effect of EDTA on Eu^{3+}. Sm^{3+} can

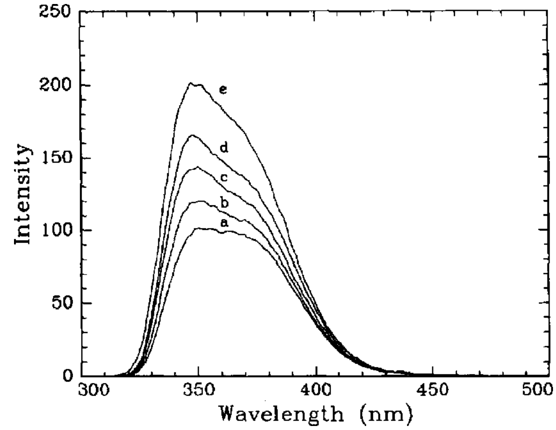

Figure 4. In-situ monitoring of cerium(III) luminescence during the condensation of a TEOS-derived gel containing 2.4% Ce/silica. Spectra were obtained at times after mixing of (a) 0, (b) 3, (c) 5, (d) 7, and (e) 8.5 h. The gel time was 3 h. Reproduced with permission from ref 181. Copyright 1995 Elsevier.

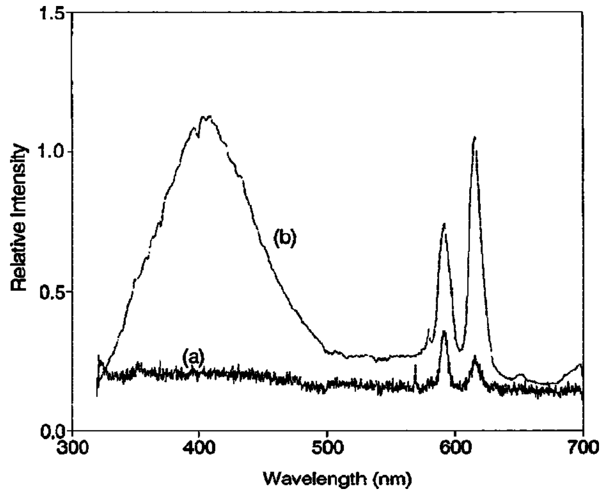

Figure 5. Luminescence spectra of (a) 10^{-3} mol/L Eu^{3+} in aqueous solution and (b) europium ions (i.e., Eu^{3+} and Eu^{2+}) in a silica sol−gel at the gelation stage. Reprinted with permission from ref 189. Copyright 1998 American Chemical Society.

be reduced to Sm^{2+} in sol−gel glasses by a hydrogen atmosphere.[191]

As already mentioned above, the good luminescence performance of lanthanide-doped xerogels and derived glasses is hampered by hydroxyl quenching and clustering of the lanthanide ions. The small absorption coefficients of the f−f transitions of trivalent lanthanide ions make efficient light absorption difficult. Because the luminescence intensity is proportional to the amount of absorbed light, the latter factor makes efficient excitation of lanthanide ions difficult. Intense research activities have been directed to find solutions for these problems.

The hydroxyl groups originating from water, solvent, and silanol groups in the sol−gel glass quench the luminescence of lanthanide ions (*hydroxyl quenching*). The high-energy vibrations associated with the hydroxyl groups can couple with the excited electronic states of the lanthanide ions, and this provides an efficient channel for deactivation of the excited states via nonradiative relaxation. This nonradiative relaxation of excited states by hydroxyl groups is especially a problem for near-infrared emitting lanthanide ions because here the energy gaps between the emitting level and the final state are smaller. The classic method to remove hydroxyl groups from the xerogel is by heat treatment of the sample so that the xerogel is transformed into a compact glass sample. The transformation of the xerogel to a silicate glass is done at quite high temperatures, up to 800 or even 1100 °C. This heat treatment lead not only to a densification of the glass matrix but also to removal of water and organic residues.[192,193] Heat treatment at lower temperatures is less effective and moreover not all organic material will be removed, although most volatile components will evaporate at temperatures below 200 °C.[194] Hydroxyl quenching is very prominent in xerogels that are not heated to temperatures above 250 °C.[161] It should be noted that heating of the sol−gel silica glass to very high temperatures up to 1300 °C, which is still below the melting point of silica, will result in crystallization of the sample.[195] Besides heating the xerogel to high temperatures, other different methods have been applied to remove hydroxyl groups as much as possible from the glass host matrix. Most of these methods are chemical modifications in which the hydroxyl groups react with reagents added to the sol−gel glass during synthesis or during the heat treatment. Examples of chemical modification are heating the sol−gel glass in a reactive atmosphere of carbon tetrachloride,[196] chlorine,[197,198] or thionyl chloride.[199] Another technique is dehydroxylation by fluorine. Fluorine can be introduced in the sol−gel glass by adding hydrofluoric acid to the initial sol−gel reaction mixture.[200] An original approach is chemical dehydroxylation via *in situ* fluorination by fluorinated counterions of the lanthanide ions. To achieve this, lanthanide salts with fluorinated anions of or lanthanide complexes with fluorinated ligands have to be used. Fluorinated species are formed during the thermal decomposition of these fluorine-containing precursors. Costa et al. used $Eu(CF_3COO)_3$, $Eu(CF_3SO_3)_3$, and $Eu(fod)_3$ as dopants.[201] These authors studied the system with lanthanide triflate salt, $Ln(CF_3SO_3)_3$, as dopant in more detail.[202] They found that it is also possible to introduce fluorine via the fluorinated sol−gel precursor $FSi(OC_2H_5)_3$.[202] If one wants to block the silanol groups at the xerogel surface at low temperature so that no heat treatment of the xerogel is necessary, the xerogel can be exposed to the vapor of 1,1,1,3,3,3-hexamethyldisilazane, $(CH_3)_3SiNHSi(CH_3)_3$, in a sealed reactor tube at about 90 °C:[186,203]

$$2(-Si-OH)(surface) + (CH_3)_3SiNHSi(CH_3)_3 \rightarrow 2-Si-O-Si(CH_3)_3(surface) + NH_3 \quad (10)$$

This reagent is also used to prepare water-repellent silica coatings.[204] Oxide gels can be transformed in fluoride glasses by fluorination with HF gas at temperatures between 100 and 800 °C. By this method, it was possible to obtain europium(III)-doped fluorozirconate glasses via the sol−gel process.[205] The prototype fluorozirconate glass ZBLAN ($53ZrF_4-20BaF_2-20NaF-4LaF_3-3AlF_3$) was prepared by first synthesizing an oxide gel via the sol−gel reaction of a mixture of zirconium *n*-propoxide, barium ethoxide, sodium methoxide, lanthanum propoxide, and aluminum ethoxide in propanol. Subsequently the oxide gel was fluorinated by anhydrous HF as fluorinating agent at 200 °C.[206] Powdered glass samples were obtained, but bulk glass samples could be prepared by melting this glass powder in a dry atmosphere. Unhydrated and low-hydroxyl silica xerogels can be produced by using a *nonhydrolytic sol−gel process*.[207] Here, the hydroxyalkoxysilanes are formed in the absence of water by reaction of the precursor molecule with a carboxylic acid (e.g., formic acid). The subsequent condensation reactions are similar to those occurring during the conventional sol−gel process. The fact that the sol−gel-derived silica glass samples still have a higher porosity than glass samples prepared via the melt process is a disadvantage for the long-term stability of sol−gel glasses and for the luminescence behavior of lanthanide-doped sol−gel glasses. It has been observed that water molecules diffuse into sol−gel glasses when they are exposed to the atmosphere under ambient conditions. The rehydration of the sol−gel glass can lead to a dramatic reduction of the luminescence intensity.[208] The tendency to rehydration can be limited by heat treatment of the samples to sufficiently high temperatures, up to 1000 °C.[209] Heat treatment allows observation of not only near-infrared luminescence in sol−gel glasses but also luminescence from less-common emitting levels. An example is the $^5D_3 \rightarrow {}^7F_J$ emission for Tb^{3+}-doped glasses.[210]

Clustering of lanthanide ions is due to aggregate formation between lanthanide ions via oxygen bridges and the clusters are characterized by short lanthanide−lanthanide distances.

Clustering is detrimental for luminescence performance, because of concentration quenching through cross-relaxation and energy-transfer processes. The clustering of lanthanide ions in sol−gel glasses has been studied by *fluorescence line narrowing* (FLN). This technique is often used to probe the local environment of lanthanide ions in glass matrices because it allows the observation of spectral fine structure, although the emission bands in the luminescence spectra of glasses are broad and featureless due to inhomogeneous line broadening. FLN is able to eliminate inhomogeneous broadening because only a small portion of the lanthanide ions that are responsible for the inhomogeneous broadening are excited. In a glass, each lanthanide ion has a slightly different local environment, resulting in slightly different crystal fields and thus in differences in the crystal-field splitting pattern, resulting in inhomogeneous spectral broadening of the emission bands. In fluorescence line narrowing studies, a narrow laser line is used to selectively excite only a small part of the lanthanide ions, which are characterized by a similar local environment, rather than all the lanthanide in the sample. This selective excitation of only a part of the lanthanide ions results in the elimination of inhomogeneous broadening. By tuning the wavelength of the laser beam, one can excite other sets of lanthanide ions in the glass matrix. The luminescence spectra generated by the FLN technique have a much higher resolution (i.e., show more crystal-field fine structure) than conventional luminescence spectra of lanthanide-doped glass, and the fine structure observed in the luminescence spectra depends on the excitation energy. Especially Eu^{3+} is a useful probe for FLN studies in glasses, with selective excitation in the $^5D_0 \rightarrow {}^7F_0$ line.[211,212] Other useful ions are Nd^{3+} and Yb^{3+}.[213] In order to selectively excite a small portion of the lanthanide ions, the lanthanide ions should be spatially separated. In the case of clustering, the small distance between the lanthanide ions will allow efficient energy transfer processes between the different ions. Therefore, selective excitation is no longer possible so that clustering makes it impossible to eliminate inhomogeneous line broadening by the fluorescence line narrowing technique. A sample in which clustering of lanthanide ions occurs is thus characterized by a lack of the line-narrowing effect. In Figure 6, examples of FLN spectra of a Eu^{3+}-doped SiO_2 glass codoped with Sr^{2+} are shown. Lochhead and Bray were able to demonstrate that codoping of silica sol−gel glasses with aluminum is effective in dispersing Eu^{3+} ions in the silicate matrix and will thus reduce the clustering in this matrix.[214] The beneficial effect of Al^{3+} ions has been attributed to the fact that Al^{3+} shows a very strong ionic field strength and strongly interacts with the silica matrix, so it is able to penetrate the lanthanide clusters and to provide a more uniform distribution. Codopants other than Al^{3+}, like Sr^{2+}, La^{3+}, Gd^{3+}, Lu^{3+}, Y^{3+}, Sc^{3+}, and Ga^{3+} are also able to inhibit clustering.[215] The strongest effect in preventing clustering was observed for the cations with the strongest charge density (Ga^{3+}, Sc^{3+}, and Lu^{3+}). A comparison with the results for Al^{3+} was found to be difficult, because Al^{3+} acts as a network former whereas the other ions act as network modifiers. Strong clustering of Eu^{3+} ions occurred in samples without inorganic cationic codopants. The luminescence intensity of Eu^{3+} in $SiO_2-Al_2O_3$ was found to be twice as high as that in the glasses without added Al_2O_3.[216] Further studies on Tb^{3+}-containing sol−gel glasses codoped with aluminum show that the dispersive action of aluminum is effective only if the Al/Tb ratio is larger than 10.[217]

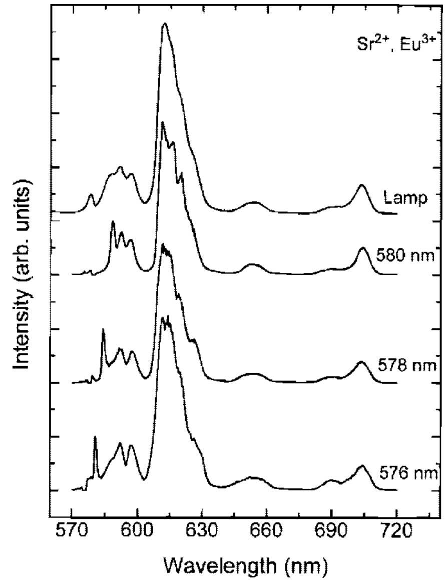

Figure 6. FLN spectra at 77 K of 1 wt % Eu_2O_3-doped sol−gel silica codoped with Sr^{2+} (molar ratio $Sr^{2+}/Eu^{3+} = 9$) at various excitation wavelengths. Intensities are normalized to the $^5D_0 \rightarrow {}^7F_1$ emission band at each excitation wavelength. The upper spectrum is the luminescence spectrum at 300 K, excited with a tungsten lamp ($\lambda_{exc} \leq 500$ nm). Reproduced with permission from ref 215. Copyright 1996 American Chemical Society.

Aluminum codoping of lanthanide-containing silica glasses is finding application for improvement of the luminescence properties of these glasses.[218] However, aluminum doping also leads to more severe hydroxyl quenching.[214] Alumina-doped glasses show a strong tendency to retain hydroxyl groups in the densified matrix after heat treatment. Therefore, aluminum codoping is less beneficial for near-infrared luminescing lanthanide ions than for lanthanide ions emitting in the visible spectral region. A less known codoping agent that improves the luminescent properties of lanthanide ions in sol−gel glasses is P_2O_5.[219,220] It has also been suggested that clustering of lanthanide ions in sol−gel glasses can be reduced by using lanthanide(III) acetate salts as lanthanide precursors.[133,221]

The classic approach to solve the problems associated with the weak light absorption by the lanthanide ions is by replacing the lanthanide salt precursors by *molecular lanthanide complexes*. In these molecular complexes, the lanthanide ions are surrounded by a shell of strongly absorbing organic ligands, which can efficiently transfer the excitation energy to the lanthanide ion. The organic ligands can shield the lanthanide ion from interaction with the hydroxyl groups in the sol−gel matrix. The incorporating of the lanthanide ion in a complex is a useful approach to avoid clustering of the lanthanide ions. In many cases, it was observed that the thermal stability of the lanthanide complex improved after incorporation in a silica xerogel. The approach of embedding molecular lanthanide complexes in a sol−gel glass matrix was first described by Matthews and Knobbe, who incorporated europium(III) β-diketonate complexes in a silica sol−gel glass prepared by hydrolysis of TEOS.[222] They studied the luminescence behavior of the complexes $[Eu(tta)_3(H_2O)_2]$ and $(pipH)[Eu(tta)_4]$. The authors selected these complexes because they display an intense photoluminescence and because they are highly soluble in DMF. As mentioned above, DMF is often added to the starting mixture for the preparation of sol−gel glasses, because this additive prevents the glass from cracking during the drying process.[152] These authors observed that the spontaneous emission cross sections for the glasses doped with these β-diketonate complexes were 2−3 orders of magnitude higher than those for glasses doped with hydrated $EuCl_3$. In a subsequent study, they investigated the concentration effects on the europium(III) luminescence.[223] Yan et al. incorporated the ternary rare-earth complexes $[Eu(dbm)_3(phen)]$ and $[Tb(acac)_3(phen)]$ into a silica sol−gel glass.[224] The luminescence lifetime of the complexes in the sol−gel matrix was found to be longer than that for the pure complexes in the solid state. Strek et al. investigated the luminescence properties of the europium(III) complexes $[Eu(acac)_3(H_2O)_2]$, $[Eu(bzac)_3(H_2O)_2]$, $[Eu(acac)_3(phen)]$, and $[Eu(bzac)_3(phen)]$ in silica sol−gel glasses.[225] Crystal-field fine structure could be observed in the emission spectra. The β-diketonate complexes have been very popular dopants for the preparation of luminescent sol−gel glasses,[226−228] although aromatic carboxylates give often better luminescence performance in the case of Tb^{3+} as dopant.[229−231]

It should be noted that a xerogel doped with molecular lanthanide complexes cannot be transformed to a compact silica glass, because the limited stability of the molecular complexes prevents heating the samples to 800 °C or higher. However, a heat treatment at 250 °C (or lower if the complexes have a low thermal stability) is beneficial for the luminescence intensities because at these temperatures water molecules and volatile organic components can be removed by evaporation. In some examples, lanthanide complexes with organic ligands have been used to obtain a homogeneous dispersion of the lanthanide ions in the glass matrix rather than to take advantage of the antenna effect.[232−234] These xerogels were heated to high temperatures in order to destroy all organic material and to remove water molecules as efficiently as possible.

Lanthanide complexes can be directly dissolved in the sol−gel precursor solution. However, the lanthanide complexes are often not stable in the acidic precursor solution. In that case, the ligands and a lanthanide salt can be added to the precursor solution instead of the complex. The complex is formed *in situ* during the transformation of the gel into a xerogel.[226,235−244] For instance, a $[Eu(tta)_3]$-doped sol−gel film was made by dip-coating of a sol codoped with europium(III) chloride and Htta.[245] The europium(III) β-diketonate complex was gradually formed upon heat treatment. This was evident from an increase in luminescence intensity. However, at temperatures above 130 °C, the luminescence intensity decreased rapidly due to thermal decomposition of the complex.

Adachi and co-workers incorporated the complexes $Ln(bipy)_2Cl_3 \cdot 2H_2O$ and $Ln(phen)_2Cl_3 \cdot 2H_2O$ (Ln = Eu, Tb) in silica sol−gel glasses.[246−249] They found a higher stability for the complexes in the glass matrix than for the pure solid complexes. The absorption spectra of several $Ln(bipy)_2Cl_3 \cdot 2H_2O$ and $Ln(phen)_2Cl_3 \cdot 2H_2O$ complexes in silica sol−gel glasses were recorded, and Judd−Ofelt intensity parameters were derived from these spectra.[177,178] $Ln(bipy)_2Cl_3 \cdot 2H_2O$ complexes (Ln = La, Nd, Tb) doped into sol−gel glasses have been investigated by luminescence spectroscopy and by photoacoustical techniques.[250] The authors conclude that the 2,2′-bipyridine ligands do not coordinate to the lanthanide ion in the xerogel before heat treatment. $Ln(phen)_2Cl_3 \cdot 2H_2O$ complexes (Ln = Eu, Tb) gave highly luminescent sol−gel glasses.[251] 2,6-Pyridinedicarboxylate (dipicolinate, dpa) is a tridentate ligand that

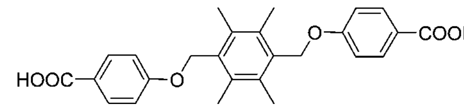

Figure 7. 3,6-Bis[(4′-carboxyphenoxy)methyl]-1,2,4,5-tetramethylbenzene (H_2BCM).

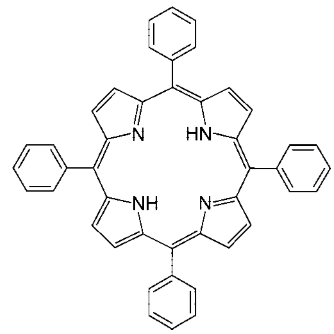

Figure 8. Tetraphenylporphyrin.

forms nine-coordinate metal complexes with lanthanide, $[Ln(dpa)_3]^{3-}$, in which the coordination polyhedron of the lanthanide ion can be described as a (distorted) tricapped trigonal prism. In this type of complex, the lanthanide ion is coordinatively saturated so that the additional coordination of solvent molecules can be efficiently prevented and thus nonradiative deactivation of excited states can be minimized. Therefore, the dipicolinate ligand is a useful ligand for the preparation of luminescent lanthanide complexes. Lai et al. incorporated tris(dipicolinate) neodymate(III) complexes in sol−gel glasses.[252] Although water molecules do not directly coordinate to the lanthanide ion, the authors were able to observe quenching of the excited state by water molecules in the sol−gel matrix. An intense $^5D_0 \rightarrow {}^7F_2$ transition was observed for the europium(III) complex of picolinic acid *N*-oxide in a sol−gel silica glass.[253] A well-adhering thin layer of a terbium(III) benzoate containing sol−gel glass was coated on a silica glass plate by dip coating.[254] Applications of these films as UV sensors have been proposed. These authors also prepared strongly luminescent microstructured silica sol−gel layers doped with terbium(III) picolinate via a photolithographical process.[255] The fact that silica sol−gel glasses doped with terbium(III) picolinate could be coated on glass fibers illustrated that coating by sol−gel materials is not restricted to flat surfaces.[256] Circularly polarized luminescence has been observed for $[Eu(dpa)_3]^{3-}$, $[Eu(oda)_3]^{3-}$, and $[Eu(bipyO_2)_4]^{3+}$ complexes in sol−gel glasses, where dpa = dipicolinate, oda = oxydiacetate, and $bipyO_2$ = 2,2′-bipyridine-*N*,*N*-dioxide.[257,258] Macrocyclic[259] and cryptand ligands[260−269] also provide a well-shielded environment for luminescent lanthanide ions in sol−gel glasses. An unusual complex for incorporation in silica sol−gel glasses is the terbium(III) complex of 3,6-bis[(4′-carboxyphenoxy)methyl]-1,2,4,5-tetramethylbenzene (H_2BCM), $Tb_2(BCM)_3$ (Figure 7).[270] Although lanthanide porphyrin complexes have been entrapped in a sol−gel matrix, in most cases only ligand-centered fluorescence could be observed and no lanthanide luminescence.[271,272] However, Cervantes et al. observed metal-centered emission from neodymium(III) and erbium(III) tetraphenylporphyrin complexes in a silica sol−gel matrix (Figure 8).[273] The strongest luminescence was observed for Er^{3+}. Notice that the authors report the $^4S_{3/2} \rightarrow {}^4I_{15/2}$ emission of Er^{3+} at 563 nm and not the near-infrared emission. The fwhm value of this transition in the silicate sol−gel material (90 cm^{-1}) was found to be a factor of 5−6 narrower than the corresponding values in erbium glasses or glass ceramics. Serra and co-workers impregnated silica gel with europium(III) complexes of 1,10-phenanthroline, 2,2′-bipyridine, benzoyltrifluoroacetone, and acetylacetone.[274] The luminescence properties were improved by functionalizing the silica gel with propyl imidazole. Notice that the silica matrix for these studies was not prepared via a sol−gel process but that silica gel for chromatographic applications was used.

Surrounding the lanthanide ion by a shell of organic ligands, which can efficiently absorb light and transfer the excitation energy to the lanthanide ion, is not the only method to sensitize lanthanide luminescence in sol−gel glasses. Another approach is to replace the organic ligands as absorbers by *inorganic nanoparticles* (see section 9.2). To enhance the luminescence of Tb^{3+} in sol−gel glasses, codoping with Ce^{3+} is an interesting option,[295,275,276] which is also being used to improve the luminescence performance of terbium(III)-doped inorganic phosphors.[277,278] Cerium(III) shows intense absorption in the ultraviolet region, and the excitation energy can be transferred to the energy levels of terbium(III). Similarly, the luminescence of Eu^{3+} in sol−gel glasses can be improved by doping with Bi^{3+}.[279] Another way to sensitize Eu^{3+} luminescence is via Eu^{2+} ions that are present in the same sample.[173,184] Partial reduction of Eu^{3+} can occur during heat treatment of the xerogel. However, it is also possible to prepare sol−gel glasses that contain only Eu^{2+} by adding $EuCl_2$ to the sol−gel precursor solution or by total reduction of the Eu^{3+}-doped xerogel by a reducing hydrogen atmosphere.[280] The emission intensity of Eu^{2+} in a silica sol−gel glass was found to be increased by about 250 times by codoping of the glass with 1% of alumina.[216] Grobelna et al. described the luminescence properties of $CaWO_4/Eu^{3+}$ and $CaWO_4/Tb^{3+}$ incorporated in silica xerogels.[281] A related study reports on samarium(III) luminescence of the wolframates $Ln_{2-x}Sm_x(WO_4)_3$ (Ln = La, Gd) in silica sol−gel glasses.[282]

Incorporation of germanium in silica glasses under the form of GeO_2 was found to increase the luminescence intensity of Tb^{3+} in silica gel glasses, possibly due to energy transfer from germanium-related defects in silica.[283,284] Whereas the as prepared samples could by efficiently excited by irradiation at 355 nm, samples annealed at temperatures between 600 and 700 °C showed additional bands in the excitation spectra and enabled efficient excitation by UV radiation of 254 nm. Quantum efficiencies up to 30% have been measured for excitation at 254 nm.

Classically, glass samples prepared by the sol−gel process are composed of silica (SiO_2). Replacement of the silicon alkoxide precursors by other easily hydrolyzable metal alkoxides will allow one to obtain other types of lanthanide-doped oxide materials like alumina (Al_2O_3),[285−289] titania (TiO_2),[290−297] zirconia (ZrO_2),[228,249,265,269,291,298−302] hafnia (HfO_2),[291,303,304] tantalum(V) oxide (Ta_2O_5)[249,299] or germania (GeO_2).[305] In general, these metal and transition-metal alkoxides are more reactive toward hydrolysis and condensation reactions than the silicon alkoxides. Typically, the metals in these alkoxides are in their highest oxidation state. These metal alkoxides can also be mixed with silicon alkoxides to prepare mixed silica−metal oxide gels.[306−312] The codoping of silica glasses by alumina, producing aluminosilicate glasses, has already been discussed above. However, because the transition metal alkoxides react in general much faster than the silicon-based precursors, they are more difficult to handle and to study. The replacement of silicon by other metals in the sol−gel glasses allows tuning of the physicochemical properties like the refractive index, but it can also be useful to obtain a more homogeneous dispersion of the lanthanide ions in the glass matrix. In the mixed oxide systems, discrete crystalline phases can be formed during synthesis. An example, is the formation of $Er_2Ti_2O_7$ in the erbium-doped SiO_2/TiO_2 system.[313,314] Zirconia coatings are an ideal medium for the preparation of active planar waveguides due to their chemical and photochemical stability, high refractive index, and low phonon energy.[300,315] Hafnia coatings possess the same advantages.[316] On the other hand, titania coatings can experience photochemical damage after long time exposure to intense excitation light.[300] Because of the low phonon energy, zirconia sol−gel glasses are an excellent medium for luminescent lanthanide ions.[300] The advantage is especially evident for near-infrared luminescent lanthanide ions. However, also the luminescence intensity of Eu^{3+} and Tb^{3+} ions is higher in zirconia than in silica sol−gel glasses. The higher luminescence intensity is attributed to the higher refractive index and the higher dielectric constant of the zirconia matrix. Interestingly, luminescence by Sm^{3+} could be observed in zirconia glasses but not in silica glasses. This was explained by the clustering of Sm^{3+} ions in silica glasses, resulting in cross relaxation. The higher refractive index of zirconia glass results in stronger light reflection than in the case of silica glass. In comparison to silica, alumina has a superior thermal conductivity.[289] For the preparation of alumina films, the preferred method of synthesis is not via an alkoxide precursor but via an aqueous sol−gel route based on the formation of hydrous aluminum oxide by hydrolysis of an aqueous $AlCl_3$ solution by an aqueous NH_3 solution.[289] Several lanthanide-doped inorganic phosphors have been prepared by sol−gel processes. For instance, YVO_4/Nd^{3+} was obtained by the reaction of yttrium(III) ethoxide, vanadyl isopropoxide, and neodymium(III) ethoxide in 2-methoxyethanol.[317] The dip-coated films crystallized to YVO_4/Nd^{3+} during heat treatment at 500 °C. YPO_4/Eu^{3+} was synthesized by a sol−gel route from yttrium(III) and phosphorus(V) isopropoxide, which were prepared *in situ* by reaction of a potassium isopropoxide solution with YCl_3 and P_2O_5.[318] Annealing the amorphous gels at 1200 °C for 12 h led to the formation of the YPO_4/Eu^{3+} phosphor. Advantages of the sol−gel process are a narrow particle size distribution and the possibility to prepare thin films by dip-coating. Other examples of rare-earth phosphors prepared by a sol−gel process include Y_2O_3/Eu^{3+},[319] Y_2O_3/Pr^{3+},[320] $LuPO_4/Ln^{3+}$ (Ln = Ce, Eu, Tb),[321] $LuBO_3/Ln^{3+}$ (Ln = Eu, Tb),[322] $Y_3Al_5O_{12}/Tb^{3+}$,[323,324] $YAlO_3/Tb^{3+}$,[319] and Sr_2CeO_4.[325] Sol−gel processes have been used for the preparation of scintillation materials like Lu_2SiO_5/Ce^{3+} and $LuBO_3/Ce^{3+}$.[326]

The possibility to obtain of a thorium(IV) phosphate gel after mixing $Th(NO_3)_4$ and H_3PO_4 has been known for a long time.[327] Brandel et al. explored thorium phosphate gels as a host for trivalent lanthanide ions.[328−331] Evaporation of a very concentrated solution of thorium(IV) phosphate at room temperature led first to the formation of a gel and upon further drying to a transparent xerogel of a good optical quality. The absorption spectra of Nd^{3+} and Er^{3+} in the gel were identical to those in aqueous solution. A small shift in the band positions and the appearance of some crystal-field fine structure was observed for these ions in xerogels. The luminescence spectra of Eu^{3+} in thorium-based gels and

Table 3. Sensitization of Lanthanide Luminescence in Glasses by Other Metal Ions

luminescent ion	sensitizing ion
Nd^{3+}	Ce^{3+}, Eu^{3+}, Tb^{3+}, UO_2^{2+}, Mn^{2+}, Cr^{3+}, Bi^{3+}
Sm^{3+}	UO_2^{2+}, Bi^{3+}
Eu^{3+}	Gd^{3+}, UO_2^{2+}, Bi^{3+}, Pb^{2+}
Tb^{3+}	Ce^{3+}, Gd^{3+}, Dy^{3+}
Ho^{3+}	Yb^{3+}, Er^{3+}
Er^{3+}	Yb^{3+}
Tm^{3+}	Ce^{3+}, Yb^{3+}, Er^{3+}
Yb^{3+}	Ce^{3+}, Nd^{3+}, (Ce^{3+} + Nd^{3+}), (UO_2^{2+} + Nd^{3+}), Cr^{3+}

xerogels were studied. For a thorium phosphate xerogel codoped with Coumarin-460 and Tb^{3+}, energy transfer was observed from the organic dye to the Tb^{3+} ion resulting in an enhancement of the Tb^{3+} luminescence.[330] Also Eu^{3+} luminescence was sensitized by Coumarin 460 in a thorium phosphate xerogel.[331] After thermal treatment of the amorphous thorium phosphate xerogel, crystalline thorium orthophosphate was formed.[328] The thorium phosphate xerogel could be processed to thin films by spin-coating and dip-coating.[332]

Examples of lanthanide ions incorporated into sol−gel xerogels and glasses have been reported for most of the spectroscopically active trivalent lanthanide ions. The studies on europium(III)- and terbium(III)-doped xerogels and glasses have been discussed in detail above. The rationale for incorporation of Eu^{3+} and Tb^{3+} ions in sol−gel glasses was on one hand the use these ions as spectroscopic probes for studying structural changes in the sol−gel matrix during transformation of gel into a xerogel and subsequently into a compact glass matrix and on the other hand the design of luminescent materials. Incorporation of lanthanide ions other than Eu^{3+} and Tb^{3+} into sol−gel matrices has at first been done to take advantage of the unique luminescent properties of lanthanide ions in the construction of luminescent materials and devices. Luminescent sol−glasses doped with cerium(III),[181,333,334] praseodymium(III),[335−338] neodymium(III),[134,339−344] samarium(III),[300,345−349] gadolinium(III),[347] dysprosium(III),[347] holmium(III),[347] erbium(III)[316,343,350−363] thulium(III),[347] and ytterbium(III)[364,365] have been studied. Special attention was paid to the Yb^{3+}−Er^{3+}-codoped glasses. Light is absorbed by Yb^{3+}, and the excitation energy is transferred to the Er^{3+} ion, which shows near-infrared luminescence.[366] Although the energy transfer from Yb^{3+} to Er^{3+} has been studied in detail, much less is known about the energy transfer between other lanthanide ions in sol−gel glasses. Buddhudu et al. studied the luminescence properties of Eu^{3+}-containing silica glasses codoped with La^{3+}, Pr^{3+}, Nd^{3+}, Sm^{3+}, Gd^{3+}, Tb^{3+}, Dy^{3+}, Er^{3+}, and Yb^{3+}.[367,368] Dai and co-workers investigated the energy transfer from uranyl to europium(III) in a sol−gel glass.[369] The emission of UO_2^{2+} is quenched in the presence of Eu^{3+}, and the luminescence lifetime of uranyl decreased with increasing concentration of Eu^{3+}. Another energy transfer study is about silica xerogels codoped with the dye Coumarin-120 and with lanthanide ions (Eu^{3+}, Tb^{3+}).[370] A glass sample codoped with chromium(III) and dysprosium(III) only showed emissive transitions due to chromium(III) ions.[371] Codoping is especially used to obtain near-infrared emitting glasses. However, the full potential of doping sol−gel glasses and similar materials by both lanthanide ions and transition metal ions has not been explored yet. In Table 3, an overview of sensitization of luminescent trivalent lanthanide ions by other metal ions is given.[131,372,373]

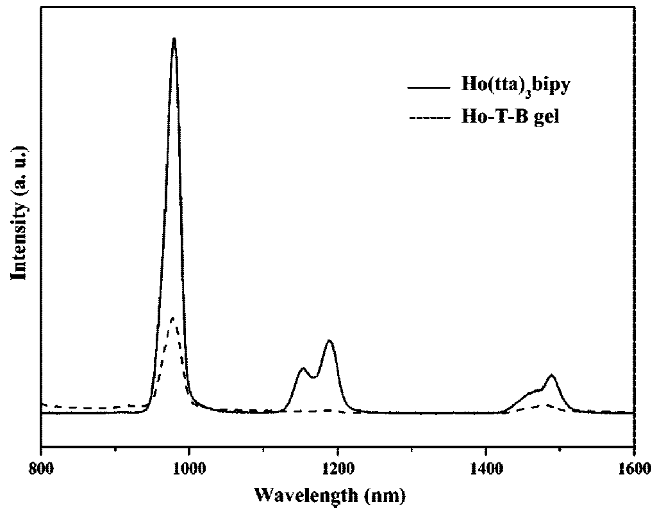

Figure 9. Luminescence spectra of the [Ho(tta)$_3$(bipy)] complex in the solid state (λ_{exc} = 386 nm) and entrapped in a silica gel glass (λ_{exc} = 362 nm). Reprinted with permission from ref 387. Copyright 2008 American Chemical Society.

For fundamental studies, the absorption spectra of lanthanide ions in sol−gel glasses have been studied: praseodymium(III),[374−378] neodymium(III).[378] samarium(III),[378] gadolinium(III),[379] holmium(III),[380] and erbium(III).[381] Strong broadband light absorption in the visible spectral region (λ_{max} at 550 nm) was observed for cerium-doped sol−gel glasses.[382] The intense absorption bands were attributed to Ce^{4+}−O−Ce^{3+} and to Ce^{4+}−O−Fe^{3+} clusters. In principle, lanthanide ions or lanthanide complexes could be incorporated into a porous xerogel by impregnation, that is, by soaking the xerogel in a solution containing a lanthanide salt or complex. Whereas this method has been used to adsorb lanthanide ions or complexes on porous Vycor glass,[383−385] this approach seems not to have often been used in the field of sol−gel glasses. Bredol et al. treated xerogels containing benzoic acid with a terbium(III) chloride solution to obtain luminescent materials.[386] Very few studies are about near-infrared emitting molecular lanthanide complexes doped into sol−gel silica glasses. Dang and co-workers doped the complexes [Ln(tta)$_3$(phen)], [Ln(tta)$_3$(bipy)], and [Ln(tta)$_3$(tppo)$_2$], where Ln = Ho, Tm, in silica glass prepared by the hydrolysis and condensation of TEOS.[387] The lanthanide complexes are introduced in the silica glass via an *in situ* synthesis procedure. Near-infrared emission was observed for both the holmium(III) and thulium(III) complexes (Figures 9 and 10). However, the luminescence intensities of the complexes in the sol−gel glasses were weaker than those of the pure solid complexes, probably due to quenching of the excited states by residual OH groups. Also the luminescence lifetimes in the sol−gel glasses are shorter than the corresponding values of the solid complexes.

An interesting phenomenon that has been observed in lanthanide-doped sol−gel glasses is *upconversion*.[388−390] Upconversion can be considered as anti-Stokes emission, that is, emission with energies larger than the excitation energy. Upconversion has been observed for several sol−gel glasses doped with Yb^{3+} or codoped with Yb^{3+} and another lanthanide ion. For instance, in Tb^{3+}−Yb^{3+}-codoped sol−gel glasses, Tb^{3+} can be excited via energy transfer processes by Yb^{3+} ions.[391] In this way, two near-infrared photons absorbed by Yb^{3+} ions can be transformed into a green photon emitted by a Tb^{3+} ion. A glass codoped with Yb^{3+} and Eu^{3+} gave yellow upconversion luminescence.[392] Blue

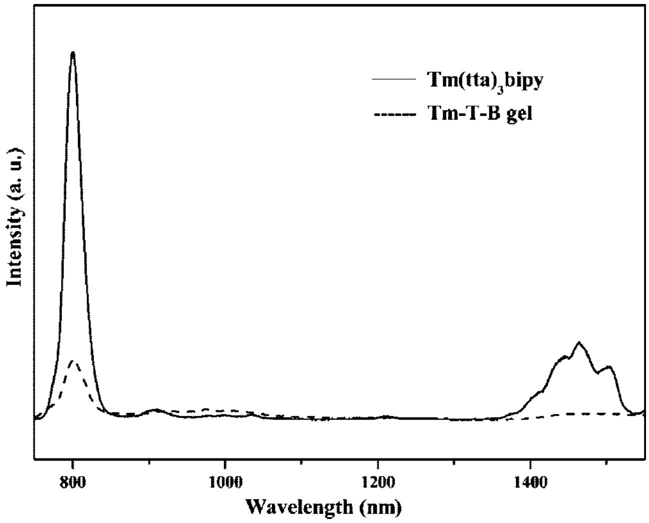

Figure 10. Luminescence spectra of the [Tm(tta)$_3$(bipy)] complex in the solid state (λ_{exc} = 384 nm) and entrapped in a silica gel glass (λ_{exc} = 370 nm). Reprinted with permission from ref 387. Copyright 2008 American Chemical Society.

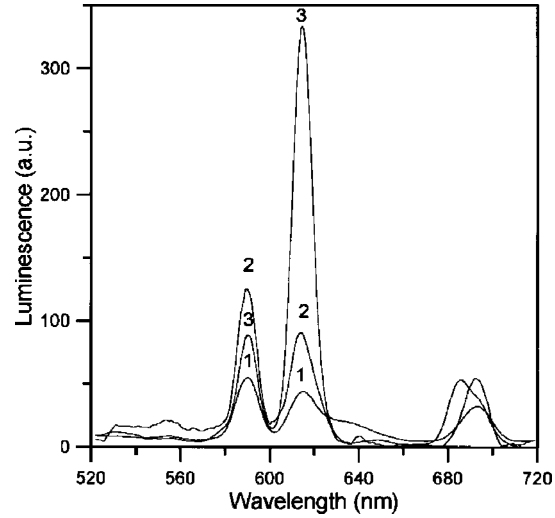

Figure 11. Luminescence spectra of Eu^{3+} in various sol–gel silica matrices containing PEG-200: (1) silica xerogel made without polymer; (2) composite xerogel containing 15 wt % PEG-200; (3) composite xerogel containing 90 wt % PEG-200. The concentration of Eu^{3+} in the sol was 0.04 mol/L in all samples. The excitation wavelength was 396 nm. Reproduced with permission from ref 400. Copyright 1999 American Chemical Society.

cooperative upconversion by Yb^{3+} was observed for a sol–gel silica glass doped with 1 mol % Yb^{3+}.[393] Red-to-green upconversion was observed for an Er^{3+}-doped sol–gel glass[394] and red-to-blue upconversion for a Tm^{3+}-doped glass.[395]

3.2. Confinement of Liquids in Silica Matrices

The silica gel formed by the sol–gel process is a two-component system consisting of an interconnected pore network and a liquid phase. The liquid phase is unwanted and is removed during the drying step. The resulting xerogel contains only a small portion of remaining liquid, and this can be removed further by heat treatment, as described in the previous section. However, the silica network can also be used to confine liquids within its porous network. Generally, these are nonvolatile liquids in which luminescent lanthanide ions or lanthanide complexes have been dissolved. Although we consider here these materials as immobilized liquids, they can also be considered as so-called class I hybrid organic–inorganic nanocomposites. Hybrid materials can be classified according to the bonding between the organic and inorganic part of the network.[396,397] In *class I materials*, organic molecules are blended into the inorganic network. In *class II materials*, the inorganic and organic constituents are linked via covalent bonds.

Poly(ethylene glycol) (PEG) with an average molecular mass of 200 g mol^{-1} (PEG-200) is a liquid that can solubilize large quantities of both lanthanide salts and 2,2′-bipyridine (bipy). Bekiari and Lianos observed a strong luminescence for solutions prepared by dissolving 2,2′-bipyridine and the lanthanide salts $Eu(NO_3)_3 \cdot 5H_2O$ or $Tb(NO_3)_3 \cdot 5H_2O$ in PEG-200 at a bipy concentration of 0.1 mol L^{-1} and a lanthanide concentration of 0.02 mol L^{-1}.[398] A spectroscopic study shows that the lanthanide ions and bipy form a complex in solution, assisted and stabilized by PEG-200. It is very likely that a PEG–lanthanide–bipy complex is formed in solution. Transparent monolithic gels could be obtained by mixing the PEG-200 solutions with prehydrolyzed TMOS. The gel formation had no effect on the photophysical properties of the original liquid mixture. This indicates that the silica network just acts to immobilize the PEG-200 solution and does not interact with the lanthanide ions. A comparison between the luminescence spectra of Eu^{3+} in a silica xerogel and in composite xerogels containing PEG-200 showed higher emission intensities, longer luminescence decay times, and smaller spectral bandwidths for the samples containing PEG-200.[399,400] In Figure 11, the luminescence spectra of Eu^{3+} in a silica xerogels are compared with those of silica–PEG hybrid materials. Similar results were obtained for PEG-400, but composite xerogels containing higher-molecular-mass PEGs were no longer transparent. Notice that the high-molecular-mass PEGs are not liquid. Although the silica network immobilizes the PEG liquid, the lanthanide ions can diffuse through the quasi-three-dimensional viscous medium. No covalent bonds are formed between the PEG chains and the silica network.[401] The luminescence properties of silica/PEG-200 nanocomposites containing 2,2′,6′,2″-terpyridine (terpy) and Eu^{3+} depended on the PEG-200 content.[402] In samples with low PEG-200 content, three emission bands coexisted: the blue luminescence associated with uncomplexed terpy, the green ligand-centered luminescence of the terpy–Eu^{3+} complex, and the red luminescence of the Eu^{3+} ion. In samples with high PEG-200 content, only green luminescence was observed.

Chuai et al. investigated the luminescence of the complex $Eu(phen)_2Cl_3$ in a silica/PEG-400 hybrid material.[403] Monolithic silica–PEG hybrid sol–gels doped with $[Ln(bpy)_2]Cl_3$, $[Ln(phen)_2]Cl_3$, $Na_3[Ln(dpa)_3]$, and $LnCl_3$ were prepared at a neutral pH.[404] The absorption spectra of the different lanthanide complexes doped in silica–PEG sol–gels were measured and the Judd–Ofelt intensity parameters were determined. Driesen et al. investigated the near-infrared luminescence of lanthanide complexes of 4′,5′-bis[*N*,*N*-bis(carboxymethyl)aminomethyl]fluorescein (calcein) (Figure 12) and pyridine-2,6-dicarboxylic acid (dipicolinic acid, dpa) doped in a silica–PEG hybrid material formed by a sol–gel process from TMOS in the presence of PEG-200.[405] The luminescence spectra of $[Nd(dpa)_3]^{3-}$, $[Dy(dpa)_3]^{3-}$ and $[Yb(dpa)_3]^{3-}$ in the hybrid matrix are shown in Figure 13, and the luminescence spectra of [Er(calc45)] is displayed in Figure 14.

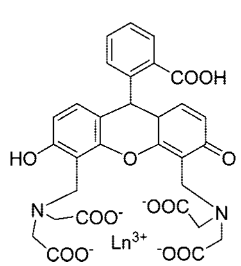

Figure 12. Structure of a lanthanide(III) complex of 4′,5′-bis[*N*,*N*-bis(carboxymethyl) aminomethyl]-fluorescein (calcein, calc45). Reproduced with permission from ref 405. Copyright 2004 American Chemical Society.

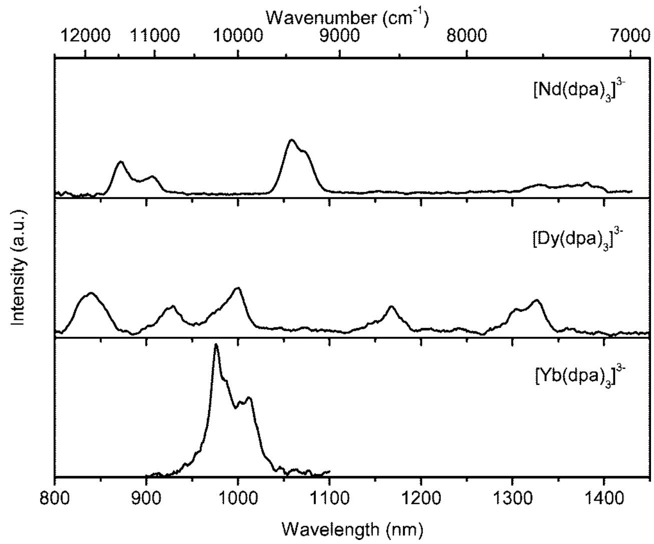

Figure 13. Room-temperature NIR luminescence spectrum of $[Nd(dpa)_3]^{3-}$, $[Dy(dpa)_3]^{3-}$, and $[Yb(dpa)_3]^{3-}$ in a silica−PEG hybrid matrix. The excitation wavelengths are 580, 390, and 290 nm respectively. Reproduced with permission from ref 405. Copyright 2004 American Chemical Society.

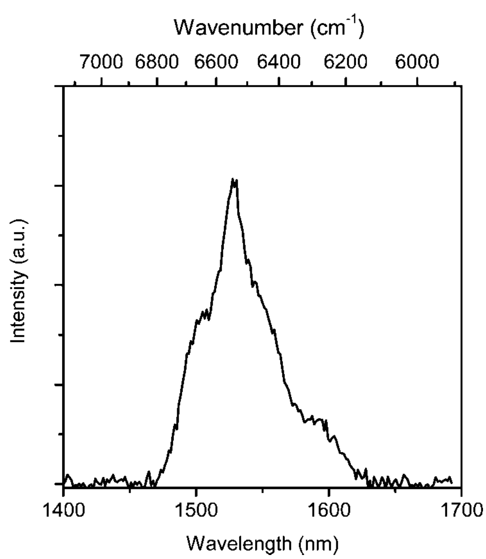

Figure 14. Typical NIR luminescence of [Er(calc45)] in a silica−PEG hybrid matrix at 1530 nm. The excitation wavelength was 480 nm. The luminescence band corresponds to the $^4I_{13/2} \rightarrow {}^4I_{15/2}$ transition. Reproduced with permission from ref 405. Copyright 2004 American Chemical Society.

Ionic liquids have been explored as new solvents for the study of spectroscopic and photophysical properties of lanthanide ions. Ionic liquids are low-melting organic salts with interesting properties like a negligible vapor pressure,

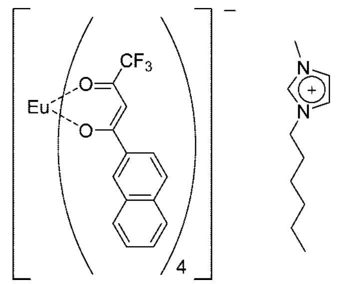

Figure 15. Structure of the complex 1-hexyl-3-methylimidazolium tetrakis(naphthoyltrifluoroacetonato)europate(III), $[C_6mim][Eu(ntac)_4]$. Notice that this structure was incorrectly drawn in the original reference.[416]

a wide electrochemical window and tunable physicochemical properties.[406,407] They are being considered as environmentally friendly solvents for organic synthesis and catalysis.[408,409] Exploratory studies have shown that carefully dried ionic liquids are excellent solvents to study the near-infrared emission of lanthanide ions in solution.[410,411] It has been found that lanthanide β-diketonate complexes dissolved in ionic liquids have a higher photochemical stability than the same complexes dissolved in conventional organic solvents like acetonitrile.[412] A recent review gives an overview of the literature about lanthanides and actinides in ionic liquids, including the literature dealing with spectroscopic properties.[413] It should be noted that it is a challenge to prepare ionic liquids in spectrograde purity.[414,415] Recently, *lanthanide-doped ionogels* have been introduced as a new type of luminescent materials.[416] By incorporation of lanthanide complexes in ionogels, a new type of luminescent material can be obtained. *Ionogels* are hybrid materials consisting of an ionic liquid confined inside the nanosized pores of a silica matrix.[417−419] The ionogels can be obtained as perfect monoliths featuring both the transparency of silica and the outstanding ionic conductivity performances of the ionic liquid, despite the nanometer scale of confinement. The conductivity of the ionogel corresponded well to that of the ionic liquid indicating an interconnecting porosity of the silica matrix. They could be made stable in water and in numerous organic solvents, in which they could be immersed without damage for months.[420] The mechanical properties of ionogels were also very similar to those of regular sol−gel hybrid materials. The volume of the ionic liquid was more or less three times the volume of the silica matrix. It is noteworthy that ionogels can contain 80 vol % ionic liquid, which was shown to preserve liquid-like dynamics.[421] The heat resistance of the ionogel depends also on the type of ionic liquid, typically being in the range of 280−350 °C. These ionic conductor materials could be excellent candidates for the design of electroluminescent devices. Lunstroot et al. prepared the first examples of lanthanide-containing ionogels by doping the 1-hexyl-3-methylimidazolium tetrakis(naphthoyltrifluoroacetonato)europate(III) complex $[C_6mim][Eu(ntac)_4]$ in an ionogel consisting of 1-hexyl-3-methylimidazolium bis(trifluoromethylsulfonyl)imide, $[C_6mim][Tf_2N]$, confined into a silica matrix (Figure 15).[416] The silica matrix was prepared by hydrolysis of a mixture of tetramethoxysilane (TMOS) and methyltrimethoxysilane (MTMS). This work shows that the photophysical properties of the europium(III) β-diketonate complex are barely changed by dissolving the complex in the ionic liquid matrix and by entrapment of the resulting solution in the silica network of the ionogel. The europium(III) complex remained dissolved in the ionic liquid, and there seemed to be no strong

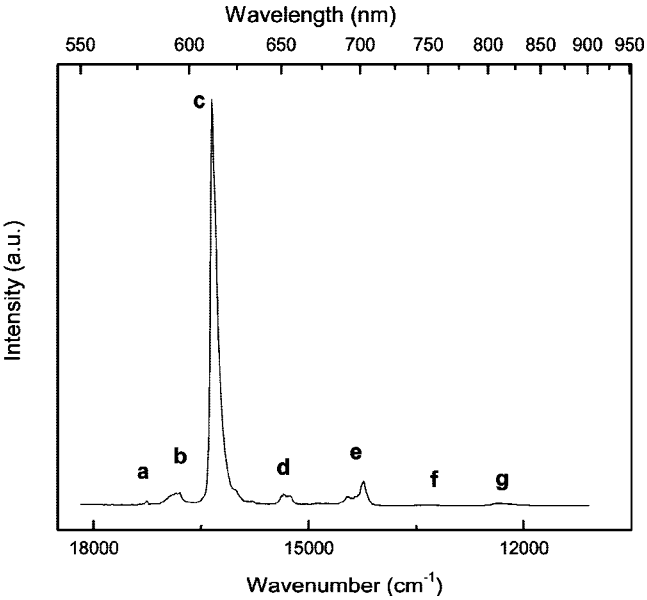

Figure 16. Room-temperature luminescence spectrum of an ionogel doped with the europium(III) complex $[C_6mim][Eu(ntac)_4]$. The excitation wavelength was 360 nm. The assignment of the lines is (a) $^5D_0 \rightarrow {}^7F_0$, (b) $^5D_0 \rightarrow {}^7F_1$, (c) $^5D_0 \rightarrow {}^7F_2$, (d) $^5D_0 \rightarrow {}^7F_3$, (e) $^5D_0 \rightarrow {}^7F_4$, (f) $^5D_0 \rightarrow {}^7F_5$, and (g) $^5D_0 \rightarrow {}^7F_6$. Reproduced with permission from ref 416. Copyright 2006 American Chemical Society.

interaction with the silica matrix. In Figure 16, the luminescence spectrum of $[C_6mim][Eu(ntac)_4]$ in the ionogel is shown. In a follow-up paper, ionogels incorporating the complexes $[C_6mim][Ln(tta)_4]$, where tta is 2-thenoyltrifluoroacetonate and Ln = Nd, Sm, Eu, Ho, Er, Yb, and $[choline]_3[Tb(dpa)_3]$, where dpa = pyridine-2,6-dicarboxylate (dipicolinate), were described.[422]

Glass-dispersed liquid crystals (GDLCs) consist of small liquid-crystal droplets dispersed in a glass matrix.[423−425] The GDLCs can be prepared via a sol−gel process. Typical glass films have dispersed liquid crystal droplets with a diameter varying between 1 and 180 μm. Although the original GDLCs contained a silica matrix, further studies have used a mixture of organoalkoxysilanes with other metal alkoxides as sol−gel precursor to decrease the differences between the refractive indices of the matrix and the liquid crystal.[425] Driesen and Binnemans prepared glass-dispersed liquid crystal films doped with the tris(β-diketonato)-europium(III) complex $[Eu(dbm)_3(gly)]$ (dbm = dibenzoylmethanate, gly = 1,2-dimethoxyethane).[426] The liquid crystal host was 4-pentyl-4′-cyanobiphenyl (5CB) and a mixed silica−titania glass with a refractive index close to that of 5CB was chosen as the glass matrix. The photoluminescence intensity was measured as a function of the temperature. A pronounced intensity decrease was observed at the nematic-to-isotropic transition upon heating of the film. This was explained by stronger scattering and therefore more efficient absorption of the excitation light in the liquid-crystal phase than in the isotropic phase.

3.3. Organically Modified Xerogels

The purely inorganic glasses that are prepared by the controlled hydrolysis of metal alkoxides have some disadvantages if one wants to entrap molecular lanthanide complexes in the glass matrix. First of all, the solubility of the lanthanide complexes in this host is quite low (a few weight percent at maximum) and crystallization of the complex in the glass matrix is often observed. This leads to loss of transparency of the silica gels. Second, these glasses easily crack due to the surface tension of the liquid in the pores. Long drying methods are necessary to reduce this cracking. Third, the mechanical properties of the glasses that have not been heat treated are poor. The resulting glasses are very brittle. It should be remembered that such glasses cannot be heat treated to a high temperature because of the limited thermal stability of the lanthanide complexes. These disadvantages can be overcome by incorporation of organic components in the backbone of the xerogel network.[15,396,397,427,428]

Different types of hybrid materials can be formed. All these compounds are characterized by the fact that the tetraalkoxysilane precursor is partially or totally replaced by trialkoxysilyl compounds with an organic group R′, the *organotrialkoxysilanes* $R'-Si(OR)_3$. The organic group R′ of the organotrialkoxysilane can be an alkyl or aryl group, but it can also bear a functional group, like an amino, and isocyanate, epoxy, or vinyl groups. Precursors with nonreactive R-groups like an alkyl or a phenyl group are *network modifiers*. Examples of organotrialkoxysilanes are methyltrimethoxysilane (MTMS) and triethoxyphenylsilane (TEPS). Network modifiers reduce the maximum functionality of the silicon atoms, and therefore, they make the network less rigid and brittle.[143] Precursors with reactive organic groups are able to form an organic as well as an inorganic network. These precursors are *network builders*. Examples are 3-methacryloxypropyltrimethoxysilane (MEMO) and 3-glycidoxypropyltrimethoxysilane (GLYMO). The hydrolysis and condensation of organically functionalized trialkoxysilanes leads to the formation of *polysilsesquioxane materials*. These are high-molecular mass macromolecules and gels with pendant organic groups. An overview of important precursors that are used for the formation of organically modified xerogels is given in Chart 3. It is common practice to copolymerize an organotrialkoxysilane with a tetraalkoxysilane like TEOS or TMOS. This leads to the formation of *polysilsesquioxane−silica copolymers*. The tetraalkoxysilane is used to ensure that there is enough cross-linking in the sol to form a gel, because many organotrialkoxysilanes do not polymerize to form a gel. This is a method to incorporate organic groups in a silica network by covalent bonds. By copolymerization of a tetraalkoxysilane with a suitable organotrialkoxysilane like methyltrimethoxysilane, it is possible to obtain nonporous xerogels. Notice that three or more hydrolyzable groups have to be present in the precursor molecule for the formation of a three-dimensional network. *Organodialkoxysilanes* lead to the formation of linear molecules, the *oligo-* and *polysiloxanes*. *Organomonoalkoxysilanes* can only form dimers or they can react with functional groups in preformed networks. The organomonoalkoxysilanes are typically used for surface modification of inorganic networks. *Bridged polysilsesquioxanes* are a special family of hybrid materials formed by sol−gel processing of monomers that contain two or more trialkoxysilyl groups connected by an organic bridging group. There is also the possibility to carry out the sol−gel net-forming process in the presence of a preformed organic polymer or to perform the polymerization of a monomer during or after the sol−gel process. This leads to the formation of *silica/polymer hybrid materials*. An overview of polysilsesquioxanes doped with lanthanide ions or lanthanide complexes

Chart 3. Precursors Used for the Synthesis of Organically Modified Xerogels

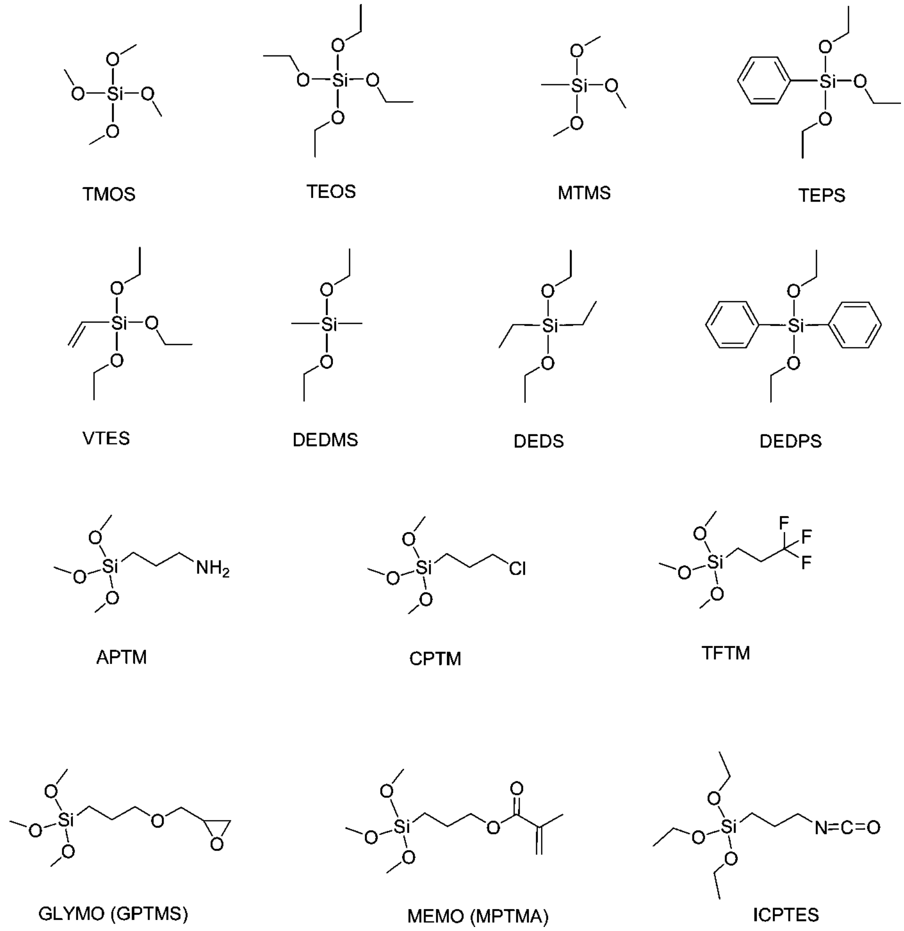

will be given in this section, whereas the bridged polysilsesquioxanes will be discussed in section 3.4 and the silica/polymer hybrids in section 3.5. The specific name *organically modified silicates* (*ormosils*) is often used denote the polysilsesquioxanes.[429−431] I will also use this term for the polysilsesquioxanes described in this section.

The refractive index of the ormosils can be tuned by a proper choice of the precursor molecules. Typically, ormosils are prepared at temperatures below 150 °C. Although they have mechanical properties that are more reminiscent of polymers than of silica glasses, their density is larger than that of polymers. Ormosils have a better processability than silica sol−gel glasses. They can be cast into molds with different shapes, and they can easily be spun to fibers or thin films. Only very few studies have focused on the influence of the type of organosilicon precursor on the luminescence performance of the resulting lanthanide-doped ormosils. However, 3-glycidoxypropyltrimethoxysilane (GPTMS or GLYMO) was found to greatly increase the luminescence output of lanthanide complexes in the hybrid matrix.[432,433] This precursor also increased the fluorescence of Nile Red in ormosils.[434] The introduction of organic groups into the silica-based matrix modifies the polarity of the matrix and its interfaces.[435] A dramatic example of the influence of the ormosil composition on the luminescence properties of lanthanide-doped materials was observed by Iwasaki et al. for Ce^{3+}-doped ormosils.[436] These hybrid materials exhibit broadband luminescence due to allowed f−d transitions in the ultraviolet to blue spectral region. Both the excitation and emission spectra, as well as the luminescence quantum yield were found to be strongly dependent on the composition of the ormosil. Organosilicon compounds with different coordinating groups were tested: 3-aminopropyltrimethoxysilane (APTM), 3-glycidoxypropyltrimethoxysilane (GPTMS or GLYMO), 3-chloropropyltrimethoxysilane (CPTM), or 3,3,3-trifluoropropyltrimethoxysilane (TFTM). The hybrid materials derived from APTM and GTMS were yellow, whereas those prepared from the other functionalized silanes as well as from unfunctionalized silane were colorless. The emission intensity of the hybrids derived from APTM or GTMS were about 100 times lower than that of the hybrid derived from unfunctionalized silanes. Notice that this observation is opposite to what was observed for the f-f transitions of the trivalent lanthanide ions where GTMS (GLYMO) has a luminescence intensity increasing effect. The emission intensity of the materials derived from CPTM or TFTM were comparable to that observed for the hybrid made of unfunctionalized silanes, but the luminescence quantum yield was higher for the materials derived from CPTM or TFTM. The emission maximum of the hybrid material derived from CPTM was strongly shifted to longer wavelengths than that of the other Ce^{3+}-doped hybrids (Figure 17).

Early examples of ormosils doped with lanthanide(III) complexes are provided by the work of Adachi and co-workers.[203,437−440] $Ln(phen)_2Cl_3 \cdot 2H_2O$ and $Ln(bpy)_3Cl_3 \cdot 2H_2O$ (Ln = Eu, Tb) were incorporated in an ormosil matrix prepared by hydrolysis and condensation of TEOS and the organosilicon compounds diethoxydiethylsilane (DEDS), diethoxydimethylsilane (DEDMS), diethoxydiphenylsilane (DEDPS), or 3-(trimethoxysilyl)propyl methacrylate (TMSPM or MEMO). Whereas silica sol−gels incorporating

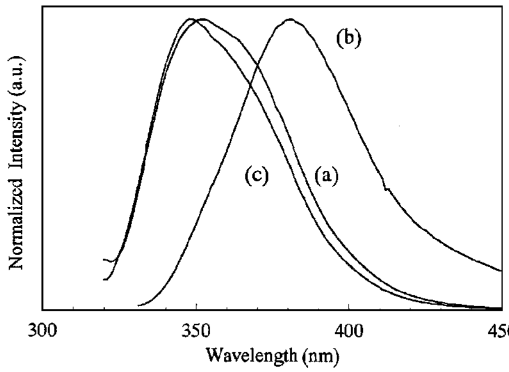

Figure 17. Normalized emission spectra of Ce^{3+}-doped ormosils with different compositions: (a) derived from unfunctionalized organosilanes; (b) derived from CPTM; (c) derived from TFTM. Reprinted with permission from ref 436. Copyright 1998 Kluwer Academic Publishers.

lanthanide complexes often have to dry for months, monolithic samples of ormosils can be prepared in about 2 weeks. A heat treatment (<150 °C) increased the luminescence intensity of the metal complexes due to elimination of water molecules from the hybrid matrix. No water molecules remain coordinated to the lanthanide(III) ion. The europium(III) and terbium(III) complexes in the ormosil matrix showed a more intense luminescence than the same complexes in a silica sol−gel matrix. In fact, the luminescence efficiency of the $Tb(bpy)_3Cl_3$-derived ormosil is 100% of that of the inorganic phosphor $LaPO_4/Ce^{3+},Tb^{3+}$ and the luminescence efficiency of the $Ln(phen)_2Cl_3$ derived ormosil is 80% of that of $Y(P,V)O_4/Eu^{3+}$. Li et al. prepared luminescent ormosils that contained [Eu(tta)$_3$(phen)].[203] The ormosils were obtained by hydrolysis of tetraethoxysilane (TEOS) and triethoxyphenylsilane (TEPS) in a THF−EtOH−H_2O mixed solvent that contained DMF. The emission intensity of the composite material increased after immersion in a dilute ammonia solution. It was argued that part of the europium(III) β-diketonate complex was decomposed in the ormosil, because of protonation of the β-diketonate ligands by the protons provided by the solvents and the acidic silanol groups. Treatment of the *ormosil* with ammonia deprotonated the β-diketone, which again bound the Eu^{3+} ion. When the europium(III)-doped ormosil samples were treated with hexamethyldisilazane (HMDS), the luminescence intensity increased markedly due to the replacement of the hydroxyl groups in the matrix by trimethylsilyl groups (−$OSi(CH_3)_3$). This modification reduced the radiationless deactivation (*multiphonon relaxation*) of the excited state $^5D_0$ of Eu^{3+} by the matrix. Additionally, the ammonia released by the trimethylsilylation by hexamethyldisilazane has the same effect as a treatment with a dilute ammonia solution. The emission intensity increased with increasing content of the organosilicon compound TEPS. It was argued that the hydrophobic phenyl group of TEPS ensures a more homogeneous dispersion of the europium(III) complex in the hybrid matrix. The thermal stability of the [Eu(tta)$_3$(phen)] complex was greatly improved by incorporation in an ormosil matrix. Transparent luminescent films were prepared on quartz plates by dip coating the plates in an ormosil sol derived from TEOS, DEDPS, and $Ln(phen)_2Cl_3$.[441] Ellipsometric measurements showed that each dip in the sol solution deposited a film with a thickness of about 0.1 μm. Dipping was repeated until films with a thickness of 0.4 μm were obtained. The coated quartz plates were used as luminescent solar concentrator panels, and they increased the photovoltaic current of crystalline silicon solar cells by 10−15%.

Just as in the case of the silica sol−gel glasses, lanthanide β-diketonates are very popular dopants for ormosils.[203,442−446] [Eu(btfac)$_3$(H$_2$O)$_2$] was incorporated in a sol−gel matrix that was formed by vinyltriethoxysilane (VTES) as the organosilicon compound.[447] The authors investigated the site symmetry of the europium(III) complex in the hybrid matrix. On the basis of the splitting of the ^7F_J levels, the authors concluded that the site symmetry of Eu^{3+} in the matrix is C_1, C_2, or C_s. Later on, the [Eu(tta)$_3$(bipy)]-containing hybrids were also investigated.[448] The latter authors also doped [Eu(tta)$_3$(tppo)$_2$] in the same type of glass matrix and investigated the temperature dependence of the lifetime of the $^5D_0$ level.[449] The lifetime remained almost constant in the temperature range between 13 and 100 K, but above 100 K, the lifetime decreased with increasing temperature. An extended study of neodymium(III) complexes in ormosils derived from vinyltriethoxysilane revealed that [Nd(tta)$_3$(tppo)$_2$] had the best luminescence performance.[450] Although in many cases, the lanthanide complexes are dissolved in the sol, it is also possible to synthesize the complex *in situ* in the sol or in the gel.[442,451] For this, the lanthanide salt and the ligand are introduced separately in the precursor solution. Because the basicity of the sol is not high enough to deprotonate a β-diketone ligand, the complex is not formed in the gel obtained at room temperature. However, during mild heat treatment, part of the H^+ is removed during vaporization of the residual water molecules and the acidity of the gel decreases to a level sufficient to allow deprotonation of the ligand. The luminescence intensity of an ormosil containing Eu^{3+}, Htta, and tppo was found to increase by a factor of no less than 1400 upon heat treatment for 24 h at 100 °C due to the *in situ* formation of a europium(III) complex.[452] High-resolution spectroscopic studies indicate that the complex that is formed *in situ* in the ormosil is identical to the [Eu(tta)$_3$(tppo)$_2$] complex. Guo et al. incorporated the ternary terbium(III) complex [Tb(tfac)$_3$(phen)] into an ormosil matrix derived from TEOS and 3-glycidoxypropyltrimethoxysilane.[453] The luminescence lifetime of the terbium(III) complex in the hybrid matrix was longer than that of the same complex in a silica matrix or that of the pure [Tb(tfac)$_3$(phen)] complex. [Eu(fod)$_3$(H$_2$O)$_2$] was doped into an inorganic−organic hybrid material, that was formed by hydrolysis of TEOS and *N*-[3-(trimethoxysilyl)propyl]-ethylenediamine.[454] The europium(III) complex was introduced in the hybrid matrix after synthesis of the matrix and stirring an ethanolic solution of the europium(III) complex with the insoluble matrix. From [Eu(tta)$_3$] and [Tb(ssa)] (where H_3ssa is sulfosalicylic acid), europium(III)- and terbium(III)-centered emission could be observed simultaneously.[455] By adjustment of the ratio of the concentration of the metal complexes, the luminescence color could be tuned. Methylated ormosils were obtained by attaching polydimethylsiloxane groups to the silica network.[433,456−458] Methylation is useful to reduce the OH-content of the hybrid matrix. This has a beneficial effect on the photophysical properties of lanthanide ions doped in such a matrix. Polydimethylsiloxane fragments can be introduced in the matrix via the dimethyldiethoxysilane precursor. As mentioned above, the hydrolysis of an organodialkoxysilane like dimethyldiethoxysilane leads to the formation of linear chains. However, network formation is possible by the cocondensation of an organodialkoxysilane with a tetraalkoxysilane. Yuh et al. obtained Er^{3+}-doped hybrid materials with low hydroxyl content based on methylsilsesquioxanes.[459,460] Ormosils of different composition doped with the erbium(III) 8-hydroxyquinolinate complex ErQ_3 were prepared to study the near-infrared luminescence of the well-known ErQ_3 complexes in a sol−gel matrix.[461] Although most of the sensitizers of lanthanide ions in sol−gel materials are organic ligands, it is also possible to use inorganic complexes like polyoxometalates as ligands. The incorporation of lanthanide-containing polyoxometalates in sol−gel derived materials is described in section 6.

Strongly luminescent materials are accessible by incorporating lanthanide complexes in hybrid materials prepared from precursors with amine groups. Ormosils with amino groups are known as *aminosils*.[462,463] These materials were developed as a new type of anhydrous protonic conductors. Stathatos and Lianos observed that the luminescence intensity of a nanocomposite material based on 3-aminopropyltriethoxysilane (APTS) and incorporating Eu^{3+} ions and 2-thenoyltrifluoroacetone (Htta) was very high and that the luminescence quantum yield was 97%.[464] The ATPS gels prepared by solvolysis with a carboxylic acid (e.g., acetic acid) are photoluminescent themselves.[465,466] This luminescence is quenched in the presence of Eu^{3+} ions, due to energy transfer from the ATPS gel to the metal ion. Interestingly, the luminescence performance of the gels strongly depended on the synthetic procedure and more particularly on the order of mixing of the three components ATPS, Eu^{3+}, and Htta. The best luminescent materials were obtained if ATPS was first mixed with Eu^{3+} and Htta was added as the last component. However, if Htta was added to ATPS before Eu^{3+} had been added, the least luminescent material was formed. If Eu^{3+} and Htta are mixed and this mixture is subsequently added to ATPS, a material with an intermediate luminescence performance is obtained. The emission luminance of the best Eu^{3+}-doped ATPS gel was 332 Cd/m^2, which is comparable to the luminance value of 357 Cd/m^2 measured for rhodamine 6G doped into PMMA. On the other hand, the luminance of a silica sol−gel glass doped with $Eu(tta)_3$ was only 148 Cd/m^2. The luminescence decay time of the $^5D_0$ state in the Eu^{3+}-doped ATPS gel was 0.97 ms, which is considerably higher than the decay time of $Eu(tta)_3$ doped into a silica sol−gel glass (0.69 ms). Carlos et al. investigated the local environment of Eu^{3+} in aminosils doped with europium(III) triflate salt, $Eu(CF_3SO_3)_3$, by luminescence spectroscopy.[467] The effect of $Eu(CF_3SO_3)_3$ doping on the nanoscopic structure of aminosils was investigated by small-angle X-ray diffraction.[468]

Trialkoxysilanes with a carbonyl function in the organic side group can facilitate a better dispersion of the lanthanide ions within the hybrid matrix by coordination of the carbonyl oxygen group to the lanthanide ion. The same effect is achieved by incorporation of other donor atoms in the organic side group. A general versatile approach to have an easy access to such precursors is by coupling of a carboxylic acid with 3-aminopropyltri(m)ethoxysilane via an amide bond, as illustrated by Yan and co-workers. The coupling reaction was in general achieved via the acid chloride. The oxygen atom of the amide bonds coordinates with the lanthanide ion. The lanthanide ions (in most studies Eu^{3+} or Tb^{3+}) were introduced as nitrate salts and sometimes 1,10-phenanthroline was added as a coligand. Precursors that have been investigated include those derived from benzoic acid,[469] 4-*tert*-butylbenzoic acid,[470,471] 2-chlorobenzoic acid,[472] *meta*-methylbenzoic acid,[473] *ortho*-acetylsalicylic acid,[474] picolinic acid,[475] nicotinic acid,[475] 2-chloronicotinic acid,[472,476] 5-bromonicotinic acid,[477] 5-hydroxyisophthalic acid,[478] 2-benzoylbenzoic acid,[479] 2-furancarboxylic acid,[480] benzimidazole 5-carboxylic acid,[481] 1,2,4-benzenetricarboxylic acid anhydride,[482] 2-bromophenylacetic acid,[483] decanoic acid,[484] and stearic acid.[484] Several of the precursors with an amide linkage are shown in Chart 4. A variation on this theme is replacement of the amide linkage by a sulfonamide linkage (Figure 18).[485] Other authors used isocyanatopropyltri(m)ethoxysilane which allows coupling of amines via a urea linkage, instead of 3-aminopropyltri(m)ethoxysilane.[486] Isocyanatopropyltri(m)ethoxysilane also reacts with COOH groups[487] or OH groups.[488−490] This silica precursor was used to graft 9-amino acridine to a silica matrix (Figure 19).[491] Different lanthanide(III) nitrate salts were added to the hybrid matrix, and the lanthanide ions were supposed to coordinate to the nitrogen atom of the acridine chromophore. No lanthanide-centered luminescence was detected, but the blue

Chart 4. Precursors with an Amide Linkage Group[a]

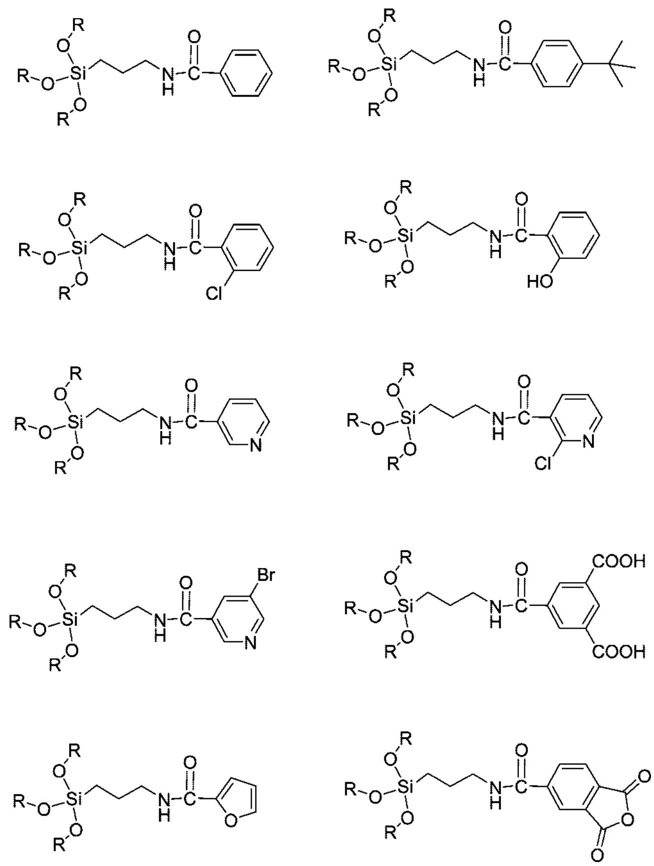

[a] R = CH_3 or C_2H_5.

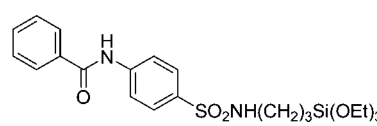

Figure 18. Precursor with a sulfonamide linkage.

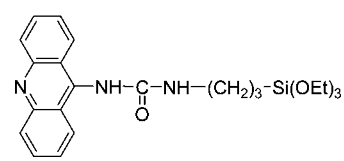

Figure 19. Precursor derived from 9-amino acridine.

luminescence of the acridine group was considerably enhanced by addition of hydrated $Ln(NO_3)_3$ salts. The reason these systems are discussed here and not together with the covalently linked complexes in section 3.6 is that although interaction occurs between the carbonyl bond of an amide function and a lanthanide ion, this interaction is rather weak if these amide bonds are not part of a multidentate chelating ligand like amide derivatives of DTPA or EDTA.

The organic *hydrosilanes*, $HSi(OR)_3$, deserve a special word of attention. The dehydrocondensation of hydrosilanes with silanols is an often used method for the formation of a siloxane linkage. Hydrogen gas is evolved during the reaction

$$\equiv Si-H + HO-Si\equiv \xrightarrow{\text{catalyst}} \equiv Si-O-Si\equiv + H_2 \quad (11)$$

The hydrogen gas released by the cleavage of the Si−H bond of the hydrosilane precursor can be used as an *in situ* reducing reagent. Sanchez and co-workers demonstrated the usefulness of hydrosilanes to generate divalent europium in hybrid materials by chemical reduction of Eu^{3+} to Eu^{2+} during the first steps of the hydrolysis and condensation reactions.[492] The reduction is done at room temperature. Further work showed that this methodology can also be used for the reduction of Ce^{4+} to Ce^{3+} during the synthesis of the hybrid matrix.[493] Typical hybrid materials were prepared by hydrolysis and condensation of a mixture of the organohydrosilanes $HSi(CH_3)(OCH_2CH_3)_2$ and $HSi(OCH_2CH_3)_3$, the alkoxysilane $Si(CH_3)(OCH_2CH_3)_3$, and zirconium(IV) propoxide in the presence of $EuCl_3$ or $(NH_4)_2[Ce(NO_3)_6]$. The Eu^{2+}-doped hybrid materials show at room temperature an intense blue photoluminescence with an emission maximum between 400 and 450 nm. This blue photoluminescence cannot be ascribed to only Eu^{2+}; the blue emission of the matrix also has to be taken into account. The fact that line transitions due to Eu^{3+} could be observed in the luminescence spectrum, besides the broad emission band, is an indication that reduction of Eu^{3+} to Eu^{2+} was not complete and that also some Eu^{3+} was present in the matrix. Interestingly, also transitions starting from the $^5D_1$ state of Eu^{3+} could be detected in these hybrid materials. It was noticed that the relative contribution of Eu^{3+} to the luminescence spectrum increased with time, which shows that the stabilization of the divalent state in the hybrid matrix still needs to be improved. The Ce^{3+}-doped hybrid material exhibited luminescence in the ultraviolet and blue regions, with an emission maximum at 370 nm. At the same time, emission from the host matrix was observed at longer wavelengths between 400 and 550 nm. Contributions to the luminescence spectrum from the host and from the lanthanide ions can be discriminated on the basis of the differences in luminescence kinetics. The luminescence decay times are ~50 ns for Ce^{3+}, <1 μs for Eu^{2+}, and 3−4 μs for the undoped matrix. Eu^{2+}-doped ormosils were prepared by photoreduction of Eu^{3+} in the host matrix by UV irradiation of the fourth harmonic wave light of a Nd:YAG laser (266 nm).[494] Irradiation with a KrCl excimer lamp (222 nm) was found to be less effective. For an efficient reduction of Eu^{3+} to Eu^{2+}, the ormosil needed to be derived from an organosilicon precursor with a terminal chlorine atom, like 3-chloropropyltrimethoxysilane, $(CH_3O)_3$-$Si(CH_2)_3Cl$ (CPTM), or a europium(III) chloride, because the Eu^{2+} ions are generated by the photodecomposition of the bond between Eu and Cl (Cl or $Cl(CH_2)_3$ of CPTM). The highest stability of Eu^{2+} was observed in pore-free materials with a high CTPM/Eu^{3+} ratio. The luminescence spectra of the Eu^{2+}-doped ormosils show a broad band in the blue spectral region, with an emission maximum between 450 and 475 nm.

In general, the organometallic components in organic−inorganic hybrid materials are organosilicon compounds. This can be explained by the fact that the Si−C bonds in the organically modified silanes have an enhanced stability toward hydrolysis in the aqueous solutions used for the sol−gel synthesis. However, the metal−carbon bonds are in most cases not stable enough to survive in the sol−gel precursor solution. It is possible to prepare organic−inorganic hybrid materials by replacing the tetraalkoxysilane precursor with a metal alkoxide, while retaining an organotrialkoxysilane compound. Depending on the type of metal alkoxide used, different types of ormosils are formed: *zirconia ormosils* (with ZrO_2), *titania ormosils* (with TiO_2), *germania ormosils* (with GeO_2), etc. Reisfeld and co-workers developed new hybrid materials on the basis of zirconia ormosils.[315,495] Highly luminescent materials were obtained by doping lanthanide complexes in this matrix.[265,269,496,497] Titania-containing ormosils where prepared from 3-(trimethoxysilyl) propyl methacrylate and tetraisopropyl-orthotitanate complexed with methacrylic acid.[498] Nassar et al. made titania−silica hybrids from tetraethylorthotitanate 3-aminopropyltriethoxysilane and deposited them on borosilicate glass by dip-coating.[499] $[Eu(fod)_3]$ complexes were incorporated in a titania-containing ormosil derived from titanium tetrabutoxide, TEOS, and *n*-[3-(trimethoxysilyl)propyl] ethylenediamine.[500]

Zirconia and titania are useful to increase the refractive index of ormosils. Zirconia has the additional advantage of a higher chemical stability and a low phonon energy. Germania ormosils were prepared by hydrolysis and condensation of germanium(IV) isopropoxide and γ-glycidoxypropyltrimethoxysilane.[501] Neodymium(III) ions were introduced in the gel as $Nd(NO_3)_3$. Europium(III)-doped polyphosphate−siloxane hybrids were obtained by reaction between sodium polyphosphate and 3-amino-propyltriethoxysilane in the presence of $EuCl_3$.[502]

Sanchez and co-workers prepared different *polydimethylsilane−metal oxide hybrid materials* doped with Eu^{3+}.[458] These hybrid matrices can be described as materials in which the linear polydimethylsilane chains are cross-linked by metal oxo domains M_xO_y (where M = Al(III), Ge(IV), Sn(IV), Ti(IV), Zr(IV), Ta(V), or Nb(V)) through covalent Si−O−M linkages.[503,504] The materials can also be considered as Eu^{3+}-doped metal oxide nanoparticles dispersed in an organosilicon matrix. Eu^{3+} was introduced in the form of the $EuCl_3$ salt and encapsulated within the metal oxo domains. The OH content of the materials can be reduced by a heat treatment at temperatures lower than the decomposition temperature. The performance of the hybrid materials very much depended on the constituting metal of the metal oxo domains. Also the local environment of Eu^{3+} depended on the metal.[505] The best results were obtained for the polydimethylsilane−metal oxide hybrids derived from titanium(IV), niobium(V), and especially tantalum(V), because of the small size and good dispersion of the nanodomains in the hybrid matrix. In addition, the resulting hybrid materials were found to be essentially free of OH groups. Aggregation of Eu^{3+} ions and poor luminescence properties were observed for the hybrid matrices derived from germanium(IV). The hybrids derived from aluminum(III), zirco-

Scheme 2. Reaction between 3-Isocyanatopropyltriethoxysilane (ICPTES) and a Jeffamine Polyetheramine Giving a Ureapropyltriethoxysilane, Which Can Be Used as a Precursor for the Synthesis of a Diureasil

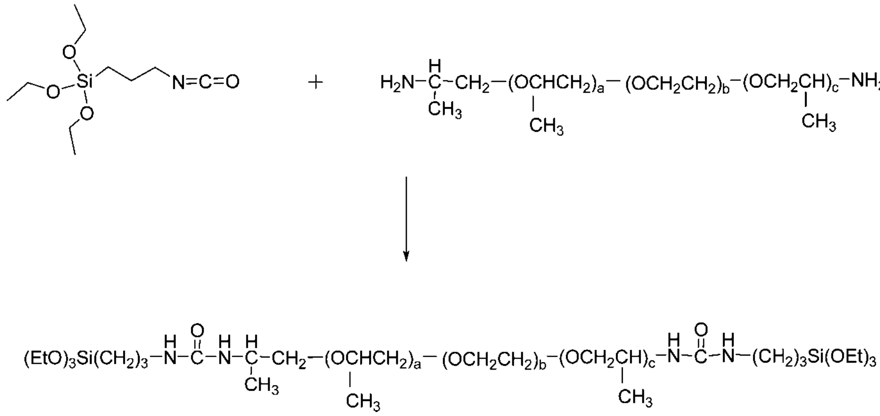

nium(IV), and tin(IV) provide a good dispersion of the Eu^{3+} ions, but their hydrophilic character resulted in a high concentration of OH groups and thus a strong quenching of the luminescence. Koslova et al. investigated thin films of luminescent siloxane−oxide hybrid matrices doped with Nd^{3+}, Sm^{3+}, Dy^{3+}, Er^{3+}, and Tm^{3+}.[506] After hydrolysis, diethoxymethylsilane (DEMS) was condensed with a mixed metallic alkoxide, prepared by reaction between zirconium(IV) propoxide and a lanthanide(III) alkoxide. The oxo domains consisted of mixed zirconium(IV)−lanthanide(III) oxo species. The authors used the reactive methyl-bearing hydridosilane precursor to obtain hybrid materials with a low hydroxyl content without the need for a thermal treatment. Similar materials were prepared starting from lanthanide chlorides, $LnCl_3$, as lanthanide precursors.[507] The luminescence decay time of Nd^{3+} could drastically be changed by variation of the concentration of Nd^{3+} ions and by playing with the experimental parameters for sol−gel processing and subsequent heat treatment.[508,509] The luminescence decay time decreased with increasing concentrations of neodymium for glasses prepared under the same experimental conditions: from 160 μs for a sample containing 0.4×10^{20} Nd^{3+} ions cm^{-3} to 200 ns for a sample containing 4×10^{21} Nd^{3+} ions cm^{-3}. The $^4F_{3/2} \rightarrow {}^4I_{11/2}$ transition was quite broad with a fwhm of about 40 nm. This inhomogeneous broadening is an indication of a broad distribution of different sites for the lanthanide ion. The luminescence became weaker at high neodymium concentrations. At high neodymium concentrations, Nd^{3+}−Nd^{3+} interactions are more likely (clustering). Moreover, there is a greater chance that a Nd^{3+} ion will be on the surface of the oxo clusters and more exposed to the remaining hydroxyl groups close to the surface. In hybrid samples codoped with the rhodamine 6G laser dye and Nd^{3+}, the rhodamine 6G emission spectra showed several dips at wavelengths corresponding to f−f transitions of the Nd^{3+} ion.[508] This phenomenon is known as the *inner filter effect*.[510] The inner filter effect is observed in luminescence spectra whenever a second substance is present that has absorption bands that overlap the luminescence bands. The result is a diminution of the luminescence intensity at the wavelengths of overlap. Near-infrared luminescence of Nd^{3+} could be observed upon excitation of the rhodamine 6G−Nd^{3+} hybrid with an argon ion laser at 488 nm in the rhodamine 6G absorption band.[508] In the absence of the dye, no Nd^{3+}-centered luminescence could be detected upon excitation at that wavelength. These experimental observations indicate that the excitation energy can be transferred from rhodamine 6G to the Nd^{3+} ion.

3.4. Bridged Polysilsesquioxanes

As mentioned in the previous section, *bridged polysilsesquioxanes* are hybrid materials formed by sol−gel processing of monomers that contain two or more trialkoxysilyl groups connected by an organic bridging group.[511−515] The bridging group can selected from a wide variety of organic groups. The structure of the hybrid material is determined by the length and the rigidity of the spacer. In contrast to pendant organic groups, the bridging groups increase the network connectivity. Aryl bridges form rigid molecular spacers. The resulting xerogels are amorphous and brittle. The properties of xerogels with alkylene bridges depend on the length of the spacer, but the flexible chains lead in general to xerogels with less stiffness and with a lower porosity. However, bridged polysilsesquioxanes with aryl or alkylene bridges have not been explored as a host matrix for luminescent lanthanide complexes yet. On the other hand, bridged polysilsesquioxanes with polyethylene bridges have been studied in detail as host matrices for lanthanide complexes. The best known examples of these materials are the *diureasils* and the *diurethanesils*.

Hybrid silica−polyether nanocomposite materials can be prepared by a sol−gel process using a hydrolyzable precursor composed of two trialkoxysilane groups connected by polyether chains of various chain lengths. In *diureasils* the trialkoxysilane groups are linked through urea (−NHC(═O)NH−) groups, whereas in *diurethanesils*, the trialkoxysilane groups are linked through urethane (−NHC(═O)O−) groups.[516,517] The polyether segments are in general poly(oxyethylene) groups, although also other segments like poly(oxypropylene) can be used. The precursor is obtained from the reaction of the isocyanate group of 3-isocyanatopropyltriethoxysilane (ICPTES) with the terminal amine groups of α,ω-diamine-poly(oxyethylene) (for diureasils) (Scheme 2) or with the terminal hydroxyl groups of poly(ethylene glycol) (for diurethanesils). Useful diamines are the commercially available Jeffamine polyether amines, which are produced by Huntsman. The Jeffamine ED series are polyether diamines which based on a predominantly poly(ethylene glycol) backbone. The diureasils and diurethanesils can be obtained as highly transparent, amorphous monoliths or thin films. These materials are gel-like, elastic, slightly hygroscopic, and thermally stable up to 200 °C. Because of the presence of the polyether groups, they can solubilize considerable quantities of inorganic salts.

Diureasils and diurethanesils can be considered as nanocomposite materials, consisting of silica nanoparticles dispersed in the organic phase provided by polyether chains. Small-angle X-ray scattering (SAXS) studies on diureasils provide evidence for a microphase separation between the silicic and polymeric domains.[518] The undoped gels are broadband photoluminescent materials.[519,520] They display a bright white emission at room temperature excitation at 365 nm. In the broadband emission spectrum (2.0−4.1 eV), a blue band at ~2.6 eV and a purplish-blue one at ~2.8−3.0 eV could clearly be distinguished by time-resolved spectroscopy.[518] At delay times longer than 10 ms, only the longer-lived blue luminescence is observed. The purplish-blue band is not present in the emission spectra for excitation wavelengths longer than 420 nm. This means that the emission is red-shifted when the excitation energy is decreased (excitation light shifted to longer wavelengths). The luminescence is the result of delocalized electron−hole recombination processes on the surface of the silica nanoparticles. It is observed that larger clusters emit at longer wavelength than smaller clusters. Another contribution to the emission spectrum originates in the NH groups of the urea or urethane linkages. Short polyether chains give a higher luminescence intensity, whereas the luminescence intensity is decreased in samples with long polyether chains due to a dilution effect. The luminescence can be enhanced by addition of large divalent ions (e.g., Cd^{2+}) or trivalent ions (rare-earth ions) to the gel matrix. These materials are quite stable against photodegradation. The first studies of lanthanide-doped diureasils were about diureasils doped with europium(III) triflate, $Eu(CF_3SO_3)_3$.[521] The hybrid material exhibited an ionic conductivity of $10^{-5}\ \Omega^{-1}\ cm^{-1}$ at 30 °C. Photoluminescence spectra showed the characteristic emission lines of the Eu^{3+} ion. Temperature-dependent luminescence measurement between 10 and 300 K revealed hardly any variation in the crystal-field fine structure, but the luminescence intensity decreased by an order of magnitude between 10 and 300 K. No luminescence from the $^5D_1$ state could be detected, not even at 10 K. In follow-up studies, the $Eu(CF_3SO_3)_3$-doped diureasils and diurethanesils were investigated in detail.[467,522−526] At low doping concentrations, the cations are coordinated to the carbonyl oxygens of the urea linkages rather than to the ether oxygens of the polyether chains. At increasing salt concentrations, the carbonyl coordination sites become saturated, and consequently, the ether oxygens start to coordinate to the cation.[523] The emission spectrum of $Eu(CF_3SO_3)_3$-doped diureasils consists of a broad green-blue band of the hybrid matrix and a series of narrow lines in the yellow-red region due to the f−f transitions of the Eu^{3+} ion.[525] To the eye, the luminescence appears white. The emission colors can be tuned across the CIE (*x*,*y*) chromaticity diagram by changing the excitation wavelength or the amount of europium(III) salt incorporated in the hybrid matrix.[527] This color tuning by changing excitation wavelength and europium(III) concentration was also observed for related types of hybrid materials.[528] Variation of the polymer chain length also allows tuning of the emission color.[529,530] Lanthanide salts other than $Eu(CF_3SO_3)_3$ that have been incorporated in diureasils are $Eu(ClO_4)_3$,[531] $EuCl_3$,[532] $Nd(CF_3SO_3)_3$,[533,534] and $Tb(NO_3)_3$.[535] 2,2′-Bipyridine acts as a sensitizer for Tb^{3+} luminescence in silica−PEO hybrid materials (Figure 20).[535] Bekiari et al. showed that the blue emission of the diureasil was strongly enhanced in the presence of Tb^{3+} ions.[535] Highly luminescent diureasils could be obtained by doping lanthanide β-diketonate complexes into the hybrid matrix.[536−542] Thin films

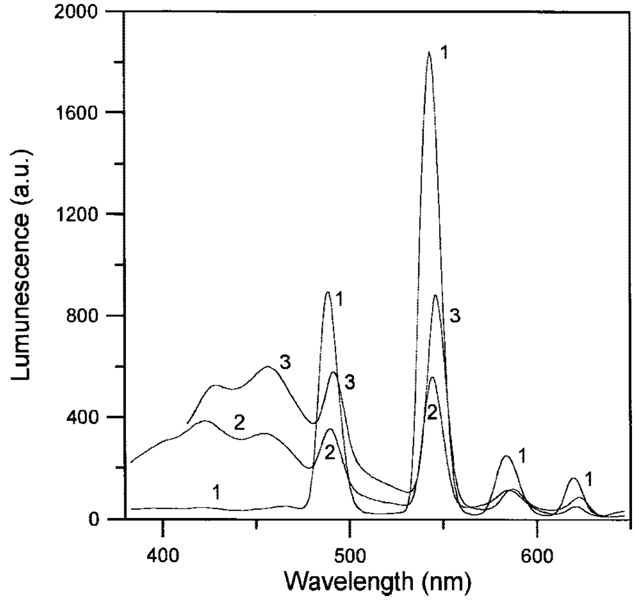

Figure 20. Luminescence spectra of (1) Tb^{3+} and 2,2′-bipyridine adsorbed by a silica−PEO hybrid gel from ethanolic solution (λ_{exc} = 318 nm), (2) the same sample upon excitation at 365 nm, and (3) a similar sample without 2,2′-bipyridine (λ_{exc} = 365 nm). Reprinted with permission from ref 535. Copyright 1999 Elsevier.

of diureasils doped with [Eu(tta)$_3$(bipy)] exhibited a very strong red photoluminescence comparable to that of the laser dye rhodamine B.[540] Energy transfer to the Eu^{3+} ion occurs not only via the coordinated ligands but also via the diureasil matrix. An interesting experimental result is the observation of near-infrared luminescence of the diureasils doped with a thulium(III) β-diketonate complex.[536]

Monourethanesils are structurally related to diurethanesils. They contain methyl end-capped oligopoly(oxyethylene) chains grafted to the silica backbone by a urethane linkage. These materials are prepared by a sol−gel process from a precursor obtained by reaction between 3-isocyanatopropyltriethoxysilane and poly(ethylene glycol) methyl ether. Because of the reduction of the number of cross-links per polymer segment, the monourethanesils have a simpler structure than the diurethanesils. De Zea Bermudez et al. studied the local Eu^{3+} coordination of monourethanesils doped with $Eu(CF_3SO_3)_3$.[543−546] Samples with different numbers of (OCH_2CH_2) moieties (*n*) per Eu^{3+} were investigated. The cations coordinated exclusively to the urethane carbonyl oxygen atoms in samples with $400 \geq n \geq 50$. At $n = 30$, the ether oxygen atoms started to coordinate to the Eu^{3+} ion. These results are similar to what was observed for the diureasils, where coordination to the ether oxygen atoms also occurred for high salt concentrations only.[523] For $n < 30$, a breakdown of the hydrogen-bonded aggregates in the matrix took place due to cation entrapment. In samples with $n = 10$, crystalline phases were detected and direct cation−anion coordination became dominant. Silver nanoparticles were found to enhance the luminescence of [Eu(tta)$_3$(phen)] in diureasil hybrid materials.[547] The luminescence intensity increased up to a silver particle concentration of 9.5 nM, but started to decrease at higher concentrations.

Many variations on the theme of diurethane cross-linked ormosils are possible. The lengths of the poly(oxyethylene) fragments can be varied, poly(oxyethylene) segments of different lengths can be built in the same hybrid matrix,[548] and poly(oxyethylene) segments can be replaced by other

Scheme 3. Reaction between 3-Aminopropyltriethoxysilane and Isocyanatopropyltriethoxysilane

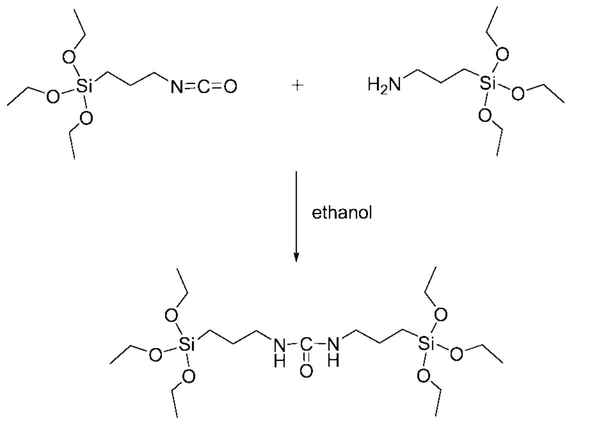

Scheme 4. Reaction between 3-Aminopropyltriethoxysilane and Sebacoyl Chloride

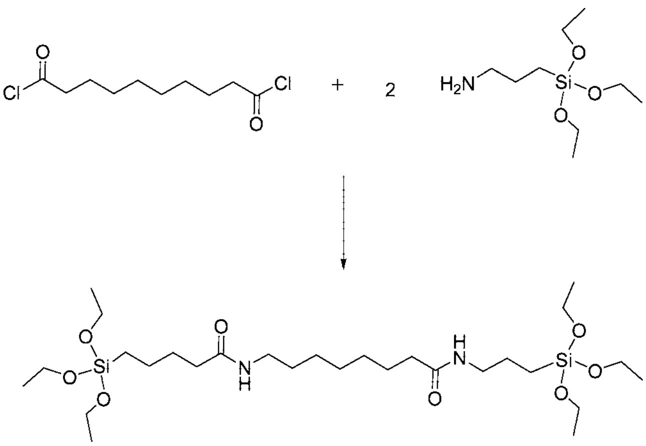

segments like poly(oxypropylene)[520] or poly(ε-caprolactone).[549] Yan and Wang prepared precursors by reaction of 3-(triethoxysilyl)propy isocyanate with amine-containing silanes like *N*-2-aminoethyl-3-aminopropyltriethoxysilane, $H_2N(CH_2)_2HN(CH_2)_3Si(OC_2H_5)_3$ (AEAPES).[550] A very short linkage between the two trialkoxysilane groups was obtained by reaction of 3-aminopropyltriethoxysilane and isocyanatopropyltriethoxysilane (Scheme 3).[551] The luminescence properties of Eu^{3+} and Tb^{3+} in a urethanesil derived from *p-tert*-butylcalix[4]arene have recently been reported.[552]

Diamidosils have amide (−NHC(=O)−) linkage groups.[553] They do not have polyether segments, but only alkyl segments. These hybrid materials are prepared by hydrolysis and condensation of a diamidopropyltriethoxysilane precursor. The precursor can be synthesized by reaction between 3-aminopropyltriethoxysilane and the acid chloride of an α,ω-dicarboxylic acid, like sebacoyl chloride (Scheme 4). Undoped diamidosils show less intense photoluminescence than undoped diureasils or diurethanesils. The spectroscopic properties of $Eu(CF_3SO_3)_3$ dissolved in diamidosils have been investigated.[554]

3.5. Silica/Polymer Nanocomposites

Organic−inorganic polymer associations can be obtained by polymerization of a monomer like methyl methacrylate in the sol. An organosilicon compound containing a vinyl group like vinyltrimethoxysilane or 3-(trimethoxysilyl)propyl methacrylate (MPTMA) can be present in the precursor solution besides the tetraalkoxysilane.[555] Polymerization can be done by photochemical or by radicalar initiation. Li et al. made a composite material by hydrolysis of tetraethoxysilane and vinyltrimethoxysilane, and they polymerized methyl methacrylate in the sol to PMMA with a radical reaction, with benzoyl peroxide as the initiator.[556] The composite silicate−PMMA matrix was doped with [Eu(tta)$_3$(phen)]. The authors chose this matrix because the refractive index of PMMA ($n = 1.4920$) is close to that of SiO_2 glass ($n = 1.4589$), so light scattering could be reduced. A related study describes results for [Eu(phen)$_2$Cl$_3$] doped in the same ormosil matrix.[557] Yan doped [Tb(acac)$_3$(phen)] in a SiO_2/PMMA hybrid matrix.[558] Yan and You incorporated [Tb(acac)$_3$(dam)] into a hybrid SiO_2/PEMA matrix, where acac = acetylacetonate, dam = diantipyrylmethane, and PEMA = poly(ethyl methacrylate).[559] The emission intensity increased with increasing Tb^{3+} concentration, and no evidence for concentration quenching was observed. This is in contrast to the terbium(III) complex in the pure PEMA polymer matrix, where the luminescence intensity reached a maximum for a Tb^{3+} content of 1%. This difference was attributed to the fact that the terbium(III) complex can be better dispersed in the hybrid matrix than in the PEMA polymer. The concentration effects on the luminescence of an ormosil made of TEOS, 3-glycidoxypropyltrimethoxysilane, and methyl methacrylate doped with [Tb(ssa)] (H_3ssa = sulfosalicylic acid) were investigated.[560] No concentration quenching was observed in the concentration range between 0.2 and 2 mol % complex. Heat treatment of the samples between 150 and 200 °C resulted in a rapid decrease of the luminescence intensity due to thermal decomposition of the sample. In contrast, the complexes showed a high photostability. A limited thermal stability of the lanthanide complexes in the ormosils was also observed for β-diketonate complexes.[442] Qian and Wang prepared *in situ* a [Eu(tta)$_3$(tppo)$_2$] complex in an ormosil matrix made of a mixture of TEOS, 3-glycidoxypropyltrimethoxysilane, and methyl methacrylate (with 0.4 wt % benzoyl peroxide).[561] A solution of Htta, tppo, and $EuCl_3$ in ethanol (3:2:1 molar ratio) was added to the starting solution for sol−gel synthesis. The precursor solution became a wet gel after a few days of gelation at 40 °C. A transparent monolithic sample was obtained after a prolonged drying period. The [Eu(tta)$_3$(tppo)$_2$] complex was formed in the sol−gel matrix by heat treatment at 100 °C for 24 h. The intensity of the $^5D_0 \rightarrow {}^7F_2$ transition in the heat-treated sample was a factor of about 1400 higher than in the sample before heat treatment! The β-diketonate complex had to be prepared *in situ* because it was not stable under the conditions at which the sol−gel matrix was synthesized (pH = 2). The precursor 3-(trimethoxysilyl) propyl methacrylate was used as a photopolymerizable component.[562] Xu et al. prepared optical waveguides from erbium-doped ormosils synthesized from 3-(trimethoxysilyl) propylmethacrylate, tetraethylorthosilicate, zirconium(IV) propoxide, and methacrylic acid.[563] Zirconia was added to increase the refractive index to 1.48−1.50. The PMMA-containing hybrid materials described in this paragraph have to be distinguished from the class I hybrid materials that are formed by dissolving a polymer in the sol−gel precursor and where no polymerization in the sol takes place.[564,565]

3.6. Covalently Bonded Complexes

A fruitful approach to avoid clustering of lanthanide ions in a hybrid matrix is grafting the lanthanide complex via a covalent bond to the backbone of the matrix. In general this

Scheme 5. Reaction between 3-Aminopropyltriethoxysilane and 2,6-Pyridinedicarbonyl Dichloride and Similar Pyridine Derivatives

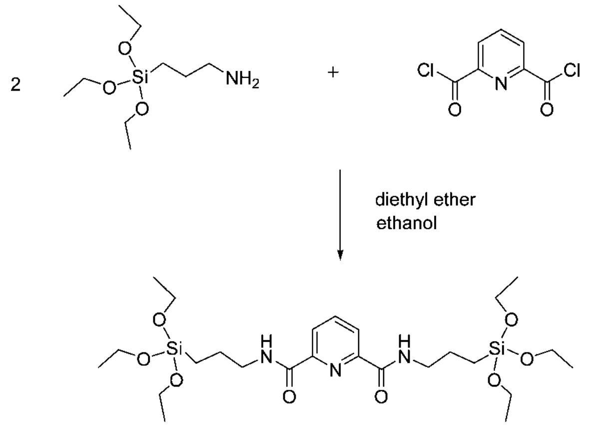

is achieved via a hydrolyzable trialkoxysilyl derivative of a polydentate ligand that can coordinate to the lanthanide ion, although linking to the silica matrix can also be achieved via trialkoxysilyl derivatives of strongly binding monodentate ligands like phosphine oxides. In other cases, more than one trialkoxysilyl group is attached to the chelating ligand. This type of hybrid material can be considered a class II hybrid material according to the classification of Sanchez.[396,397] The covalent bonding of lanthanide complexes to the hybrid matrix also reduces the risk of leaching the complex out from the matrix. Leaching is often observed for lanthanide complexes impregnated in porous hybrid matrices, and this is of course very disadvantageous for the luminescence properties of the hybrid materials. Additional advantages of covalent attachment of lanthanide complexes to the matrix are that in general higher doping concentrations can be reached and that the luminescent hybrid materials have a better homogeneity. The design of new luminescent hybrid systems based on covalently bonded lanthanide complexes is at the present a very active research field. Here in this section, we review the research on lanthanide complexes that are covalently coupled to the more conventional sol−gel-derived silica hybrid materials. In section 4.2, lanthanide complexes covalently grafted to mesoporous silicates will be discussed.

Pioneering work in this field have been done by Franville and co-workers, who prepared europium(III)-containing hybrid materials based on derivatives of pyridine-2,6-dicarboxylic acid (dipicolinic acid).[566−568] A typical ligand was prepared by reaction between 3-aminopropyltriethoxysilane and 2,6-pyridinedicarbonyl dichloride (Scheme 5). Different types of ligands were obtained by attaching phenyl groups or other substituents on the amide nitrogens or on the pyridine ring (Chart 5). The europium(III)-doped hybrid materials were obtained by hydrolysis and condensation of the functionalized dipicolinate ligands in ethanol. The Eu^{3+} ion was introduced in the sol solution as $Eu(NO_3)_3\cdot 6H_2O$, and the Eu^{3+}/ligand ratio was 1/3. Only in one study, TEOS was additionally added to the precursor solution.[566] These materials can be compared with the bridged polysilsesquioxanes described in section 3.4. A schematic representation of such a hybrid material is shown in Figure 21. The samples could be obtained as monoliths but were ground for luminescence studies. It was found that the europium(III) complexes in the silica hybrid matrix had a much higher thermal stability than the complex with the organic part alone.

Chart 5. Hydrolyzable Precursors Derived from Pyridine-2,6-dicarboxylic Acid (Dipicolinic Acid)

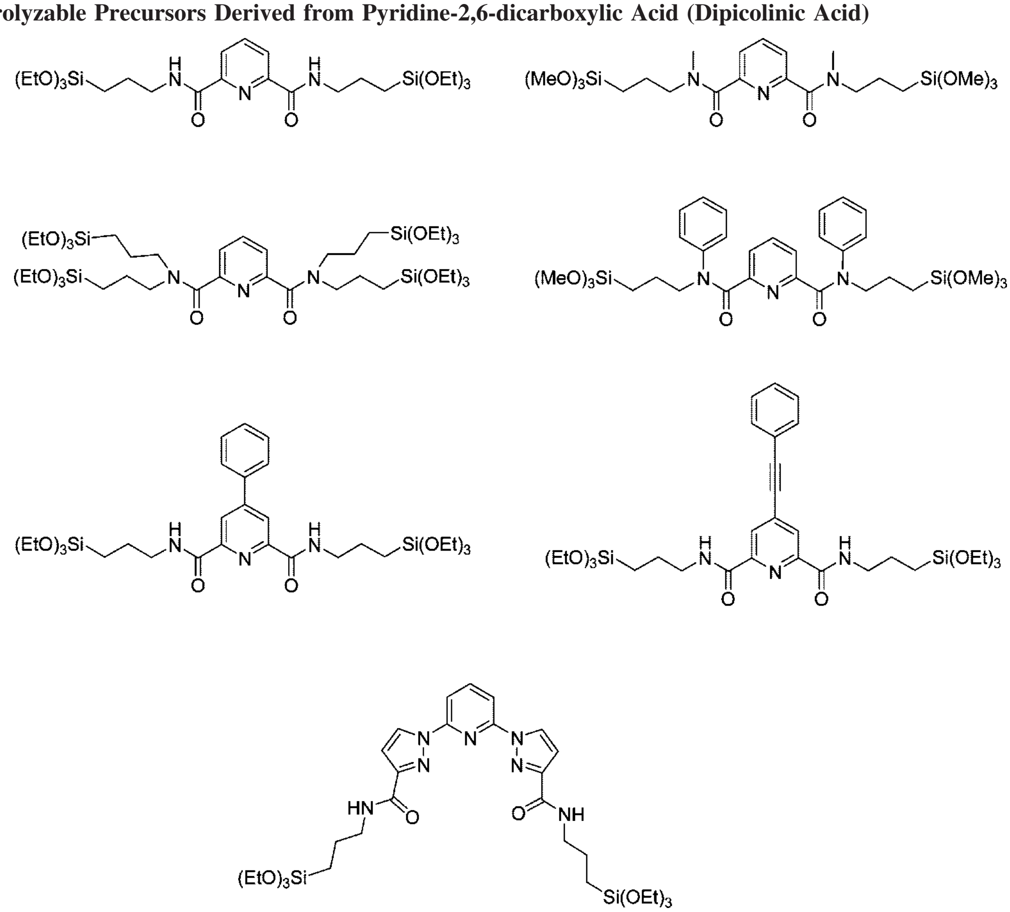

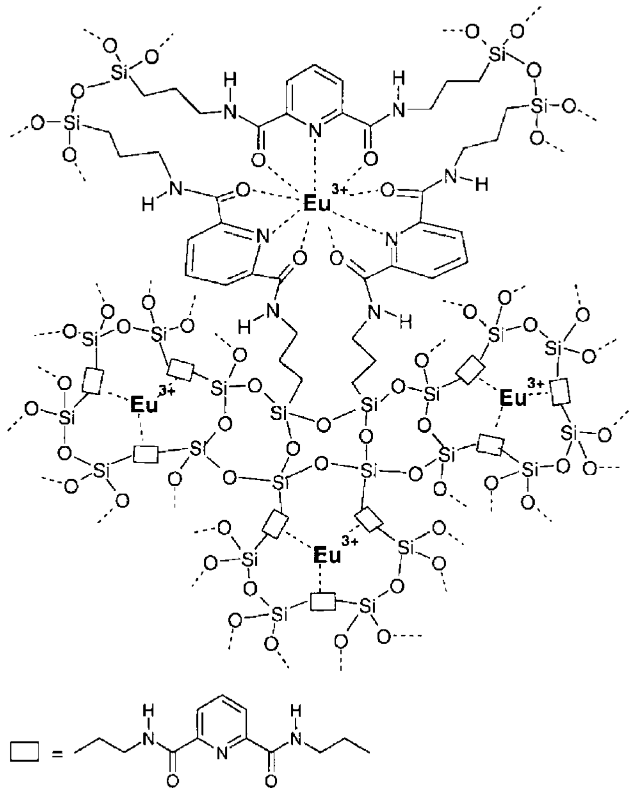

Figure 21. Schematic representation of a europium(III)-containing hybrid material derived from functionalized dipicolinic acid ligands. Reproduced with permission from ref 567. Copyright 2000 American Chemical Society.

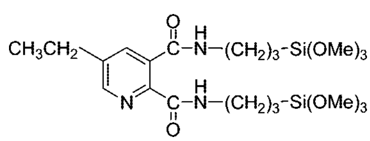

Figure 22. Triethoxysilyl derivative of 5-ethylpyridine-2,3-carboxylic acid.[569]

For instance, a europium(III) complex that started to decompose at 150 °C did not decompose below 300 °C after incorporation in the hybrid matrix. The authors could detect only minor differences between the luminescence properties of the europium(III)-containing hybrid materials and the corresponding europium(III) complexes without trialkoxysilyl groups. The most pronounced effect of the silica matrix was a broadening of the emission peaks, whereas the relative intensities of the emission bands and the luminescence decay times were relatively unaffected. The luminescence decay times were slightly lower in the hybrid materials than in the organic complexes, and this was attributed to the residual silanol groups in the hybrid matrix. These silanol groups do not necessarily interact directly with the Eu^{3+} ion, but their presence in the second coordination sphere also influences the luminescence properties, for instance, via hydrogen bonding with the chelating groups of the ligands. However, the total luminescence intensities of the hybrid matrices were found to be strongly dependent on the modifications of the parent dipicolinic acid ligand. The substituents also shifted the maxima in the excitation spectra to longer wavelengths, making a more efficient excitation with long-wave UV radiation possible. Although 5-ethylpyridine-2,3-carboxylic acid gives a triethoxysilyl derivative that is very similar to that of pyridine-2,6-dicarboxylic acid (Figure 22), the resulting lanthanide-containing hybrid materials are very different

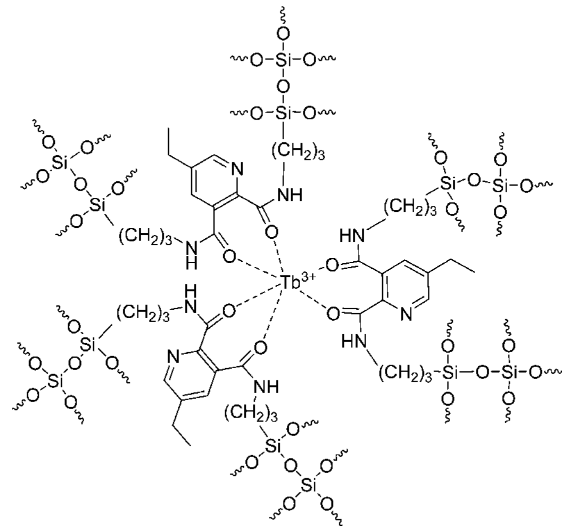

Figure 23. Terbium(III)-containing hybrid material derived from 5-ethylpyridine-2,3-carboxylic acid.[569]

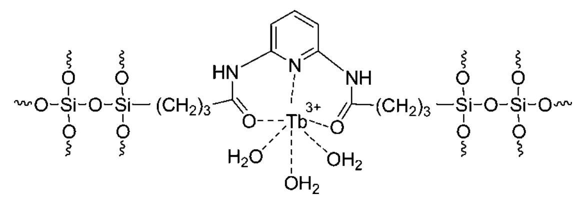

Figure 24. Terbium(III)-containing hybrid material derived from 2,6-bis(propyltriethoxysilylureylene)pyridine.[570]

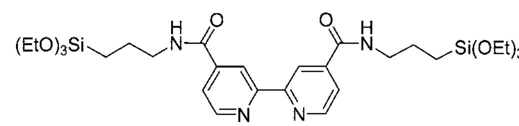

Figure 25. Hydrolyzable derivative of 2,2′-bipyridine.

because the lanthanide ion cannot coordinate to the nitrogen atom of the pyridine ring in 5-ethylpyridine-2,3-carboxylic acid (Figure 23). Nevertheless, the terbium(III)-containing hybrid materials showed a good luminescence performance.[569] Zhang and co-workers prepared 2,6-bis(propyltriethoxysilylureylene)pyridine by reaction of isocyanatopropyltriethoxysilane with 2,6-diaminopyridine.[570] Hydrolysis and condensation of the ligand in the presence of $TbCl_3$ in DMF followed. Transparent luminescent films were obtained by dip-coating of the sol on a quartz substrate. The authors proposed that the Tb^{3+} ion is coordinated by one functionalized pyridine ligand, acting as a tridentate ligand (N atom of pyridine ring and two O atoms of carbonyl groups) and by three water molecules (Figure 24). Structurally related to hybrid materials derived from pyrdinecarboxylic acids are those derived from triazine functionalized with hydrolyzable silylated groups via urea bridges.[571]

Different polypyridine ligands have been used for grafting lanthanide complexes to a silica hybrid matrix. Zhang and co-workers modified 2,2′-bipyridine to obtain a hydrolyzable derivative (Figure 25).[572] They transformed 2,2′-bipyridine-4,4′-dicarboxylic acid first to the corresponding acid chloride, followed by reaction with 3-aminopropyltriethoxysilane. Hybrid materials with Eu^{3+} and Tb^{3+} were obtained by hydrolysis of the ligand in the presence of hydrated $EuCl_3$ or $TbCl_3$. Each lanthanide ion was coordinated by two 2,2′-bipyridine ligands and four water molecules (Figure 26). The chloride ions did not bind to the lanthanide ion. Silylated 2,2′-bipyridine derivatives were also grafted to silica nano-

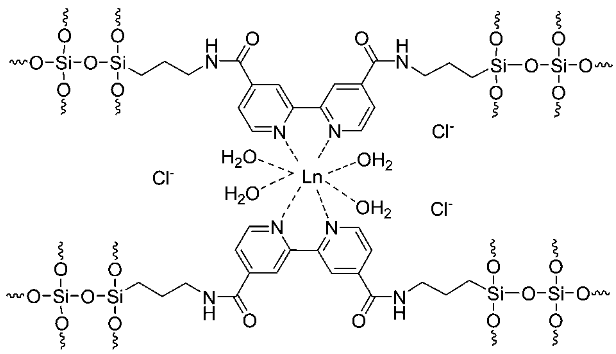

Figure 26. Lanthanide-containing hybrid material with covalently bonded 2,2′-bipyridine ligands.[572]

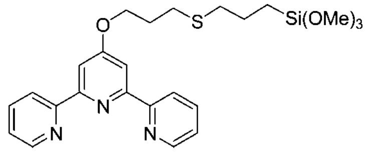

Figure 27. Hydrolyzable derivative of terpyridine.

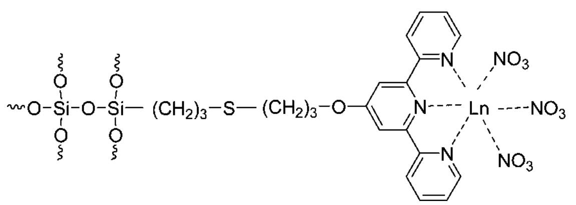

Figure 28. $Ln(NO_3)_3$ complex of a covalently bonded terpyridine ligand.[574]

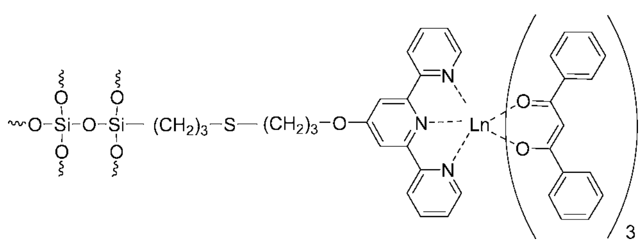

Figure 29. $Ln(dbm)_3$ complex (Ln = Nd, Er) of a covalently bonded terpyridine ligand.[575]

particles.[573] Reaction with $Eu(tmhd)_3$ led to the formation of luminescent hybrids. Tong et al. used a modified terpyridine ligand, which was prepared by the thiol−ene photopolymerization between γ-mercaptopropyltrimethoxysilane and 4′-allyloxy-2,2′:6′,2″-terpyridine (Figure 27).[574] Hybrid materials incorporating Eu^{3+} and Tb^{3+} were made (Figure 28). The lanthanide ion was coordinated to one terpyridine ligand and to three nitrate groups. To observe near-infrared luminescence in the corresponding Nd^{3+} and Er^{3+} complexes, dibenzoylmethane had been added as a coligand to exclude water molecules from the first coordination sphere of the lanthanide ion (Figure 29).[575]

Kloster and Watton described the synthesis of the hydrolyzable 1,10-phenanthroline derivative 5-(*N*,*N*-bis-3-(triethoxysilyl)propylureyl-1,10-phenanthroline (abbreviated to phen-Si) (Figure 30), which they used to immobilize iron(II) on a silica matrix.[576,577] In a seminal paper, Li et al. used this ligand to prepare europium(III)-doped hybrids, in which the Eu^{3+} ion was coordinated by two 1,10-phenanthroline ligands and two water molecules (Figure 31).[578] The europium(III) complex was thus linked to the silica matrix via two attachment points. The resulting hybrid material showed a stronger luminescence than a hybrid material prepared by

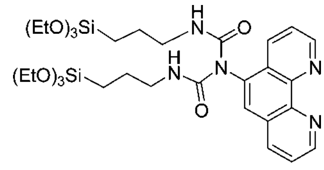

Figure 30. 5-(*N*,*N*-Bis-3-(triethoxysilyl)propylureyl-1,10-phenanthroline (Phen-Si).

simply mixing 5-amino-1,10-phenanthroline, TEOS, and hydrated $EuCl_3$, although the luminescence intensity was not extremely high due to the coordinated water molecules. Thermal treatment of dip-coated thin films to temperatures up to 200 °C could increase the luminescence intensity, but treatment at higher temperatures caused a rapid decrease in intensity, probably due to thermal decomposition of the europium(III) complex.[579] Also the corresponding hybrid materials of terbium(III) have been prepared.[580] Because $[Eu(tta)_3(phen)]$ is a europium(III) complex with excellent luminescence properties, Binnemans and co-workers decided to covalently attach this complex to a silica hybrid matrix via the functionalized 1,10-phenantroline, phen-Si (Figure 32).[581] The phen-Si ligand, tetramethoxysilane (TMOS), and diethoxydimethylsilane (DEDMS) were hydrolyzed and condensed at a neutral pH to a sol−gel glass. By reaction of tris(2-thenoyltrifluoroacetonato) europium(III) dihydrate with the hybrid matrix containing the pendant 1,10-phenanthroline group, the final luminescent hybrid matrix with grafted $[Eu(tta)_3(phen)]$ complexes was obtained. The presence of the 2-thenoyltrifluoroacetonate ligands resulted in much higher luminescence intensities due to the exclusion of water molecules from the first coordination sphere of Eu^{3+} and the enhanced antenna effect of the 2-thenoyltrifluoroacetonate ligands. The covalent attachment of the $[Eu(tta)_3(phen)]$ complex to a silica matrix had only limited influence on its photophysical properties. It should be noted that in this type of hybrid material only one linking point between the lanthanide complex and the silica matrix exists. In a follow-up study, other $[Ln(tta)_3(phen)]$ complexes (Ln = Nd, Sm, Tb, Er, Yb) were incorporated in this matrix. This allowed observation of near-infrared emission for the complexes containing Nd^{3+}, Sm^{3+}, Er^{3+}, and Yb^{3+}.[582] Sun et al. prepared similar near-infrared-emitting hybrid materials (Ln = Nd, Er, Yb) by replacing the 2-thenoyltrifluoroacetonate ligands by dibenzoylmethanate ligands.[583] The sol−gel material was prepared by condensation of the phen-Si ligand in the presence of TEOS. The authors made a detailed study of the spectroscopic properties. They determined the Judd−Ofelt parameters for the neodymium(III)-containing hybrid material: $\Omega_2 = 94.88 \times 10^{-20}$ cm^2; $\Omega_4 = 3.771 \times 10^{-20}$ cm^2; $\Omega_6 = 2.818 \times 10^{-20}$ cm^2. However, the Ω_2 value is unrealistically high and, judging from the reported absorption spectrum, should be corrected to $\Omega_2 = 9.488 \times 10^{-20}$ cm^2. Binnemans and co-workers replaced the phen-Si ligand with a 2-substituted imidazo[4,5-*f*]-1,10-phenanthroline (Figure 33) and incorporated lanthanide complexes of 2-thenoyltrifluoroacetonate in the hybrid matrix (Ln = Pr, Nd, Sm, Eu, Dy, Ho, Er, Tm, Yb) (Figure 34). Thin films were obtained by spin-coating on a quartz plate or on a silicon wafer.[584] Because the 2-thenoyltrifluoroacetonate ligand is not a good sensitizer of terbium(III) luminescence, Binnemans and co-workers replaced this ligand by nicotinic acid in hybrid materials based on the phen-Si ligand (Figure 35).[585] The nicotinate ligand was selected because it forms mononuclear

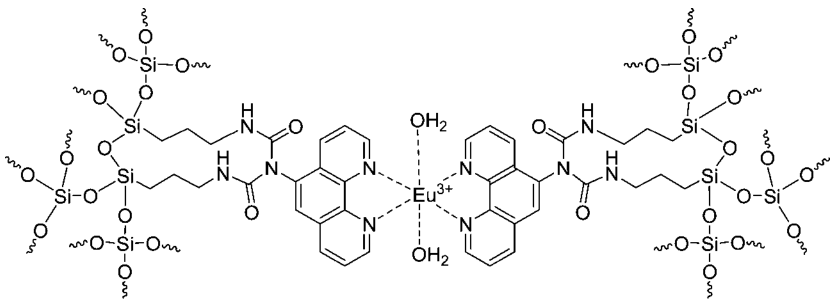

Figure 31. $[Eu(phen)_2(H_2O)_2]$ complex covalently linked to a silica hybrid matrix.[578]

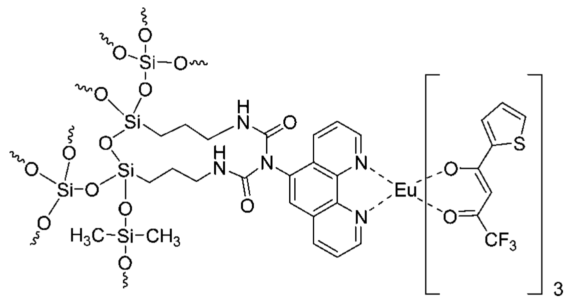

Figure 32. $[Eu(tta)_3(phen)]$ complex covalently linked to a silica hybrid matrix.[581]

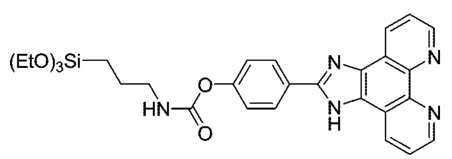

Figure 33. Hydrolyzable derivative of imidazo[4,5-*f*]-1,10-phenanthroline.

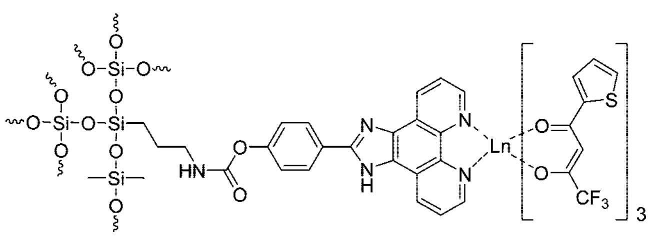

Figure 34. Luminescent hybrid material with lanthanide complexes covalently linked to a silica matrix via an imidazo[4,5-*f*]-1,10-phenanthroline derivative.[584]

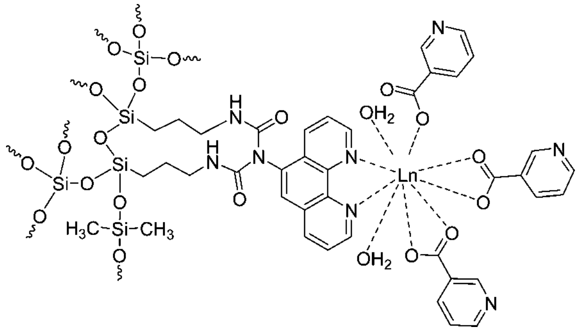

Figure 35. Luminescent silica hybrid matrix containing a lanthanide(III) nicotinate complex.[585]

complexes in the presence of 1,10-phenanthroline with lanthanide ions, in contrast to many other aromatic carboxylic acids.

Other types of bidentate ligands that have been used for covalent attachment of lanthanide complexes to a silica hybrid matrix include trialkoxysilyl derivatives of a salicylaldimine Schiff base,[586] 1,3-bis(2-formylphenoxy)-2-propanol,[587] *ortho*-aminobenzoic acid,[588] *meta*-aminobenzoic acid,[589] *para*-aminobenzoic acid,[590] phenylmalonic acid,[591] and 8-hydroxyquinoline.[592] An overview of these precursors in given in Chart 6. Liu and Yan used 3-alkyl-4-amino-5-ylsulfanyl-1,2,4-triazole derivatives to graft lanthanide complexes to a silica matrix (Chart 6).[593] Samples containing europium(III) and terbium(III) were prepared. Dong et al. selected *N*-(3-propyltriethoxysilane)-4-carboxyphthalimide as a precursor for luminescent hybrid materials with covalently attached lanthanide complexes (Chart 6).[594−597] Europium(III)- and terbium(III)-containing samples have been synthesized. Coordination of the lanthanide ions to the hybrid matrix occurs via the carboxylate groups of the ligand. Thin films could be prepared by spin-coating of the sol on quartz plates. An ormosil containing silylated tetraethylmalonamide (Figure 36) was prepared for the purpose of solid−liquid extraction of lanthanide and actinide ions but could in principle also be used as a host for luminescent lanthanide ions.[598] Nassar et al. attached β-diketonate ligands to a silica matrix, albeit not via a sol−gel process.[599] The authors started by reacting silica gel with 3-chloropropyltrimethoxysilane, resulting in a chloropropyl-functionalized silica gel. This was reacted with the sodium salts of acetylacetone or dibenzoylmethane in a methanolic solution so that the β-diketone ligand was bonded via the 2-position to the silica matrix (Figure 37). Complex formation with the Eu^{3+} ion resulted in the formation of a luminescent material. In a later study by another Brazilian group, ethyl 4,4,4-trifluoroacetoacetate was linked in a similar way as the β-diketones to a silica matrix.[600] It was observed that the luminescence intensity of the europium(III) complexes was greatly enhanced by addition of 1,10-phenanthroline as a coligand, because of expulsion of some water molecules from the first coordination sphere of the Eu^{3+} ion (Figure 38). Guo et al. covalently grafted europium(III) complexes of *o*-hydroxydibenzoylmethane to a silica matrix via the hydroxy group of the β-diketonate ligand.[601] The authors found a more efficient energy transfer from the matrix to the Eu^{3+} ion and a higher luminescence quantum yield for the hybrid material with the covalently bonded complex in comparison with a SiO_2 matrix doped with $Eu(dbm\text{-}OH)\cdot 2H_2O$ complex. Yan and coworkers prepared luminescent hybrid materials by linking *p-tert*-butylcalix[4]arene and calix[4]arene to a silica matrix and formation of the corresponding europium(III) and terbium(III) complexes.[602,603]

Phosphine oxides are often used as a coligand in lanthanide complexes and, in general, the resulting complexes exhibit good luminescence properties. Corriu et al. incorporated $Eu(NO_3)_3$ and $EuCl_3$ into inorganic−organic hybrid materials by the hydrolytic polycondensation of europium(III) with phosphine oxide ligands bearing one hydrolyzable $Si(OR)_3$

Chart 6. Hydrolyzable Precursors for Covalent Attachment of Lanthanide Complexes to a Silica Hybrid Matrix

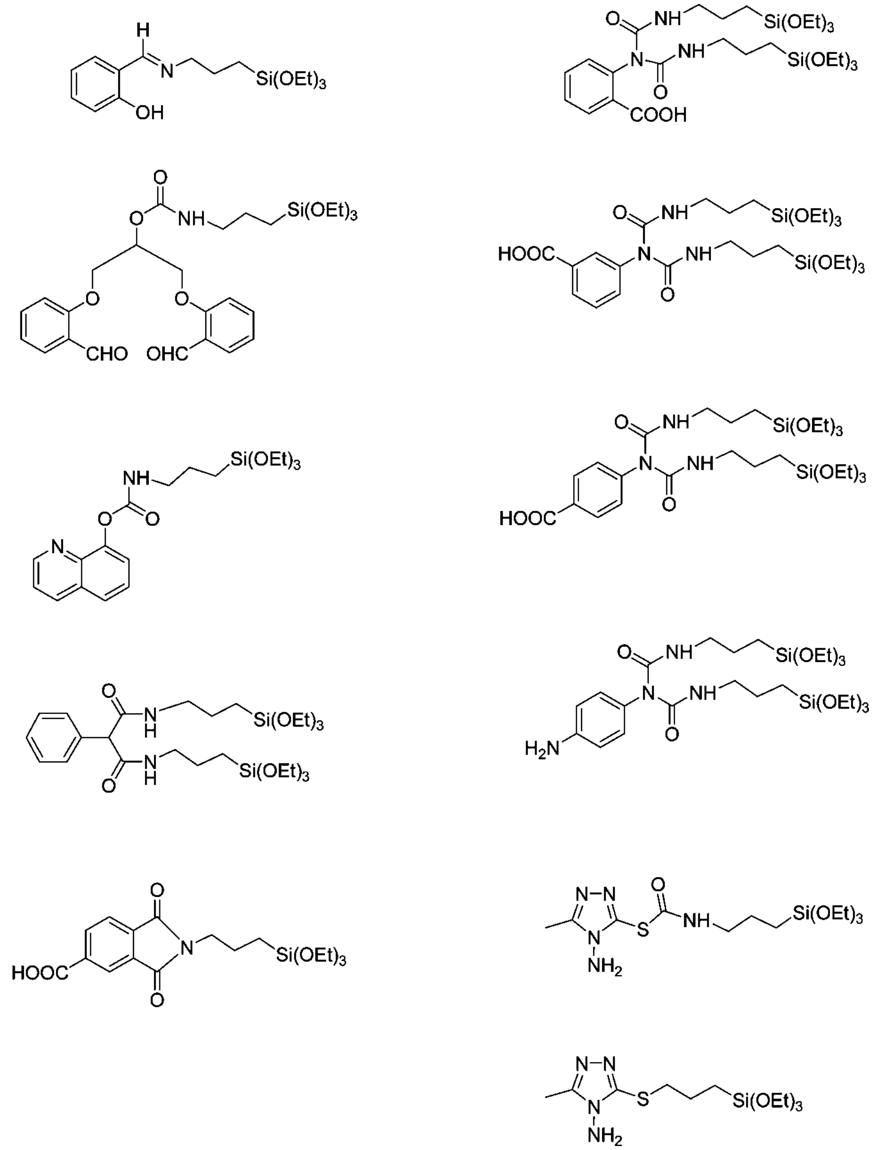

group (Chart 7).[604] Three phosphine oxide groups coordinate to a Eu^{3+} ion, and the coordination sphere is completed by chloride or nitrate anions (Chart 8). The authors found that using complexes derived from phosphine oxide with two or three hydrolyzable $Si(OR)_3$ groups resulted in the decomplexation of the ligands during the sol−gel process and the europium(III) salt was lost. Therefore only phosphine oxides bearing one hydrolyzable $Si(OR)_3$ group were considered for the hybrid materials. By use of solid-state ^{31}P NMR spectra, it was possible to calculate the percentage of complex P=O groups. This percentage varied between 81% and 91%. The highest values were observed for ligands with more flexible groups. No loss of europium(III) salt from the hybrid matrix occurred upon washing with different solvents, which indicates that the Eu^{3+} ions were strongly bound by the P=O groups of the phosphine oxide ligands. Raman spectra

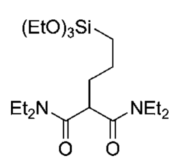

Figure 36. Silylated tetraethylmalonamide.

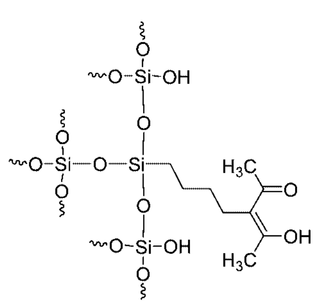

Figure 37. Silica gel functionalized with a *β*-diketone.

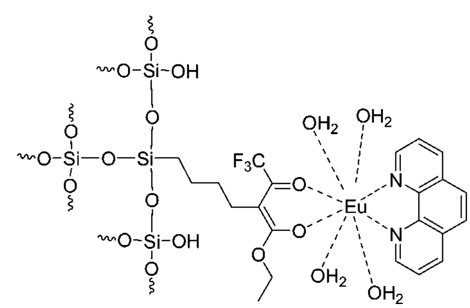

Figure 38. Europium(III) covalently bonded to silica matrix via a *β*-diketonate ligand.

Chart 7. Phosphine Oxide Ligands with Hydrolyzable $Si(OR)_3$ Groups

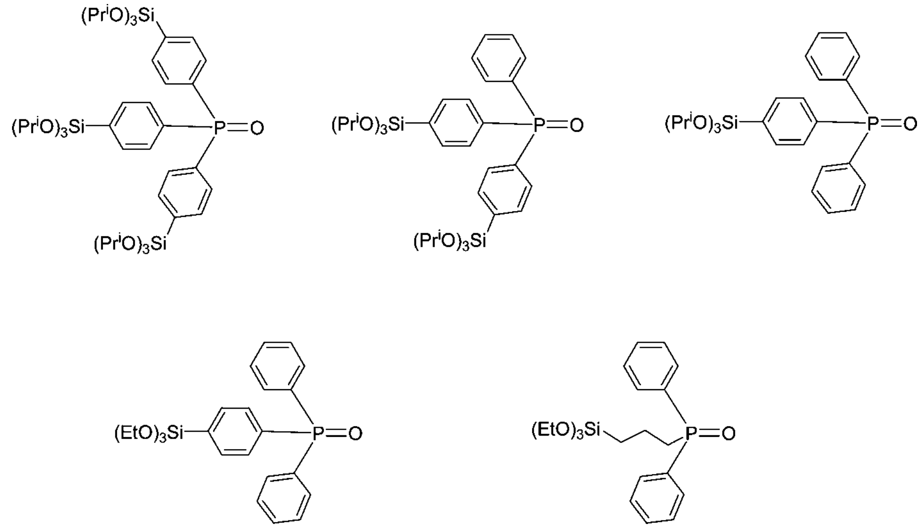

Chart 8. Lanthanide Complexes of Phosphine Oxide Ligands with Hydrolyzable $Si(OR)_3$ Groups

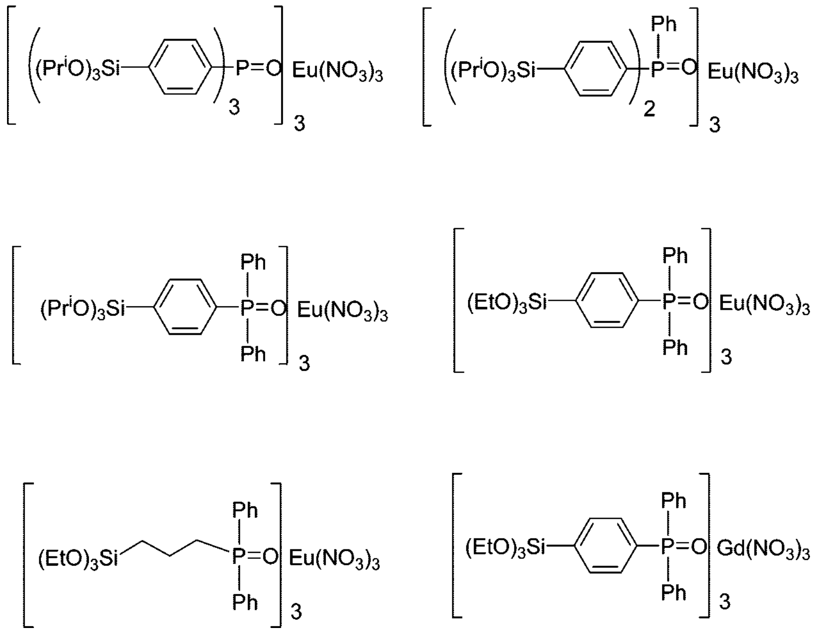

showed that the Eu^{3+} NO_3^- contact ion pair survived during the sol–gel process. Interestingly, the authors observed that co-condensation of the hydrolyzable phosphine oxide precursors with TEOS resulted in the formation of a hybrid material in which clustering of the Eu^{3+} took place. Addition of TEOS to the precursor solution had thus a negative effect on the properties of the resulting luminescent hybrid material. The europium(III)-containing hybrid exhibited a strong red photoluminescence and the luminescence spectra did not depend on the nature of the phosphine oxide ligands. However, phosphine oxide ligands with aromatic groups can act as an antenna for capturing excitation energy and can transfer this excitation energy to the Eu^{3+} ion. In a later paper, the authors first made the hybrid host matrix with appended phosphine oxide groups and subsequently formed complexes with $Eu(NO_3)_3\cdot 6H_2O$.[605] Two types of hybrids were prepared. The first type was obtained by hydrolysis and condensation of a mixture of $Ph_2P(CH_2)_3Si(OCH_3)_4$ and n equivalents of TEOS (n = 4, 7, 9, 12, 14, 19, and 35) in the presence of n-hexadecylamine as a templating surfactant. A second type was prepared in the absence of the surfactant but in the presence of 1% of Bu_4NF as catalyst. The phosphine groups in the hybrid materials were oxidized to the phosphine oxide groups by treatment with a large excess of an aqueous H_2O_2 solution. The first type of hybrid was mesoporous, while the second type was macroporous. The incorporation of $Eu(NO_3)_3\cdot 6H_2O$ in both types of hybrids was only possible if $7 \leq n \leq 14$. The amount of incorporated Eu^{3+} was found to be strongly dependent on the type of material and on the dilution of the relative amount of silica. In general, the uptake of Eu^{3+} was much higher for the mesoporous materials, in which the P=O groups were on the surface of the pores, than for the macroporous materials, in which the distribution of P=O groups was uncontrolled. The complexation of Eu^{3+} was optimum for mesoporous materials with n = 9. However, the porosity of the matrix (mesoporous or macroporous) had only limited influence on the fine structure of the luminescence spectra, showing that the Eu^{3+} are in similar environments in both types of matrices. In addition to $Eu(NO_3)_3$, $Er(NO_3)_3$ and $Yb(NO_3)_3$ were incorporated into silica matrices with pendant phosphine oxide groups, but no luminescence studies on these compounds were reported.[606] Khimich et al. prepared lanthanide-doped hybrid materials

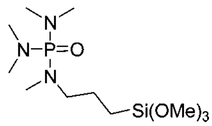

Figure 39. Trimethoxysilyl derivative of hexamethyl phosphoric triamide (HMPA).

by hydrolysis and condensation of a trimethoxysilyl derivative of hexamethyl phosphoric triamide (HMPA) (Figure 39).[607]

Corriu and co-workers incorporated the macrocyclic cyclam (1,4,8,11-tetraazacyclotetradecane) in a silica matrix (Chart 9).[608] As expected, the resulting hybrid material showed a strong tendency for complex formation with first row transition metal ions like Cu^{2+}. However, it was a surprise that also coordination between the macrocycle and Eu^{3+} could be observed, because the cyclam does not form stable complexes with Eu^{3+} in solution, in contrast to the tetramethylcarboxy-functionalized cyclam macrocycle DOTA. It was found that complex formation occurred at a ratio of one Eu^{3+} ion per two cyclam moieties. The fact that the Eu^{3+} ion forms a complex with two cyclam macrocycles suggested that the cyclam groups are in close proximity within the hybrid matrix. It was proposed that the coordination number of Eu^{3+} was eight. In related work by an Italian team, a europium(III) complex of 1,4,7,10-tetraazacyclododecane-1,4,7-triacetic acid (DO3A) was covalently linked to a silica matrix (Figure 40).[609] A methoxy-acetophenone unit in the linker acted as an antenna chromophore. The quantum yield of Eu^{3+} in thin glassy layers of this hybrid material was 10%. Thin silica films of 40 nm thick containing both Eu^{3+} and Tb^{3+} complexes of this ligand were prepared by dip-coating.[610] The relative intensities of the emission bands of Eu^{3+} and Tb^{3+} depended on the ratios of these ions in the hybrid matrix, allowing the emission color to be tuned from red over orange to yellow and green.

Raehm et al. reported that bright yellow emission could be obtained at room temperature from Eu^{2+} coordinated to two 2,9-functionalized 1,10-phenanthroline ligands (Figure 41), which were covalently bonded to the host matrix.[611] The Eu^{2+} was spontaneously formed in the hybrid matrix by reduction of Eu^{3+} during synthesis with electron transfer from ethanol. The divalent oxidation state of europium is strongly

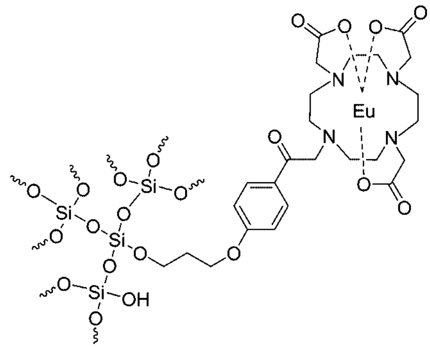

Figure 40. Europium(III) complex of 1,4,7,10-tetraazacyclododecane-1,4,7-triacetic acid (DO3A) covalently linked to a silica matrix.[609]

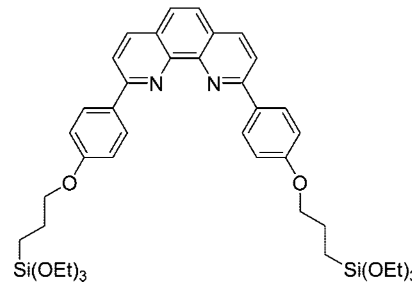

Figure 41. 2,9-Functionalized 1,10-phenanthroline ligand for stabilization of divalent europium.

stabilized by the 1,10-phenanthroline ligands in the hybrid matrix. Transitions due to the Eu^{3+} ions could not be observed in the luminescence spectra. This work shows that the emission color of Eu^{2+} strongly depends on the local environment of the Eu^{2+} ion and is not limited to the violet-blue regions.

Qiao and Yan prepared a hybrid polymer/silica material with lanthanide(III) complexes grafted to it via a modified 2-thenoyltrifluoroacetylacetonate ligand.[612] So far most of the studies of on covalently bonded complexes have been restricted to silica-based materials. However, just as in the case of simple inorganic sol−gel systems, silica (SiO_2) can be replaced by other oxide matrices like alumina (Al_2O_3), zirconia (ZrO_2), or titania (TiO_2). Li et al. grafted lantha-

Chart 9. Hydrolyzable Derivatives of 1,4,8,11-Tetraazacyclotetradecane (Cyclam)

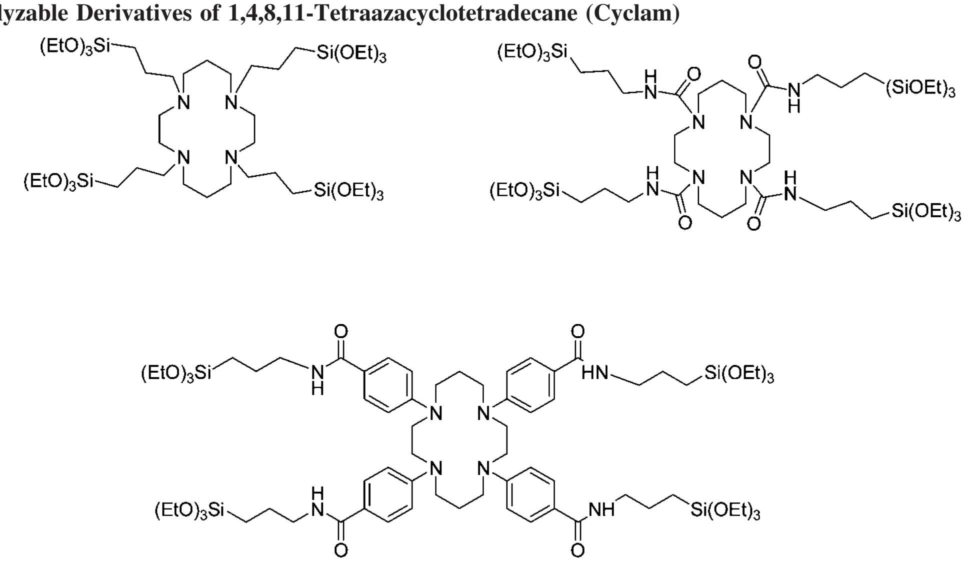

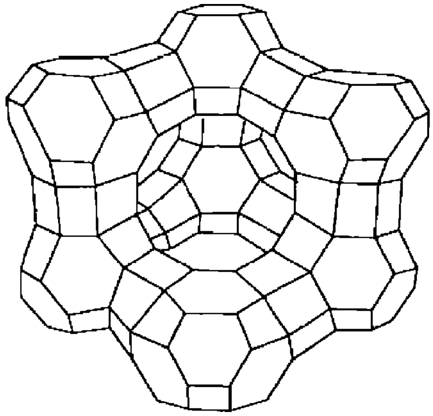

Figure 42. Structure of zeolites X and Y (faujasite structure).

nide(III) 2-thenoyltrifluoroacetonate complexes (Ln = Eu, Nd, Er) on titania via modification of titanium(IV) isopropoxide by isonicotinic acid, followed by binding of the lanthanide complexes to the matrix via the nitrogen atoms of isonicotinic acid.[613]

4. Porous Hybrid Materials

4.1. Zeolites

Zeolites are microporous crystalline aluminosilicates, whose general formula can be represented as $M^{n+}_{x/n}[(AlO_2)_x(SiO_2)_y]\cdot mH_2O$.[614−616] The *y*/*x* ratio varies between 1 and 5. Their structure consists of $[AlO_4]^{5-}$ and $[SiO_4]^{4-}$ tetrahedra linked by bridging oxygen atoms to a three-dimensional network. The negative electric charge generated in the framework when a silicon atom is isomorphically replaced by an aluminum atom, must be compensated by counterions M^{n+} present in the micropores of the zeolite. In this way, zeolites act as cation ion exchangers. Additional water molecules are located in the cavities. The pores of the zeolites have a very regular shape and size and are defined by the crystal structure. A typical feature of zeolites is also the presence of large central cavities, the so-called *supercages*. About 50 zeolites occur as minerals in nature, but more than 150 different types of zeolites have been synthesized in the laboratory. Two types of zeolites that are often used as hosts for lanthanide ions or lanthanide complexes are the synthetic zeolites *zeolite X*[617,618] and *zeolite Y*,[619,620] which have the cubic *faujasite* structure (Figure 42). The basic building block of this zeolite is the *sodalite cage* (or *β*-cage). The sodalite cage has the shape of a truncated octahedron and thus possesses square and hexagonal faces. Its name derives from the aluminosilicate sodalite whose structure consists of a cubic array of truncated octahedra sharing their square faces. Alternate hexagonal faces, at positions corresponding to the vertices of a tetrahedron, are connected via hexagonal prisms. Each sodalite cage is thus connected to four other sodalite cages via the hexagonal prisms, which form the small pore system of the zeolite. The α-*cage* or *supercage* is created by eight *β*-cages. The faujasite structure has large channels and voids and thus is useful in catalysis and as a molecular sieve. Zeolite Y is very often used as a cracking catalyst. The diameter of the entrance to the supercage is about 7.5 Å, whereas the diameter of the supercage itself is about 12 Å. In contrast, the diameter of the sodalite cage is 6.6 Å and that of the hexagonal prism 1.8 Å. The differences between zeolite X and Y are the Si/Al ratios: zeolite X is rich in alumina, whereas zeolite Y is rich in silica. Typical formulas are $Na_{86}[(AlO_2)_{86}(SiO_2)_{106}]\cdot 264H_2O$ for NaX zeolite (zeolite X in Na^+ form) and $Na_{56}[(AlO_2)_{56}(SiO_2)_{136}]\cdot 264H_2O$ for NaY zeolite (zeolite Y in Na^+ form).[621] The water molecules in the zeolite structure can be removed by dehydration and their number is variable. Indeed, a typical feature of zeolites is that they can absorb and lose water without damage to their crystal structures. The Si/Al ratio can be varied, but the constraints are that the sum of the number of Si atoms and the number of Al atoms equals 192 and that the total charge of the cations equals the number of Al atoms. The total number of Al atoms varies between 77 and 96 for X-type zeolites and between 48 and 76 for Y-type zeolites.[622] In *zeolite A* (*zeolite Linde type A*), the sodalite cages are interconnected by tetragonal prisms via the square faces. The main use of zeolite A is as ion exchanger. It has also replaced phosphates in household detergents.

Zeolites can be converted into luminescent materials by replacing the sodium counterions by lanthanide ions. Ion exchange is generally carried out by stirring a zeolite suspension in an aqueous solution of a lanthanide salt at a suitable pH at room temperature or at reflux temperature. For instance, Jüstel et al. incorporated lanthanide ions in zeolite X by immersing the zeolite in the sodium form in an aqueous solution of a lanthanide chloride salt (0.5 mol/L; pH = 6, adjusted by aqueous ammonia) and heating the solution to reflux temperature for 48 h.[623] After filtering, the samples were calcined at 600 °C. It is also possible to introduce the lanthanide ions in the zeolite matrix mechanochemically by grinding the zeolite and the lanthanide salt. Nassar and Serra introduced Eu^{3+} in zeolite Y by ball-milling the zeolite with hydrated $EuCl_3$, followed by calcination at 300 °C.[624,625]

Lanthanide ions have frequently been used as luminescent probes to investigate zeolite structures. Luminescence studies are helpful to locate the lanthanide ion within the zeolite framework and to study the local environment of the lanthanide ion. Traditionally, most of these studies have used the Eu^{3+} and Tb^{3+} ions. The luminescence studies are often complemented by studies with other spectroscopic techniques like EXAFS, EPR, and Mössbauer spectroscopy. This work was motivated by the importance of rare-earth-exchanged zeolites in catalysis. Luminescence and EXAFS studies of Eu^{3+}-exchanged zeolite Y and zeolite A showed that the coordination of Eu^{3+} in the supercage of zeolite Y is the same as in aqueous solution, whereas a lower coordination number is found for Eu^{3+} in zeolite A.[626] A comparative high-resolution luminescence study of hydrated Eu^{3+} ions in zeolite A and zeolite Y indicated that the hydrated ions are coordinated to the framework oxygen atoms of zeolite A but not to those of zeolite Y.[627] Heating of a europium-exchanged zeolite Y to 100 °C did not change the local environment of the Eu^{3+} ion in comparison to the as exchanged sample, but heating to 200 °C caused the Eu^{3+} to migrate from the supercage to the sodalite cages.[628] Three different sites were found for Eu^{3+} in dehydrated zeolite Y.[629] The Eu^{3+} ions located at different sites in the zeolite have different luminescent decay times.[630,631] Although the existence of Eu^{4+} in zeolite A had been postulated on the basis of X-ray crystallography data,[632,633] these results could not be confirmed by other studies.[634] Jørgensen argued that the existence of europium(IV) in this matrix is highly unlikely and that Eu^{4+} cannot be colorless.[635] The occupation of zeolite sites by lanthanide ions changes over time. Blasse and co-workers found that in freshly prepared samples, hydrated Gd^{3+} ions

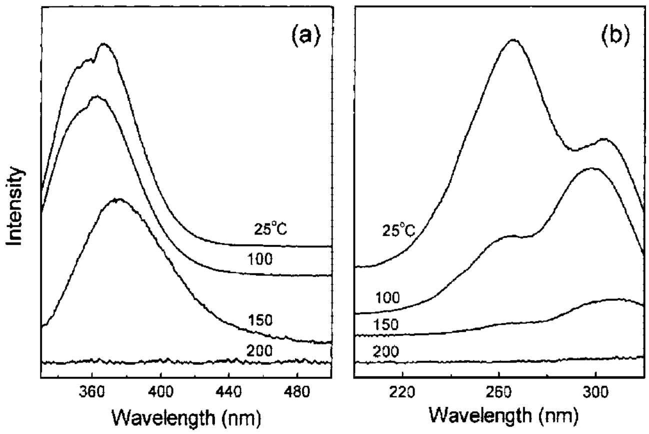

Figure 43. Emission (a) and excitation (b) spectra of CeNa-zeolite pretreated at different temperatures. The emission spectra were recorded with an excitation wavelength of 300 nm, and the excitation spectra were monitored at 370 nm. Reprinted with permission from ref 643. Copyright 2001 American Chemical Society.

occupy only one site in zeolite A samples, whereas three different sites were found to be occupied after several months.[636] In general, hydrated lanthanide ions are located in the supercage of the zeolite, but upon thermal treatment they migrate to the sodalite cages or to the hexagonal prisms. Hong et al. found that the thermally induced migration of Tb^{3+} within faujasite-type of zeolite hosts strongly depended on the Si/Al ratio.[637] For a low-silica zeolite (Si/Al = 1.37), most of the Tb^{3+} ions exchanged into the supercages start to migrate directly to the hexagonal prisms at 150 °C, without staying at the sodalite cages. In contrast, the Tb^{3+} ions in a high-silica zeolite (Si/Al = 3.40) migrate first to the sodalite cages at 100 °C and subsequently to the hexagonal prisms at temperatures above 100 °C.[638] In zeolite A with different Si/Al ratios, the Tb^{3+} ions migrate from the supercage to the sodalite cages at 100 °C.[639] Two different species could be detected for hydrated Tb^{3+} ions in the supercage of Tb^{3+}-exchanged zeolite X.[640] Tiseanu et al. investigated the dehydration and rehydration of different Tb^{3+}-exchanged zeolites of the ZSM-5 type (MFI type) by luminescence spectroscopy.[641,642] The local order of the Tb^{3+} ions and the behavior toward rehydration were found to be dependent on the type of zeolite host. Luminescence spectroscopy studies showed that an intrazeolitic $Ce^{4+} \leftrightarrows Ce^{3+}$ redox process took place within the hexagonal prism (double six-ring, D6R).[643] In Figure 43, the excitation and luminescence spectra of CeNa-Y zeolite (zeolite Y in the Na^+ form, with Na^+ partially exchanged by Ce^{3+}) pretreated at different temperatures. The luminescence spectrum sample dried at room temperature after Ce^{3+} ion exchange, show a broad band at 367 nm and a shoulder at 356 nm, which were assigned to the $^2T_{2g} \rightarrow {}^2F_{7/2}$ and $^2T_{2g} \rightarrow {}^2F_{5/2}$ transitions between the 5d and 4f levels of the Ce^{3+} ion, respectively ($4f^05d^1 \rightarrow 4f^1$ transitions). The band positions and their relative intensity were found to strongly depend on the temperature of heat treatment. For samples heated to a temperature above 200 °C, no emission bands could be observed. Based on group theory, these results were interpreted as the Ce^{3+} ions first migrating at 100 °C to the sodalite cages, then above 150 °C to the hexagonal prisms. The disappearance of the luminescence in the samples heated to above 200 °C can be attributed to oxidation of Ce^{3+} to Ce^{4+} within the hexagonal prisms.

Lanthanide-exchanged zeolites have been investigated as cheap inorganic phosphor material as replacements for the conventional inorganic phosphors like $BaMgAl_{10}O_{17}/Eu^{2+}$ (BAM), $LaPO_4/Ce^{3+},Tb^{3+}$ (LAP), and Y_2O_3/Eu^{3+} (YOX) for lighting applications. Efficient emission in the ultraviolet region with quantum yields up to 100% was observed for Ce^{3+} incorporated in zeolites X and Y, thanks to allowed f−d transitions.[644] Kynast and co-workers investigated the luminescence properties of zeolite X doped with Ce^{3+} and Tb^{3+} ions.[645] In samples doped with only Tb^{3+}, a quantum yield of 18% could be reached for excitation at 254 nm. However, due to the weak light absorption of Tb^{3+} at this wavelength, the total luminescence output was relatively weak. Higher luminescence intensities were observed for the Tb^{3+}-containing zeolite codoped with Ce^{3+} ions. Ce^{3+} strongly absorbs light of 254 nm and can transfer the excitation energy to the Tb^{3+} ion. The efficiency of the energy transfer $Ce^{3+} \rightarrow Tb^{3+}$ was over 90%, so less than 10% Ce^{3+} emission remained in the samples. Depending on the Tb^{3+}/Ce^{3+} ratio, quantum yields between 40% and 50% could be obtained, with the highest quantum yields for samples with high Tb^{3+} content and low Ce^{3+} content. High Tb^{3+} contents require low Ce^{3+} contents because it was observed that samples containing more than 28 lanthanide ions per unit cell suffer from lower efficiencies. However, the quantum yield of the Tb^{3+}/Ce^{3+} could be increased to 85% by changing the excitation wavelength from 254 to 330 nm. Tb^{3+} luminescence sensitized by Ce^{3+} ions was also studied in zeolites of types A and Y and ZSM-5.[646]

The luminescence efficiency of zeolites doped with Eu^{3+} ions is very low (quantum yield lower than 1% for Eu-loaded zeolite X).[647] Although this is partly due to the presence of water molecules in the zeolite cage, dehydration experiments show that this is not the only cause: even after dehydration (600 °C, *in vacuo*) the quantum yield remained as low as 5%. The main cause seems to be a low-lying O → Eu^{3+} charge transfer band, which efficiently deactivates the excited state of Eu^{3+}. The increase of the luminescence upon heat treatment is not only due to dehydration, but also due to migration of the Eu^{3+} ions from the supercage to the sodalite cages.[627] Because of the weak light absorption by the f−f transitions of Eu^{3+}, the total luminescence output remained low, even after heat treatment, and one had to rely on the antenna effect to increase the luminescence efficiency. A tremendous gain in luminescence intensity was observed when the Eu^{3+} ions in the cage were complexed with β-diketonate ligands. Sendor and Kynast found an increase by a factor of 350 after treatment of a {Eu_8-X} sample (i.e., a zeolite-X with eight Eu^{3+} ions per unit cell) with an excess of solid 2-thenoyltrifluoroacetone (Htta), followed by washing and rehydration.[647] The rehydration step was necessary for complex formation, because otherwise the Htta ligands could not be deprotonated in the zeolite cage and the Eu^{3+} ions could not be released from the walls of the supercage. The luminescence efficiency depended on the Eu/tta ratio. A strongly emissive species was found to be {[$Eu(tta)_3$]-X}, where the complexes remained attached to the zeolite cage. Increasing the number of Eu^{3+} ions per unit cell resulted in an increase of the luminescence intensity up to eight Eu^{3+} per unit cell. Further addition of Eu^{3+} led to a decrease in the luminescence intensity. The corresponding complex could be represented as {[$Eu_8(tta)_{13.5}$]-X}. Bright luminescent materials could also be obtained by encapsulating [$Eu(tta)_3(phen)$] in the zeolite cage. In this case, the

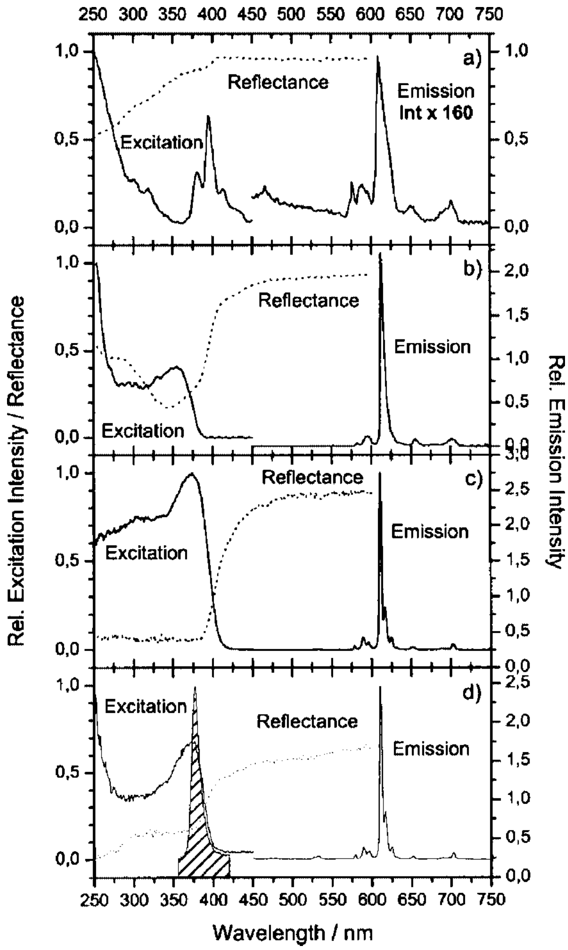

Figure 44. Excitation, emission, and reflectance spectra of europium-containing zeolite X hybrid materials: (a) {Eu_8-X}; (b) {[$Eu(tta)_3$]-X}; (c) {[$Eu(tta)_3$(phen)]}; (d) {[$Eu(tta)_3$(phen)]-X}. The excitation wavelength was 250 nm for {Eu_8-X} and was set at the excitation maximum for the tta complexes. The hatched curve in panel d represents the emission spectrum of a commercial UV-LED (Nichia). Reprinted with permission from ref 647. Copyright 2002 Copyright Wiley-VCH Verlag GmbH & Co. KGaA.

β-diketonate complex was no longer linked to the walls of the zeolite cage. The increase in luminescence intensity of Eu^{3+}-doped zeolites by complex formation with β-diketonate ligands was illustrated by a spectacular experiment.[647] {Eu_8-X} hardly showed visible luminescence upon irradiation by a 366 nm UV source. However when solid Htta was added to a vial containing {Eu_8-X} powder and the mixture shaken, a bright red luminescence was visible within a few seconds. In Figure 44, the luminescence spectra of Eu^{3+}-doped zeolite X are compared with those of the same zeolite loaded with $Eu(tta)_3$ and $Eu(tta)_3$phen complexes. From this figure, it is also evident that these materials can efficiently be excited by an UV-LED. The luminescence of the $[Eu(bipy)_2]^{3+}$ complex in zeolite Y was studied by Rosa et al.[648] The authors point to the feasibility of using zeolites as host matrices for luminescent lanthanide complexes. The $I(^5D_0 \rightarrow {}^7F_2)/I(^5D_0 \rightarrow {}^7F_1)$ intensity ratio was 1.45. Alvaro et al. prepared complexes of europium(III) with benzoyltrifluoroacetone (Hbfac), 1,10-phenanthroline (phen), 2,2′-bipyridine (bipy), and dipicolinic acid (H_2dpa) in the zeolites zeolite Y, mordenite, and ZSM-5.[649] For the europium(III) benzoyltrifluoroacetonate complexes in zeolite Y and mordenite, the Eu/ligand ratio was in all cases lower than the ratio expected for a 1:3 complex. For instance, for zeolite Y, no Eu/ligand ratios higher than 1:1.35 could be obtained. Because of steric hindrance, the pores of the zeolite Y and mordenite are too small to host a [$Eu(bfa)_3$] or even a $[Eu(bfa)_2]^+$ complex. The most abundant species seemed to be $[Eu(bfa)]^{2+}$. Encapsulation of the europium(III) complexes in the zeolite matrix resulted in an increase of the luminescence lifetime in comparison with the complexes in solution. An increase in lifetime by a factor of 2 was found when the zeolite Y containing $[Eu(bfa)]^{2+}$ complex was dehydrated and rehydrated by D_2O. Surprisingly no difference in lifetime was found when a zeolite Y containing Eu^{3+} without organic ligands was treated by the same procedure. This is an indication that the emitting Eu^{3+} ion was not hydrated. The type of both ligand and zeolite host was found to have an influence on the luminescence decay times. The decay times followed the order dpa > phen > bipy > bfa and ZSM-5 > mordenite > zeolite Y. The $^5D_0$ state decayed faster as the amount of Eu^{3+} in the zeolite increased. The luminescence decay time increased as the amount of ligand increased. The shortest decay times were found for the Eu^{3+}-loaded zeolites without organic ligands. Dexpert-Ghys et al. studied the complexes between the dipicolinate ion and the lanthanide ions La^{3+} and Eu^{3+} in faujasite-type zeolite X and zeolite Y.[650] The authors found that the dpa/Ln ratio never exceeded 1. Moreover, not all lanthanide ions in the zeolite matrix were able to form complexes with the dpa ligand, only those within the supercages. The europium(III) complexes within the zeolite matrices were luminescent, and energy transfer from the dipicolinate ligand to the Eu^{3+} ion could be observed. Although the 2-thenoyltrifluoroacetonate (tta) ligand is a very efficient ligand for the sensitization of Eu^{3+}, it should be remembered that $Tb(tta)_3$ complexes are poor emitters. Terbium(III) benzoate was found to be an efficient green-emitting molecular luminescent material for incorporation in zeolite Y.[651] The terbium(III) benzoate was formed *in situ* in the zeolite by refluxing the Tb^{3+}-exchanged zeolite with benzoyl chloride. Unreacted benzoyl chloride could be removed by solvent extraction with hexane or diethyl ether. Europium(III) and terbium(III) complexes of different carboxylic acids, including benzoic acid, salicylic acid, and phenoxyacetic acid, as well as adducts of these carboxylates with 1,10-phenanthroline in zeolite A were prepared, and their luminescence properties were investigated.[652] The highest luminescence output was observed for the terbium(III) complex of *ortho*-chlorobenzoic acid. The integrated luminescence intensity of this complex in zeolite A was 55% that of the inorganic phosphor Gd_2O_2S/Tb^{3+} for excitation at 254 nm. The luminescence of the terbium(III) complexes was much weaker if an excitation wavelength of 365 nm was used. The best luminescence performance of the europium(III) complexes was observed for the complexes with α-phenoxybutyric acid, *ortho*-chlorobenzoic acid, or *ortho*-methoxybenzoic acid with an excitation wavelength of 365 nm. However, the europium(III) complexes of these ligands could only be efficiently excited at 254 nm if 1,10-phenanthroline was present as coligand. In a related paper, the europium(III) and terbium(III) complexes of diphenacylphosphinic acid in zeolite A were investigated.[653] Liu et al. incorporated [$Eu(dbm)_3$(bath)] in zeolite Y and zeolite L.[654] Higher thermal stabilities, longer luminescence lifetimes, and high quantum yield were observed for the complex incorporated in the zeolite matrix in comparison with the pure complex. The authors concluded that zeolite L is better host material of the two.

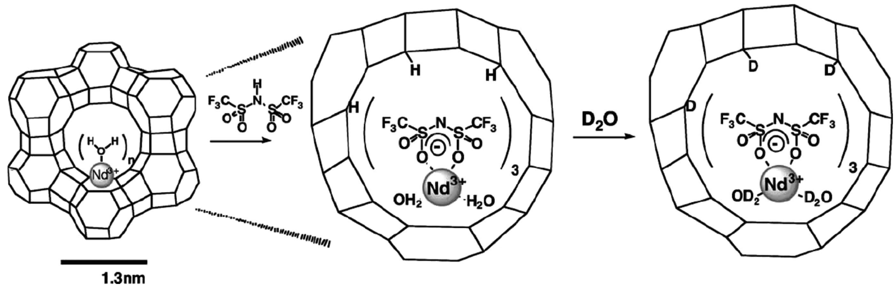

Figure 45. Conceptual process of ship-in-bottle synthesis of $Nd(Tf_2N)_3$ complexes within a faujasite host matrix and the effect of treatment with D_2O. Reprinted with permission from ref 657. Copyright 2000 American Chemical Society.

It is not easy to observe near-infrared luminescence for lanthanide-exchanged zeolites, due to the strong nonradiative relaxation of the excited states of the near-infrared emitting lanthanide ions by the water molecules within the pores of the zeolite host. Lezhina and Kynast reported that they were unsuccessful in detecting near-infrared luminescence for Nd^{3+} ions in a zeolite X matrix.[655] Rocha et al. were able to observe strong luminescence for Er^{3+}-doped narsursukite that was obtained from the microporous titanosilicate ETS-10 by calcination at high temperatures.[656] Wada et al. succeeded in observing near-infrared emission of Nd^{3+} ions in a nanosized faujasite zeolite powder by coordination of bis(trifluoromethylsulfonyl)imide ligands to the Nd^{3+} ion.[657] The Nd-exchanged zeolite was exposed to vapors of hydrogen bis(trifluoromethylsulfonyl)imide, HTf_2N, and to D_2O vapor. $Nd(Tf_2N)_x$ complexes were assembled from the Nd^{3+} ions and the Tf_2N^- ligands within the supercage (*ship-in-bottle synthesis*, Figure 45). It was estimated that one or two neodymium(III) complexes reside within the supercage of the faujasite. The exposure to D_2O was done to convert the OH groups into OD groups, which have a much lower vibrational frequency. Emission spectra were measured on powdered samples in vacuum and dispersed in DMSO-d_6. Whereas the Nd^{3+}-exchanged faujasite treated with D_2O alone did not show detectable luminescence, strong luminescence was observed for the samples that were also treated with bis(trifluoromethylsulfonyl)imide ligands. The quantum yield of the Nd^{3+}-containing zeolite in DMSO-d_6 was determined to be 9.5% $\pm$ 1.0%, which is not only very high for neodymium(III) complexes but also much higher than the value measured for $Nd(Tf_2N)_3$ dissolved in DMSO-d_6. This is an indication that in DMSO-d_6 solution, Nd^{3+} remains incorporated in the zeolite host matrix. The luminescence lifetime of the Nd^{3+}-containing zeolite in DMSO-d_6 was 22 μs. The high emission of Nd^{3+} indicated that the bis(trifluoromethylsulfonyl)imide ligands efficiently prevent radiationless deactivation of the excited states of Nd^{3+} by OD vibrations and by the wall vibrations of the zeolite cage. The entrapment of the neodymium(III) complex in the supercage also excludes clustering of Nd^{3+} ions. Subsequent studies report that the Nd-exchanged faujasite contained the tetramethylammonium (TMA^+) ion, originating from the synthetic procedures.[658] The TMA^+ ions in the supercage can be exchanged by Nd^{3+} ions, whereas the TMA^+ ions in the sodalite cage are not exchanged. Up to 14.3 Nd^{3+} could be introduced per unit cell. The ease of complex formation between the Nd^{3+} ions and the Tf_2N^- ligands within the faujasite host was attributed to the fact that the Nd^{3+} ions are located in the supercage and not in the sodalite cages. Besides nanocrystalline powders, also microcrystalline powders were investigated. High-resolution emission spectra show smaller band widths for Nd^{3+} ions in the zeolite than for Nd^{3+} ions in a glass, which is an indication that the environment of the Nd^{3+} ion is better defined in the zeolite host. The splitting of the $^2P_{1/2}$ level into two bands suggests that at least two different neodymium(III) complexes were present, which were tentatively assigned as $[Nd(Tf_2N)]^{2+}$ and $[Nd(Tf_2N)_2]^+$. Heat treatment had only a small effect on the luminescence intensities. If a Na^+-containing faujasite instead of a TMA^+-containing faujasite was used as the starting material for the preparation of Nd^{3+}-exchanged faujasite, it was observed that thermal treatment resulted in higher luminescence intensities, while treatment with Tf_2N^- ligands had only a minor effect. The increase in luminescence could be explained by loss of water of hydration and migration of the Nd^{3+} ions from the supercage to the sodalite cages and the hexagonal prisms. Here, the Nd^{3+} ions can no longer form complexes with Tf_2N^- ligands. Judd−Ofelt parameters were determined for different samples of Nd-exchanged faujasite. The emission intensity was found to increase with increasing loading with Nd^{3+} ions.[659,660] This looks contradictory, because concentration quenching of the luminescence is expected at high concentrations of lanthanide ions. However, at low Nd^{3+}-loading the $Nd(Tf_2N)_3$ complexes contained coordinating water molecules, whereas at high Nd^{3+}-loading $Nd(Tf_2N)_3$−zeolite complexes without coordinating water molecules were formed. The luminescence efficiency of the material could be increased by coexchange with La^{3+} ions, because this suppressed the energy migration between Nd^{3+} ions while maintaining the possibility to form anhydrous $Ln(Tf_2N)_3$−zeolite complexes.

Multicolored luminescence can be created by codoping several lanthanide ions in the same zeolite matrix. Tricolor emission, namely, blue (434 nm), green (543 nm), and red (611 nm), was observed for zeolite Y codoped with Tb^{3+} and Eu^{3+} and heat treated at 800 °C.[661] More fine-tuning of the emission colors was possible by doping a photosensitizer with the lanthanide ions in the zeolite. Wada and co-workers exchanged the sodium ion of a NaX zeolite with Eu^{3+} and Tb^{3+} in different amounts and Eu^{3+}/Tb^{3+} ratios, and the dehydrated samples were either exposed to benzophenone vapor or stirred in a solution of 4-acetylbiphenyl in ethanol.[662] The function of the photosensitizer is to efficiently absorb the excitation light and to transfer it to the lanthanide ions (Figure 46). If the efficiency of the energy transfer was not 100%, emission by the photosensitizer was observed as well. The luminescence colors of the samples varied from red to green, blue, and violet by changing the amounts and ratios of lanthanide ions and the nature of the sensitizer. For instance, a sample containing Eu^{3+}, Tb^{3+}, and 4-acetylbiphenyl showed simultaneously blue emission (4-acetylbiphenyl), green emission (Tb^{3+}), and red emission (Eu^{3+}). On the other hand, a sample containing Eu^{3+}, Tb^{3+}, and benzophenone showed only red and green emission, because

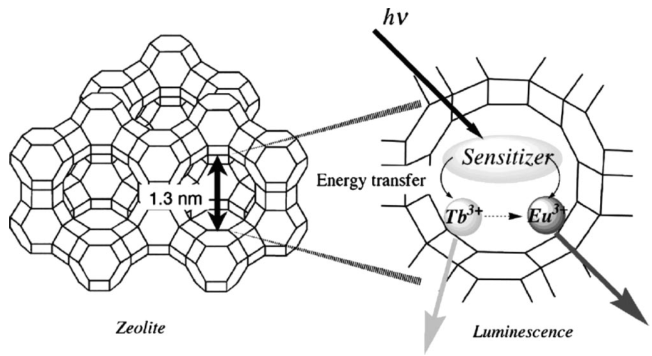

Figure 46. Sensitized luminescence of Tb^{3+} and Eu^{3+} in the supercage of zeolite X through energy transfer from a sensitizer. Reprinted with permission from ref 663. Copyright 2008 Elsevier.

the photosensitizer benzophenone does not emit blue light. The relative intensities of the red and green emissions could be changed by varying the Eu^{3+}/Tb^{3+} ratios in the samples. The intensity ratios could also be tuned by changing the excitation wavelength of the 4-acetylbiphenyl photosensitizer or by changing the temperature. By choice of the correct experimental parameters, the zeolite hybrid materials were white light emitters. In a later paper, the authors described the energy transfer processes in a Eu/Tb-exchanged zeolite X containing the benzophenone sensitizer more in detail.[663] In Figure 47, it is shown how the relative intensities of the green and red emission depend on the relative amounts of Eu^{3+} and Tb^{3+}.

4.2. Mesoporous Silicates

The mesoporous molecular sieves of the M41S family were developed by researchers at Mobil Corporation.[664−666] These materials exhibit narrow pore size distributions, similar to those found for zeolites. Whereas the pore sizes of zeolites are typically less than 10 Å, the pores of the M41S materials can be tailored between 15 and more than 100 Å. The M41S materials can be obtained in different compositions, either as pure silica or as aluminosilicate. They are synthesized hydrothermally in the presence of a long-chain alkyltrimethylammonium surfactant. The surfactant acts as a template for the formation of the mesoporous network and the length of the alkyl chain determines the size of the pores. The M41S family has several well-known members like *MCM-41* (*Mobil Composition of Matter No. 41*) and *MCM-48*. A unique feature of these materials is that although they are composed of amorphous silica, they have a long-range ordered framework with uniform mesopores. The structure of MCM-41 (hexagonal phase) consists of a hexagonal packing of one-dimensional channels with a pore diameter ranging between 20 and 100 Å. MCM-48 (cubic *Ia*3*d* structure) has a bicontinuous structure, which consists of two independent and intricately interwoven networks of mesoporous channels. A mesoporous material related to the M41S family is *SBA-15* (*Santa Barbara Amorphous No. 15*). SBA-15 is a hexagonal silica that is prepared with poly(alkylene oxide) triblock copolymer surfactants as template.[667] A typical surfactant for the synthesis of SBA-15 is Pluronic P123, which is poly(ethylene oxide)$_{20}$−poly(propylene oxide)$_{70}$−poly(ethylene oxide)$_{20}$ (Figure 48). SBA-15 has a larger pore size than MCM-41 (from 89 to more than 300 Å) and thicker silica cell walls. Instead of the expensive block copolymer nonionic surfactants, it is also possible to use the much cheaper poly(ethylene glycol)s as template.[668] It should be noted that these mesoporous materials are synthesized via a sol−gel process by hydrolysis and condensation of a tetraalkoxysilane or an organosilicon compound in the presence of a surfactant. Therefore, these materials can also be considered as sol−gel-derived materials. Reviews on the use of mesoporous and mesostructured materials for optical applications are available.[669,670]

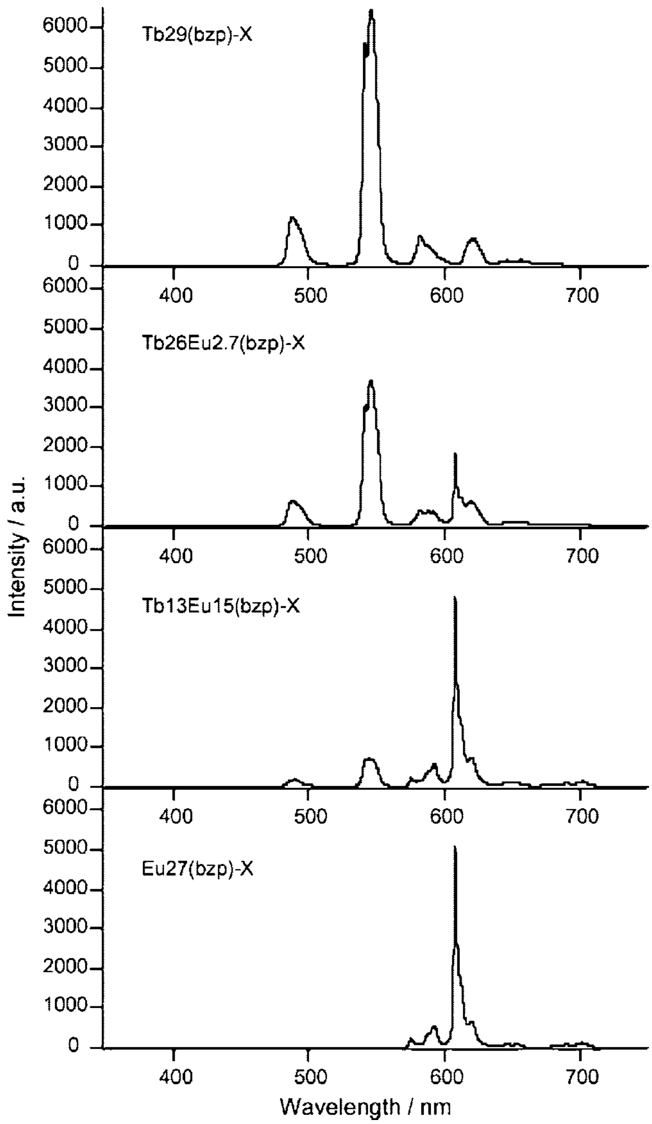

Figure 47. Luminescence spectra (λ_{exc} = 342 nm, 300 K) of samples of Eu/Tb-exchanged zeolite X containing benzophenone as photosensitizer with different Eu^{3+}/Tb^{3+} ratios. Reprinted with permission from ref 663. Copyright 2008 Elsevier.

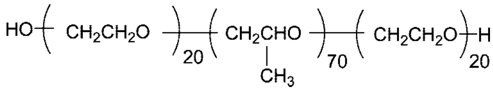

Figure 48. Structure of the Pluronic 123 surfactant.

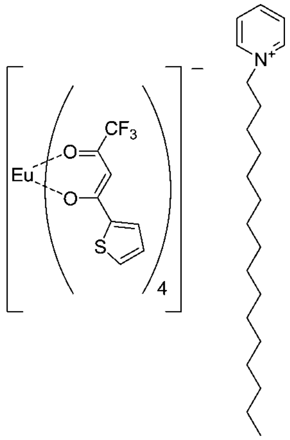

Figure 49. Structure of the $[Eu(tta)_4]^-(C_5H_5NC_{16}H_{33})^+$ complex.

The pores of these mesoporous materials are large enough to encapsulate lanthanide complexes without the need for the "ship-in-bottle" approach that is necessary for introduction of these complexes in conventional zeolites. Xu et al. used MCM-41 as a host for a luminescent europium(III) β-diketonate complex.[671,672] Before encapsulation of the $[Eu(tta)_4]^-(C_5H_5NC_{16}H_{33})^+$ complex (Figure 49), the authors modified MCM-41 with *N*-(3-trimethoxysilyl)ethylethylenediamine in order to reduce the number of silanol groups in the host matrix. The high-energy vibrations of the Si−OH groups would otherwise partially quench the luminescence of the Eu^{3+} ion. The most remarkable property of the europium(III) complex in the modified MCM-41 was the very strong intensity of the hypersensitive transition $^5D_0 \rightarrow {}^7F_2$ at 612 nm. The authors even report that the intensity ratio $I(^5D_0 \rightarrow {}^7F_2)/I(^5D_0 \rightarrow {}^7F_1)$ is $+\infty$, because the $^5D_0 \rightarrow {}^7F_1$ could not be observed. Of all the luminescent europium(III) complexes presently known, this material has the highest color purity. The intensity ratio for the same europium(III) complex in unmodified MCM-41 is only 5.5. The intensity increase has been attributed to the reduced size of the pores in the modified MCM-41 (14.26 Å) in comparison with the unmodified MCM-41 (29.31 Å). The europium(III) complex with a diameter of about 12 Å can enter the pores of the modified MCM-41 matrix, but NH groups of the modifying agent form strong H-bonds with the F-atoms of the 2-thenoyltrifluoroactylacetonate ligands. Due to this H-bonding, the symmetry of the complex is decreased, and this renders the electric dipole transition $^5D_0 \rightarrow {}^7F_2$ dominant. The luminescence lifetime of the complex $[Eu(tta)_4]^-(C_5H_5NC_{16}H_{33})^+$ in the modified MCM-41 matrix (2.18 ms) is much longer than that of neat $[Eu(tta)_4]^-(C_5H_5NC_{16}H_{33})^+$ powder (0.84 ms). Encapsulation of the europium(III) complex in the MCM-41 host improved the photostability of the complex as well. In a follow-up study, the MCM-41 host was modified with (3-chloropropyl)triethoxysilane and (1*R*,2*R*)-(−)-1,2-diaminocyclohexane.[673] This resulted in the formation of nonpolar chiral channels. The luminescence properties of $[Eu(tta)_4]^-(C_5H_5NC_{16}H_{33})^+$ in this host were better than that of the same complex in MCM-41. Fu et al. modified MCM-41 with 3-aminopropyltriethoxysilane (APTES) or *N*-[(3-triethoxysilyl)propyl]ethylenediamine (TEPED), and encapsulated the europium complex $[Eu(dbm)_3(phen)]$ in the modified hosts.[674] In this case, the $I(^5D_0 \rightarrow {}^7F_2)/I(^5D_0 \rightarrow {}^7F_1)$ intensity ratio was much lower (2.7 for the host modified by APTES and 1.7 for the host modified by TEPED) than for the tetrakis(2-thenoyltrifluoroactylacetonato)europate(III) complex discussed above. The thermal stability of the $[Eu(tta)_3]$ complex was improved by encapsulation in MCM-41.[675] The $[Eu(tta)_3]$ molecules were found to be present within the cetyltrimethylammonium micelles that were used as template to prepare MCM-41.[676] Acid treatment of the molecular sieve to remove the surfactant template also removed the europium(III) complex. Europium luminescence was not observed in the precursor solution that was used to make the molecular sieve. A luminescent complex was formed upon heat treatment, because the 2-thenoyltrifluoroacetonate molecules could then diffuse to the Eu^{3+} sites to form $[Eu(tta)_3]$ complexes. The luminescence lifetime of $[Eu(tta)_3]$/MCM-41 (228 μs) was found to be similar to that measured for $[Eu(tta)_3]$ in ethanolic solution (226 μs). $[Eu(dbm)_3(H_2O)_2]$ was impregnated in cubic MCM-48.[677] Fernandes et al. incorporated $[Eu(thd)_3]$ and $[Eu(dbm)_3]$ complexes in MCM-41, either by wet impregnation of the MCM-41 with a solution of the europium(III) complex or by reaction between the matrix and the europium(III) complex in the gas phase.[678] The europium(III) complexes were immobilized on the silica matrix by grafting them on the free silanol groups at the surface. The luminescence spectra of the europium(III) complexes changed after incorporation in the MCM-41, but ligand-to-metal energy transfer could still be observed. The luminescence performance of these materials could greatly be improved by coordination of 1,10-phenanthroline or 2,2′-bipyridine to the Eu^{3+} ion.[679] Different terbium(III) complexes of the type $Tb(phen)_x(bipy)_{4-x}(NO_3)_3$ ($x = 4, 3, 2, 1, 0$) were incorporated in mesoporous molecular sieves.[680] It was observed that the luminescence of the complexes encapsulated in the polar pores of MCM-41 was weaker than that of complexes in the nonpolar pores of trimethylsilyl-functionalized MCM-41, $(CH_3)_3Si$-MCM-41. In the trimethylsilyl-functionalized (or silylated) MCM-41, the silanol groups on the surface are replaced by trimethylsilyl groups. The advantage of silylation of MCM-41 for improving lanthanide luminescence was also reported for europium(III) dibenzoylmethanate complexes in mesoporous MCM-48.[681] Another method to block the silanol groups on the surface is by reaction of the walls of the mesoporous host with phenyltriethoxysilane, $PhSi(OEt)_3$.[682] Incorporation of $[Eu(phen)_2]^{3+}$ in a surface-functionalized MCM-41 host resulted in a material that emits both in the blue (1,10-phenanthroline emission) and in the red region (Eu^{3+} emission). Lanthanide(III) complexes of bis(perfluoroalkylsulfonyl)imide impregnated MCM-41 were described as heterogeneous catalysts for aromatic nitration.[683] These hybrid materials could have some potential as near-infrared-emitting materials, but this has not been investigated yet.[684] The same remark can be made for lanthanide(III) triflates impregnated in MCM-41.[685] The $[Eu(dbm)_3(phen)]$ complex was formed *in situ* in mesophase thin films, which were prepared by hydrolysis of TEOS in the presence of Pluronic P123 triblock copolymer surfactant. A higher quantum yield was reported for the europium(III) complex in the mesostructured thin silica films than for the pure europium(III) complex.[686] Most of the MCM-41 host materials used for the preparation of lanthanide-containing hybrid materials are

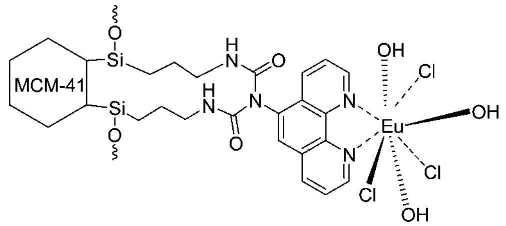

Figure 50. Europium(III) phenanthroline complex covalently linked to the mesoporous MCM-41 matrix.[699]

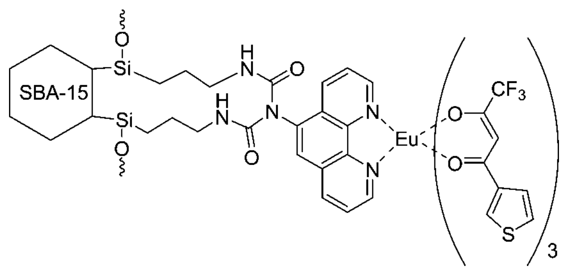

Figure 51. [Eu(tta)$_3$(phen)] complex covalently attached to the mesoporous SBA-15 matrix.[701]

made of mesoporous amorphous silica, prepared by the hydrolysis of TEOS in the presence of a cationic surfactant. Studies on MCM-41 materials with an aluminosilicate composition are less common. Aquino et al. prepared aluminum-containing MCM-41 impregnated with Eu-$(NO_3)_3$.[687] The thermostability and photostability of [Eu(tta)$_3$(tppo)$_2$] and [Eu(bzac)$_3$(tppo)$_2$] was found to be improved after incorporation in SBA-15.[688] Multicolor emission was observed for hexagonal mesostructured silica doped with Eu^{3+} (red emission), Tb^{3+} (green emission), and 1,10-phenanthroline (blue emission).[689] The emission color covered the whole visible range and could be fine-tuned by changing the ratios among the different components and by fine-tuning the excitation wavelength. Tiseanu et al. compared the photoluminescence properties of europium(III) complexes grafted via different coordinating groups on silica and on mesoporous MCM-41.[690]

Although the surfactants used for the synthesis of SBA-15 are generally removed after synthesis, Bartl et al. obtained luminescent mesostructured block-copolymer/silica thin films activated by lanthanide(III) 1,10-phenanthroline complexes by leaving the surfactant molecules intact in the mesoporous silica matrix.[691] The high solubility of 1,10-phenanthroline in the Pluronic 123 block copolymer facilitated the formation of the lanthanide(III) complexes. Mesoporous materials that still contain the templating surfactant can be used to spatially separate different doping molecules.[692−695] Mesostructured silicate films templated by cationic surfactants contain three spatially separated regions: a silicate framework, an organic region formed by the hydrocarbon tails of the surfactants, and an intervening ionic interface formed by the charged surfactant head groups. Lipophilic molecules can be solubilized by the nonpolar chains of the surfactant molecules. Hydrophilic molecules are incorporated in a region close to the charged headgroup of the surfactant molecules or are adsorbed by the walls of the mesoporous host. Functionalized molecules can be covalently bonded to the silica walls of the host matrix.

The classic methods for incorporation of lanthanide complexes in the mesoporous host are based on wet chemical routes. Volatile lanthanide complexes, like those derived from the β-diketones 2,2,6,6-tetramethyl-3,5-heptanedione (Hthd) or 6,6,7,7,8,8,8-heptafluoro-2,2-dimethyl-3,5-octanedione (Hfod) can be introduced in the host in the vapor phase.[696−698] This method is called *chemical vapor infiltration* (CVI), and has two variants, the *static vapor phase (SVP)* method and the *dynamic vapor phase (DVP)* method. The SVP method makes use of a sealed container, whereas the DVP method is based on a continuous flow reactor. This methodology has been applied for the incorporation of europium(III) and gadolinium(III) complexes into MCM-41.

Just like in the case of ormosils, it is possible to covalently bind luminescent lanthanide complexes to the host matrix, in this case the wall of the mesoporous host materials. The grafting of the complexes to the walls of the host is a good strategy to prevent leaching of the lanthanide complex out of the host matrix. Li et al. grafted 1,10-phenanthroline to the walls of MCM-41 and prepared the corresponding europium(III) complex by reaction with hydrated $EuCl_3$ (Figure 50).[699] The luminescence of this material was mainly caused by blue emission of the 1,10-phenanthroline ligand. The characteristic red emission of Eu^{3+} was only weak and always observed in combination with the blue ligand emission. This indicates that the energy transfer from 1,10-phenanthroline to Eu^{3+} is not efficient. The luminescence performance of these hybrid materials could significantly be improved by using β-dike-

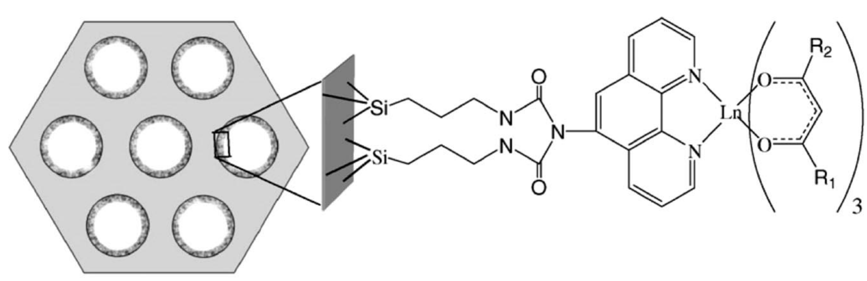

Ln	R_1	R_2
Er, Nd, Yb, Sm		C_3F_7
Pr	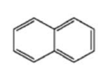	CF_3

Figure 52. Schematic structure of hybrid materials [Ln(hfth)$_3$phen−MCM41] (Ln = Sm, Nd, Er, Yb) and [Pr(tfnb)$_3$phen−MCM41] mesoporous materials. Reprinted with permission from ref 702. Copyright 2006 Elsevier.

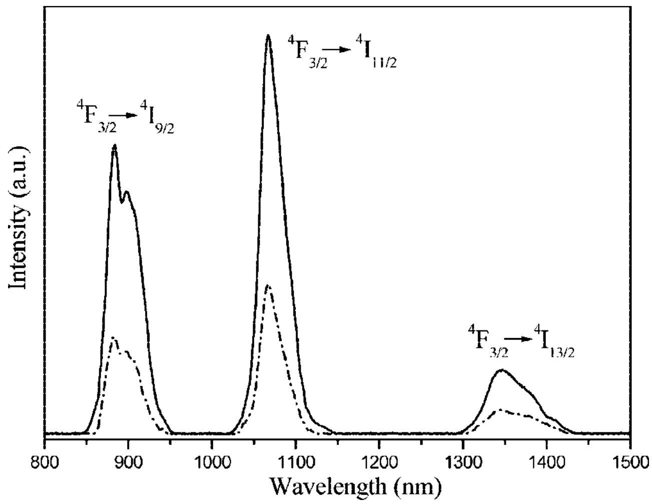

Figure 53. Luminescence spectra of [Nd(dbm)$_3$(phen)]−MCM-41 (−•−) and [Nd(dbm)$_3$(phen)]−SBA-15 (—) (λ_{exc} = 397 nm). Reprinted with permission from ref 704. Copyright 2006 American Chemical Society.

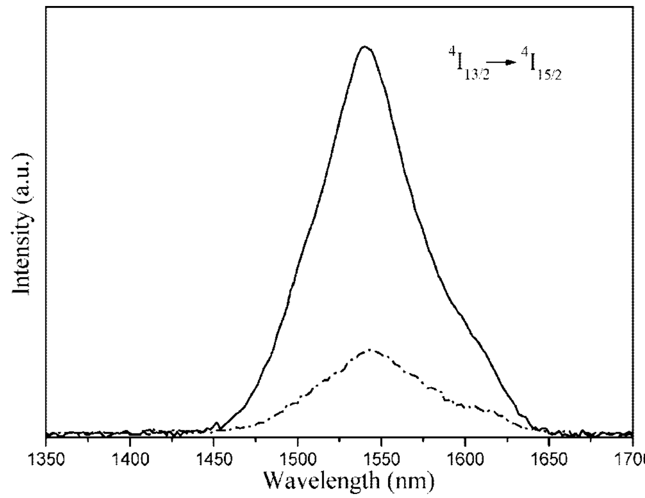

Figure 54. Luminescence spectra of [Er(dbm)$_3$(phen)]−MCM-41 (−•−) and [Er(dbm)$_3$(phen)]−SBA-15 (—) (λ_{exc} = 397 nm). Reprinted with permission from ref 704. Copyright 2006 American Chemical Society.

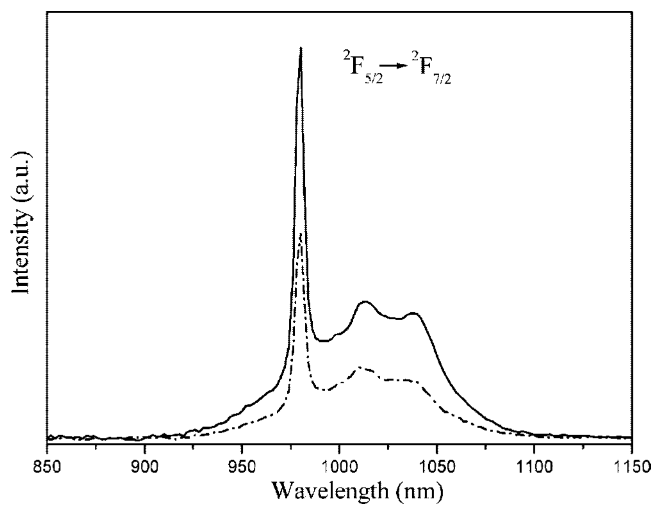

Figure 55. Luminescence spectra of [Yb(dbm)$_3$(phen)]−MCM-41 (−•−) and [Yb(dbm)$_3$(phen)]−SBA-15 (—) (λ_{exc} = 397 nm). Reprinted with permission from ref 704. Copyright 2006 American Chemical Society.

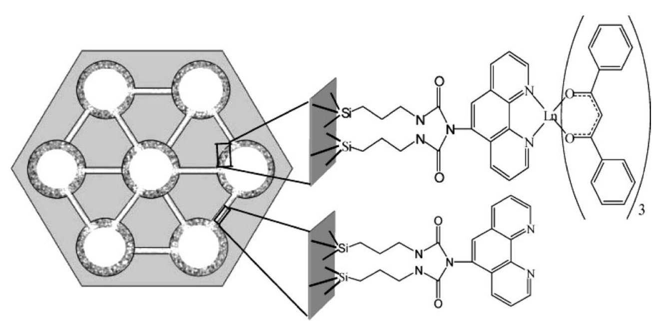

Figure 56. Schematic representation of the [Ln(dbm)$_3$(phen)]−SBA-15 structure with micropores, in which the grafted 1,10-phenanthroline ligands are not accessible for coordination to [Ln(dbm)$_3$]. Reprinted with permission from ref 704. Copyright 2006 American Chemical Society.

tonate ligands besides 1,10-phenanthroline. Peng et al. obtained highly luminescent materials by grafting [Eu(tta)$_3$phen] complexes to mesoporous SBA-15 (Figure 51).[700,701] The integrated luminescence intensity of Eu(tta)$_3$(phen)−SBA-15 was about six times higher than that of the corresponding material without tta ligands, Eu(phen)−SBA-15, and about 30 times higher than that of Eu(tta)$_3$•2H$_2$O adsorbed on SBA-15. Whereas Eu(phen)−SBA-15 samples showed blue luminescence of the 1,10-phenanthroline ligand besides the red Eu^{3+} luminescence, no ligand emission could be detected for Eu(tta)$_3$(phen)−SBA-15. This indicates that the energy transfer from the ligands to the Eu^{3+} ion was very efficient in Eu(tta)$_3$(phen)−SBA-15. The work on Eu^{3+} complexes was extended to the near-infrared-emitting complexes of Pr^{3+}, Sm^{3+}, Nd^{3+}, Er^{3+}, and Yb^{3+} with the perfluorinated β-diketonates 4,4,5,5,6,6,6-heptafluoro-1-(2-thienyl)hexane-1,3-dionate (hfth) and 4,4,4-trifluoro-1-(2-naphthyl)-1,3-butanedionate (tfnb) (Figure 52).[702] The ligand hfth was used to form complexes with Ln = Sm, Nd, Er, or Yb and tfnb for Ln = Pr. Near-infrared emission was also observed for [Tm(dbm)$_3$(phen)] covalently linked to MCM-41.[703] A comparative study of [Ln(dbm)$_3$(phen)] (Ln = Nd, Er, Yb) complexes immobilized via the 1,10-phenanthroline ligand on MCM-41 and SBA-15 showed that higher luminescence intensities could be obtained for the complexes in the SBA-15 matrix (Figures 53−55).[704] At the same time, the luminescence lifetimes were shorter for the lanthanide complexes in MCM-41 than in SBA-15. The poorer luminescence performance of the MCM-41-based materials was attributed to the higher number of residual silanol groups on the walls of MCM-41. In general, the materials derived from SBA-15 have a lower lanthanide content than those derived from MCM-41 because the 1,10-phenanthroline ligands in the micropores of SBA-15 are unavailable for complex formation with Ln(dbm)$_3$ (Figure 56). The luminescence behavior of [Eu(tta)$_3$phen] grafted to SBA-15 was compared with that of the same complex tethered to a mesoporous organosilica host, and the best luminescence performance was found for the material derived from SBA-15.[705]

Covalent linking of Eu(β-diketonate)$_3$(phen) complexes to a mesoporous host matrix is not restricted to grafting via a functionalized 1,10-phenanthroline. Li et al. illustrated that the immobilization of the lanthanide complex can also be achieved via functionalized β-diketonate ligands (Figure 57).[706] They reacted naphthoyltrifluoroacetone with 3-(triethoxysilyl)propyl isocyanate, which resulted in the formation of a reactive β-diketonate ligand with two 3-(triethoxysilyl-

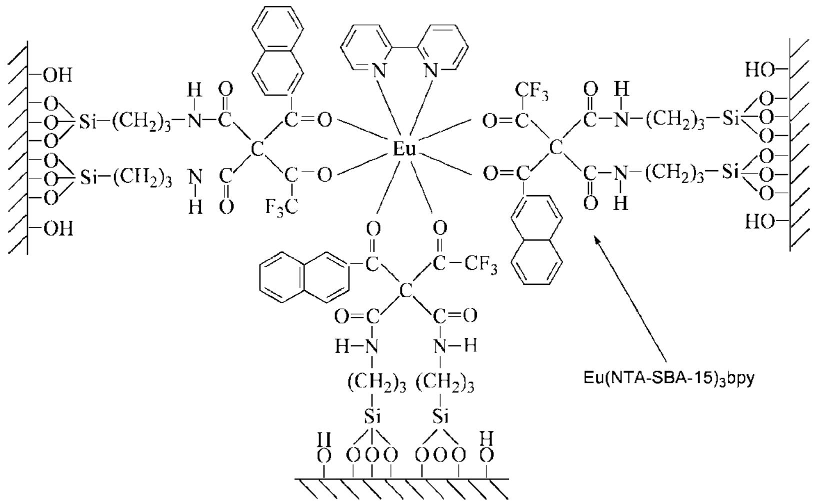

Figure 57. Structural model for the hybrid materials Eu(nta−SBA-15)$_3$(bipy). Reprinted with permission from ref 706. Copyright 2008 American Chemical Society.

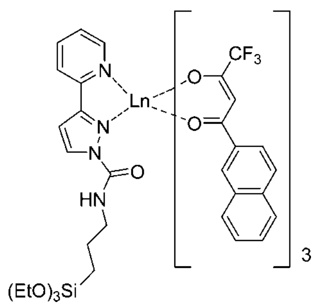

Figure 58. Europium(III) β-diketonate complex with a functionalized pyrazolylpyiridine ligand.

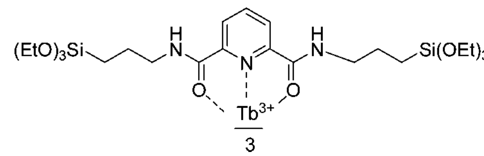

Figure 59. Terbium(III) complex of dipicolinic acid derivative with triethoxysilyl groups.

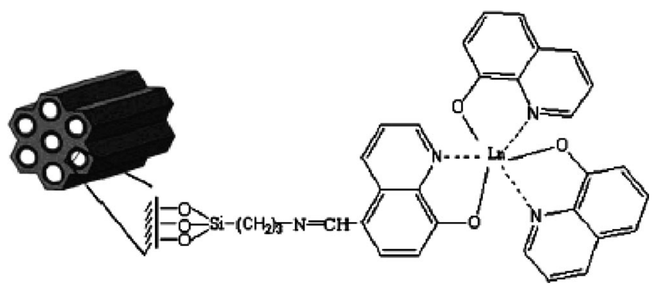

Figure 60. Lanthanide(III) 8-hydroxyquinolinate complex covalently bonded to the SBA-15 mesoporous host. Reproduced with permission from ref 715. Copyright 2008 American Chemical Society.

)propyl groups attached to the 2-position. A difference between the resulting material and that obtained by grafting via 1,10-phenanthroline is that the lanthanide complex is attached via three positions to the host matrix instead of one. The coordination sphere of the Eu^{3+} complex formed by these ligands was completed by a 2,2′-bipyridine coligand. In a subsequent paper, the authors showed that also other β-diketonates like acetylacetone and dibenzoylmethane can be functionalized in a similar way.[707] Dibenzoylmethane was functionalized in the 2-position by reaction with 3-chloropropyltrimethoxysilane, and this functionalized ligand was incorporated into hexagonal porous silica. Reaction of the sodium salt of the immobilized dibenzoylmethane ligand with $EuCl_3$ in the presence of sodium dibenzoylmethanate resulted in the formation of Eu(dbm)$_3$ complexes linked via one spacer to the porous silica matrix.[708] In a similar way Eu(tta)$_3$ was grafted to MCM-41[709] and Tb(acac)$_3$ to SBA-15.[710] Li and Yan linked Eu^{3+} and Tb^{3+} to MCM-41 via a modified *meta*-methylbenzoic acid.[711] Guo et al. prepared a mesoporous material through a one-step co-condensation of 1,2-bis(triethoxysilyl)ethane and a benzoic acid-functionalized organosilane using cetyltrimethylammonium bromide as the templating agent.[712] Impregnation of the solid material with terbium(III) chloride resulted in the formation of a green-emitting mesoporous luminescent material. Gago et al. grafted a Eu(nta)$_3$ complex via a functionalized pyrazolylpyridine ligand to MCM-41 (Figure 58).[713] Dipicolinic acid derivatives with trialkoxysilyl groups were used to graft Eu^{3+} and Tb^{3+} ions to hexagonal mesostructured silica thin films (Figure 59).[693,694] Codoping of Tb^{3+}-containing films with rhodamine 6G caused quenching of the Tb^{3+} luminescence, because of energy transfer from the Tb^{3+} to the organic fluorescent dye. Although europium(III) and terbium(III) complexes of 8-hydroxyquinoline do not show lanthanide-centered luminescence, 8-hydroxyquinoline is a useful ligands to obtain near-infrared-emitting lanthanide complexes.[714] Sun and co-workers prepared hybrid materials by grafting 8-hydroxyquinoline complexes of Nd^{3+}, Er^{3+}, and Yb^{3+} to SBA-15 (Figure 60).[715] Pyridyl groups were grafted to the surface of MCM-41 by reaction with 3-triethoxysilylpropyl 4-pyridylacetamide.[716] Upon treatment of the pyridyl-functionalized MCM-41 with a chloroform solution of europium(III) tris-1-(2-naphthoyl)-3,3,3-trifluoroacetonate, a luminescent hybrid material was obtained. Residual coordinated water molecules were subsequently replaced by pyridine or methyl phenyl sulfoxide. Eu(dbm)$_3$ complexes were tethered to MCM-41 via a modified bidentate bis(phosphino)amine oxide ligand.[717]

Corriu and co-workers prepared mesoporous SBA-15 with *N*-propylcyclam macrocycles coordinated to the pore walls.[718] Treatment of the solids with different amounts of cyclam moieties with $EuCl_3$ in ethanol gave 1:1 Eu^{3+}/cyclam complexes (Figure 61). EXAFS measurements revealed that

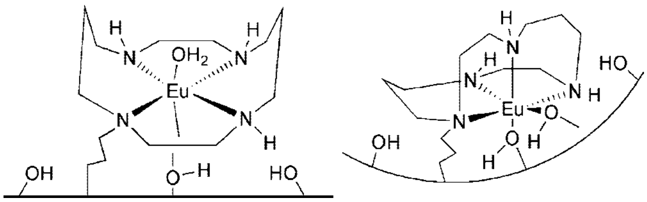

Figure 61. Different coordination spheres of six-coordinate Eu^{3+} ions in a cyclam-functionalized SBA-15 mesoporous matrix. Reproduced from ref 718 (http://dx.doi.org/10.1039/b307526e) by permission of The Royal Society of Chemistry (RSC) for the Centre National de la Recherche Scientifique (CNRS) and the RSC. Copyright 2004 Royal Society of Chemistry.

Chart 10. Organosilylated Quinizarin Derivatives

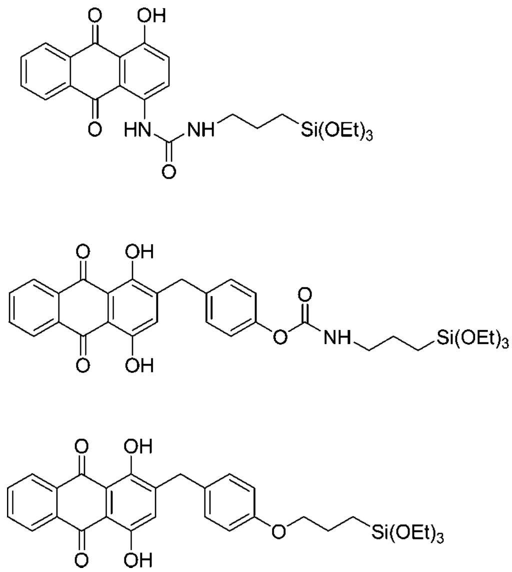

the coordination number of Eu^{3+} is six, irrespective of the concentration of cyclam moieties in the mesoporous material. It was proposed that the Eu^{3+} is octahedrally coordinated, with the octahedron being formed by the four nitrogen atoms of the cyclam macrocycle and by two additional oxygen groups from either water molecules or silanol groups. No coordination by chloride ions occurred.

Europium(III)-doped mesoporous materials with quinizarin chromophores were obtained by co-condensation of TEOS with an organosilylated quinizarin derivative in the presence of a cationic surfactant (CTAB), followed by soaking of the thin films in a solution of a europium(III) salt (Chart 10).[719] Europium(III) salts investigated were $Eu(acac)_3 \cdot xH_2O$, $EuCl_3 \cdot xH_2O$, and $Eu(NO_3)_3 \cdot xH_2O$. The complex formation between quinizarin and Eu^{3+} ions could be visually detected by a color change of the films upon complexation. The Eu^{3+} ions quench the fluorescence of quinizarin, because of energy transfer from the organic ligand to the Eu^{3+} ion. The highest luminescence intensity was observed for the acetylacetonate complexes. The encapsulation of lanthanide-containing polyoxometalate complexes in mesoporous hosts is described in section 6.

Europium(III) β-diketonate complexes have been tethered to a so-called Si(HIPE), which is a foam-like organosilica-based hybrid material exhibiting a hierarchically structured bimodal porous structure.[720] These hierarchical inorganic porous materials can be obtained as monoliths using concentrated emulsion and micellar templates.[721] The texture of the monoliths can be tuned by varying the pH of the continuous aqueous phase, the emulsification process, or the oil volumic fraction. Si(HIPE) shows interconnected macroporosity associated with vermicular-type mesostructuration.

5. Intercalation Compounds

Intercalation compounds are formed by the inclusion of molecules between the layers of a solid matrix with a lamellar structure. By intercalation of the guest, the layer-to-layer distance in the host is increased. Typical examples are *layered double hydroxides* (*LDHs*) containing organic guests[722] or coordination compounds.[723] Intercalation of lanthanide(III) complexes into a layered inorganic host has a beneficial effect on both the complex stability and the luminescence performance. This observation is similar to what is noticed for lanthanide complexes doped in hybrid sol−gel matrices.

Inorganic−organic materials with a controlled porosity can be obtained by replacing the acidic phosphates exposed in the lamellae of γ-zirconium phosphate, $Zr(PO_4)(H_2PO_4) \cdot 2H_2O$ by organic diphosphonic acids. Brunet et al. described a γ-zirconium phosphate modified with poly(ethylene oxide) chains and doped with lanthanide(III) ions (Ln = Eu, Tb) and with 2,2′-bipyridine as sensitizer.[724] Xu et al. prepared the layered compound zirconium bis(monohydrogenphosphate) intercalated with the europium(III) complex $[Eu(dbm)_3(phen)]$ or the terbium(III) complex $[Tb(acac)_3(phen)]$ by exchanging the lanthanide complexes into the *para*-methyoxyaniline (PMA) preintercalated compound $Zr(O_3POH)_2 \cdot 2PMA$.[725,726] Different lanthanide ions (Ln = Sm, Eu, Tb, Dy) were incorporated in a mixed zirconium phenyl and *meta*-sulfophenyl phosphonate host matrix.[727] The energy transfer from uranyl to europium(III) ions in α-carboxyethyl zirconium(IV) phosphonate was described.[728] The binding of the uranyl donors and the europium(III) acceptors to the matrix resulted in an enhanced energy transfer from the donor to the acceptor in comparison with these ions in solution. Lanthanide bisphosphonates were pillared with chiral crown ethers.[729] Composite materials of exfoliated titania nanosheets, $Ti_{0.91}O_2$, and the complexes $Eu(phen)_2Cl_3 \cdot 2H_2O$ and $Tb(phen)_2Cl_3 \cdot 2H_2O$ were described.[730] Although red luminescence was observed for the europium(III)-containing material, no metal-centered luminescence could be measured for the corresponding terbium(III)-containing material. A series of pyridine intercalation compounds, $(py)_xLnOCl$, was prepared by reactions of pyridine with lanthanide oxides (Ln = Ho, Er, Tm, and Yb).[731] An acid−base interaction was proposed for the mode of intercalation of pyridine into the lanthanide oxychlorides. It was found that the C_2-axes of the pyridine molecules were oriented perpendicular to the LnOCl layers.

Crystalline lanthanide oxide layers separated by organic layers of intercalated benzoate molecules were prepared by reaction of lanthanide(III) isopropoxides with benzyl alcohol in an autoclave at a temperature between 250 and 300 °C.[732−735] The rare-earth oxide catalyzed two low-temperature hydride transfer reactions to form benzoic acid and toluene from benzyl alcohol via benzaldehyde, whereas a C−C bond formation occurred between benzyl alcohol and the isopropanolate ligand.[736] Although the lamellar structure is kept together by only the $\pi-\pi$ interactions between the phenyl rings, these materials have a remarkably high thermal stability to temperatures up to 400 °C. The phenyl rings act as antennas, which transfer the excitation energy to the lanthanide ion. Luminescence has been demonstrated for Eu^{3+}, Tb^{3+}, Nd^{3+}, and Er^{3+} ions. An advantage of such hybrid materials is that the excitation wavelength is shifted to the visible region in comparison with that of conventional inorganic lanthanide phosphors. Related nanostructured materials were obtained by reaction between lanthanide(III) isoproxides and 4-biphenyl methanol.[737]

Sousa et al. reported on luminescent polyoxometalate anion-pillared layered double hydroxides (LDHs) containing the polyoxotungstate anions $[EuW_{10}O_{36}]^{9-}$, $[Eu(BW_{11}O_{39})(H_2O)_3]^{6-}$, and $[Eu(PW_{11}O_{39})_2]^{11-}$.[738] The europium(III) complex $[Eu(EDTA)]^-$ was incorporated into a Mg−Al layered double hydroxide.[739] Also $[Ln(pic)_4]^-$ complexes (pic = picolinate) (Ln = Eu, Tb) were enclosed into that matrix.[740] The energy transfer in mixed Eu^{3+}/Tb^{3+} systems was investigated.[741] A Zn−Al layered double hydroxide pillared by 2,2′-bipyridine-5,5′-dicarboxylate (BDC) anions was selected as a porous matrix to intercalate $LnCl_3$ (Ln = Eu, Gd).[742] Li et al. incorporated europium(II) complexes of ethylenediaminetetraacetate (EDTA) and nitrilotriacetate (NTA), $[Eu(EDTA)(H_2O)_3]^-$ and $[Eu(NTA)_2(H_2O)]^{3-}$, in Zn−Al layered double hydroxides.[743] The authors have investigated the orientation of the anionic europium(III) complexes within the layers of the inorganic host.

Different types of clay minerals have been used as a host for luminescent lanthanide complexes. The europium(III) complexes $[Eu(bipyO_2)_4Cl_2]^+$ and $[Eu(bipyO_2)_4]^{3+}$ were intercalated into the interlayer spacing of montmorillonite clay.[744] A luminescent lanthanide-containing hectorite clay was obtained by first exchanging the cations in the clay by Tb^{3+} ions, followed by exposing the terbium(III)-exchanged clay to 2,2′-bipyridine vapor.[745] The gas-phase reaction resulted in the formation of $[Tb(bipy)_3]^{3+}$ complexes in the hectorite clay. Although the resulting hybrid material showed intense green luminescence, it was found that iron impurities had a negative effect on the luminescence efficiency. Europium(III)-containing composites were made by incorporation of $[Eu(bipy)_3]^{3+}$ in bentonite clay.[746] Complexes of europium(III) and terbium(III) with 2,2′-bipyridine and 1,10-phenanthroline were incorporared in a Na-bentonite via an ion exchange reaction.[747]

6. Polyoxometalates (POMs)

Polyoxometalates (*POMs*) are oxygen cluster anions formed by early transition metals (V, Nb, Ta, Mo, W) in their highest oxidation state. The chemistry of POMs is dominated by molybdenum and tungsten in their +6 oxidation state. An amazing rich variety of polyoxometalate complexes has been described in the literature.[748−750] Polyoxometalates find applications in many fields including materials sciences,[751,752] analytical chemistry,[753] medicine,[754] and catalysis.[755,756] Some polyoxometalate clusters can acts as ligands for lanthanide ions.[757−759] Lanthanide-containing polyoxometalates have recently been reviewed by Pople[760] and by Yamase.[761] Of all the known lanthanide-containing polyoxometalates, the lanthanide decatungstates, and especially the europium decatungstate or decatungstoeuropate(9−) anion, shows the best luminescence performance. This polyoxoanion was first prepared as a potassium salt by Peacock and Weakley and originally formulated as $[EuW_{10}O_{35}]^{7-}$,[762] but later studies revealed that its composition is in fact $[EuW_{10}O_{36}]^{9-}$.[763] The crystal structure of $Na_9[EuW_{10}O_{36}]\cdot 32H_2O$ was described by Sugeta and Yamase.[764] The $[EuW_{10}O_{36}]^{9-}$ anion consists of two $[W_5O_{18}]^{6-}$ fragments (each consisting of five WO_6 octahedra sharing edges) coordinating to the Eu^{3+} ion. The eight oxygen atoms (four of each W_5O_{18} fragment) around Eu^{3+} define a slightly distorted square antiprism (Figure 62). The approximate symmetry is C_{4v}. No water molecules are directly coordinated to the Eu^{3+} ion. The spectroscopic properties of the $[EuW_{10}O_{36}]^{9-}$ complex have been studied by several authors.[765−769] Photoexcitation in the intense ligand-to-metal excitation band (O → W LMCT band) between 250 and 360 nm led to the observation of the typical red photoluminescence of the Eu^{3+} ion. Besides the $[EuW_{10}O_{36}]^{9-}$ complex, strong luminescence was observed for $[Eu(SiW_{10}Mo_{39})_2]^{13-}$ and for $[Eu_2CeMo_{12}O_{42}]^{6-}$.[770,771] In contrast, the luminescence of the complexes $[Eu(SiW_{11}O_{39})_2]^{13-}$, $[Eu(PW_{17}O_{61})_2]^{17-}$, $[EuP_5W_{30}O_{110}]^{12-}$, $[EuAs_4W_{40}O_{140}]^{25-}$, and $[EuSb_9W_{21}O_{86}]^{16-}$ was much weaker.[759] No charge transfer from the ligand to the Eu^{3+} ion occurred. Notice that in the complexes $[EuP_5W_{30}O_{110}]^{12-}$, $[EuAs_4W_{40}O_{140}]^{25-}$, and $[EuSb_9W_{21}O_{86}]^{16-}$, the Eu^{3+} is encapsulated inside the polyoxometalate. The polyoxometalate acts as an inorganic cryptand, although the ligands cannot efficiently shield the Eu^{3+} ions from coordinating water molecules. The W atoms in $[Eu(SiW_{11}O_{39})_2]^{13-}$ can partially or totally be replaced by Mo atoms, giving rise to the formation of a series of complexes with the general formula $[Eu(SiW_{11-x}Mo_xO_{39})_2]^{13-}$. The luminescence intensity of the complexes decreases with an increase in Mo content (increase in x). Most of the attention about lanthanide ions in polyoxometalate complexes has been given to Eu^{3+} and Tb^{3+}. Very few studies report on complexes with near-infrared-emitting lanthanide ions. NIR emission was described for a series of neodymium-containing polyoxometalates in aqueous solution.[772]

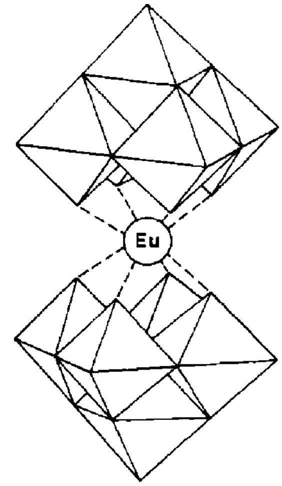

Figure 62. Structure of the $[EuW_{10}O_{36}]^{9-}$ anion. Reprinted with permission from ref 768. Copyright 1984 American Chemical Society.

Typically, lanthanide-containing polyoxometalate complexes have Na^+, K^+, or NH_4^+ counterions, and the resulting salts are water-soluble. In order to obtain polyoxometalate complexes soluble in organic solvents, the small inorganic counterions can be replaced by large organic counterions. These counterions range from tetrabutylammonium ions[773−775] over brucinium[776] to different phosphorus-containing ions like $Ph_3P^+CPh_3$, Ph_3P^+Et, $Ph_3P^+C_{16}H_{33}$, Ph_4P^+, or Bu_4P^+.[777] In some cases not all counterions are replaced by organic counterions, and the negative charge of the polyoxoanion is partially compensated by protons. An example is a complex like $(Bu_4N)_5H_2[\alpha_1\text{-}Eu(H_2O)_4P_2W_{17}O_{61}]$, where α_1 points to the fact that the compound is a monolacunary polyoxometa-

Chart 11. Hydrophobic Cations Used in Hybrid Polyoxometalate Hybrid Materials

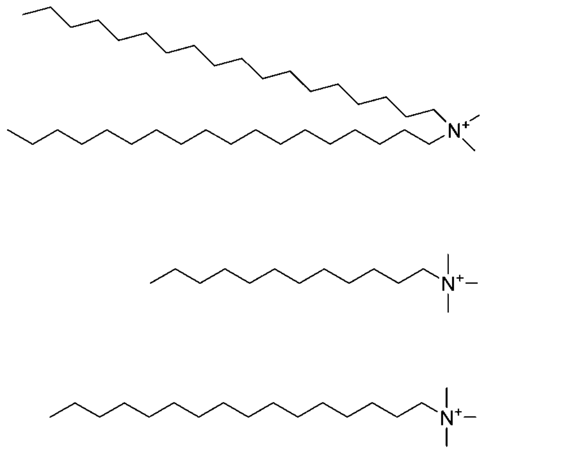

late.[778] *Surfactant encapsulation* is a technique that is often used for obtaining polyoxometalates that are soluble in organic solvent.[779−784] This technique consists of replacing the inorganic countercations with cationic surfactant molecules. By creation of a hydrophobic shell around the polyoxometalate cluster, water molecules are expelled from the direct environment of the POM. This has a beneficial effect on the luminescence properties of lanthanide-containing POMs. Typical hydrophobic counterions are dimethyldioctadecylammonium (DODA), dodecyltrimethylammonium (DDTA), or hexadecyltrimethylammonium (CTA) (Chart 11). Incorporation of the $[EuW_{10}O_{36}]^{9-}$ ion gave strongly red-emitting hybrid materials. Orange photoluminescence was observed for $(DDTA)_9[SmW_{10}O_{36}]\cdot xH_2O$ in chloroform.[785,786] Some of these surfactant-encapsulated polyoxometalate complexes exhibited liquid-crystalline behavior. Stable smectic mesophases were observed for materials based on the surfactant *N*-[12-(4-carboxylphenoxy)dodecyl]-*N*-dodecyl-*N*,*N*-dimethylammonium, which is a benzoic acid terminated surfactant.[787] The mesophases are stabilized by the intermolecular hydrogen bond interactions between the benzoic acid moieties. Zhang et al. described a luminescent logic gate based on surfactant-encapsulated $[EuW_{10}O_{36}]^{9-}$ complexes.[784] The cationic surfactant contained a stilbazole function, which can undergo a *cis*−*trans* isomerization under UV irradiation (Figure 63). The logic gate was able to generate the INHIBIT and NOR logic functions. The input were metal ions (Zn^{2+}) or UV radiation (365 nm), whereas the output was luminescent light at 480 nm (stilbazole emission) or 614 nm (Eu^{3+} emission). The luminescence was excited with UV radiation of 260 nm. The irradiation at 365 nm induces *cis*−*trans* isomerization in the stilbazole group of the surfactant. The luminescence intensity at 480 nm was high only when UV radiation was absent and Zn^{2+} ions were present. This expresses the INHIBIT logic function. The luminescence intensity at 614 nm was high when both UV radiation and Zn^{2+} were absent. This expresses the NOR

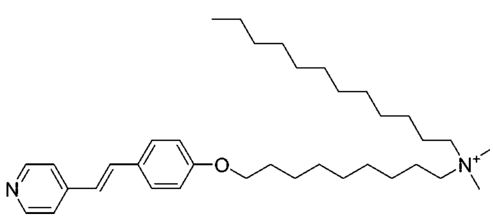

Figure 63. Quaternary ammonium cation containing a photoactive stilbazole group.

Figure 64. Sulfonated polystyrene polyelectrolyte (left) and poly(allylamine hydrochloride) polyelectrolyte (right)

logic gate function. For more background information on molecular logic, the reader is referred to other review papers.[788−790]

Thin films of lanthanide-containing polyoxometalates have been prepared by several methods, including via the Langmuir−Blodgett (LB) technique, electrostatic self-assembly (ESA), or simple solvent casting. Langmuir−Blodgett films of polyoxometalates are generally prepared by spreading a solution of a cationic surfactant on the surface of a dilute aqueous solution of the POM. The POMs are absorbed on the positively charged Langmuir monolayer of the cationic surfactant on a substrate. By repetition of the procedure, Langmuir−Blodgett multilayers are formed. A review on polyoxometalates incorporated in Langmuir−Blodgett films is available.[791] After the pioneering work of Sousa et al., who deposited Langmuir−Blodgett films of a polyoxotungstoeuropate complex with different surfactant cations on a quartz glass slide,[792] several other papers on LB films of lanthanide-containing polyoxometalates have been published. Polyoxometalate fragments entrapped in LB films include $[EuW_{10}O_{36}]^{9-}$,[793−799] $[Eu(XW_{11}O_{39})_2]^{n-}$ (X = Ge, Si, B; n = 13, 15),[800] $[SmW_{10}O_{36}]^{9-}$,[797,801] and $[Tb(XW_{11}O_{39})_2]^{n-}$ (X = P, Si, B, n = 11, 13, 15).[802] Langmuir−Blodgett films of $[EuW_{10}O_{36}]^{9-}$ were found to be sensitive to acidic and basic gases.[795] When films with *n*-octadecylamine (ODA) or 4-hexadecylaniline (HDA) were exposed to HCl gas, their photoluminescence disappeared completely, but the photoluminescence was recovered upon exposure to NH_3 gas. The protonation of the amine group plays an important role in the switching of the luminescence from on to off. The *layer-by-layer self-assembly* technique involves repeated dipping of a charged-surface slide in polycation and polyanion solutions, with intermediate washing steps, resulting in the alternate deposition of the corresponding polyions.[803−805] Typical polyelectrolytes are sulfonated polystyrene and poly(allylamine hydrochloride) (Figure 64). Other terms used to designate *layer-by-layer self-assembly* are *electrostatic layer-by-layer self-assembly* (ELSA),[806] *electrostatic self-assembly* (ESA),[807] or *ionic self-assembly* (ISA).[808] Thin films incorporating the Preyssler-type anion $[Eu(H_2O)P_5W_{30}O_{110}]^{12-}$ were prepared by a layer-to-layer self-assembly process on an ITO plate with poly(allylamine hydrochloride) and poly(styrene sulfonate) as the oppositely charged polyelectrolytes.[809] The films showed an electrochromic behavior: they are colorless in the oxidized forms, while they are blue in the oxidized form (exhibiting a broad absorption band with maximum at ca. 700 nm). A film with a thickness of 1 μm in the oxidized form had an absorbance of about 1 at 700 nm. The electrochromic system was found to be stable over more than 500 reduction−oxidation cycles. The blue color persisted for more than 30 min without power consumption. Luminescent inorganic−organic hybrid films incorporating $K_{10}H_3[Eu(SiMo_9W_2O_{39})_2]\cdot xH_2O$ and $[Ru(bipy)_3]^{2+}$ were prepared via electrostatic self-assembly.[810] The emission spectra were dominated by the broadband red emission of the $[Ru(bipy)_3]^{2+}$ complex, but upon direct excitation in the $^5L_6$ level of Eu^{3+} at 393 nm, the characteristic narrow f−f transitions of Eu^{3+} were observed superimposed on the broad $[Ru(bipy)_3]^{2+}$ emission band. The films showed electrocatalytic activity toward the reduction of IO_3^-, H_2O_2, BrO_3^- and NO_2^-, as well toward the oxidation of $C_2O_4^{2-}$. Films of $[Eu(SiMoW_{10}O_{39})_2]^{13-}$ with quaternized poly(4-vinyl pyridine) partially complexed with osmium bis(2,2′-bipyridine)[811] or with polyacrylamide were made by layer-by-layer deposition.[812] Polarized luminescence was observed for self-organized films of $(DODA)_9$-$[EuW_{10}O_{36}]\cdot 9H_2O$ that were prepared by solvent casting.[813] Differences were observed for the intensities of the transitions in the luminescence spectra, depending on the position of the polarizers before and after the sample. Only the total luminescence intensity was found to change and not the relative intensity of the different transitions. $(CTA)_9[EuW_{10}O_{36}]$ films were prepared by solvent casting chloroform solutions of the complexes on hydrophilic substrates.[814]

Antonietti and co-workers described the encapsulation of polyoxometalate complexes in a sol−gel silica matrix by blending.[815] The first examples of lanthanide-containing polyoxometalate complexes in sol−gel glasses were described by Lis, Klonkowksi, and co-workers.[773,816] The complexes $Na_9[EuW_{10}O_{36}]$ and $Eu_2TeMo_6O_{24}$ were incorporated in SiO_2 glass and in hybrid materials derived from TMOS and polydimethylsiloxane, and tri(ethylene glycol). The best luminescence performance was observed for $Na_9[EuW_{10}O_{36}]$ in the silica−polydimethylsiloxane hybrids. Lis and co-workers doped ormosils with heteropolyoxometalates of the type $K_{13}[Eu(SiMo_xW_{11-x}O_{39})_2]$ ($x = 1, 3, 5$).[456] Not only the compositional parameter x but also the composition of the ormosil matrix were found to have an effect on the photophysical properties. The highest luminescence intensity was observed for $K_{13}[Eu(SiMoW_{10}O_{39})_2]$ doped in a hybrid matrix derived from 3-glycidoxypropyltrimethoxysilane. On the other hand, the longest luminescent lifetimes were observed for the same complexes in a methylated ormosil. Unfortunately, the Eu^{3+}-containing ormosils derived from 3-glycidoxypropyltrimethoxysilane showed a lower thermal and photochemical stability than other ormosils with a lower organic content. Good luminescence properties were observed for the polyoxometalate complex $Na_9EuW_{10}O_{36}$ in different ormosils. Hungford et al. described the luminescence properties of the decatungstoeuropate(9−) anion, $[EuW_{10}O_{36}]^{9-}$, in a silica sol−gel glass.[817] The intensity ratio $I(^5D_0 \rightarrow {}^7F_2)/I(^5D_0 \rightarrow {}^7F_1)$ ranged from 1.54 to 2.71 during the 20 day aging process of the gels. These ratios are higher than that for the complex in aqueous medium, where the value is only 1.06. The surfactant-encapsulated polyoxometalates entrapped in a sol−gel hybrid matrix form a new class of hybrid materials.[818] Highly luminescent hybrid materials based on the $[EuW_{10}O_{36}]^{9-}$ anion were obtained. The use of a functional cationic surfactant with two terminal hydroxyl groups, di(11-hydroxyundecyl)dimethylammonium bromide (DODHA) (Figure 65), was found to be necessary to obtain optically transparent hybrid materials. The cationic head groups replace the sodium cation in $Na_9[EuW_{10}O_{36}]$ and combine with the POM via electrostatic interactions. The alkyl chains create a hydrophobic microenvironment, which protects the Eu^{3+} in the POM from residual water molecules and hydroxyl groups. The alkyl chains make the hybrid materials less brittle and easier to prepare without cracks. The hydroxyl groups link the POM complexes to the silica backbone. The authors could not prepare transparent hybrid materials by physical blending of $Na_9[EuW_{10}O_{36}]$ in the sol−gel precursor solution, and they obtained an inhomogeneous material. The luminescence decay time of the surfactant-encapsulated Eu^{3+}-containing POM in the hybrid matrix was significantly lower than that of the pure surfactant-encapsulated europium(III) complex but still longer than 1 ms. The complexes $[LnW_{10}O_{36}]^{9-}$ (Ln = Eu, Dy) were built in a citric acid/poly(ethylene glycol) matrix by a sol−gel process.[819] Branched polyesters are formed by reaction of citric acid with poly(ethylene glycol). Thin films were obtained by dip-coating on a quartz glass slide. The luminescent decay times were much shorter in the hybrid films than in the pure solids. The same technique was used to encapsulate $[Eu(XW_{11}O_{39})_2]^{n-}$ (X = Ge, Si, B; $n = 13, 15$) complexes in that hybrid matrix.[820]

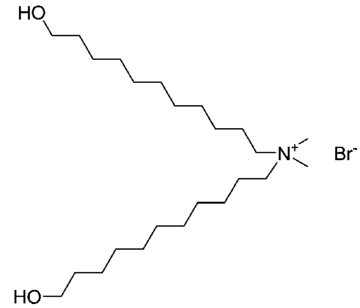

Figure 65. Di(11-hydroxyundecyl)dimethylammonium bromide (DODHA).

The polyoxoanion $[Eu(H_2O)_3(\alpha\text{-}1\text{-}P_2W_{17}O_{61}]^{7-}$ was encapsulated within MCM-41.[821] To aid the incorporation of the negatively charged polyoxoanion, it was necessary to functionalize the walls of MCM-41 using 3-aminopropyltriethoxysilane and to adjust the pH to protonate the amino groups. At pH 5, the promotion of the encapsulation of the polyoxoanion was promoted by the electrostatic interactions between the negatively charged polyanion and the positively charged NH_3^+ groups on the walls of the mesoporous host. At lower pH, the polyoxoanion could capture protons and formed a neutral weak acid, which was difficult to incorporate in MCM-41. At high pH, the polyoxoanion was decomposed into smaller anions. The luminescence spectra of the polyoxoanion in the pure solid state were very similar to the polyoxoanion/MCM-41 composite material, which is an indication for weak electrostatic interactions between the host and the guest. On the basis of luminescence and Raman measurements, it was concluded that the host−guest interaction involves mainly the negatively charged terminal oxygen atoms and not the oxygen atoms coordinated to the Eu^{3+} ions. In a subsequent paper, the incorporation of the polyoxoanion $[(Eu_2PW_{10}O_{38})_4(W_3O_8(H_2O)_2(OH)_4)]^{22-}$ in MCM-41 was described.[822]

Lanthanide-containing polyoxometalate−PMMA composites were prepared using a surfactant-encapsulated $[EuW_{10}O_{36}]^{9-}$ polyoxometalate complex with the polymerizable surfactant dodecyl(11-methacryloyloxyundecyl)dimethylammonium bromide (DMDA) (Figure 66) by copolymerization of this surfactant with methyl methacrylate.[823] The free-radical polymerization was initiated by azoisobutyronitrile (AIBN). The authors noticed that simple blending of a nonpolymerizable surfactant-encapsulated polyoxometalate complex and poly(methyl methacrylate) gave phase separation, which resulted in hybrid materials of poor optical

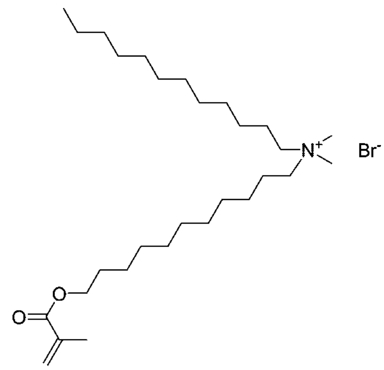

Figure 66. Dodecyl(11-methacryloyloxyundecyl)dimethylammonium bromide (DMDA).

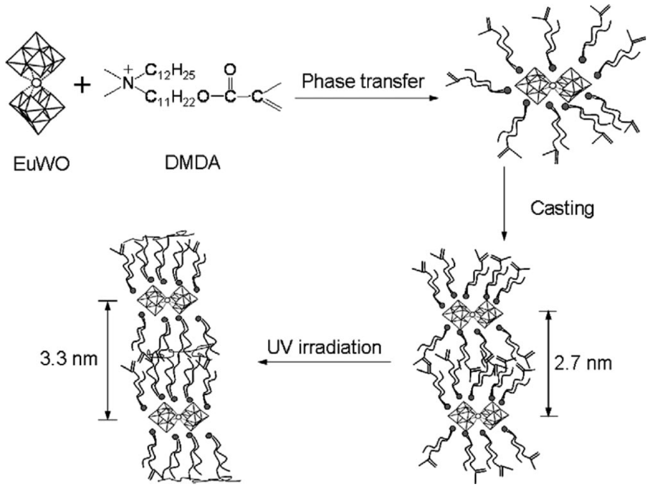

Figure 67. Schematic illustration of the preparation of a surfactant-encapsulated polyoxometalate complex and its packing in a solvent cast film before and after photopolymerization. Reproduced with permission from ref 825. Copyright 2008 Elsevier.

quality. $[EuW_{10}O_{36}]^{9-}$ was also incorporated in micrometer-sized polystyrene latex particles by the same copolymerization methodology as that used for the PMMA films.[824] The $I(^5D_0 \rightarrow {}^7F_2)/I(^5D_0 \rightarrow {}^7F_1)$ ratio for powder samples was only 0.87. Thin films of surfactant-encapsulated polyoxometalate complexes containing surfactants with polymerizable groups were first solvent cast and then *in situ* photopolymerized (Figure 67).[825] Poly(vinyl alcohol)/$[EuW_{10}O_{36}]^{9-}$ composite fibers could be obtained by the electrospinning technique.[826] In this case, no phase separation was observed and the resulting composite material was highly luminescent.

Sanchez and co-workers reviewed different approaches to incorporate metal-oxo clusters including polyoxometalate complexes in class I and class II hybrid materials.[827] From this work, it is evident that by far not all different approaches to lanthanide-containing polyoxometalates have been investigated yet. Research has mainly been focused on class I hybrid materials, that is, materials without a covalent bond between the POMs and the host matrix. Good examples of this approach are the surfactant-encapsulated polyoxometalates and the Langmuir–Blodgett films. Although the functionalization of polyoxometalates is a very active research field,[828] preliminary functionalization of the POMs and subsequent grafting to the matrix still have to be developed for lanthanide-containing systems.

A few studies describe the binding of organic ligands (mostly carboxylic acids) to lanthanide-containing polyoxometalates. Polynuclear tungsten(VI) and molybdenum(VI) complexes with 3-hydroxypicolinic acid (HpicOH) and europium(III), $[M_4O_{12}Eu(picOH)_3]$ (M^{VI} = Mo, W) were prepared by hydrothermal methods.[829] The europium(III) luminescence was found to be sensitized both by the 3-hydroxypicolinate and by the inorganic clusters. Inorganic–organic hybrid materials were obtained by combining $[Ln(W_5O_{18})_2]^{n-}$ polyoxoanions (Ln = Eu, Tb, Er, Yb) and 3-hydroxypicolinic acid via reaction of an aqueous solution of $Na_9[Ln(W_5O_{18})_2]\cdot 14H_2O$ with an aqueous solution of 3-hydroxypicolinic acid (HpicOH).[830] The general formula of the compounds is $[Ln(W_5O_{18})_2(picOH)_x]^{n-}$, with $x = 6$ or 8 for Ln = Eu, $x = 2$ for Ln = Tb and Er, and $x = 4$ for Ln = Yb. Luminescence was observed for Eu^{3+} and Tb^{3+} complexes but not for the near-infrared-emitting Er^{3+} and Yb^{3+}. But and Lis prepared several complexes with acetate or oxolate ligands like $K_{12}[\{Eu(SiMo_xW_{11-x}O_{39})(H_2O)\}_2(CH_3COO)_2]\cdot nH_2O$, $K_{16}[\{Eu(CH_3COO)(H_2O)_2(P_2W_{17}O_{61})\}_2]\cdot nH_2O$ and $(NH_4)_{29}K_5[\{Eu(P_2W_{17}O_{61})\}_4(C_2O_4)_3(H_2O)_4]\cdot nH_2O$, where $x = 0$ or 1.[831]

Chart 12. Fluorinated and Deuterated Polymers Used as Hosts for near-Infrared-Emitting Lanthanide Complexes

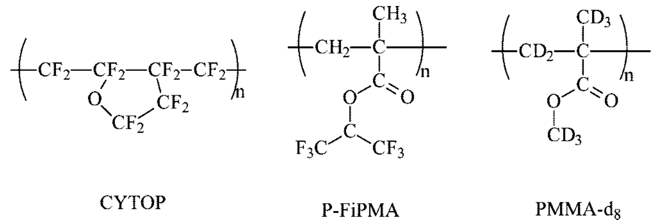

7. Polymer Materials

7.1. Complexes Blended with Polymers

An advantage of polymers as host matrix for luminescent lanthanide complexes is their easy processability. Polymer films can be obtained by spin coating or melt casting and objects of virtually any desired shape (sheets, rods, fibers, etc.) or size can be made from polymeric materials. Polymers have several advantages over glasses besides the better processability, including a lighter density and higher flexibility. In general the production of polymers is cheaper than that of glasses, and much less energy is required. Lanthanide complexes can be incorporated in many types of optically transparent polymers. Examples are poly(methyl methacrylate) (PMMA), poly(vinyl alcohol) (PVA), polyethylene (PE), polystyrene (PS), polyurethanes, polyesters, polycarbonates, polyimides, and epoxy resins. Fluorinated or deuterated polymers are of interest as a host matrix for infrared luminescent lanthanide complexes. Examples of perfluorinated polymers are CYTOP (cyclic transparent optical polymer; developed by Asahi Glass Company) and poly(hexafluoro isopropyl methacrylate) (P-FiPMA). An example of a deuterated polymer is deuterated poly(methyl methacrylate) (PMMA-d_8). An overview of fluorinated and deuterated polymer matrices used as hosts for lanthanide complexes is given in Chart 12.

There are different methods for incorporating lanthanide complexes into polymers. First of all, one has to distinguish between host–guest systems and systems in which the lanthanide complexes are an integral part of the polymer. In a *host–guest system*, the lanthanide complex is dissolved in the polymer matrix or blended with the polymer matrix. To prepare host–guest systems, two techniques can be used. The first technique involves dissolution of the lanthanide complex directly into the monomer or into the monomer solution. After addition of an appropriate initiator, the monomer solution is polymerized by either thermal polymerization of photopolymerization to form a uniformly doped polymer. In the second technique, the lanthanide complex and the pure polymer are both dissolved in a cosolvent. The solvent is then evaporated, and a uniformly doped polymer is obtained. There is a limit to the amount of dopant that can be incorporated in the polymer host. This limit is determined by the solubility of the lanthanide complex in the host polymer. Beyond this limit, aggregation of the complexes occurs, and this ruins the optical quality of the doped polymer. Lanthanide complexes that contain polymerizable groups can be copolymerized together with another monomer. This results in a copolymer in which the lanthanide complex is part of the polymer backbone or of the side chain. Alternatively, a polymer with pendant ligands such as 1,10-phenanthroline can form adducts with lanthanide complexes. The covalent linking of lanthanide complexes to a polymer matrix is described in section 7.2. Polymers doped with lanthanide-containing nanoparticles are described in section 9.3.

The first experiments on optical materials based on polymers doped with β-diketonate complexes go back to the 1960s when lanthanide β-diketonates had been tested as active components in chelate lasers (see section 10.3). For instance, Wolff and Pressley doped [Eu(tta)$_3$] into a poly(methyl methacrylate) (PMMA) matrix and observed stimulated emission around 613 nm in this material upon excitation with a xenon lamp at 340 nm a 77 K.[832] Huffman described laser action of [Tb(tta)$_3$] at 545 nm in this same type of polymer matrix at 77 K (λ_{exc} = 335 nm).[833,834] Besides PMMA, polystyrene and epoxy resins were also used as hosts for the lasing chelate complexes. After this initial interest in lanthanide-doped polymers, during the next three decades not much further research has been done on these materials. Recently, luminescent lanthanide-containing polymers regained interest because of their possible application in light-emitting diodes (LEDs) and in optical amplifiers and waveguides. The application of rare-earth doped polymers in LEDs is reviewed in section 10.4 and the application in optical amplifiers and waveguides in section 10.2. Here we also mention the review of Kuriki et al. in the thematic *Chemical Reviews* issue "Frontiers in Lanthanide Chemistry".[835] The references to older work on lanthanide complexes blended with polymer matrices will not be reviewed into detail. The interested reader is referred to the most important papers in the original literature.[836−842]

Simple organic salts like lanthanide(III) chlorides or nitrates have a poor solubility in polymers. Therefore, lanthanide(III) alkanoates are often the compounds of choice for doping lanthanide ions in polymer matrices. Neodymium(III) octanoate has been used to dope PMMA films or fibers with neodymium(III) ions.[843−848] The choice of the octanoate salt is mainly due to its relatively high solubility in the PMMA matrix. The absorption spectrum of PMMA/Nd^{3+} was found to be similar to that of Nd^{3+} in silica glass, although a slight blue shift was found in the PMMA/Nd^{3+} spectrum.[849] At high neodymium(III) octanoate concentration, clustering of Nd^{3+} ions was observed.[850] The localized luminescence spectra of the clusters have been detected by near-field scanning optical spectroscopy.[851] The local structure of Eu^{3+} and Sm^{3+} doped into PMMA via the corresponding octanaoate salts has been investigated by EXAFS in fluorescence mode.[852] Besides Eu^{3+} also Eu^{2+} was found in the polymer samples.

Lanthanide β-diketonate complexes are often selected as dopants in polymer matrices because of their good solubility in the host matrix and because of their good luminescence performance. The luminescence behavior of [Eu(dbm)$_3$] and [Eu(dbm)$_3$(phen)] in PMMA was investigated.[853] Europium(III)-doped polymer films were made by dissolution of PMMA and the europium(III) complex in chloroform, followed by casting of the solution on a clean glass or quartz slide and evaporation of the solvent. The lifetimes of the $^5D_0$ level of the two complexes in PMMA were found to be different. The decay curve of [Eu(dbm)$_3$(phen)] in PMMA could be fitted by a single-exponential function, whereas the decay of [Eu(dbm)$_3$] in PMMA is biexponential. These results indicate that all Eu^{3+} ions experience the same environment in [Eu(dbm)$_3$(phen)] but different environments in [Eu(dbm)$_3$]. No changes in the local environment of Eu^{3+} in [Eu(dbm)$_3$(phen)] could be observed with increasing complex concentration in PMMA.[854] In a follow-up study, the 1,10-phenanthroline ligand in [Eu(dbm)$_3$(phen)] was replaced by other bidentate N-donor ligands: 4,4-di-*tert*-butyl-2.2′-dipyridine, 4,4′-dinonyl-2,2′-dipyridine, and 2,2′-biquinoline.[855] With the exception of the complex with 2,2′-biquinoline, the europium(III) complexes showed a strong red luminescence in the polymer matrix. Addition of triphenylphosphate was found to increase the luminescence intensity, luminescence lifetime, and quantum yield of europium(III) tris-β-diketonate complexes in PMMA.[856] For instance, the luminescence intensity of Eu(tta)$_3$ in PMMA doped with triphenylphosphate is twice as high as that of a similar matrix without triphenylphosphate. A study of the miscibility of blends formed by bisphenol A polycarbonate (PC) with poly(methyl methacrylate) (PMMA) doped with europium(III) acetylacetonate was made to investigate whether the complex remained preferentially resolved in one of the polymer components.[857] Although TGA analysis suggested that the europium(III) complex remained preferably in the polycarbonate microphase, SEM analysis revealed that europium(III) acetylacetonate was homogeneously distributed within the blend. These results were further supported by photoluminescence measurements.[858] Other lanthanide β-diketonate complexes of which the optical absorption spectra have been investigated in a PMMA matrix include [Nd(dbm)$_3$(phen)],[859] [Nd(dbm)$_3$(tppo)$_2$],[860] [Nd(tta)$_3$(tppo)$_2$],[861] [Er(dbm)$_3$(phen)],[862] and [Sm(dbm)$_3$].[863] [Eu(fod)$_3$] was doped in a fluorinated copolymer of PMMA, obtained by copolymerization of methyl methacrylate and heptafluorobutyl methacrylate (HFBMA).[864] Fluorination of PMMA enabled tailoring of the refractive index, the glass transition temperature, and the intensity ratios of the transitions in the luminescence spectra. Hasegawa and co-workers investigated the luminescence properties of adducts of deuterated tris(hexafluoroacetylacetonato)europium(III) with different phosphine oxides (Chart 13), triphenyl phosphine oxide (tppo), diphenyl-*p*-fluorobenzene phosphine oxide (dpfbpo), and (tri-*n*-butylphosphine oxide) (tbpo), in PMMA.[865] The highest luminescence intensities were observed for the polymer matrix doped with [Eu(hfac-*d*)(dpfbpo)$_2$]. A study of the effect of the concentration of [Eu(hfac)$_3$] in PMMA on the luminescence intensity revealed that the intensity linearly increased with increasing concentration of the europium(III) complex up to a concentration of 5 wt %.[866] At higher concentrations, the linear relationship was lost because of

Chart 13. Phosphine Oxides

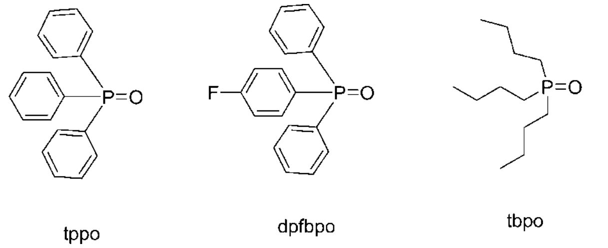

concentration quenching due to the formation of aggregates. Addition of cryptands to [Eu(hfac)$_3$] in PMMA led to an increase of the luminescence intensity, probably due to the formation of ternary complexes of the type [Eu(hfac)$_3$(cryptand)].[866] However, the increase in luminescence depended on the type of cryptand, and the most pronounced increases were observed for cryptate 211. Interestingly, the luminescence decay time of [Eu(hfac)$_3$] only slightly increased upon addition of the cryptand. [La(dbm)$_3$(phen)] had a sensitizing effect on the luminescence of [Eu(dbm)$_3$(phen)] in PMMA films.[867] In the same study, it was also shown that the molecular mass of PMMA has an influence on the luminescence efficiency of [Eu(dbm)$_3$(phen)] sensitized by [La(dbm)$_3$(phen)], with the highest efficiency for the complex doped into PMMA with the highest molecular mass. It was argued that PMMA with high molecular mass enwrapped the europium(III) complexes and kept the donor [La(dbm)$_3$(phen)] and the acceptor [Eu(dbm)$_3$(phen)] close, which resulted in a effective intermolecular energy transfer and a high sensitization efficiency. Also [Tb(dbm)$_3$(phen)] sensitized the luminescence of [Eu(dbm)$_3$(phen)] in PMMA.[868] Films consisting of neodymium(III) nitrate hexahydrate in PMMA were suggested for use as absorbing color filters to improve the primary color purity of OLEDs.[869]

A comparative study of [Eu(hfac)$_3$] in different types of polymer matrix revealed that the luminescence intensity depends on the polymer matrix.[866] The highest luminescence intensities were observed for poly(methyl methacrylate) (PMMA). Reasonable luminescence performances were also observed in poly(vinyl alcohol) (88% hydrolyzed) and poly(2-vinyl pyridine). Poorer luminescence properties were observed for poly(vinyl pyrrolidinone), cellulose acetate, polystyrene, and polycarbonate, and the weakest luminescence intensities were observed in polyolefins (e.g., polyethylene). No correlation was found between the luminescence intensity and the luminescence decay time for the [Eu(hfac)$_3$] complexes in polymer matrices. The luminescence intensities of many different combinations of europium(III) complexes and polymer matrices were screened. The best performance was observed for a sample consisting of 10 wt % of [Eu(hfac)$_3$(cryptand-211)] in poly(2-vinyl pyridine).[866] Long luminescence decay times (>1.5 ms) were measured for Na$_3$[Eu(dpa)$_3$] and (NBu$_4$)$_3$[Eu(dpa)$_3$] doped in polymers.[866] A disadvantage of these complexes is that their absorption maximum is located around 270 nm, so they can only be efficiently excited by short-wave UV radiation. Liu et al. doped [Eu(dbm)$_3$(H$_2$O)$_2$], [Eu(tta)$_3$(H$_2$O)$_2$], and [Eu(phen)$_2$(H$_2$O)$_2$]Cl$_3$ complexes into a poly(vinyl pyrrolidone) (PVP) matrix.[870] It was shown by XRD that the β-diketonate complexes can be dispersed well in the polymer matrix. There was evidence that the water molecules in the complexes were partially replaced by C═O groups of the PVP polymer. However, the complex [Eu(phen)$_2$(H$_2$O)$_2$]Cl$_3$ was found to dissociate in the PVP matrix due to interaction with the C═O groups. The differences of luminescence properties of [Eu(phen)$_2$(H$_2$O)$_2$]Cl$_3$ in PMMA and PVP have been discussed in detail.[871,872] Replacement of 1,10-phenanthroline in [Eu(phen)$_2$(H$_2$O)$_2$]Cl$_3$ by 4,4′-dinonyl-2,2′-bipyridine or 4,4′-di-*tert*-butyl-2,2′-bipyridine in PMMA has an influence not only on the luminescence properties but also on the miscibility of the complexes and PMMA.[873] The complex [Eu(tta)$_3$(H$_2$O)$_2$] doped in poly(vinyl pyrrolidone), poly(ethylene oxide), and poly(vinyl stearate) showed host-matrix-dependent luminescence characteristics, which indicates that the complex interacts with the polymer matrix.[874] The polymer composite exhibited a stronger photoluminescence than the pure terbium(III) complex. Pagnot et al. investigated by scanning near-field optical microscopy (SNOM) the photostability of [Eu(dbm)$_4$](piperidinium) complexes in polystyrene thin films.[875] As could be expected, the photostability of this β-diketonate complex was found to be quite low. By blending europium(III) and terbium(III) complexes in different concentration ratios in polystyrene, de Souza and co-workers were able to obtain luminescent polymer films with different emission colors, ranging from red over yellow to green.[876] Brito and co-workers blended [Eu(tta)$_3$(H$_2$O)$_2$] with poly(β-hydroxybutyrate)(PHB).[877] A significant increase of the quantum efficiency was observed for the europium(III) complex after doping into the polymer. A study of polymer films with different europium(III) complex concentrations showed concentration quenching above 5 mass % of complex. [Eu(dbm)$_3$(phen)] was doped in poly(*N*-vinylcarbazole) for the preparation of OLEDs.[878] De Farias et al.[454] doped [Eu(fod)$_3$-(H$_2$O)$_2$] and [Eu(fod)$_3$(terpy)] into films of 3-trimethylsilylpropyl)ethylene diamine and of an acrylic resin, and these authors studied the luminescence properties of these films. The luminescence properties of [Eu(tta)$_3$(H$_2$O)$_2$] in an epoxy resin were investigated by Parra et al.[879] The epoxy resin was a diglycidyl ether of bisphenol A (Araldite GT 7004). The epoxy matrix acted as an antenna, which absorbed light and channeled it to the europium(III) ion. Oxygen sensors made of fluoropolymers doped with europium(III) complexes are described in section 10.5. Lin et al. investigated the solubility of the neodymium(III) complexes [Nd(thmd)$_3$], [Nd(hfac)$_3$], and [Nd(tfac)$_3$] in different polymers: PMMA, polystyrene, the polyimide Ultem, and the fluorinated polyimide of the Ultradel 9000 series (Figure 68).[880] The best solubility was found for [Nd(hfac)$_3$] in the fluorinated polyimide. Both the complex and the solvent could be dissolved in γ-butyrolactone. Thin films of the neodymium(III)-doped polymer could be obtained by spin-coating of a solution in γ-butyrolactone. However, in order to obtain an optically transparent film without scattering particles, it was found necessary to remove particles by filtration from the solution before spin coating. After spin coating, the films were heated for several hours in air at 110 °C to remove solvent residues. Subsequently the films were exposed to UV radiation to cross-link the polymer. Finally, the films were heated at 175 °C in nitrogen atmosphere to improve the film quality and to remove traces

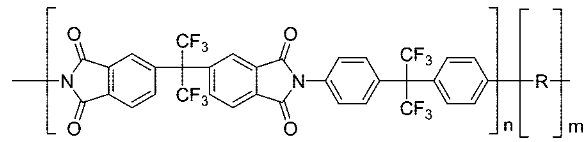

Figure 68. Generic formula of the Ultradel 9000 fluorinated polyimides.

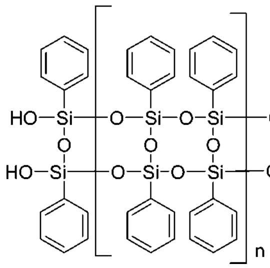

Figure 69. Structure of a polyphenylsilsesquioxane (PPSQ) polymer.

of water. The films showed three emission bands at 880, 1060,and 1330 nm. The luminescence lifetime of the $^4F_{3/2}$ level was about 1 μs. Polyphenylsilsesquioxane (PPSQ) is a polymer with a excellent optical transparency, in combination with very good chemical, thermal, and mechanical stabilities (Figure 69). PPSQ has been used as a host matrix for luminescent lanthanide clusters. Strong green luminescence was observed a for nonanuclear terbium(III) cluster with 16 hexylsalicylate ligands in PPSQ.[881] The luminescence quantum yield of this complex dissolved in methanol is over 90%,[882] and the efficient photoluminescence is attributed to J-type $\pi-\pi$ stackings, which are enhanced by the interactions of the hexyl groups in the hexylsalicylate ligands.[883]

One has to be aware of the fact that during the processing of the polymer, the lanthanide complexes can dissociate in coordinating solvents. Gao et al. investigated the effect of dissociation of the samarium(III) and europium(III) β-diketonate complexes on the optical properties of the doped PMMA polymers. In contrast to the benzoyltrifluoroacetylacetonate complexes, the hexafluoroacetylacetonate complexes $[Sm(hfac)_4]^-(Et_4N)^+$ and $[Eu(hfac)_4]^-(Et_4N)^+$ were found to be quite stable and did not show evidence for dissociation.[884] By dispersing lanthanide complexes into polymers, it is possible to reduce the concentration quenching of the luminescence.

The research groups of Bazan and Heeger were able to observe polarized emission from [Eu(dnm)$_3$(phen)] in stretched polyethylene films.[885,886] The presence of the rigid naphthyl groups allowed the three β-diketonate ligands to align parallel to the direction in which the polymer film had been stretched. This resulted in a quasi-uniaxial alignment of the chelate complex. The emission of Eu^{3+} was found to be highly polarized. When the luminescence was detected with the polarization parallel to the orientation direction of the film, intensity of the strongest emission line of the $^5D_0 \rightarrow {}^7F_2$ manifold (ca. 612 nm) increased by a factor of 10 when the polarization of the incident beam was changed from perpendicular to parallel to the orientation direction of the film. The reason for these intensity differences is that the aligned chromophores of the β-diketonate ligands absorb light more strongly when the incident light beam is parallel to the orientation direction of the polymer film. More light absorption by the ligands means that more energy can be transferred to the Eu^{3+} ion. When the experimental setup was changed so that the incident light beam was always parallel to the orientation direction of the film and that the luminescence was detected either parallel or perpendicular to the orientation direction, the crystal-field transitions of the $^5D_0 \rightarrow {}^7F_J$ transitions were found to be polarized. However, in this case the differences in total luminescence intensity were less pronounced. The fact that the crystal-field fine structure of the $^5D_0 \rightarrow {}^7F_2$ transitions in solid [Eu(dnm)$_3$(phen)] differed from the fine structure observed for [Eu(dnm)$_3$(phen)] in the

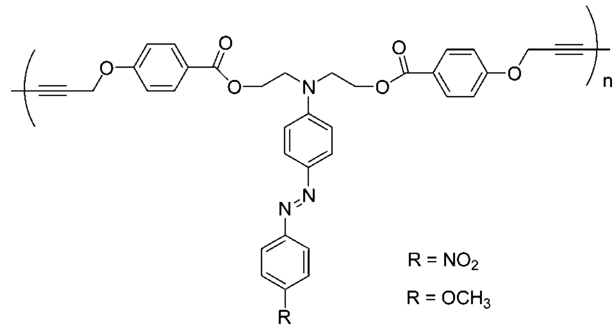

Figure 70. Azopolymer.

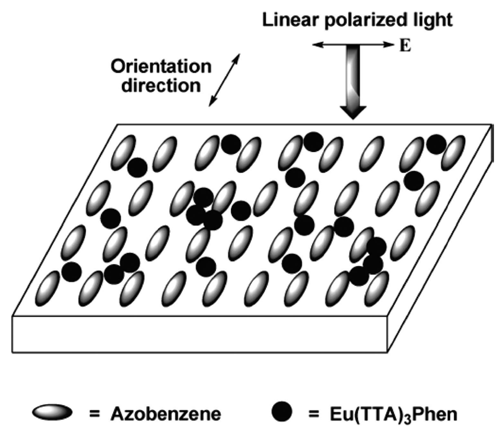

Figure 71. Schematic model of the photoinduced alignment of the azobenzene groups in an azopolymer film doped with [Eu(tta)$_3$(phen)]. Upon irradiation with linearly polarized light, the azobenzene groups are oriented in a direction perpendicular to the direction of the electric field of the incident light beam. Reprinted with permission from ref 887 (http://dx.doi.org/10.1039/b802198h). Copyright 2008 The Royal Society of Chemistry.

stretched polymer film indicates that the β-diketonate ligands rearrange upon stretching. Zhang and co-workers observed polarized luminescence by doping [Eu(tta)$_3$(phen)] in photoaligned azopolymer films (Figure 70).[887] The azobenzene groups of the polymer were oriented upon irradiation with linearly polarized light in a direction perpendicular to the polarization direction of the electric field vector in the film plane (Figure 71). The polarized emission was caused by the "polarizer effect" of the aligned azobenzene groups. The oriented polymer matrix acted as a polarizer toward the emission light that travels through it. Therefore, the intensity of the emission light was stronger when the direction of the electric field vector was parallel to the alignment layer and lower when the direction of the electric field was perpendicular to it (Figure 72). In contrast to the work of Bazan and Heeger mentioned above, the polarization effects here were not caused by the alignment of the [Eu(tta)$_3$(phen)] molecules. This is evident from the fact that the total intensity of the luminescence spectrum differed in the two polarization directions, rather than that there were differences in the relative intensities of the crystal-field components.

In order to observe near-infrared luminescence of lanthanide complexes doped into a polymer matrix, it is advantageous to select complexes with deuterated or fluorinated ligands, as well as deuterated or perfluorinated polymer hosts. Nonradiative relaxation by high-energy vibrations of C−H groups can be reduced by replacing these C−H bonds by C−D or C−F bonds. Of course, also OH groups in the vicinity of the lanthanide ion have to be avoided. In general, it is easier to observe near-infrared luminescence for lan-

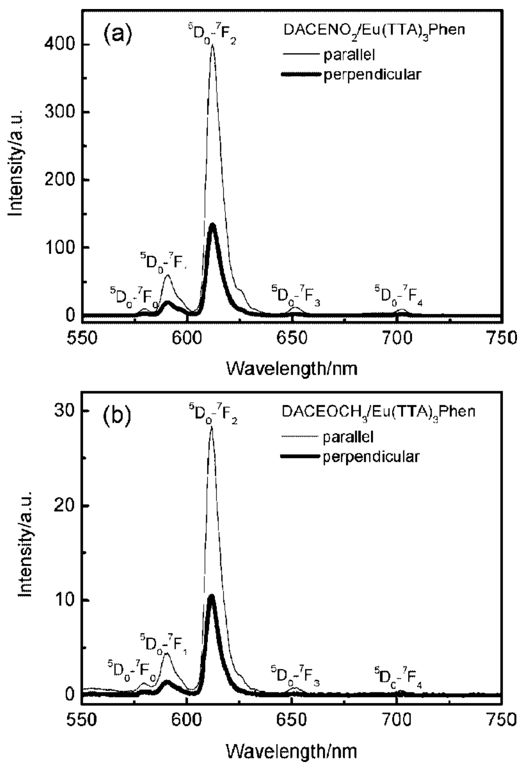

Figure 72. Polarized luminescence spectra of photoaligned $[Eu(tta)_3(phen)]$-doped azopolymer films. The polarizer in the emitted light beam was either parallel or perpendicular to the alignment direction of the azobenzene groups. Reprinted with permission from ref 887 (http://dx.doi.org/10.1039/b802198h). Copyright 2008 The Royal Society of Chemistry.

thanide ions in polymer matrices than in solution, because in solution the lanthanide complexes can diffuse and collide. These collisions lead to energy transfer via cross-relaxation and excitation migration.[888] Pioneering work on near-infrared-emitting deuterated and perfluorinated lanthanide complexes has been done by Hasegawa and co-workers. [Nd(hfac-*d*)$_3$] was synthesized by reaction of deuterated hexafluoroacetone in methanol-d_4.[889] Near-infrared emission was observed for [Nd(hfac-*d*)$_3$] dissolved in deuterated acetone-d_6. In a follow-up study, the authors showed that this complex showed near-infrared luminescence in other perdeuterated solvents as well: methanol-d_4, THF-d_8, DMF-d_7, and DMSO-d_6.[890] Enhanced emission properties were observed for [Nd(hfac-*d*)$_3$] in DMSO-d_6, probably because this coordinating ligand replaced water molecules from the first coordination sphere of the neodymium(III) ion. Deuterated tris(bis-(perfluorooctanoyl)methanato)neodymium(III), Nd(POM-*d*)$_3$, gave enhanced luminescence in DMSO-d_6 by minimizing the energy migration during diffusional collisions in the liquid matrix.[891] These authors obtained luminescent polymers by doping [Ln(hfac-*d*)$_3$] (Ln = Nd, Eu) and DMSO-d_6 in poly(alkyl methacrylate).[892] Kuriki et al. doped the complexes of deuterated 1,1,1,2,2,6,6,7,7,7-decafluoro-3,5-heptanedione, [R(fhd-*d*)$_3$] (R = Pr, Nd, Er, Tm), into a perfluorocarbon liquid (3 M PF-5080) and into the perfluorinated polymer CYTOP.[893] A comparison of the peak positions in the emission spectrum of [Nd(fhd-*d*)$_3$] in PMMA-d_8 with that of the same complex in a perfluorocarbon liquid shows that the $^4F_{3/2} \leftarrow {}^4I_{9/2}$ transition in PMMA-d_8 is shifted to shorter wavelengths. Near-infrared emission around 1550 nm was observed for an octupolar erbium(III) complex in PMMA (Figure 73).[894]

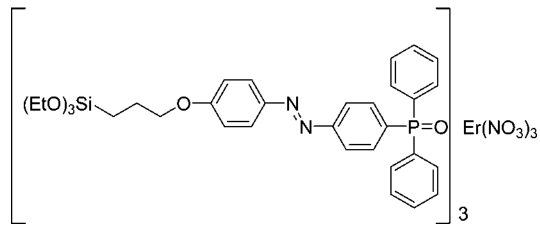

Figure 73. Structure of an octupolar erbium(III) complex.[894]

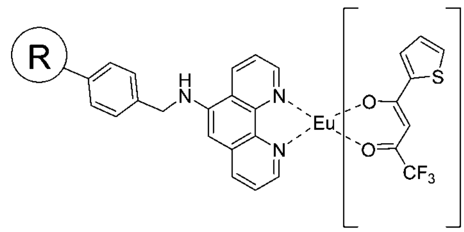

Figure 74. $[Eu(tta)_3(phen)]$ covalently linked to a Merrifield resin.[895]

7.2. Complexes Covalently Bonded to the Polymer Matrix

Just like in the case of sol−gel-derived hybrid materials, it is possible to reduce clustering of lanthanide ions in polymers by covalently attaching lanthanide complexes to the polymer backbone rather than just blending the lanthanide complex with the polymer matrix. In general, a ligand with a polymerizable group is copolymerized together with another polymer and the final luminescent polymer is obtained by reaction of a lanthanide salt of the complex with the pendant coordinating groups of the polymer matrix. It is also possible to have a lanthanide complex with a reactive group coupled to a polymer containing reactive groups itself. The latter approach is nicely illustrated by Binnemans and co-workers who coupled luminescent $[Ln(tta)_3(phen)]$ complexes to a Merrifield resin (Figure 74).[895] The Merrifield resin is the standard solid support for solid-state organic synthesis. It consists of polystyrene cross-linked by divinyl benzene, and the phenyl rings bear chloromethyl groups in the *para*-position. The Merrifield resin is able to react with different functional groups including alcohol and amino groups. By reaction of the Merrifield resin with 5-amino-1,10-phenanthroline, it was possible to covalently attach 1,10-phenanthroline groups to the surface of the Merrifield resin. Reaction of the modified Merrifield resin with $[Ln(tta)_3(H_2O)_2]$ complexes allowed the authors to obtain the luminescent hybrid materials. Strong red luminescence was observed for the Eu^{3+} complex, whereas near-infrared luminescence was detected for complexes where Ln = Sm, Nd, Er, or Yb. Notice that this is one of the few studies in which a near-infrared luminescence spectrum of a samarium(III)-containing hybrid material is reported (Figure 75).

Ueba et al. made europium(III) complexes of β-diketone-containing polymers (Figure 76).[896] In this way, it was possible to attach the Eu^{3+} ion directly to the polymer, either through the backbone or through the side chain. The europium-containing polymers were prepared by adding a $EuCl_3$ solution in tetrahydrofuran and methanol (1:1 v/v) to a tetrahydrofuran solution of the polymers (1−2% solution). The pH of the solution was adjusted to pH 8 by adding piperidine. The polymer precipitated and could be recovered by filtration. The luminescence intensity reached a maximum at a Eu^{3+} content of 1 wt % and remained constant upon further increase of the Eu^{3+} content. Chauvin and co-workers

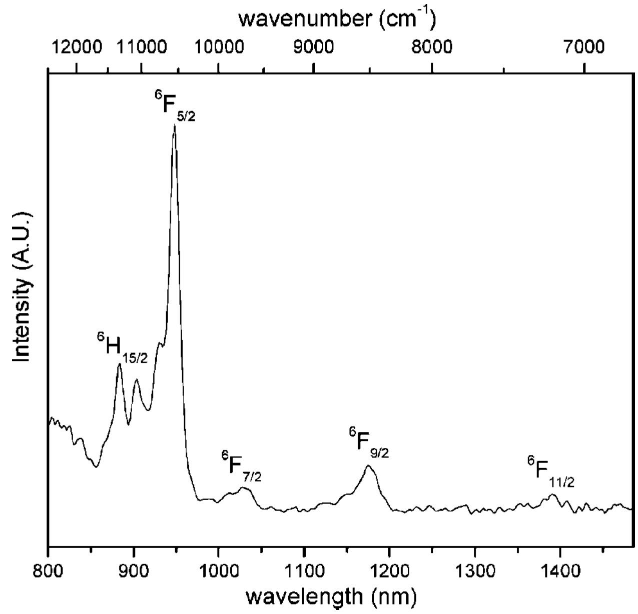

Figure 75. Near-infrared luminescence spectrum of a [Sm(tta)$_3$(phen)] complex immobilized on a Merrifield resin. Reprinted with permission from ref 895. Copyright 2005 American Chemical Society.

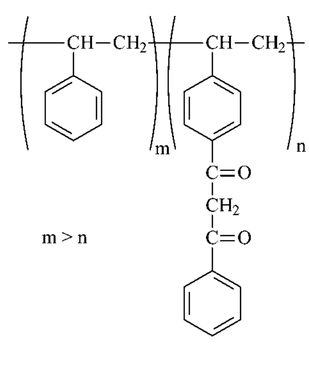

poly(*p*-benzoylacetylstyrene)

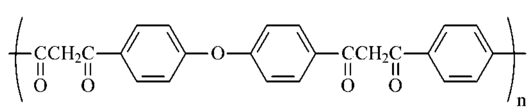

poly(aryl β-diketone)

Figure 76. Polymeric β-diketones used for incorporation of Eu^{3+} ions in a polymer matrix.[896]

have used the metal ion imprinted concept to imprint coordination cages derived of dipicolinic acid in styrene-based polymeric materials.[897,898] The resulting resins were selective for extraction of lanthanide ions. Europium(III) luminescence has been used to probe the local environment of the lanthanide ions.

Upon addition of dibenzoylmethanate ligand to a styrene-*co*-acrylic acid oligomer complex, Tang and co-workers found an increase of the photoluminescence intensity of Eu^{3+}.[899] These authors also observed an intense luminescence for a ternary complex formed between europium(III) ion, dibenzoylmethanate ligands, and oligo(acrylic acid).[900] Wang and co-workers obtained luminescent resins by free radical copolymerization of styrene and methylacrylic acid in the presence of a europium(III) or terbium(III) complex.[901] Complexes that were considered are [Eu(tta)$_3$(phen)],

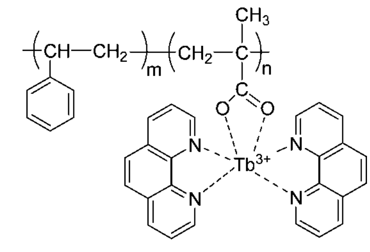

Figure 77. Terbium(III) phenanthroline complex covalently bound to a polymer backbone via an acrylate group.

[Eu(dmb)$_3$(phen)], [Tb(phen)$_2$Cl$_3$]$\cdot$2H$_2$O, and [Tb(sal)$_3$]. The lanthanide complexes were bound via the carboxylic acid group of the acrylic acid moieties to the polymer backbone (Figure 77). The emission lines of Eu^{3+} and Tb^{3+} were found to be narrower and more intense in the resin than in the corresponding pure solid complexes. The luminescence decay times were longer after incorporation in the matrix.

Wang et al. made europium(III)-containing copolymers by copolymerization of methyl methacrylate and [Eu(β-diketonato)$_2$(aa)] complexes that contain two β-diketonate ligands (tta, acac, bzac, and dbm) and one acrylate ligand.[902] The europium(III) complexes were synthesized by the reaction of 1 equiv of europium(III) isopropoxide with 2 equiv of a β-diketone and 1 equiv of acrylic acid in a 1:1 mixture of anhydrous 2-propanol and anhydrous benzene. The copolymers were prepared by radical copolymerization of the europium(III) complexes with methyl methacrylate in DMF using AIBN as the initiator. The copolymers were found to be soluble in chloroform, 1,2-dichloroethane, THF, benzene, and toluene and could be easily cast into uniform thin films with good mechanical flexibility and high thermal stability. The number-average molecular weight (M_n) of the copolymers was in the range between 53 700 and 72 600, whereas the polydispersity index (PDI) was between 4.79 and 5.96. These M_n values are lower than of the homopolymer PMMA that was obtained by the same polymerization technique, whereas at the same time the polydispersity was higher. The luminescence intensities, the luminescence lifetimes, and the intensity ratio $I(^5D_0 \rightarrow {}^7F_2)/I(^5D_0 \rightarrow {}^7F_1)$ of the europium(III)-containing copolymers are higher than those of the corresponding europium(III)-containing monomers and of blends of the europium(III) complexes with PMMA. The emission intensities increased linearly with increasing europium(III) content, and no significant concentration quenching of the luminescence could be observed in the concentration range between 0 and 6.39 mol % Eu^{3+}. This latter effect is because the europium(III) complexes were uniformly distributed along the polymer backbone, so that $Eu^{3+}-Eu^{3+}$ interactions were avoided. The luminescence intensity of the copolymers depended on the β-diketonate ligand and increased in the order acac < bzac < dbm < tta.

Pei and co-workers grafted [Eu(dbm)$_3$], [Eu(tta)$_3$], and [Eu(ntac)$_3$] to a fluorene type of conjugated polymer by complex formation via 2,2′-bipyridine groups in the side chains.[903] The complexes were prepared by heating at reflux for 2 days a solution of the polymer and a europium(III) complex in a 1:1 mixture of THF and ethanol. The authors made special efforts to purify the europium(III)-containing polymer. After synthesis, the polymer was placed in a Soxhlet extractor and extracted with hot acetone for 2 days, in order to remove all of the excess europium(III) β-diketonate complex. In these electroluminescent polymers, the blue light emitted by the fluorene groups was transformed into red light

Scheme 6. Synthesis of Polybenzimidazoles with Pendant Acetylacetonate Groups and Formation of the Corresponding Lanthanide Complexes

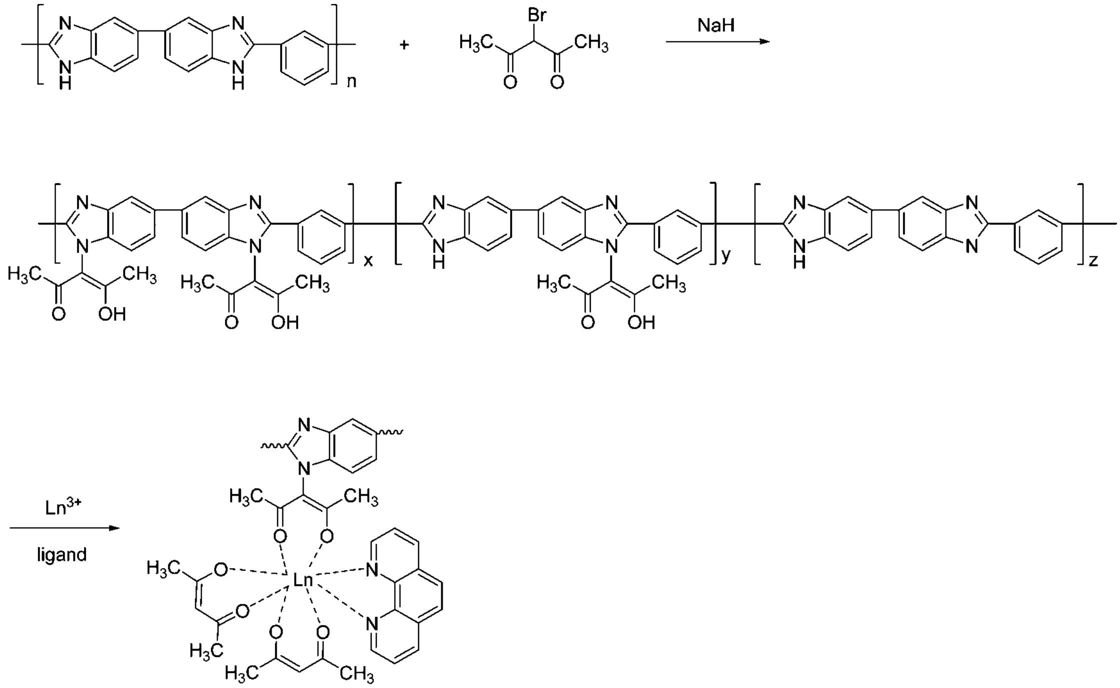

by energy transfer to the europium(III) ion. The best efficiency for energy transfer from the blue-emitting conjugated polymer to the europium(III) ion was observed for the [Eu(dbm)$_3$] complex. No concentration nor self-quenching was observed. Feng and co-workers formed lanthanide(III) grafted polymers by reaction between [Eu(tta)$_3$] and polymer-bound triphenylphosphine, triphenylarsine, triphenylstibine, or triphenylbismutine.[904] It was assumed that the P, As, Sb, or Bi group of the polymer interacted with the lanthanide(III) ion (R = Sm^{3+}, Eu^{3+}, Tb^{3+}). Among the europium(III)-containing polymers, the best luminescence performance was observed for the polymer-bound triphenylarsine system. By coupling a functionalized dibenzoylmethanate ligand to poly(lactic acid) through an ester bond, site-isolated luminescent europium(III) complexes were obtained.[905]

Wu et al. functionalized polybenzimidazoles with pendant acetylacetone groups by reaction of the parent polybenzamidazole polymer with 2-bromo-acetylacetone in DMSO in the presence of sodium hydroxide.[906] The functionalized polymers were allowed to react with a lanthanide salt in the presence of a coligand (1,10-phenanthroline and 2,2′-bipyridine) (Scheme 6). Only gadolinium(III) and dysprosium(III) complexes were made. For the dysprosium(III)-containing samples, f−f transitions could be observed superimposed on a broad background emission in the luminescence spectra. These compounds surely have good potential for study of near-infrared-emitting lanthanide complexes. Ling et al. prepared a copolymer containing carbazole side chains and europium(III) complexes by free radical copolymerization of 9-vinylcarbazole, methyl methacrylate, and a europium(III) acrylate complex.[907] This composite material was prepared with the intention of using it for making OLEDs. The carbazole units should enable hole transport, while the europium(III) complexes are responsible for electron transport and emission. The photoluminescence and electroluminescence properties of these materials were described in a later paper.[908] An OLED was made, but it had a maximum brightness of only 0.228 cd/m^2 at 29 V. Ling et al. prepared a copolymer containing 9,9-dihexylfluorene and benzoate groups able to coordinate to Eu^{3+} ions.[909] The benzoate groups were introduced via the 4-vinylbenzoate monomer. A similar europium(III)-containing polymer was synthesized by copolymerization of *N*-vinylcarbazole and 4-vinylbenzoate complexed with Eu^{3+} ions (Figure 78).[910] This hybrid material was used for the construction of a polymer memory device.[911,912] The device had two distinctive bistable conductivity states. Application of a potential set the device to the high-conductivity ON state by generation of holes in the polymer material. Erbium(III) porphyrin complexes were incorporated as erbium(III)(acetylacetonato-)diphenylporphyrin or erbium(III)(acetylacetonato)-dimesitylporphyrin in the backbone of a conjugated poly(arylene ethynylene) copolymer.[913] The material could be processed by spin-coating and emits at 1550 nm. Because of the greatly increased electronic delocalization throughout the conjugated polymer backbone, the complexes could be excited with a wavelength as long as 750 nm.

7.3. Complexes of Dendrimeric Ligands

The negative impact of clustering (aggregation) of lanthanide ions on the luminescence properties of lanthanide-containing hybrid materials has already been mentioned several times in this review. Clustering is a problem for lanthanide ions dispersed in sol−gel-derived materials or in

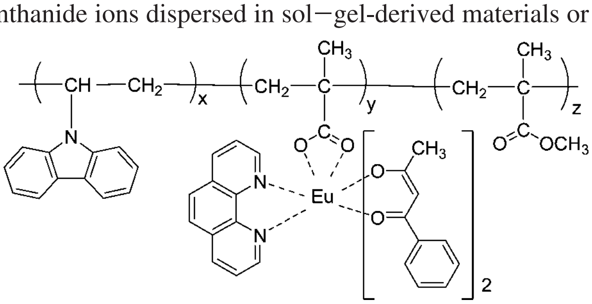

Figure 78. Europium(III)-containing copolymer of *N*-vinylcarbazole and 4-vinylbenzoate.

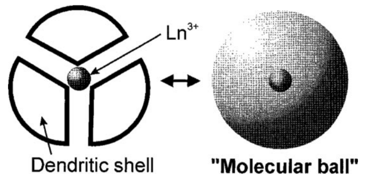

Figure 79. Molecular ball with a lanthanide(III) ion at the core created by three dendrimeric ligands coordinated to a central lanthanide ion. Reprinted with permission from ref 914. Copyright 1998 American Chemical Society.

polymers because of cooperative energy-transfer processes, which cause nonradiative relaxation of the excited states and thus a quenching of the luminescence. A general used approach to reduce the clustering of lanthanide ions is surrounding the lanthanide ion by organic ligands. The shell of organic ligands has also additional benefits besides reducing the effects of clustering, because the organic ligands can also act as an antenna to capture and transfer excitation energy and because the ligands can protect the lanthanide ion from coordination with water molecules or with other ligands possessing high-energy vibrations. This approach of surrounding the lanthanide ion by a shell of organic ligands has been extended to an extreme by Kawa and Fréchet, who coordinated the lanthanide ions with dendrimeric ligands of different generations.[914,915] Three dendrons containing a carboxylate group bind to the lanthanide ion and create in this way a "*molecular ball*" with the lanthanide ion residing at the core (Figure 79). These complexes are examples of noncovalent assembly of the dendrons to a dendrimer, based on the electrostatic interaction of the carboxylate group of the dendrons and the lanthanide(III) at the focal point (Figure 80). The metal complexes were prepared by an exchange reaction between the carboxylic acid terminated dendrons and lanthanide(III) acetate salts. The luminescence properties of the europium(III), terbium(III), and erbium(III) complexes were investigated in solution. Luminescence was detected for the europium(III) and terbium(III) complexes but not for the erbium(III) complexes. The higher generation dendrimers showed a more intense luminescence. This was attributed both to the antenna effect and to the site isolation of the lanthanide ions. The luminescence performance of the terbium(III) complexes was better than that of the europium(III) compounds. Excitation in the aromatic groups of the ligands was only possible with UV radiation of a wavelength between 290 and 315 nm. Thin films could be prepared by dissolving a europium(III) complex and an ester derivative of the dendrimeric carboxylate ligand in chlorobenzene, followed by casting the solution and hot-pressing the film after evaporation of the solvent. Luminescence of Eu^{3+} was observed after direct excitation in the $^5D_2$ level at 462 nm. These results show that dendrimeric lanthanide complexes can be processed into thin films without the need for another polymeric matrix.

Kawa and Takahagi structurally modified poly(benzyl ether) dendrimers to optimize the luminescence properties of the corresponding terbium(III) complexes.[916] Smith and co-workers encapsulated lanthanide ions in a dendritic shell of dendrons derived from L-lysine with a carboxylic group at the focal point. However, these authors have not investigated the luminescence properties of the europium(III) and terbium(III) complexes of these dendrimeric ligands, but rather the application of these complexes as selective Lewis acid catalysts for Diels−Alder reactions.[917] Lindgren and co-workers prepared lanthanide complexes of fluorinated den-

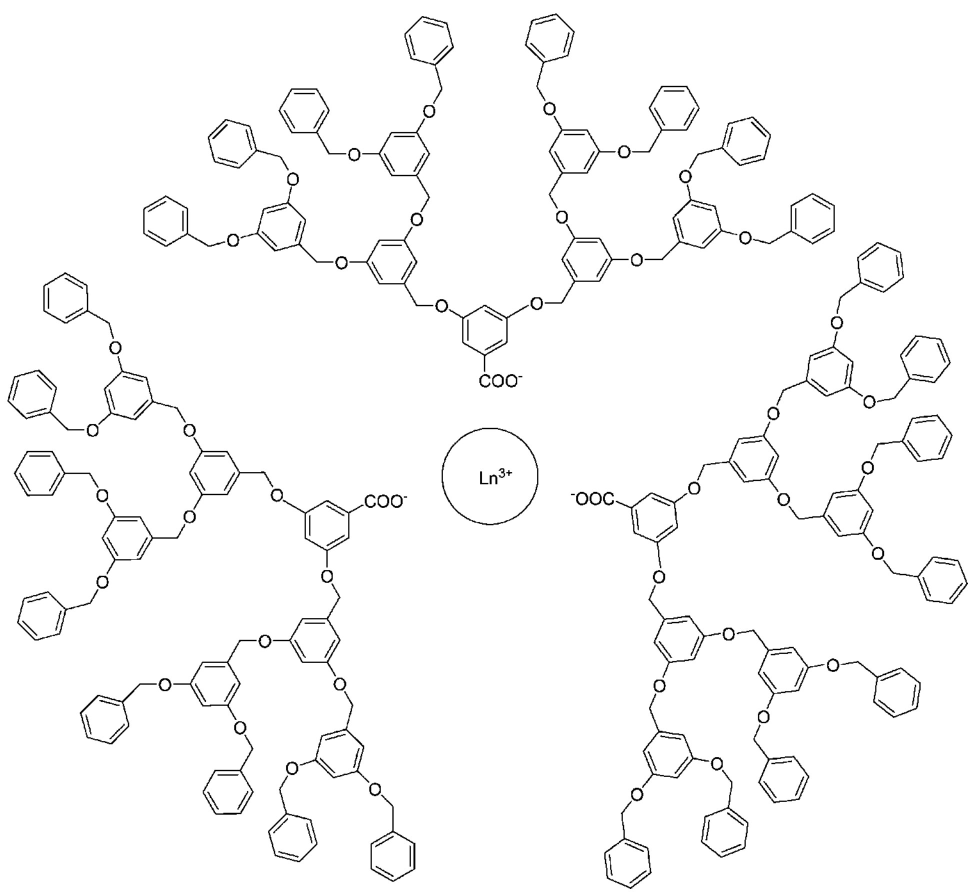

Figure 80. Lanthanide complexes of Fréchet type dendrons with carboxylate groups (Ln = Eu, Tb, Er).[914]

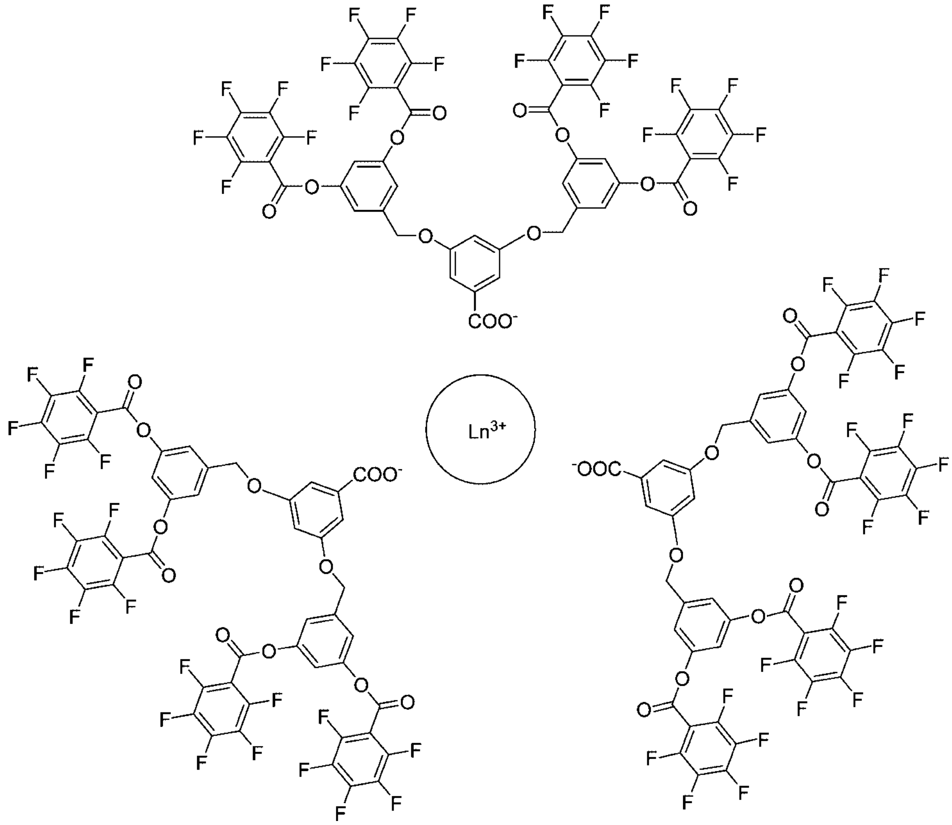

Figure 81. Lanthanide complex of fluorinated dendrons with a carboxylate group.[919]

drons with carboxylic acid groups.[918,919] The dendrimers were capped at the periphery with fluorinated phenyl groups (Figure 81). The function of these fluorinated phenyl groups was to enhance the rigidity of the dendrimer complexes, to lower the moisture penetration to the dendrimer core, and to reduce the absorption in the near-infrared region. The materials with Ln = Nd and Er showed near-infrared emission and those with Ln = Eu, Tb visible luminescence. No luminescence could be detected for Ln = Pr. The film-forming properties of the dendritic europium(III) complexes were investigated at the air−water surface.[920] The dendrimer rearranged at the surface to asymmetric conformations so that the lanthanide ions point to the water phase and the fluorinated groups to the air. Ordered Langmuir monolayers were obtained for generations G1 to G4. Zhu et al. formed terbium(III) complexes of amphiphilic linear−dendritic block copolymers of poly(acrylic acid) and a dendritic polyether (Figure 82).[921] The materials exhibited intense green photoluminescence. The luminescence intensity showed a pronounced increase with increasing the generation of the dendrimer. This increase was due to not only an improvement of the antenna effect but also the fact that less water molecules were coordinated to the Tb^{3+} ion in the higher-generation dendrimers.

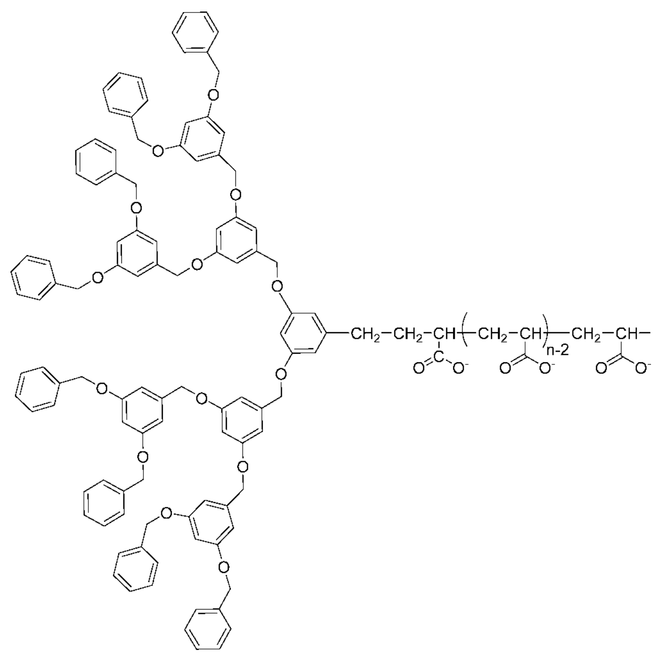

Figure 82. Amphiphilic linear−dendritic block copolymers of poly(acrylic acid) and a dendritic polyether.

Vögtle and co-workers have investigated the complex formation of a dendrimer derived from poly(L-lysine) that contains 21 amide groups in the interior and 24 5-dimethyl-amino-1-naphthalenesulfonamido (dansyl) groups in the periphery with the lanthanide ions Nd^{3+}, Eu^{3+}, Gd^{3+}, Tb^{3+}, Er^{3+}, and Yb^{3+} (Figure 83).[922] Although the coordination of the lanthanide(III) ions was not discussed in detail, it can be expected that the lanthanide(III) ions are incorporated as salts inside the dendrimer and that they interacted with the internal amide bonds of the dendrimer. The number of lanthanide(III) ions entrapped in the dendrimeric host depended on the metal ion concentration. The poly(L-lysine) dendrimer exhibited remarkably large molar absorption coefficients ε of 3×10^5 L mol^{-1} cm^{-1} at 253 nm and 9.2×10^4 L mol^{-1} cm^{-1} at 338 nm. The photophysical properties of the dansyl groups in the dendrimer were similar to those of a monomeric dansyl group, which indicates that little interaction occurred between the different dansyl groups at the periphery of the dendrimer. The lanthanide(III) ions partially quenched the fluorescent excited states of the dansyl units. The strongest quenching effects were observed for

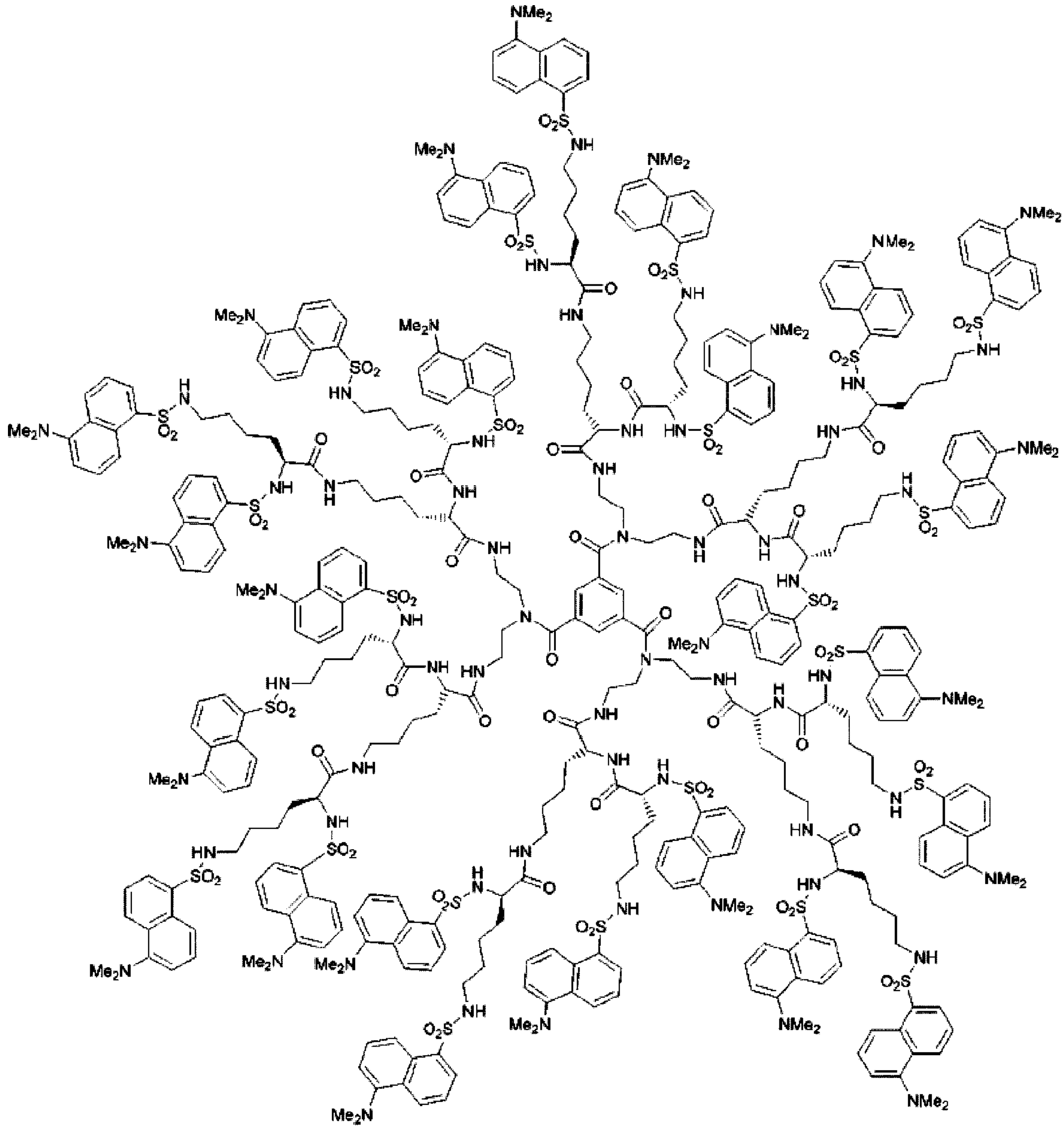

Figure 83. Dendrimer derived from poly(L-lysine) with dansyl groups in the periphery. Reproduced with permission from ref 922. Copyright 2002 American Chemical Society.

Nd^{3+} and Eu^{3+}, moderate effects for Er^{3+} and Yb^{3+}, small effects for Tb^{3+}, and negligible effects for Gd^{3+}. The quenching of the dansyl fluorescence in solution (acetonitrile/dichloromethane 5:1 v/v) was accompanied by sensitization of the luminescence of the near-infrared-emitting lanthanide ions Nd^{3+}, Er^{3+}, and Yb^{3+}. Sensitized luminescence of Eu^{3+} and Tb^{3+} could not be observed in solution but only in the vitrified organic matrix at 77 K where the dansyl groups were protonated. The quantum yield of the metal-centered luminescence of the Nd^{3+} complex was found to be 0.27% by comparison with [Nd(hfac)$_3$] in D_2O.[923] No metal-centered luminescence was observed for lanthanide complexes of cyclam-derived dendrimers with dimethoxy and naphthyl groups (Figure 84).[924] However, it was noticed that when neodymium(III) triflate was added to an acetonitrile/dichloromethane solution of the dendrimer and the ruthenium(II) complex [Ru(bipy)$_2$(CN)$_2$] in a 1:1 molar ratio, a three-component system was formed in which the luminescence of both the dendrimer and the ruthenium(II) complex was quenched and the Nd^{3+} near-infrared luminescence was sensitized.[925] It is assumed that the [Ru(bipy)$_2$(CN)$_2$] complex coordinated through its cyanide ligands to the Nd^{3+} ion. This is an efficient light-harvesting system because the dendrimer ligand absorbs in the UV spectral region and the [Ru(bipy)$_2$(CN)$_2$] complex in both the ultraviolet and visible spectral regions, so ultraviolet and visible radiation is converted into near-infrared luminescence. The synthesis of cyclam-derived dendrimers with dansyl groups and oligo(ethylene glycol) chains was described and the interaction of the dendrimer with Nd^{3+}, Eu^{3+}, and Gd^{3+} was reported (Figure 85).[926] Pétoud and co-workers synthesized a PAMAM-type of dendrimer of generation 3, with 32 external 2,3-naphthalimide groups and 60 internal amide bonds suitable for coordination with lanthanide(III) ions (Figure 86).[927] The 2,3-naphthalimide chromophore can sensitize europium(III) luminescence. The stoichiometry of the lanthanide−dendrimer complexes was determined by luminescence titrations, and it was found that the coordination number of the Eu^{3+} ion varied between 7 and 9. The quantum yield at 298 K was quite low (0.06%), but this was compensated by the very large molar absorption coefficient and the large number of Eu^{3+} ions bound to the dendrimer. A europium(III)-contain-

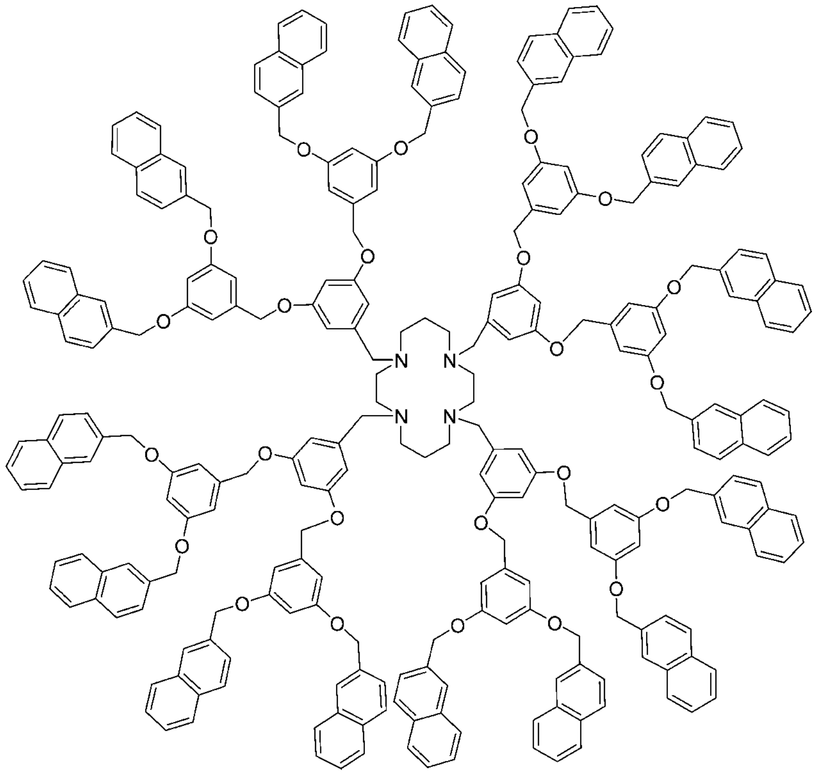

Figure 84. Cyclam-derived dendrimers with naphthyl groups.[924]

ing dendrimer was obtained by linking dendron wedges via *click chemistry* to a DOTA derivative functionalized with four alkyne groups.[928] The alkyne function reacted with the azide function at the focal point of the dendron upon formation of a triazole ring. The triazole ring acts not only as a linker between the cyclen-related macrocycle but also as an antenna to sensitize the Eu^{3+} luminescence. Light in the ultraviolet region between 270 and 290 nm is efficiently absorbed by this chromophore. An increase of the luminescence decay time of the $^5D_0$ excited state was observed with increasing dendrimer size.

Visible-light sensitization of erbium(III) luminescence was possible via platinum(II)-porphyrin ligands decorated with aryl ethyl-functionalized Fréchet-type dendrons (Figure 87).[929−931] Three porphyrin ligands bind via a carboxylic acid group to the Er^{3+} ion, and the coordination sphere of Er^{3+} is saturated by an additional terpyridine ligand, resulting in a nine-coordinated complex. The terpyridine ligand prevents water molecules from coordinating to the Er^{3+} ion.[932] The dendrons on the porphyrin ligand cause a more efficient site isolation of the Er^{3+} ion and result in an increase in the luminescence intensity by a factor of 7 in comparison with the luminescence intensity of the corresponding complex without attached dendrons. In the complex, the high-energy excitation light is first absorbed by the aryl groups of the dendrons, then transferred to the porphyrin complex, and finally transferred to the Er^{3+} ion. Direct excitation of the porphyrin complexes with light of longer wavelength is also possible. The site isolation effect has been found of more importance to increase the luminescence intensity than a more efficient antenna effect in the higher-generation dendrons.[930,933] The luminescence performance of similar complexes obtained by replacing the platinum(II) porphyrin by a zinc(II) analogue is much weaker.[934] This is attributed to a better intersystem crossing efficiency of the platinum(II) complex compared with that of the zinc(II) complex. The energy transfer occurs from the triplet level of the ligand to the $^4F_{9/2}$ and $^4I_{9/2}$ levels of Er^{3+}.[935] It has been proposed to build integrated planar waveguide-type amplifiers on the basis of these highly efficient light-harvesting dendritic arrays.[936,937] Intense luminescence of Er^{3+} at 1530 nm was observed for dendrimer complexes of Fréchet-type aryl ether dendrimeric ligands with diphenyl naphthalene and diphenyl anthracene groups and with a coordinating carboxylate group (Figure 88).[938] The polyaromatic groups take over the function of the platinum(II) porphyrin complexes present in the dendrimers described above. The highest luminescence efficiency was observed for the complexes with the diphenyl anthracene groups. Thin films with a thickness of about 3 μm of a good optical quality were obtained by spin-coating a solution of the erbium(III) complexes in 1,2-dichloroethane.

7.4. Coordination Polymers

Although lanthanide-containing coordination polymers have been an active research field for about a decade,[939−943] for a long time most of the attention has been paid to the structural characterization of these compounds, and luminescence studies have largely been neglected until quite recently.[944,945] However, many of the coordination polymers based on carboxylate ligands show good luminescence properties. Moreover, porous coordination polymers (*metal−organic frameworks* or *MOFs*)[946] offer the opportunity for fine-tuning the luminescence behavior because of the possibility to entrap in the network pores molecules that can influence the lanthanide emission. The polycarboxylates 1,4-benzenedicarboxylate (BDC) and 1,2,5-benzenetricarboxylate (BTC) are building blocks for the synthesis of robust metal−organic frameworks, including *lanthanide-containing MOFs* (Chart 14).[947−952] The coordination poly-

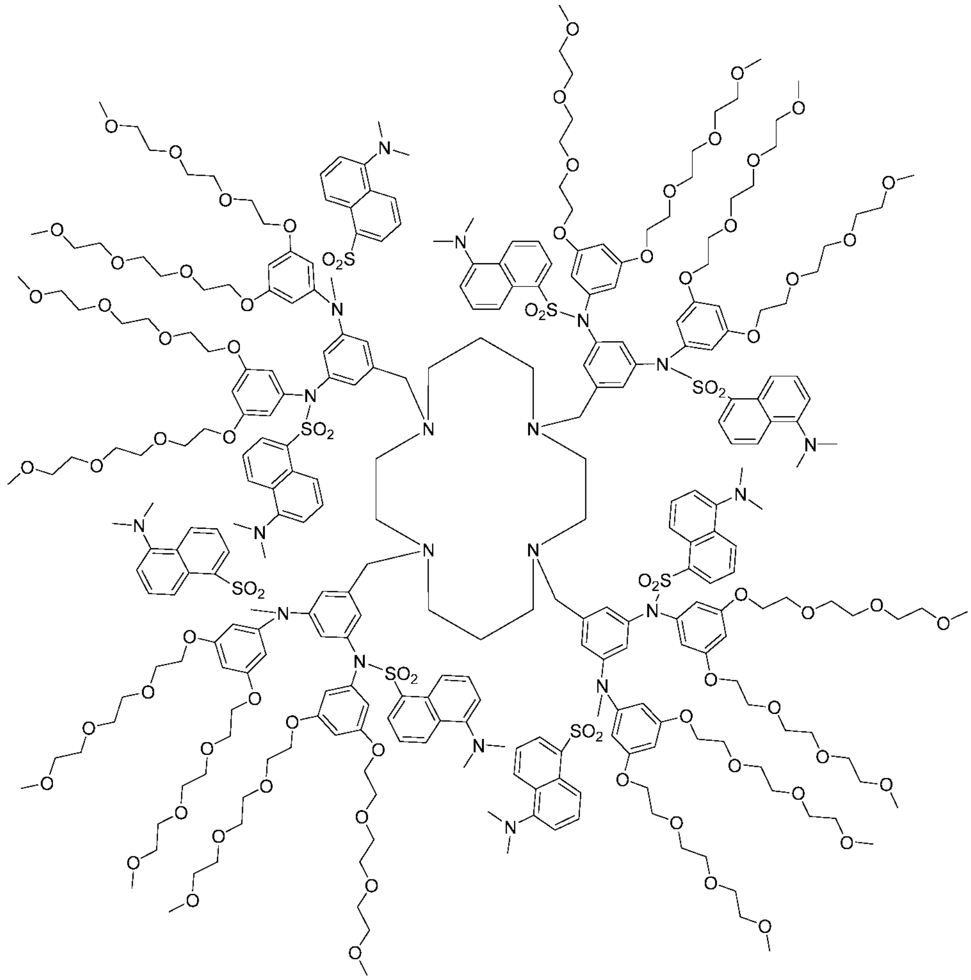

Figure 85. Cyclam-derived dendrimers with dansyl groups and oligo(ethylene glycol) chains.[926]

mers are typically prepared via a hydro(solvo)thermal method by dissolving a lanthanide(III) salt and the organic acid in a mixture of water and an organic solvent like ethanol, DMF, or acetonitrile, followed by heating the mixture in an autoclave. Related ligands for synthesis of lanthanide-containing MOFs are 1,2-benzenedicarboxylate,[953] 1,3-benzenedicarboxylate,[954,955] 5-nitro-1,3-benzenedicarboxylate,[956] 1,3,5-benzenetricarboxylate,[957] 2,6-naphthalenedicarboxylate,[958,959] 1,4-naphthalenedicarboxylate,[960] 1,4,5,8-naphthalenetetracarboxylate,[961] 2,6-pyridinedicarboxylate,[962] 2,5-pyridinedicarboxylate,[963] 2,5-thiophenedicarboxylate,[964] 1,4-phenylenediacetate,[963] 4,5-imidazoledicarboxylate,[965] 2,2′-bipyridine-4,4′-dicarboxylate,[966] 1,3-cyclohexanedicarboxylate,[967] 1,3,5-cyclohexanetricarboxylate,[968] and 1,3-adamantanedicarboxylate (Chart 14).[969] More flexible networks are formed by α,ω-dicarboxylate ions like the adipate ion.[970−974]

Liu and co-workers prepared lanthanide-containing coordination polymers $\{Na[LnL(H_2O)_4]\cdot 2H_2O\}_n$ (Ln = La, Sm, Eu, Gd) based on the macrocyclic ligand 1,4,8,11-tetraazacyclotetradecane-1,4,8,11-tetraproprionic acid (H_4L) (Figure 89). The compounds form a 3D network with channels. The tetraazacyclotetradecane macrocycle is not occupied in the basic structures and interaction of the coordination polymers with transition metals like Cu^{2+}, Ag^+, Zn^{2+}, Cd^{2+}, and Hg^{2+} results in coordination of these metals to this site. Whereas the Cu^{2+}, Zn^{2+}, Cd^{2+}, and Hg^{2+} ions lead to a quenching of the europium(III) luminescence, a strong enhancement of the luminescent intensity was found in the presence of silver(I) ions, and a spectacular increase of the intensity of the hypersensitive transition $^5D_0 \rightarrow {}^7F_2$ was noticed.[975] On the other hand, the energy transfer of silver(I) to europium(III) in a heterometallic Ag−Eu coordination polymer derived from isonicotinate and 1,3-benzenedicarboxylate was found not to be efficient.[976] The luminescence of 3d−4f heterometallic coordination polymers $\{Ln(dpa)_3Mn_{1.5}(H_2O)_3]\cdot 3.25H_2O\}_\infty$ with 1D channels (Ln = Eu, Tb, dpa = pyridine-2,6-dicarboxylate) dissolved in DMF is strongly enhanced in the presence of Zn^{2+} ions, so these materials have been proposed as active components for zinc sensors.[977] Addition of Ca^{2+} and Mg^{2+} did not influence the luminescence intensity, whereas quenching of the emission was observed in the presence of Fe^{2+}, Co^{2+}, and Ni^{2+}. MOFs formed by 1,4,8,11-tetraazacyclotetradecane-1,4,8,11-tetraacetic acid (H_4TETA) and lanthanide ions (Ln = Nd, Eu, Tb, Dy) were found to be efficient luminescent materials, emitting either in the visible or in the near-infrared region.[978] Sensitized luminescence was observed for the lanthanide-containing coordination polymer $\{Ba_2(H_2O)_4[LnL_3(H_2O)_2](H_2O)_nCl\}_\infty$, where Ln = Sm, Eu, Tb, or Dy and L is 4,4′-disulfo-2,2′-bipyridine-*N*,*N*′-dioxide.[979] Schiff base coordination polymers were obtained by reaction of *N*,*N*′-bis(salicylidene)propane-1,2-diamine with a solution of $Ln(NO_3)_3$ salt (Ln = La, Sm, Eu).[980] Red emission was observed for the europium(III) and samarium(III) complexes, while blue ligand emission was detected for the lanthanum(III) compound. Kerbellec et al. showed that the emission properties of lanthanide-containing

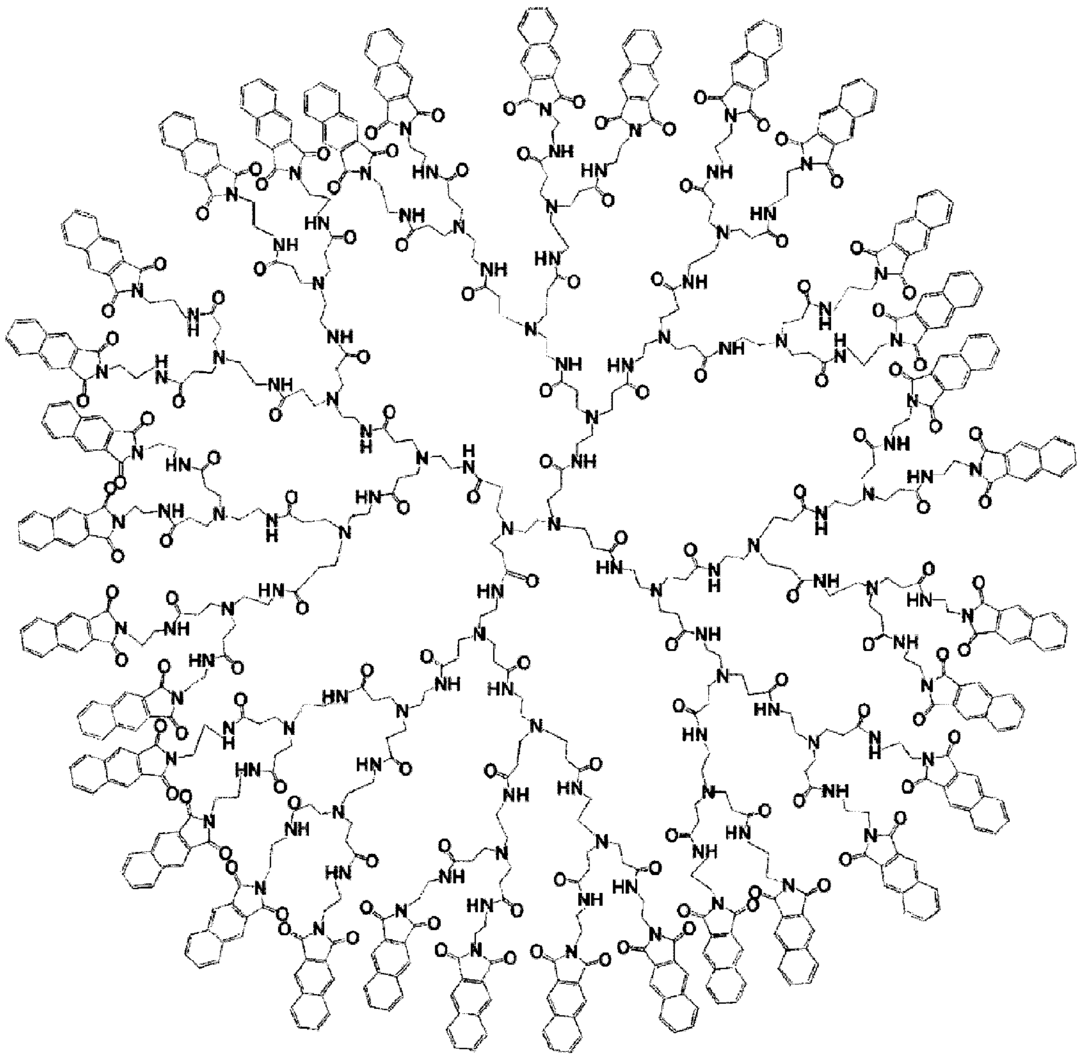

Figure 86. PAMAM-type of dendrimer of the third generation, with 32 external 2,3-naphthalimide groups and 60 internal amide bonds suitable for coordination with lanthanide(III) ions. Reproduced with permission from ref 927. Copyright 2004 American Chemical Society.

coordination polymers can be tuned by using a mixture of emitting lanthanide ions so that the different lanthanide ions are statistically distributed over the metal sites of the coordination polymer network. For instance, the emission color could be varied from green over yellow and orange to red by adjusting the ratio of Tb^{3+} to Eu^{3+}.[981]

The possibility to sense small molecules in the pores of microporous metal−organic frameworks by lanthanide luminescence was illustrated for polymeric europium(III) 1,3,5-benzenetricarboxylate by Chen et al.[982] The microporous europium polymer was first activated by heating at 140 °C *in vacuo* to expel the water molecules from the pores. The activated polymer was dispersed in different organic solvents (methanol, ethanol, 1-propanol, 2-propanol, acetone, acetonitrile, chloroform, DMF, and THF). The strongest enhancement of the luminescence was observed for DMF, while the luminescence was nearly totally quenched in acetone. Further studies included dispersion of the europium polymer in 1-propanol with different amounts of DMF or acetone added. The increase (or decrease) of the emission intensity was found to be proportional to the DMF (or acetone) concentration. Polymeric terbium(III) 1,3,5-benzenetricarboxylate forming a microporous network was used for luminescence sensing of anions.[983] The heat-activated polymer was immersed in methanol solutions of sodium salts (NaF, NaCl, NaBr, Na_2CO_3, and Na_2SO_4). An enhancement of the terbium(III) luminescence was noticed for all anions, with the strongest effect for fluoride ions.

Two-photon upconversion luminescence was reported for a metal−organic framework containing neodymium(III) and 1,3,5-benzenetricarboxylate ions.[984] Comparison of the near-infrared luminescence of coordination polymers derived from erbium(III) and 1,4-benzenedicarboxylate or 2,3,5,6-tetrafluorobenzenedicarboxylate shows a strong enhancement of the luminescence by fluorination of the benzene ring.[985] Intense terbium luminescence was observed for terbium(III) imidazolate networks with ammonia molecules entrapped in the network pores.[986] Highly green-luminescent terbium(III) coordination polymers were obtained by reaction of the amino groups in terbium(III) *p*-aminobenzoate with aromatic or aliphatic diisocyanates.[987]

8. Hydrogels and Organogels

Hydrogels and *organogels* are soft materials that are formed by immobilization of water or organic solvents, respectively, by means of a *gelator*.[988,989] A typical gelator is a low-molecular weight organic compound, which is able to form by self-assembly polymer-like fibers with lengths on the micrometer scale and diameters on the nanometer

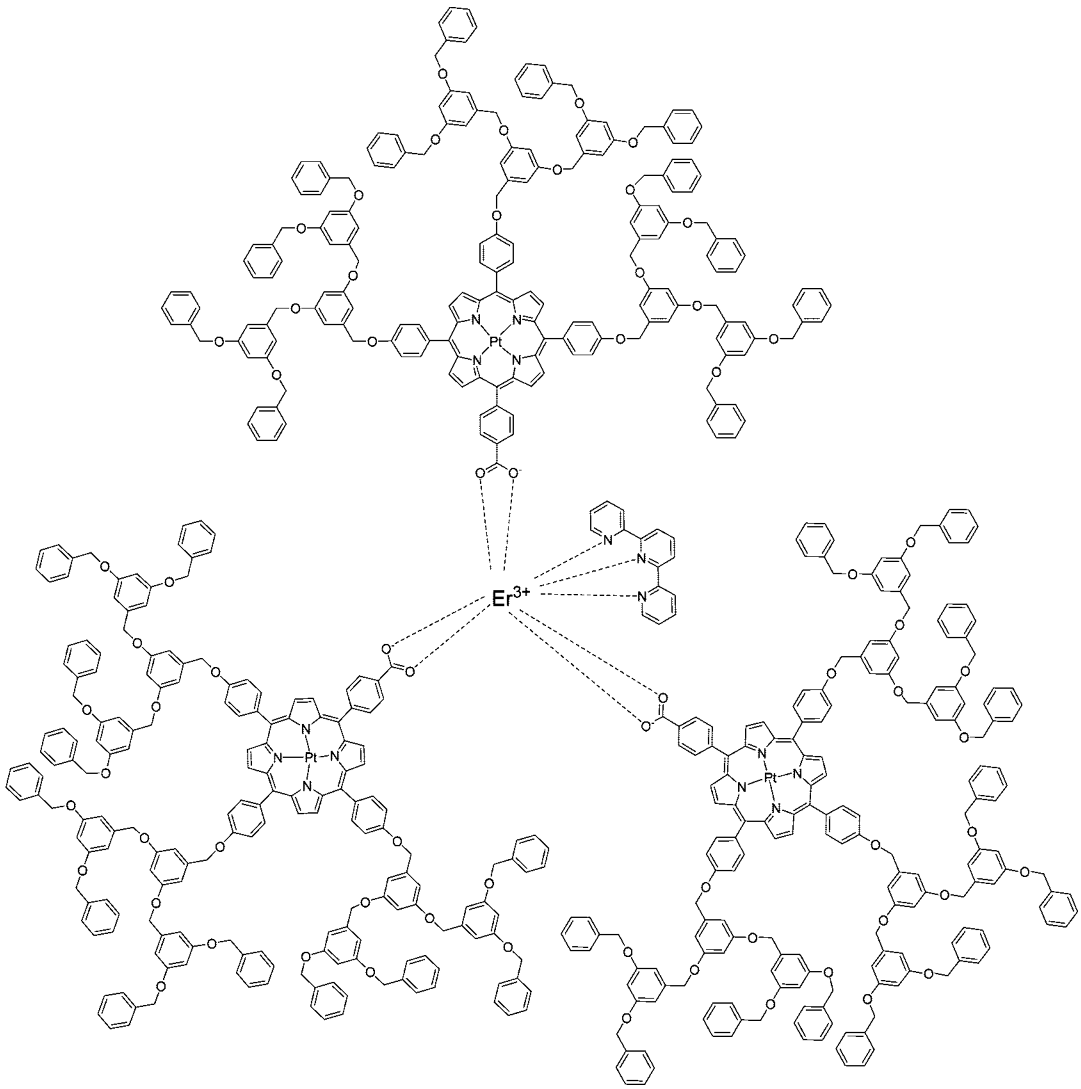

Figure 87. Erbium(III) complex of platinum(II)-porphyrin ligands decorated with Fréchet-type dendrons.[930]

scale. The entanglement of a large number of the fibers results in the formation of a network that entraps solvent molecules in the fibrillar network compartments. The gels formed by low-molecular weight gelators are considered physical gels or supramolecular gels. Other types of gels are *polyelectrolyte gels*, which are, for instance, formed by poly(acrylic acid) or by poly(methacrylic acid),[990] and hydrogel gels formed by polymers like poly(*N*,*N*-dimethylacrylamide). The gels are viscoelastic solid-like materials with the solvent being the major component. Luminescent hydrogels and organogels can be obtained by incorporation of luminophores in the gelator or by dissolution of luminescent compounds in the water or organic solvent phase. Only very few studies of lanthanide-containing hydrogels and organogels have been reported to date.

De Paoli et al. prepared luminescent gels doped with a hemicaged europium(III) complex (Figure 90) using a carboxylate-based aliphatic gelator (Figure 91) to gelate DMF and a *N*,*N'*-bis(*O*-methyl-tyrosine) oxalamide derivative (Figure 92) to gelate water.[991] The luminescence characteristics of the Eu^{3+} ion did not significantly changed upon gelation of the solvent. This is an indication that the complex remained dissolved in the solvent pockets and that it was not involved in the network formation. An amphiphilic gallamide derivative bearing three hydrophobic tetradecyl chains and a hydrophilic triethoxysilyl group was used as gelator of an ethanol solution containing lanthanide(III) nitrate salts (Ln = Tb and Dy) (Figure 93).[992] The terbium(III)-containing organogel showed green emission and the luminescence intensity gradually decreased upon heating. On the other hand, the blue luminescence of the dysprosium(III)-containing organogel was suddenly quenched when the samples were heated above the order−disorder phase transition point. The luminescence of lanthanide(III)-doped ionogels consisting of ionic liquids immobilized into a nanostructured silica network has been described in section 3.2.

Smirnov et al. studied the chemically cross-linked gels of europium(III), terbium(III), and neodymium(III) salts of poly(methacrylic acid) swollen in methanol.[993] The lanthanide ions bound to the polymer network formed multiplets consisting of clusters of three to four lanthanide ions. The aggregation number of the multiplets was estimated by energy transfer from Eu^{3+} to Nd^{3+}. Binding of the carboxylate groups of poly(acrylic acid) or poly(methacrylic acid) to europium(III) in hydrogels resulted in the expulsion of up to five water molecules from the first coordination sphere of the europium(III) ion.[994] The changes in hydration number of the Eu^{3+} ion upon coordination to the carboxylate groups did not seem to depend much on the molecular mass of the poly(acrylic acid).[995] Bekiari and Lianos described hydrogels formed by poly(*N*,*N*-dimethylacrylamide) doped with lan-

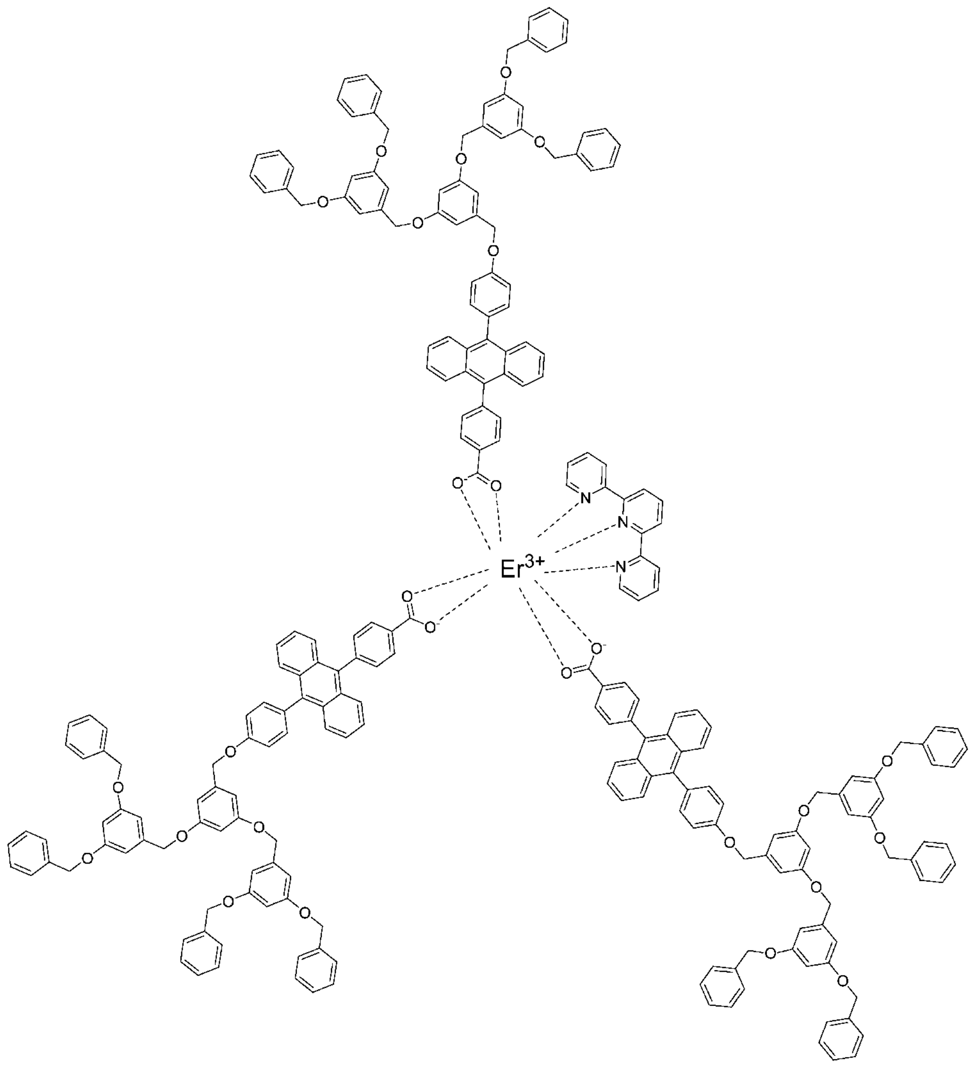

Figure 88. Erbium(III) complex of a Fréchet-type dendron with a diphenyl anthracene group and with a coordinating carboxylate group.[938]

Chart 14. Selected Building Blocks for Metal−Organic Frameworks (MOFs)

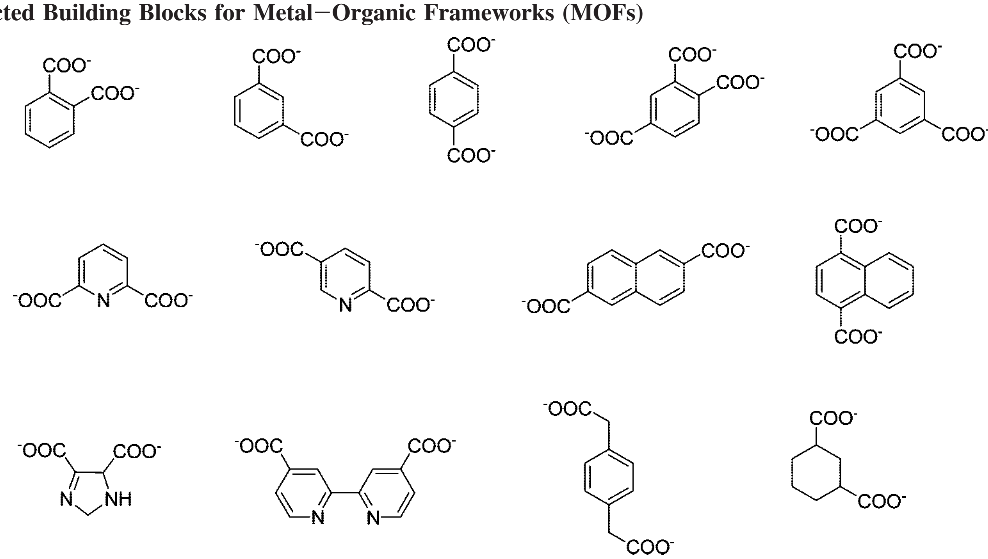

thanide(III) terpyridine complexes.[996] The hydrogels were investigated in three different states: swollen in water, lyophilized (dried by freeze-drying), in which case it loses the solvent but preserves the swollen configuration, and dried in air, in which case it shrinks. Interestingly, the gels doped with the Eu^{3+} ion exhibited the typical metal-centered red luminescence in the solvent-swollen and lyophilized gels, but green ligand-centered luminescence in the air-dried gel samples. Kawa and Takahagi obtained a transparent green-emitting hydrogel by radical copolymerization of a terbium(III) complex of a poly(benzyl ether) dendrimer containing terminal vinyl groups with *N*-isopropylacrylamide in

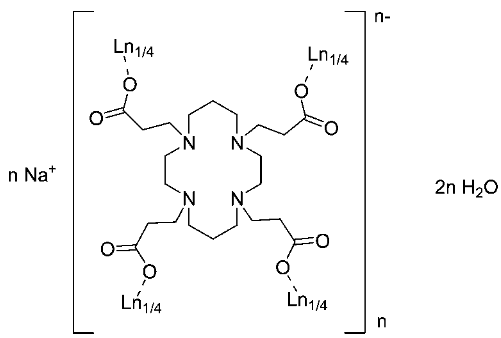

Figure 89. Lanthanide-containing coordination polymers derived from 1,4,8,11-tetraazacyclotetradecane-1,4,8,11-tetraproprionic acid. Ln = La, Sm, Eu, or Gd.

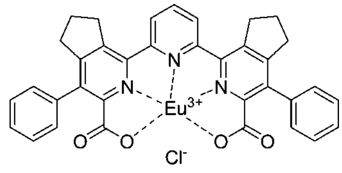

Figure 90. Hemicaged europium(III) complex.

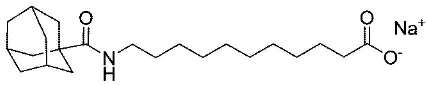

Figure 91. Carboxylate-based aliphatic organogelator.

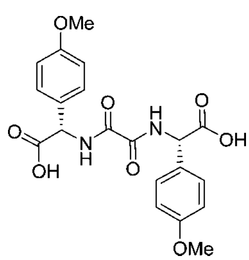

Figure 92. *N*,*N′*-Bis(*O*-methyl-tyrosine) oxalamide gelator.

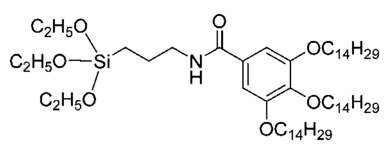

Figure 93. Hydrolyzable amphiphilic gallamide precursor.

DMSO, followed by immersion of the DMSO gel in a large excess of water to ensure solvent exchange.[916] The hydrogel was found to be stable in strong electrolyte solutions like a saturated NaCl solution. Another type of terbium(III)-containing hydrogel was obtained by gelation of an aqueous solution of a terbium(III) calix[4]arene complex by gelatin.[997] A europium(III) complex of a quinoline-derivatized cyclen (1,4,7,10-tetraazacyclododecane) was incorporated in a hydrogel derived from cross-linked poly(methyl methacrylate-*co*-2-hydroxyethyl methacrylate) (Figure 94).[998,999] The luminescence of the europium(III) complex in the hydrogel was found to be highly pH-sensitive, and the luminescence could be switched on and off as a function of the pH. Whitesides and co-workers obtained a hydrogel responsive to an external magnetic field by cross-linking alginic acid in aqueous solution by (paramagnetic) Ho^{3+} ions.[1000] Although no luminescence of these materials was reported, they can easily be transformed into luminescent magnetic-field-responsive materials by incorporation of emissive lanthanide ions. A europium(III)-containing chitosan−poly(acrylic acid) hydrogel was prepared by radical solution polymerization

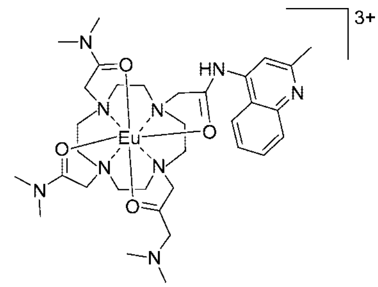

Figure 94. Europium(III) complex of a quinoline-derivatized cyclen.[998] The triflate ($CF_3SO_3^-$) counterions are not shown.

in water, using chitosan as the basic material, *N*,*N′*-methylene-diacrylamide as the cross-linking agent, and potassium persulfate as the initiator.[1001]

9. Nanocomposite Materials

Lanthanide-doped nanoparticles are interesting compounds, because they possess the excellent luminescent properties of inorganic phosphors and because they are compatible with molecular materials. For instance, the quenching of lanthanide luminescence in sol−gel-derived materials by concentration quenching and remaining hydroxyl groups can be avoided by doping lanthanide-containing nanoparticles instead of molecular lanthanide complexes in the sol−gel matrix. The same reasoning can be applied for lanthanide-doped polymer materials. Despite the huge potential of luminescent materials based on lanthanide-doped nanoparticles, this field is still underdeveloped. This is in contrast to the intense research activities on lanthanide-doped nanopartices dispersed in water or organic solvents. The older (pre-1998) work on lanthanide-doped nanoparticles has been reviewed by Tissue.[9] Several reviews describe the more recent developments.[1002−1006] Here, we will mainly focus on the use of luminescent nanoparticles in hybrid materials and will therefore discard a discussion about nanosized lanthanide phosphors or lanthanide nanoparticles dispersed in solutions. An exception is made for surface-modified nanoparticles, which are discussed in section 9.1.

9.1. Surface-Modified Nanoparticles

Lanthanide-doped nanoparticles are often coated with polymers or with long-chain organic molecules to improve the stabilities of the nanoparticles. The organic coating protects the nanoparticles against close contact with other nanoparticles and thus avoids their aggregation to larger particles. However, it is also possible to covalently attach additional organic molecules or metal complexes to the surface of these nanoparticles in order to add an additional functionality. On the other hand, it is also possible to anchor luminescent lanthanide complexes via a linking group on nanoparticles.

$LaF_3/(Tb^{3+}/Ce^{3+})$ nanoparticles functionalized with glucose were developed as fluorescent labels for the determination of glucose.[1007] LaF_3/Eu^{3+} nanoparticles were coated with the biopolymer chitosan, not only to stabilize these nanoparticles but also to have hydroxyl and amino groups on the surface to which other biomolecules can be attached.[1008] Coating of lanthanide-containing nanoparticles by organic molecules can be done to sensitize the lanthanide luminescence. This was illustrated, for instance, for (LaF_3/Eu^{3+})−AEP nanoparticles (AEP = aminoethylphosphate) coated with 6-carboxy-5′-methyl-2,2′-bipyridine[1009] or for $Eu(OH)_3$ nanorods with

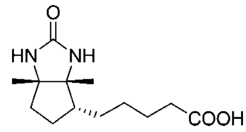

Figure 95. Biotin.

coating of a chromophore-containing organically modified silicate layer.[1010]

The lanthanide complexes [Ln(btac)$_3$(phen)] (Ln = Sm, Eu, Tb) were doped into polystyrene and PMMA nanoparticles.[1011] It was found that it was impossible to obtain a homogeneous distribution of [Eu(tta)$_3$(phen)] in the nanoparticles so that some of the nanoparticles were not luminescent. The same problem was observed for [Eu(btac)$_3$(phen)] in PMMA but not in polystyrene. Polystyrene nanoparticles doped with luminescent lanthanide complexes have been developed for use in *time-resolved fluoroimmunoassay* (TR-FIA). Europium(III) β-diketonate containing polystyrene nanoparticles were coated with streptavidin. Because of the high affinity of the protein streptavidin for biotin (Figure 95), the streptavidin-coated nanoparticles could be used for interaction with biotinylated antibodies, and this approach allowed ultrasensitive detection of nanoparticles to zeptomolar (10^{-21} mol/L) concentrations.[1012] Further elaboration of this methodology has been described in follow-up papers.[1013−1015] Luminescent europium(III)-containing silica nanoparticles with surface amino groups were used for biolabeling.[1016] Streptavidin-labeled nanoparticles were used for time-resolved fluoroimmunassays of carcinoembryonic antigens (CEA) and hepatitis B surface antigens (HBsAg) in human sera. Nanoparticles labeled with transferrin were used for staining cultured Hela cells.[1017] Van Veggel reported on LaF_3/Ln^{3+} (Ln = Eu, Tb, Nd, Tm, Yb) nanoparticles to which biotin was covalently bonded for interaction studies with the protein avidin.[1018,1019]

The streptavidin coating of nanoparticles was also applied to nanoparticles consisting of a core of magnetic iron oxide particles, an inner shell of $NaYF_4/(Yb^{3+},Er^{3+})$ phosphor, and an outer shell of silica.[1020] The silica was activated with glutaraldehyde, and subsequently streptavidin was immobilized on the nanoparticles. The nanoparticles were found to bind specifically to a glass slide spotted with biotinylated IgG. The $NaYF_4/(Yb^{3+},Er^{3+})$ coating allows observation of infrared-to-visible upconversion for these nanoparticles (Figure 96). Hur and co-workers coated magnetic ferrite (Fe_3O_4) nanoparticles with a silica shell and 2,2′-bipyridine-4,4′-dicarboxylate molecules were attached to the silica surface.[1021] The chelating groups on surface of the nanoparticles were allowed to react with $EuCl_3$ or $TbCl_3$, and as a result, nanoparticles that showed both magnetic and luminescent properties were obtained. These luminescent nanoparticles could be manipulated by external magnetic fields. Such multifunctional magnetic−luminescent nanocomposites are of interest for biomedical uses, like biological imaging, cell tracking, magnetic bioseparation, biosensing, and chemosensing.[1022] Another type of luminescent/magnetic nanoparticle was obtained by coating Fe_3O_4 nanoparticles with a shell of Gd_2O_3/Eu^{3+} or Gd_2O_3/Tb^{3+}.[1023,1024]

Pikramenou and co-workers described luminescent lanthanide complexes bonded via thiol groups to gold nanoparticles (Figure 97).[1025] Thomas and co-workers attached thiol-functionalized 2,2′-bipyridine ligands to gold nanoparticles (Figure 98).[1026] Around a gold nanoparticle with a diameter of about 4 nm, an estimated 340 2,2′-bipyridine

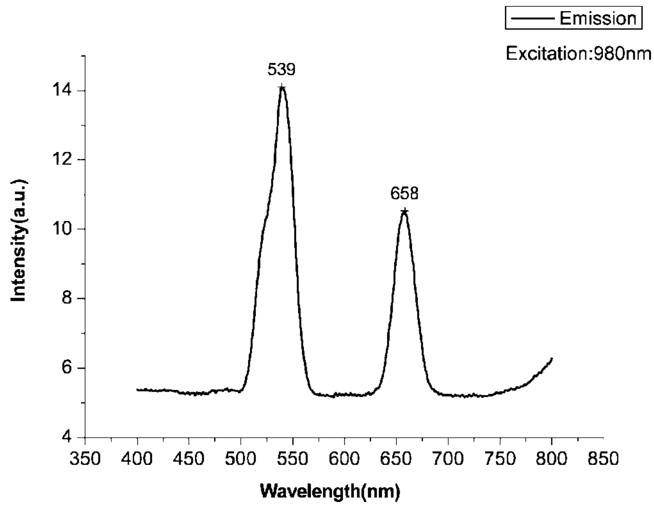

Figure 96. Near-infrared-to-visible upconversion luminescence spectrum of magnetic iron oxide nanoparticles, an inner shell of $NaYF_4/(Yb^{3+},Er^{3+})$ phosphor, and an outer shell of silica. The excitation wavelength was 980 nm. Reproduced with permission from ref 1020 (http://dx.doi.org/10.1039/b315103d). Copyright 2004 Royal Society of Chemistry.

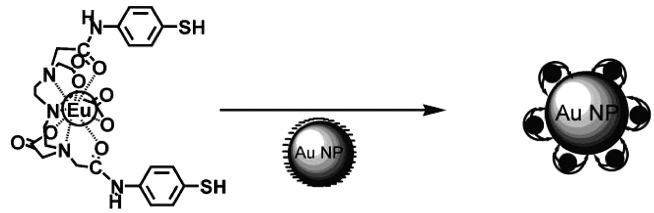

Figure 97. Europium(III) complex of a thiol-functionalized DTPA derivative and its anchoring to a gold nanoparticle. Reproduced with permission from ref 1025 (http://dx.doi.org/10.1039/b518091k). Copyright 2006 Royal Society of Chemistry.

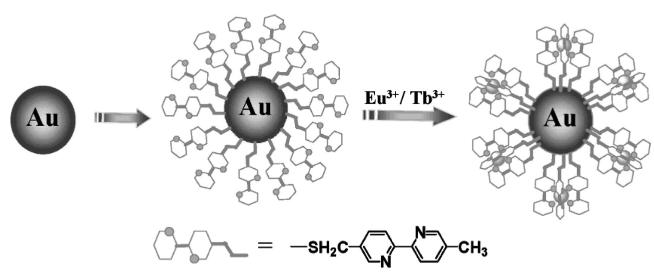

Figure 98. Design of luminescent europium(III) and terbium(III) complexes of gold nanoparticles functionalized with 2,2′-bipyridine groups. Reproduced with permission from ref 1026. Copyright 2006 American Chemical Society.

ligands were present, creating an environment with a high ligand concentration (5 mol/L). The 2,2′-bipyridine ligands formed complexes with Eu^{3+} and Tb^{3+} in a 1:3 metal-to-ligand ratio. The europium(III)-containing nanoparticles are useful for cation sensing, because the europium luminescence is quenched upon addition of Mg^{2+}, Ca^{2+}, Ni^{2+}, Zn^{2+}, and Cu^{2+} (Figure 99). Na^+ and K^+ ions had no influence on the luminescence intensity. Gunnlaugsson connected a macrocyclic europium(III) cyclen derivative via a long alkyl spacer and a thiol group to gold nanoparticles.[1027] The luminescence of these nanoparticles could be strongly increased upon addition of the naphthoyltrifluoroacetonate ligand, which binds to the Eu^{3+} ion and acts as an antenna for light capture. However, subsequent addition of flavin monophosphate decreased the luminescence intensity, because this ligand

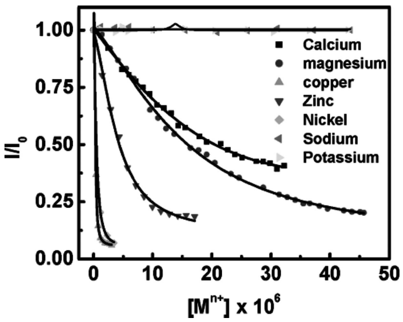

Figure 99. Relative decrease of the luminescence intensity of europium(III) complexes of 2,2′-bipyridine-functionalized nanoparticles upon addition of metal ions. Reproduced with permission from ref 1026. Copyright 2006 American Chemical Society.

replaces naphthoyltrifluoroacetonate in the first coordination sphere of the Eu^{3+} ion.

9.2. Nanoparticles in Sol−Gel Glasses

In order to overcome the weak light absorption of lanthanide ions dispersed in a sol−gel glass, the glass matrix can be codoped with inorganic nanoparticles like ZnS or CdS. These nanoparticles show a strong light absorption, and they can transfer the excitation energy to excited energy levels of the lanthanide ion. Reisfeld and co-workers have studied CdS nanoparticles doped with Eu^{3+} and Tb^{3+} in zirconia sol−gel glasses.[1028] A detailed study by Meijerink and co-workers on the sensitization of lanthanide luminescence by ZnS and CdS nanoparticles showed that the trivalent lanthanide ions are very likely not incorporated in the nanoparticles but are rather adsorbed on the nanoparticles surface.[1029] The distribution of the Eu^{3+} ions and CdS nanoparticles within a silica sol−gel matrix could be varied by changing the synthesis conditions.[1030] It is possible to introduce CdS nanoparticles in a Eu^{3+}-doped silica sol−gel glass after synthesis by immersion of the glass sample in a colloidal CdS solution.[1031,1032] Zalewska and Klonkowski studied the influence of CdS nanoparticles on Tb^{3+} luminescence in sol−gel glasses, and they observed a decrease in the luminescence intensity of Tb^{3+} with decreasing size of the CdS nanoparticles.[1033] Incorporation of Mn^{2+} in ZnS was found to distort the ZnS lattice and to generate many blue-emitting defect states. Therefore, Eu^{3+} and Mn^{2+} codoped nanocrystals dispersed in a silica glass exhibit not only the typical europium(III) line emission but also broad-band blue emission due to the defect states.[1034] This work also shows that Eu^{3+} is not incorporated in the ZnS lattice but that the Eu^{3+} ions are in close vicinity of the ZnS nanoparticles. Otherwise no efficient energy transfer from ZnS to Eu^{3+} would be possible. Several other studies on sol−gel glasses doped with semiconductor nanoparticles (ZnS, ZnSe, CdS, CdSe) and lanthanide ions have been reported.[1035−1042] SnO_2 nanocrystals have been used to sensitize the luminescence of samarium(III)[1043] and europium(III)[1044] ions in silica xerogels. Klonkowski and co-workers considered silica sol−gel glasses or ormosils doped with ZnO nanoparticles and codoped with Eu^{3+} or Tb^{3+} ions or both.[1045] The ZnO nanoparticles were found to sensitize Tb^{3+} luminescence but not Eu^{3+} luminescence. However, Eu^{3+} luminescence could be enhanced by adding Tb^{3+} ions to the sol−gel materials containing both ZnO nanoparticles and Eu^{3+} ions. This behavior can be explained by a ZnO → Tb^{3+} energy transfer, followed by a Tb^{3+} → Eu^{3+} energy transfer. Also TiO_2 nanoparticles can sensitize Tb^{3+} luminescence in sol−gel glasses.[1046]

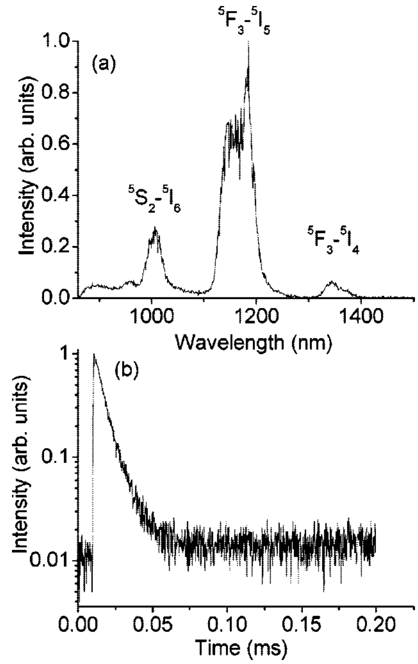

Figure 100. Luminescence spectrum (a) and decay curve (b) for silica sol−gel films doped with LaF_3/Ho^{3+} nanoparticles with Ho/Si ratio = 0.0015 and heated in air at 800 °C for 12 h. The samples were excited at 448 nm. The decay curve was monitored at 1180 nm ($^5F_3 \rightarrow {}^5I_5$ transition). Reproduced with permission from ref 1058. Copyright 2005 American Chemical Society.

Instead of semiconductor nanoparticles, also metal nanoparticles like gold[1047,1048] or silver[1049−1054] can be used to sensitize lanthanide luminescence in sol−gel glasses. For more information on *metal-enhanced luminescence*, the reader is referred to the specialized literature.[1055−1057] The photoluminescence enhancement is maximal if the lanthanide luminescence is resonant with the nanoparticle plasmon modes. The transition dipoles of the f−f transitions are coupled with these plasmon modes.

A third approach toward nanocomposite sol−gel materials is to dope luminescent lanthanide-containing nanoparticles in a sol−gel matrix. Van Veggel and co-workers doped LaF_3/Ln^{3+} nanoparticles (Ln = Nd, Eu, Er, Ho) in sol−gel-derived thin films of SiO_2, Al_2O_3, ZrO_2, HfO_2, and In_2O_3 (Figure 100).[1058,1059] Energy transfer of the semiconductor thin film to the lanthanide ion was observed after excitation in the absorption bands of the semiconductor. By incorporation of the lanthanide ions in the LaF_3 nanoparticles, quenching of the luminescence by OH vibrations could be avoided, and this resulted in an increase in the luminescence lifetimes. In Figure 101, the luminescence spectra of LaF_3/Eu^{3+} nanoparticles is shown.[1060] A remarkable property of Eu^{3+} in the LaF_3 matrix is the weak relative intensity of the $^5D_0 \rightarrow {}^7F_2$ transition in comparison to the intensity of the $^5D_0 \rightarrow {}^7F_1$ transition. Also transitions starting from the $^5D_1$ excited state can be observed in the room-temperature luminescence spectrum. Via an upconversion process, it was possible to generate white light from SiO_2 or ZrO_2 sol−gel matrices doped with $LaF_3/(Eu^{3+},Yb^{3+})$, $LaF_3/(Er^{3+},Yb^{3+})$, and $LaF_3/(Tm^{3+},Yb^{3+})$ (Figure 102).[1061] The codoping with Yb^{3+} makes excitation with 980 nm radiation (from a cheap CW laser) possible. Eu^{3+} generates red light, Er^{3+} generates red and green light, and Tm^{3+} generates blue light via the upconversion process after energy absorption via the Yb^{3+}

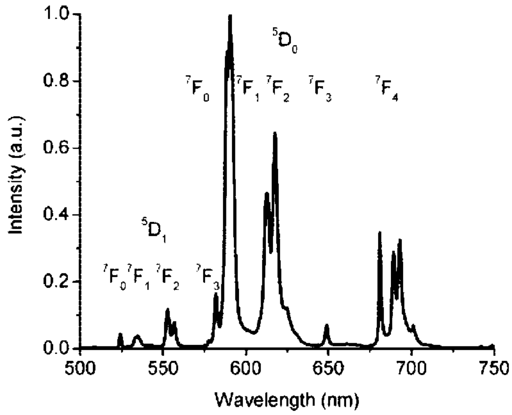

Figure 101. Luminescence spectrum of LaF_3/Eu^{3+} nanoparticles dispersed in dichloromethane (excitation wavelength = 397 nm). Reproduced with permission from ref 1060. Copyright 2004 American Chemical Society.

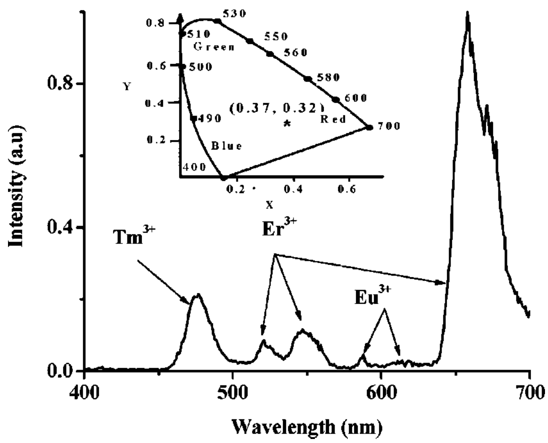

Figure 102. Upconversion emission spectrum of silica thin films prepared at 800 °C made with $La_{0.45}Yb_{0.5}Er_{0.05}F_3$, $La_{0.75}Yb_{0.2}Tm_{0.05}F_3$, and $Yb_{0.75}La_{0.2}Eu_{0.05}F_3$ nanoparticles under 300 mW 980 CW laser excitation. The inset shows the CIE color coordinates of the resulting white light. Reproduced with permission from ref 1061. Copyright 2005 American Chemical Society.

ion. The CIE coordinates of the emitted light could be adjusted by controlling the relative concentration of the lanthanide ions in the nanoparticles as well as the concentration of the nanoparticles in the sol−gel film. The spatial separation of the different nanoparticles avoids energy transfer between the Eu^{3+}, Er^{3+}, and Tm^{3+} ions. Thin films were obtained by spin-coating on a quartz plate. A control experiment in which La^{3+}, Eu^{3+}, Er^{3+}, and Tm^{3+} were doped directly in the sol−gel thin film rather than first incorporating them into LaF_3 nanoparticles resulted in a material that showed only green Er^{3+} emission. Bo et al. doped $LaF_3/(Er^{3+},Yb^{3+})$ nanoparticles coated with oleic acid in sol−gel-derived silica thin films.[1062] These materials were used for the preparation of optical waveguide amplifiers. Nd_2O_3 nanoparticles (5−60 nm)[1063] and Er_2O_3 nanoparticles (5−30 nm)[1064] were prepared by an inverse microemulsion technique and were dispersed in a titania/GLYMO hybrid material. Erbium(III) oxalate nanoparticles incorporated into a titania/GLYMO matrix showed relatively intense green upconversion luminescence at room temperature.[1065] Neodymium(III) oxalate nanoparticles in this hybrid matrix gave violet upconversion luminescence (399 nm) upon excitatation with yellow light (587 nm).[1066]

Y_2O_3/Eu^{3+} nanocrystals were incorporated in mesoporous MCM-41, porous silica aerogels, and porous alumina with

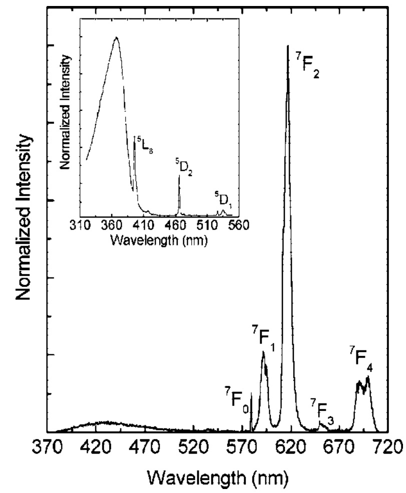

Figure 103. Luminescence spectrum of a $[Eu(H_2O)(picOH)_2(\mu\text{-HpicO})]\cdot 3H_2O/SiO_2$ nanocomposite material excited at 327 nm. The inset shows the excitation spectrum monitored at 617 nm. Reprinted with permission from ref 1069. Copyright 2003 American Chemical Society.

pore sizes ranging between 2.7 to 80 nm.[1067] A remarkable observation was that luminescence decay was 3 times larger than that of a Y_2O_3/Eu^{3+} bulk sample. Monoclinic Eu_2O_3 nanoparticles are stabilized in MCM-41 and show a higher luminescence intensity than cubic Eu_2O_3 nanoparticles or the bulk powder.[1068]

It is also possible to prepare silica nanoparticles by a sol−gel method. Molecular lanthanide complexes can be incorporated in these silica colloids during synthesis. This was illustrated for lanthanide complexes of 3-hydroxypicolinic acid (HpicOH).[1069] In Figure 103, the luminescence spectrum of the $[Eu(H_2O)(picOH)_2(\mu\text{-HpicO})]\cdot 3H_2O/SiO_2$ nanocomposite material is shown. Iwu et al. used reverse micelles to prepare nanoparticles consisting of europium(III) or terbium(III) complexes of 3-hydroxypicolinic acid as a core and with a silica shell around it.[1070] Inverse silica opals were synthesized via centrifugation of monodisperse colloidal poly(methyl methacrylate) spheres (330−400 nm) to a close-packed structure, followed by infiltration of a silica sol−gel precursor, gel formation, and calcination. Lanthanide complexes of fluorinated β-diketonates were loaded in the voids of the inverse opal structure by vacuum sublimation. Thermal decomposition of the fluorinated complexes led to formation of lanthanide(III) fluorides inside the voids. The fluorides could be transformed into oxyfluorides by heating of the fluorides in air. Typical red Eu^{3+} luminescence was observed for EuF_3, EuOF, GdF_3/Eu^{3+} and $GdOF/Eu^{3+}$.[1071]

9.3. Nanoparticle−Polymer Composites

Composites consisting of luminescent nanoparticles dispersed in a polymer matrix are interesting materials because they combine the advantages of both polymers (good processability and good mechanical properties) and inorganic luminescent materials (high luminescence efficiency and long-term chemical stability). Whereas polymer composites with microsized particles suffer from strong light scattering, polymers composites with nanoparticles can be highly transparent.[1072] Particle sizes below 40 nm are required to reduce the Rayleigh scattering to such an extent that transparent materials are obtained. However, the required size also depends on the difference of refractive index between the polymer matrix and the nanoparticles, because the larger the difference the greater the light scattering will be. The easiest way to prepare nanoparticle−polymer composites is by dispersing the nanoparticles in a solution of a polymer in an organic solvent, followed by preparation of the films by spin-coating, dip-coating, or casting. Goubart et al. reported on green-emitting poly(ethylene oxide) films doped with Gd_2O_3/Tb^{3+} nanoparticles.[1073] Dekker et al. prepared near-infrared emitting PMMA films doped with LaF_3/Nd^{3+} nanoparticles.[1074] Strong near-infrared emission at about 1550 nm upon excitation at 980 nm was observed for oleic acid modified $LaF_3/(Yb^{3+},Er^{3+})$ nanoparticles that were incorporated in a PMMA polymer matrix.[1075] In order to overcome the problems with the strong absorption of the PMMA matrix in the 1600−1700 nm region, Riman and co-workers proposed to incorporate the nanoparticles in perfluorocyclobutyl polymers. These authors doped the fluorinated polymers with CaF_2/Er^{3+} and LaF_3/Nd^{3+} nanoparticles.[1076] Quantum efficiencies as high as 95% for LaF_3/Nd^{3+} and 51% for CaF_2/Er^{3+} were measured. The particle sizes of the nanoparticles in the polymers was less than 100 nm. Loading of the semiconducting polymer poly(phenylene vinylene) (PPV) with erbium-doped silicon nanocrystals was found to have a significant effect on the carrier transport and the visible electroluminescence of this polymer.[1077] No erbium-centered near-infrared emission was reported. Tranparent nanocomposites consisting of YVO_4/Eu^{3+} nanoparticles in polymer matrices were prepared by in situ polymerization of particle dispersions in methyl methacrylate (MMA) and lauryl acrylate (LA).[1078] Near-infrared-emitting materials were obtained by doping $Y_2O_3/(Yb^{3+},Er^{3+})$ nanoparticles into a PMMA matrix. Upon excitation at 980 nm, emission of 1550 nm was observed.[1079] White-emitting organic−inorganic hybrid films consisting of Eu_2O_3 nanocrystals, *N*,*N*′-diphenyl-*N*,*N*′-bis(3-methylphenyl)-1,1′-biphenyl-4,4′-diamine (TPD) and poly(methyl methacrylate) (PMMA) were prepared by spin-coating.[1080,1081] Poly(vinylidene difluoride) (PVDF)/$(Y_{0.97}Eu_{0.03})_2O_3$ nanocomposites were prepared by a coprecipitation method.[1082] The optical band gap of the nanocomposites showed a decreasing trend with the increase of $(Y_{0.97}Eu_{0.03})_2O_3$ content in the polymer matrices. Luminescent composite fibers of poly(vinyl pyrrolidone) (PVP) and Y_2O_3/Eu^{3+} nanocrystals were prepared by electrospinning. The composite fibers were in a random orientation, with an average diameter of about 300 nm and length up to several tens of micrometers.[1083] Ln^{3+}-doped $NaYF_4$/poly(vinyl pyrrolidone) (PVP) nanocomposite fibers with an average diameter of 300−800 nm were prepared by electrospinning. The $NaYF_4$ nanoparticles have a size between 5 and 20 nm. Upon laser excitation at 980 nm, blue upconversion emission was observed for the PVP-dispersed $NaYF_4$ nanoparticles codoped with Yb^{3+} and Tm^{3+}. White light with more stable color balance (blue of Tm^{3+}, green and red of Er^{3+}) was obtained for the triply doped $NaYF_4/(Yb^{3+},Tm^{3+},Er^{3+})$ nanoparticles.[1084] Addition of dielectric Y_2O_3 nanocrystals resulted in a blue shifting and broadening of luminescence spectra of the conjugated polymer poly(*p*-phenylene vinylene) with a simultaneous disappearance of its vibronic structure.[1085] On the other hand, incorporation of the same nanocrystals in a poly[2-(6-cyano-6′-methylheptyloxy)-1,4-phenylene] matrix cause red shifting and spectral broadening. These results were explained by referring to a model that accounts for the change in the polarization component of the carrier and exciton energy in the vicinity of inclusions. PMMA and polystyrene films containing Eu_2O_3 nanoparticles coordinated by 2-thenoyltrifluoroacetonate and 1,10-phenanthroline have been prepared by laser ablation of a Eu_2O_3 in a flowing solution of the polymer and the organic ligands in cyclohexane.[1086] The hybrid polymer films were obtained by dropping of the solution on a glass plate, followed by evaporation of the organic solvent. During the laser ablation process, a pulsed laser beam (532 nm; frequency-doubled Nd/YAG laser) was focused on the solid Eu_2O_3 target, resulting in Eu_2O_3 nanoparticles with an average size of 20 nm. Nanocomposites were made by dispersing SiO_2 nanoparticles doped with Eu^{3+} ions in isotactic polypropylene.[1087] The fine structure of the luminescence spectra depended on the crystallinity of the polymer matrix. Higher luminescence intensity was noticed for polypropylene of higher crystallinity. Luminescent transparent layers were made by inkjet printing of $LaPO_4/Ce^{3+},Tb^{3+}$ (green luminescence) and $LaPO_4/Eu^{3+}$ (red luminescence) nanophosphors on standard overhead transparencies.[1088] The average size of the nanoparticles was 15 nm, and they were applied as a dispersion in ethanol for printing. Layer thicknesses of about 30 nm were obtained by a layer-by-layer process via repeating the printing process 10 times. The nanophosphors were prepared by a microwave synthesis in an ionic liquid.[1089−1091]

Europium(III)-containing hybrid materials were prepared by first introducing the complex $[Eu(dbm)_3(phen)]$ in monodisperse colloidal silica spheres, followed by dispersion of these microspheres in poly(methyl methacrylate) or in polystyrene.[1092] It was found that the europium(III) complex in such polymer systems showed higher spontaneous emission rates than for the spheres in air. Embedding of the europium-doped spheres in a polymer matrix is thus a method to modify the spontaneous emission rates. The $[Eu(dbm)_3(phen)]$ complex retained the same molecular conformation in the silica spheres as in the pure europium(III) complex.[1093] Nanosized lanthanide phosphates could be incorporated inside hollow poly(allylamine hydrochloride)/poly(styrene sulfonate) capsules.[1094] Daiguebonne et al. prepared poly(vinyl pyrrolidone) nanoparticles doped with lanthanide terephthalate coordination polymers $[Ln_2(C_8H_4O_4)_3(H_2O)_4]_n$ (Ln = Eu, Tb, Er).[1095] Although the encapsulation of the coordination polymers in the polymeric nanoparticle matrix resulted in a somewhat reduced luminescence intensities and luminescence lifetime, the fact that nanoparticles could be dispersed in water and remained unchanged in this medium for more than 20 h is a main advantage over the coordination polymers.

10. Applications

10.1. Luminescent Thin Films

Thin transparent polymer films of poly(vinyl chloride) or polyethylene find widespread use in agriculture and horticulture as covers for hotbeds and greenhouses to protect the plants from low temperatures or damage by intense UV radiation. It has been proposed to add luminescent molecular lanthanide complexes or lanthanide-doped inorganic compounds to such polymer films. The luminescent compounds can absorb the UV part of the solar spectrum and transform it into visible light. The absorption of UV radiation protects the polymer films against photodegradation and makes it possible to convert a part of the solar spectrum that cannot be used for photosynthetic processes into wavelengths that can be absorbed by the chlorophyll molecules in plants. The doping of luminophores into the films has thus a double advantage: (1) stabilization of the polymer films so that their service life will be extended and (2) a more efficient use of solar energy. The luminescent light of interest in this agricultural application is the red light emitted by the Eu^{3+} ion, because red light is essential for the growth of plants during all their stages of development. Inorganic europium(III)-containing compounds for dispersion in polymer films are being commercialized under the name Ksanta by Ranita (Regensburg, Germany).[1096] The polymer films incorporating the Ksanta additive are commercially available under the name *Redlight*. Productivity increases up to 100% for plants in greenhouses have been reported after the use of polymer films with these additives. The faster growth and development of plants under such films is known as the *Polysvetan effect*,[1097−1099] which is thought to be caused by the effect of low-intensity red luminescent radiation on the plant hormonal balance.[1100] Examples of europium(III)-containing dopants for polymer films are Y_2O_2S/Eu^{3+},[1101−1103] Y_2O_3/Eu^{3+},[1102] and $Eu(phen)_2(NO_3)_3$.[1102] Yang and coworkers describe luminescent films for agricultural applications prepared by doping [Pr(sal)$_3$(phen)] and [Eu(sal)$_3$(phen)], where sal = salicylate and phen = 1,10-phenanthroline, in different molar ratios in linear low-density polyethylene (LLDPE).[1104] The thermal and photochemical stability of the red-emitting films was tested.

Europium(III) β-diketonate complexes are used in *safety inks*.[1105] These inks are used as counterfeiting countermeasures for protecting banknotes, bank cards, and value documents. The safety inks are invisible but glow in different colors (red in the case of Eu^{3+}) under irradiation with UV light. The euro notes show under UV radiation blue-, green-, and red-emitting fibers and patterns. Although the exact composition of these safety inks is kept secret for good reasons, Meijerink could show by luminescence measurements that the blue and green color are caused by inorganic europium(II) compounds and that the red color is very likely due to a europium(III) β-diketonate complex.[1106] Thus, one can state that "*europium protects teh euro*"!

It has been demonstrated that europium(III)- and terbium(III)-doped ormosil glass films placed on top of silicon solar cells can improve the efficiency of these *photovoltaic devices*.[1107−1109] This can be attributed to the fact that ultraviolet radiation is converted by the luminescent complex into visible radiation, which is more efficiently absorbed by silicon than the ultraviolet radiation. Cerium(III)-containing silica sol−gel glasses were deposited on top of solar concentrator plates consisting of organic fluorophores doped in PMMA. The function of the cerium(III) ions was to absorb a large part of the ultraviolet spectrum so that the fluorescent dyes in the PMMA plate were protected against photodegradation.[1110]

An exotic application is the use of *tritiated polymers doped with lanthanide(III) complexes* as a *light source*.[1111] The radioactive decay energy of the tritium atoms excites the lanthanide(III) complexes, and the excitation energy is converted into visible light. This is thus a form of *radioluminescence*, instead of the usual photoluminescence generated by UV irradiation. The tritium is introduced in the polymer by tritiation of the monomers prior to polymerization. It is advisible to select polymers with a good resistance against radiation damage, like polystyrene. These self-luminescent materials are suggested for use as *luminescent markers*.

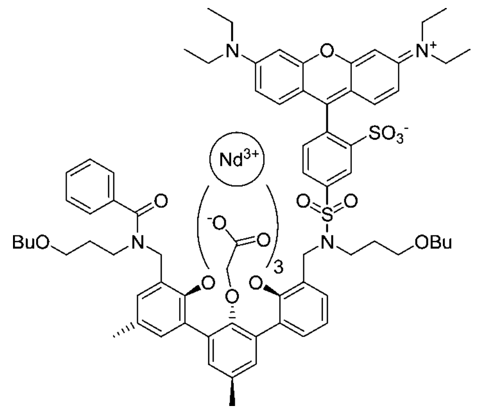

Figure 104. Terphenyl-based neodymium(III) complex functionalized with a lissamine chromophore.[1116]

10.2. Polymeric Optical Amplifiers

Lanthanide complexes have been often tested as luminescent materials in *polymer optical fiber amplifiers* and in *planar optical waveguides*. This research has been reviewed by Kuriki et al.[835] and by Slooff et al.[1112] The most often used lanthanide(III) ion for telecommunication applications is Er^{3+}, because it emits at a wavelength of 1540 nm, which is within one of the telecommunication windows. In an optical amplifier, the Er^{3+} ion is incorporated in the core of an optical fiber or in a planar optical waveguide.[1113] The Er^{3+} ion is excited to a higher lying energy level by an external laser source (pump laser), typically by a 1480 nm or a 980 nm diode laser. When sufficient pump power is applied, population inversion can be achieved with more Er^{3+} ions in the first excited state ($^4I_{13/2}$) than in the ground state ($^4I_{15/2}$). An optical signal of 1540 nm, which travels through the erbium-doped waveguide, will induce stimulated emission from the first excited state to the ground state, and this results in signal amplification. Besides the Er^{3+} ion, which emits at 1540 nm, the Nd^{3+} ion, which emits at 1340 nm, is sometimes used in telecommunication applications.

Lin et al. doped the neodymium(III) complex [Nd(hfac)$_3$] into a fluorinated polyimide (Ultradel 9000 series of the Amoco Chemical Company) and used this material to prepare slab and channel optical waveguides.[880] Although they observed photoluminescence at 880, 1060, and 1330 nm, the luminescence intensity was weak and the lifetime was short compared with the luminescence characteristics of neodymium-doped inorganic hosts. Another study used $NdCl_3 \cdot 6H_2O$ as the dopant in Ultradel 9000 series fluorinated polyimides for making optical waveguides.[1114] The authors demonstrated optical amplification at 1060 nm. An optical gain of about 8 dB was observed in a 5 cm long multimode channel waveguide. It was difficult to obtain films of a good optical quality. Kuriki et al. prepared a graded index optical fiber of PMMA-d_8 doped with the neodymium(III) complex of deuterated hexafluoroacetylacetone, [Nd(hfa-d)$_3$], or with the neodymium(III) complex of deuterated 1,1,1,2,2,6,6,7,7,7-decafluoro-3,5-heptanedione, [Nd(fhd-d)$_3$].[1115] A terphenyl-based neodymium(III) complex functionalized with a lissamine chromophore was doped into partially fluorinated polycarbonate polymer, and the material was used to prepare planar waveguides by spin coating (Figure 104).[1116] The lissamine acted as a sensitizer for Nd^{3+} luminescence. The undoped polymer had optical losses of <0.05 dB/cm at 1060 nm and 0.08 dB/cm at 1305 nm. Although room-temperature near-infrared luminescence could be observed both upon direct excitation of the Nd^{3+} and upon excitation via the sensitizer, the excitation efficiency was a factor of 10^4 higher upon excitation via the sensitizer. The luminescence lifetime in the polymer was short (0.8 μs). Although the neodymium(III)-doped waveguides showed excellent waveguide properties, photodegradation of the doped films was observed upon continued illumination.

Kobayashi et al. made graded index polymer optical fibers of PMMA doped with the europium(III) complexes [Eu(tta)$_3$] and [Eu(hfac)$_3$].[1117] An increase in luminescence intensity was observed when 20 wt % of triphenyl phosphate was added to the polymer, whereas the luminescence intensity decreased upon addition of benzyl *n*-butyl phthalate. The attenuation loss of the graded index PMMA fiber doped with [Eu(hfac)$_3$] was found to be 0.4 dB/m around 650 nm. Mataki et al. fabricated planar polymer optical waveguides from PMMA doped with Eu−Al nanoclusters.[1118] Optical amplification was successfully demonstrated at a wavelength of 614 nm under both pulsed operation using a N_2 laser (λ = 337 nm) and CW operation using a frequency-doubled diode-pumped Nd:YAG laser (λ = 532 nm). The optical gain was found to be as high as 5.57 dB/mm, which is a very high value for a lanthanide-doped planar optical waveguide. Polymer channel waveguides containing [Eu(dbm)$_3$(phen)] and [Er(dbm)$_3$(phen)] in ethylene glycol dimethacrylate were made by hot embossing.[1119]

10.3. Lasers

The possibility to use lanthanide β-diketonate complexes for the design of lasers gave a strong impulse to the spectroscopic study of these complexes in the early 1960s. In a seminal paper, Schimitschek and Schwarz pointed to the fact that europium(III) complexes have optical properties that make them very attractive as potential laser materials.[1120] The authors suggested that laser action should be experimentally observed for these complexes dissolved in both organic solvents and a polymer matrix. Around the same time, the potential application of lanthanide chelates in lasers was suggested by other authors as well.[1121,1122] In 1963, Lempicki and Samelson were the first to obtain stimulated emission at 613.1 nm ($^5D_0 \rightarrow {}^7F_2$ transition) from an alcohol solution (3:1 ethanol/methanol) of europium(III) benzoylacetonate at −150 °C by pumping with a xenon flash lamp.[1123] Samelson et al. observed room-temperature operation of a europium(III) chelate laser.[1124] From then on, a considerable number of studies on laser action of europium(III) and terbium(III) β-diketonate complexes in frozen organic solutions and in polymers were reported within a few years.[1125−1133] The ligands included benzoylacetone, dibenzoylmethane, trifluoroacetylacetone, 2-thenoyltrifluoroacetone, and benzoyltrifluoroacetone. A great deal of this older work was done by physicists on poorly characterized or on impure compounds. During these studies, it was realized that, in contrast to earlier belief, lanthanide(III) tris β-diketonate complexes are much less common than Lewis base adducts of these tris complexes and than the tetrakis β-diketonate complexes. It was shown that the active components in the best performing laser systems were the tetrakis complexes.[1134] Although in most of the studies on laser chelates, europium(III) has been chosen as the emitting ion, some studies report on laser action of terbium(III) complexes,[1135−1137] whereas Whittaker observed laser action by neodymium(III) in a tetrakis 2-thenoyltrifluoroacetonate complex prepared from a didymium salt (mixture of praseodymium and neodymium salts).[1138]

Strong light absorption by the β-diketonate ligands is an advantage for sensitizing the luminescence of lanthanide ions by the antenna effect, but this property limits the usefulness of the lanthanide β-diketonate complexes as laser materials. In order to achieve uniform excitation of the solutions containing the lanthanide chelate at the concentration required for laser action (ca. 0.01 M), only thin samples (ca. 1−6 mm) could be used.[1139] Therefore, most of the studies of liquid lasers have been performed on laser solutions in a capillary tube or on lanthanide doped polymers drawn to fibers. Another serious problem with the chelate lasers was the low photostability of the lanthanide β-diketonate complexes under ultraviolet irradiation. This severely limits the lifetime of these laser systems. Third, the lasing thresholds are high for these chelate lasers at room temperature. Because of the high input energy needed, excessive warming of the laser solutions was observed. To circumvent the latter problem, circulation of the liquid through the cell and cooling with an external heat exchanger was proposed.[1140] Finally, the energy output of the lanthanide chelate lasers was low, because of the existence of efficient pathways for the radiationless deactivation of the excited states.

For a long time after 1970, no research had been done on lanthanide chelate lasers, due to the development of lasers based on lanthanide ions in single crystals or glasses. In 1995, Taniguchi et al. demonstrated ultralow threshold lasing due to morphology-dependent resonances from the europium(III) complex [Eu(dbm)$_3$(phen)] dissolved in liquid microdroplets with ca. 90 μm diameters.[1141] These microdroplets consisted of a viscous ethanol−glycerol mixture. The same year, authors from the same research consortium described a solid chelate laser based on [Eu(dbm)$_3$(phen)] dispersed in polystyrene spheres.[1142] The advantage of this type of chelate laser in comparison with a liquid chelate laser is that the former is free of solvent effects. Hasegawa and co-workers observed laser action in polystyrene thin films doped with the europium(III) complex [Eu(hfac)$_3$(tppo)$_2$].[1143] The thin films were prepared by spin coating from a solution in cyclohexanone. The microcavity was constructed by a high refractivity film on a glass substrate. The authors report that the required properties of a europium(III) complex to make it useful for applications in lasers is a high luminescent quantum yield (to increase the energy density) and fast radiation rates (to get a high Einstein coefficient *B*). As a continuation of this work, the lasing properties of europium(III) complexes in polymer thin films of polyphenylsilsesquioxane (PPSQ) were investigated.[1144] The complexes were adducts of phosphine oxides to tris(hexafluoroacetylacetonato)europium(III): [Eu(hfac)$_3$(tppo)$_2$], [Eu(hfac)$_3$(oppo)$_2$], and [Eu(hfac)$_3$(biphepo)], where tppo is triphenylphosphine oxide, oppo is 1,2-phenylenebis(diphenylphosphine oxide), and biphepo is 1,1′-biphenyl-2,2′diylbis(diphenylphosphine oxide). Thin films were prepared by spin-coating from an anisole solution. An advantage of the PPSQ polymer is its high transmission in the ultraviolet and visible spectral regions. The optical microcavity was constructed by forming a highly refractive film of PPSQ (n = 1.558) on the glass substrate. The thin films were excited by the third harmonic generated by a nanosecond Nd:YAG laser (355 nm). The emitted light beam was monitored along the edge of the film. The threshold for amplified spontaneous emission was found to be <0.05 mJ for [Eu(hfac)$_3$(tppo)$_2$] and

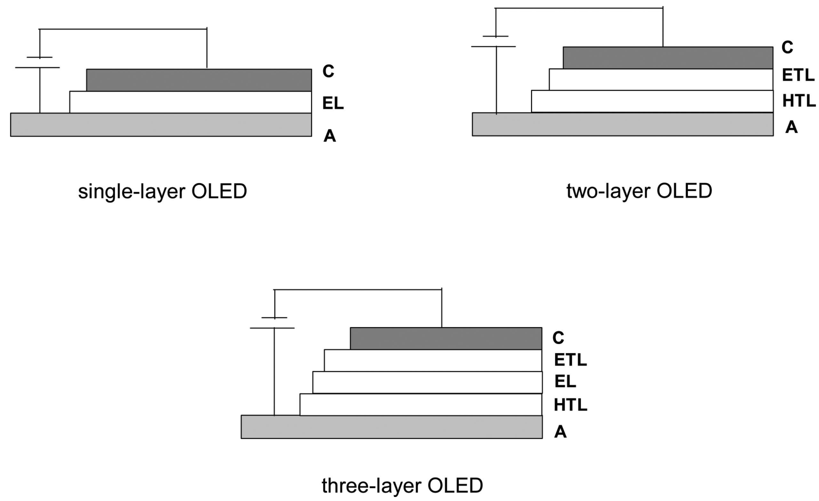

Figure 105. Different types of OLEDs. C = cathode (typically aluminum); EL = emitter layer; ETL = electron transport layer; HTL = hole transport layer; A = anode (typically ITO glass).

[Eu(hfac)$_3$(biphepo)], but the threshold energy was much larger (0.5 mJ) for [Eu(hfac)$_3$(oppo)$_2$].

10.4. OLEDs

Light emitting diodes (LEDs) will probably become the most important type of light source for artificial lighting in the 21st century and will probably replace the incandescent lamps and even the mercury-containing discharge lamps. Typically, a LED consists of inorganic p- and n-type semiconductors. The holes and electrons are driven to the p−n junction by the applied electric field. The electrons and holes recombine at this p−n junction, and the excess of energy is emitted as visible or infrared radiation. In a LED, electrical energy is transformed into light (electroluminescence). In *organic light emitting diodes* (OLEDs), the active components are organic molecules instead of inorganic semiconductors.[1145−1147] OLEDs are mainly developed for display applications. One hopes to use OLEDs for the design of large flat panel displays with very wide viewing angles. The advantages of OLEDs are that they are easier and cheaper to fabricate than their inorganic counterparts, that they can be made very large (luminescent sheets), and that they can be deposited on almost every substrate including flexible ones, like plastics, to yield flexible displays. Although the phenomenon of organic electroluminescence was discovered by Pope in 1963, the development of the first OLEDs began in the Chemistry Division of Kodak Research Laboratories at the end of the 1970s. One has to mention here the pioneering work of Tang and Van Slyke, who introduced an injection type of electroluminescent device that operated at driving voltages as low as a few volts.[1148] They used a hole transport layer for hole injection from the electrode into the emitting organic layer, and they used tris(8-hydroxyquinolinato)aluminum(III) (AlQ) as the emissive material. Tris(8-hydroxyquinolinato)aluminum(III) emits bright green light. This multilayer device had a luminance of more than 1000 cd/m^2 below 10 V with an external quantum efficiency of 1% (i.e., one photon is emitted for 100 injected electrons). Another milestone was the work of Burroughes et al.[1149] Their OLED consisted of a single layer of the π-conjugated polymer poly(phenylene vinylene) (PPV) between metallic electrodes. Since that time, many research efforts have been invested in optimizing the performance of OLEDs, and now OLEDs with a broad variety of emitting colors are available.[1147]

An OLED consists of very thin layers sandwiched by two electrodes. These layers can be deposited by various techniques such as chemical vapor deposition, plasma deposition, or spin coating from a solution. Electrons are injected into the emitting layer from the cathode, and holes are injected from the anode. The cathode is typically a layer of a metal with a low work function such as aluminum, magnesium, or calcium or a magnesium/aluminum alloy to guarantee efficient injection of electrons. The anode is typically a transparent layer of *indium tin oxide* (ITO). ITO is a nonstoichiometric composition consisting of In_2O_3 (80−90%) and SnO_2 (10−20%). The recombination of the injected holes with the injected electrons allows the formation of singlet and triplet excitons. Because of spin statistics, 75% of the recombinations give rise to triplet excitons and 25% to singlet excitons. Only singlet excitons can produce electroluminescence. The triplet excitons decay nonradiatively and do not generate electroluminescence. For this reason, the maximum internal quantum efficiency of an OLED is limited to 25%. Different types of OLEDs have been described (Figure 105). A *single-layer OLED* is made of a single organic layer sandwiched between the cathode and the anode. This layer must not only possess a high quantum efficiency for photoluminescence but also have good hole and electron transport properties. In a *two-layer OLED*, one organic layer is specifically chosen to transport holes and the other layer is chosen to transport electrons. Recombination of the hole−electron pair takes place at the interface between the two layers, which generates electroluminescence. In a *three-layer OLED* an additional layer is placed between the hole-transporting layer and the electron-transporting layer. The emitting layer is primarily the site of hole−electron recombination and thus of electroluminescence. This cell structure is useful for emissive materials that do not possess high carrier (either electron or hole) transport properties. Often the cathode is covered by a very thin layer (0.5−1 nm) of LiF or CsF, which strongly reduces the injection barrier and also protects the electron transport layer from chemical reactions with the cathode material. Ohmic losses due to imbalance between the electron current and hole current can be avoided by introduction of a hole blocking layer between

Chart 15. Active Components in OLEDs: The Hole-Transporting Materials Poly(*N*-vinylcarbazole) (PVK) and *N*,*N*′-Diphenyl-*N*,*N*′-bis-(3-methylphenyl))-1,1′-biphenyl-4,4′-diamine (TPD) and the Electron-Transporting Material 2-*tert*-Butylphenyl-5-biphenyl-1,3,4-oxadiazole (PBD)

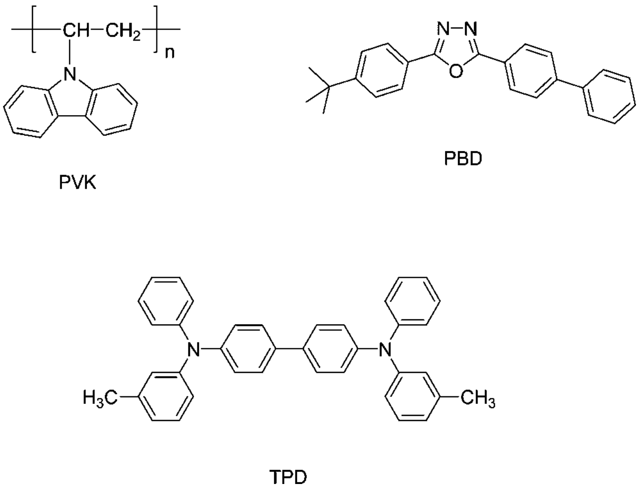

the electron transport layer and the emitting layer or of an electron-blocking layer between the hole transport layer and the emitting layer. In an OLED, electrons are transported via the lowest unoccupied molecular orbital (LUMO). The LUMO is analogous to the conduction band of semiconductors. Holes are transported via the highest occupied molecular orbital (HOMO). The HOMO can be compared with the valence band of a semiconductor.

The performance of OLEDs is tested by measuring the current density−voltage and the luminance−voltage characteristics. The *luminance* is a measure of luminous intensity in a given direction. It describes the amount of light that passes through or is emitted from a particular area and falls within a given solid angle. The SI unit for luminance is the candela per square meter (cd/m^2). The *candela* (cd) is the SI unit for *luminous intensity*, that is, the power emitted by a light source in a particular direction weighted by the luminous function (a standardized model of the sensitivity of the human eye to different wavelengths). The luminous intensity of a common candle is roughly 1 cd. The *turn-on voltage* is defined as the voltage necessary to have a luminance of 1 cd/m^2. Ideally, this value should be as low as possible, but in many lanthanide-based OLEDs, the values are between 5 and 10 V. The luminance will increase with increasing voltage up to a maximum value. Increasing the voltage further will then cause a decrease of luminance. In OLEDs one can distinguish the *external quantum efficiency* (η_{ex}) and the *power efficiency* (η_p). The external quantum efficiency is defined as the ratio of the number of emitted quanta to the number of charge carriers. The power efficiency is the ratio of the luminous flux emitted by the OLED and the consumed electric power. Molecules often used as active components in OLEDs are depicted in Chart 15.

Kido and Okamoto published in this journal a review article on lanthanide-containing OLEDs, which gives an overview of the developments in the field until 2001.[1150] More recent reviews have been written by Katkova et al.[1151] de Bettencourt-Dias,[1152] and Bian and Huang.[1153] Comby and Bünzli have reviewed the developments in the field of near-infrared-emitting OLEDs.[37] Because of the availability of good review papers, I will not cover the literature on lanthanide-doped OLEDs exhaustively but only describe the most remarkable experimental results and developments. In theory, incorporation of lanthanide complexes in the emitting layer of OLEDs offers two main advantages: (1) improved color saturation and (2) higher efficiency of the OLED. Because of the sharp emission bands of the trivalent lanthanide ions (with a full-width at half-maximum of less than 10 nm), lanthanide luminescence is highly monochromatic. This results in a much better color saturation than when organic molecules are used as the emissive material. In this case the band widths of the emission bands are typically around 80 to 100 nm. A saturated monochromatic emission is necessary for the development of full-color displays based on OLEDs. Broad emission bands will give dull colors. As mentioned above, the efficiency of OLEDS is limited to 25% by spin statistics. However, when lanthanide complexes are used, the efficiency is in theory not limited because the excitation energy can be transferred from either an excited singlet or triplet to the lanthanide ion. Although one often predicts a bright future for lanthanide-doped OLEDs, it has been learned from practice that the use of lanthanide complexes in OLEDs generates several problems. One difficulty is the poor film-forming properties of low-molecular weight lanthanide coordination compounds. Other problems are the low electroluminescence efficiency (due to poor charge-carrier transporting properties), and the bad long-term stability of many types of lanthanide complexes.

Kido and co-workers were the first to propose a lanthanide complex as the emissive material in an OLED.[1154] These authors built an electroluminescent device consisting of *N*,*N*′-diphenyl-*N*,*N*′-(3-methyl phenyl)-1,1′-biphenyl-4,4′-diamine (TPD) as the hole-injecting layer and [$Tb(acac)_3$] as the emitting and electron-transporting layer. The cathode was an aluminum layer and the anode an ITO-coated glass plate. The OLED was made by vacuum deposition. The green-emitting OLED had a luminance of only 7 cd/m^2 at 20 V, but the importance of this paper is that it gives the proof-of-principle of using electroluminescent lanthanide complexes in OLEDs. The electroluminescence spectrum was found to be identical to the corresponding photoluminescence spectrum. The relative intensities of the emission bands were independent of the current density. It should be noticed that the [$Tb(acac)_3$] compound described in this paper was not characterized, so it is not clear whether the compound under investigation was a hydrate or a partially hydrolyzed compound. Later research on lanthanide-doped OLEDs was mainly concentrated on the red-emitting europium(III) complexes, because with tris(8-hydroxyquinolinato)aluminum(III) (AlQ) a very efficient green-emitting material was available. Kido and co-workers made a red-emitting OLED based on a europium(III) compound.[1155] Their electroluminescence cell consisted of 2-*tert*-butylphenyl-5-biphenyl-1,3,4-oxadiazole (PDB) as the electron-transporting layer and poly(methylphenylsilane) (PMPS) as the hole-transporting layer doped with [$Eu(tta)_3$]. Luminescence started at 12 V, and a maximum luminance of 0.3 cd/m^2 was obtained at 18 V. The first types of lanthanide-based OLEDs were prepared by vacuum deposition of the different layers (hole-injection layer, emitting layer, electron-transport layer, cathode) on the ITO substrate. This technique is applicable only for volatile and thermally stable lanthanide complexes. Unfortunately, the most volatile lanthanide β-diketonate complexes are not the ones with the best luminescence properties. Many types of lanthanide complexes cannot be sublimed without

Chart 16. Low-Molecular Weight Red-Emitting Europium(III) β-Diketonate Complexes and Green-Emitting Terbium(III) β-Diketonate Complexes That Are Used as Active Components in the Emitter Layer of Lanthanide-Doped OLEDs

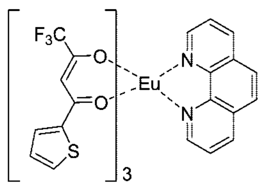

[Eu(tta)$_3$(phen)]

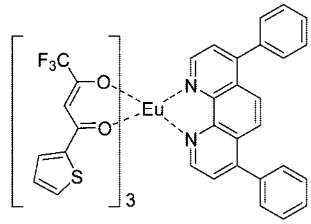

[Eu(tta)$_3$(bath)]

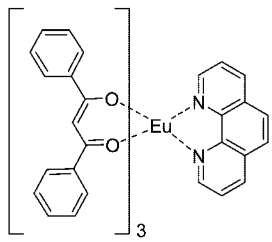

[Eu(dbm)$_3$(phen)]

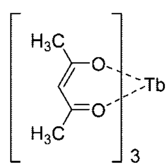

[Tb(acac)$_3$]

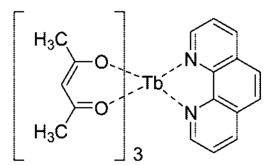

[Tb(acac)$_3$(phen)]

considerable thermal decomposition or give deposited layers of an inferior quality. The films of lanthanide complexes produced by vacuum deposition have often poor charge-carrier properties. Especially the transport of electrons is problematic. Because of the unbalanced injection and transport of charge carriers, recombination often takes place at sites other than the emitting layer. This not only leads to low electroluminescence efficiency, but also to a reduced lifetime of the OLED. One approach to improve OLEDs based on lanthanide compounds was to replace the tris-β-diketonate complexes originally used by Lewis base adducts (i.e., by ternary complexes). In this way, not only the volatility and the thermal stability but also the film-forming properties and the carrier-transport ability were improved. By replacing the [Eu(tta)$_3$] complex with [Eu(tta)$_3$(phen)], the luminance could be increased from 0.3 cd/m^2 to 137 cd/m^2.[1156] Replacement of [Eu(tta)$_3$(phen)] by [Eu(dbm)$_3$(phen)] gave a further improvement of the OLED efficiency, and a luminance of 460 cd/m^2 could be achieved.[1157] An OLED incorporating [Eu(hfnh)$_3$(phen)], where hfnh is 4,4,5,5,6,6,6-heptafluoro-1-(2-naphthyl)hexane-1,3-dione, was successfully used to obtain a maximum brightness of 957 cd/m^2.[1158] On the basis of Eu(tta)$_3$ complexes with the substituted phenanthrolines pyrazino[2,3-*f*][1,10]phenanthroline (PyPhen), 2-methylpyrazino[2,3-*f*][1,10]phenanthroline (mpp), dipyrido[3,2-*a*:2′,3′-*c*]phenazine (dppz), 11-methyldipyrido[3,2-*a*:2′,3′-*c*]phenazine (mdpz), 11,12-dimethyldipyrido[3,2-*a*:2′,3′-*c*]phenazine (ddpz), and benzo[*i*-]dipyrido[3,2-*a*:2,3-*c*]phenazine (bdpz)), Sun et al. were able to make OLEDs with a luminescence of more than 1000 cd/m^2, with a maximum of 1670 cd/m^2 for the complex with dipyrido[3,2-*a*:2′,3′-*c*]phenazine (dppz).[1159] The latter device showed an external quantum efficiency of 2.1%, a current efficiency of 4.4 cd/A and a power efficiency of 2.1 lm/W. In the same way, the luminescence of the green-emitting OLED could be improved to 90 cd/m^2 by use of [Tb(acac)$_3$(phen)] instead of [Tb(acac)$_3$].[1160] The structures of low-molecular weight europium(III) and terbium(III) β-diketonate complexes that have found application in lanthanide-based OLEDs are shown in Chart 16. In Table 4, an overview of the performance of OLED devices based on red-emitting europium(III) complexes is given.[1161−1174]

Although 1,10-phenanthroline is often used as Lewis base to form ternary complexes, better results can be obtained when 4,7-diphenyl-1,10-phenanthroline (bathophenanthroline, bath) is used instead. Other phenanthroline derivatives that have been applied to make electroluminescent ternary europium complexes are 5-amino-1,10-phenanthroline, 4,7-dimethyl-1,10-phenanthroline, 1,10-phenanthroline disulfonic acid, and 5-chloro-1,10-phenanthroline.[1175] Tsaryuk et al. discussed the problem of optimizing the performance of ternary complexes of europium(III) β-diketonates with 1,10-phenanthroline for OLED applications.[1176] 2,2′-Bipyridine is much less popular than 1,10-phenanthroline to form ternary complexes.[1177] Huang et al. made ternary complexes with 2-(2-pyridyl)benzimidazole (Hpbm) and 1-ethyl-2-(2-pyridyl)benzimidazole (epbm).[1178] The ligands derived from 2-(2-pyridyl)benzimidazole have the advantage that they can be easily substituted by alkyl chains on the benzimidazole group. The europium(III) complex made of 1-octadecyl-2-(2-pyridyl)benzimidazole (opb), [Eu(dbm)$_3$(opb)], has a melting point of 119 °C, and starts to decompose at 337 °C.[1179] The large temperature interval between the melting point and the onset of thermal decomposition facilitates processing of this complex by vacuum vapor deposition. Moreover, the long alkyl chain stabilizes the amorphous phase. It is known that crystallization of the emissive layer has an unfavorable effect on the electroluminescence. Gao et al. studied the performance of the [Eu(dbm)$_3$(piphen)] complex, where piphen is 2-phenyl-imidazo[4,5-*f*]1,10-phenanthroline (Figure 106).[1180] Another type of 1,10-phenanthroline derivative is dipyrido[3,2-*a*:2′,3′-*c*]phenazine (dppz). This ligand was used to make [Eu(tta)$_3$(dppz)] complexes.[1181] Hu et al. chose triphenyl phosphine oxide (tppo) as the reagent to make ternary [Eu(dbm)$_2$(tppo)] complexes, and the corresponding OLEDs had a high luminance (up to 380 cd/m^2).[1182,1183] In order to improve the charge-transport properties, an oxadiazole-functionalized

Table 4. Performance of Selected Red-Emitting Europium(III)-Containing OLEDs[a]

emitter layer[b]	L (cd/m^2)	V (V)	J (mA/cm^2)	η_{ext} (%)	η_p (lm/W)	ref
[Eu(tta)$_3$]/PMPS	0.3	18				1155
[Eu(tta)$_2$(pmbbp)(phen)]	16	12.5	125			1170
[Eu(tta)$_3$(phen)]	30	15	182			1173
Na[Eu(tta)$_4$]/PVK	36.7	26				1174
[Eu(dbm)$_3$(phen)]	50	15				1168
[Eu(tfac)$_3$(bipy)]]	68	20				1171
[EuY(tta)$_6$(phen)$_2$]	99	11	246.5			1169
[Eu(dbm)$_3$(tppo)]	320	14.5				1172
[Eu(dbm)$_3$(oxd-pbm)]	322	21		1.7		1185
[Eu(dbm)$_3$(bath)]	400	15				1161
[Eu(tta)$_3$(cppo)$_2$]/BCP	414	17.6	204.78	1.55	0.77	1166
[Eu(tta)$_3$(phen)]/PBD,PVK	417	25	175			1163
[Eu(dtp)$_3$(bath)]	450	15	200			1164
[Eu(dbm)$_3$(phen)]/PBD (1/3)	460	16				1157
[Eu(tta)$_3$(phen)]/CBP (1%)	505	12	0.4	1.4		1165
[Eu(dbm)$_3$(bath)]/TPD (3/1)	820	18	0.6	1.0	1.0	1162
[Eu(dcnp)(dbm)$_2$(phen)]/PBD (10%)	924		0.17	3.5	2.0	1167
[Eu(tta)$_3$(dppz)]/CBP (4.5%)	1670	13.6	1.23	2.1	2.1	1159

[a] Parameters: operating voltage (V); current density (J); external quantum efficiency (η_{ext}); luminance (L); power efficiency (η_p). [b] Abbreviations: bath = 4,7-diphenyl-1,10-phenanthroline (bathophenanthroline); bipy = 2,2′-bipyridine; cppo = 9-[4-(diphenyl-phosphinoyl)-phenyl]-9*H*-carbazole; dbm = dibenzoylmethanate; dcnp = 1,3-dicyano-1,3-propanedione; dppz = dipyrido[3,2-*a*:2′,3′-*c*]phenazine; dtp = 1,3-di(2-thienyl)-1,3-propanedionate; oxd-pbm = oxadiazole-functionalized 2-(2-pyridyl)benzimidazole; phen = 1,10-phenanthroline; pmbbp =1-phenyl-3-methyl-4(4-butylbenzoyl)-5-pyrazolonate; tfac = 1,1,1-trifluoro-2,4-pentanedionate (trifluoroacetylacetone); tppo = triphenylphosphine oxide; tta = 2-thenoyltrifluoroacetonate; BCP = bathocuproin or 2,9-dimethyl-4,7-diphenyl-1,10-phenanthroline; CBP = 4,4′-*N*,*N*′-dicarbazole-biphenyl; PBD = 2-*tert*-butylphenyl-5-biphenyl-1,3,4-oxadiazole; PMPS = poly(methylphenylsilane); PVK = poly(*N*-vinylcarbazole); TPD = *N*,*N*′-diphenyl-*N*,*N*′-(3-methyl phenyl)-1,1′-biphenyl-4,4′-diamine.

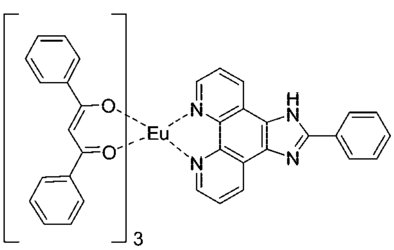

Figure 106. Structure of the complex [Eu(dbm)$_3$(piphen)].

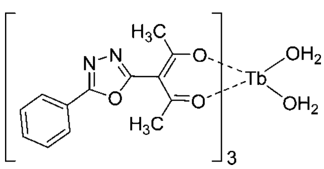

Figure 107. Structure of an oxadiazole-functionalized terbium(III) β-diketonate.[1184]

β-diketone ligand was designed and the electroluminescence of the corresponding tris-β-diketonate dihydrate was studied (Figure 107).[1184] The turn-on voltage of the device was 8 V. At 15 V, the luminance was 100 cd/m^2 (η_{ex} = 1.1%), and at 20 V the luminance increased to 550 cd/m^2 (η_{ex} = 0.6%). The improved charge transport was evident from the high current densities (25 mA/cm^2 at 15 V, and 275 mA/cm^2 at 20 V). The same type of device with [Tb(acac)$_3$] as the emitter had current densities of only 0.6 and 1.3 mA/cm^2 under the same conditions. The terbium compound described by Wang et al. had two water molecules in the first coordination sphere.[1184] The luminescence efficiency could be enhanced by replacing these water molecules by a bidentate Lewis base. Liang et al. used 2-(2-pyridyl)benzimidazole functionalized with an oxadiazole group to form a ternary complex with [Eu(dbm)$_3$].[1185] The complex tris[1-(*N*-ethylcarbazoyl)(3′,5′-hexyloxybenzoyl)methane](1,10-phenanthroline)europium(III) was designed to incorporate the same complex groups that improve both the electron transport (1,10-phenanthroline) and hole transport (the carbazole fragment) (Figure 108).[1186] Moreover, crystallization was

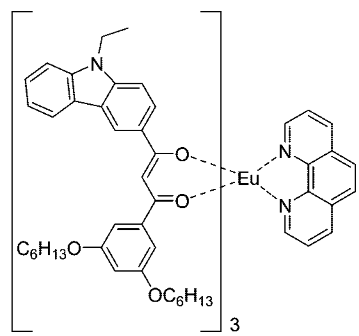

Figure 108. Structure of tris[1-(*N*-ethylcarbazoyl)(3′,5′-hexyloxybenzoyl)methane](1,10-phenanthroline)europium(III).[1186]

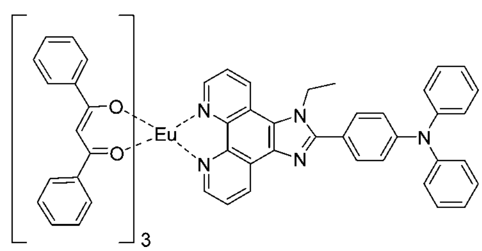

Figure 109. Structure of tris(dibenzoylmethanato)(2-4′-triphenylamino)imidazo[4,5-*f*]1,10-phenanthroline)europium(III).[1188]

prevented by the presence of six hexyloxy groups and a stable amorphous phase was obtained. Noto et al. studied the electroluminescence of an OLED that contained the complex [Eu(dbm)$_2$(dcnp)(phen)], where H(dcnp) is 1,3-dicyano-1,3-propanedione.[1187] A luminance of 1305 cd/m^2 at 16 V was reported for an OLED based on a europium(III) complex containing an imidazo[4,5-*f*]1,10-phenanthroline ligand (Figure 109).[1188]

Instead of depositing the emissive layer by vacuum vapor deposition, it is also possible to dope the lanthanide complex into a polymer matrix. In this case the lanthanide complex and the polymer are dissolved in a suitable solvent and the emissive layer is cast directly from solution by spin coating. The doped polymers have several advantages. First of all, the thermal decomposition of the electroluminescent complexes by vacuum sublimation is avoided. Second, the processing of the films is simplified. Third, the polymers have better film-forming properties than the low-molecular-weight lanthanide complexes. Fourth, the polymer matrix can have good hole- and electron-transporting properties, so that the electroluminescence performance is improved. Finally, the energy of blue-emitting polymers can be transferred to the lanthanide complex. Heeger and co-workers reported red-emitting OLEDs with a high color saturation in which the energy from the blue-emitting conjugated polymer poly[2-(6′-cyano-6′-methyl-heptyloxy-1,4-phenylene] (CN-PPP) is transferred to europium(III) β-diketonate complexes.[1189] The complexes [Eu(acac)$_3$(phen)], [Eu(bzac)$_3$(phen)], [Eu(dbm)$_3$(phen)], and [Eu(dnm)$_3$(phen)] were studied. The external quantum efficiency of the OLEDs incorporating these complexes were 0.03%, 0.1%, 0.7%, and 1.1%, respectively. The best performance was thus observed for the OLED based on [Eu(dnm)$_3$(phen)]. In order to have a good energy transfer from the polymer to the europium(III) complex, the position of the triplet level of the β-diketonate ligand has to lie above the $^5D_0$ level of Eu^{3+}, and there must be an overlap between the emission spectrum of the polymer and the absorption spectrum of the β-diketonate ligand. Diaz-Garcia et al. investigated the energy transfer from the OLED-components PVK, PBD, and TPD to the lanthanide complexes [Eu(tmhd)$_3$], [Eu(tfc)$_3$], and [Sm(tmhd)$_3$].[1190] To have a better intramolecular energy transfer, Jiang et al. prepared β-diketones bearing two phenanthryl groups.[1191] These authors also synthesized dendron-substituted β-diketones to provide site isolation of the Eu^{3+} ion in the corresponding complexes; this results in less self-quenching of the luminescence.[1192] It is possible to bind the lanthanide complexes directly onto the polymer backbone. Zhao et al. linked a europium(III) complex consisting of two dibenzoylmethanate (dbm) ligands and one 1,10-phenanthroline group to a copolymer of methacrylate and acrylic acid.[1193] The efficiency of the OLED made of this material was low; the luminance was only 0.32 cd/m^2 at 18 V. Ling et al. made a copolymer containing both a europium(III) complex and carbazole groups.[1194] However, a LED based on this polymer had a very high turn-on voltage (24 V) and a very low luminance (0.228 cd/m^2 at 29 V). Pei et al. designed conjugated polymers with europium(III) β-diketonate complexes grafted to fluorene-type conjugated polymers through pendant 2,2′-bipyridine groups in the side chains.[1195] An OLED based on this conjugated polymer had a turn-on voltage of 15 V, an external electroluminescence efficiency of 0.07% and a luminance of about 11 cd/m^2 at 25 V. Although most of the lanthanide complexes applied in OLEDs are ternary complexes (Lewis base adducts of tris-β-diketonate complexes), there is evidence that the tetrakis-β-diketonate complexes give a good performance as well. This was illustrated for Li[Eu(tta)$_4$], Na[Eu(tta)$_4$], and K[Eu(tta)$_4$].[1196] An advantage of these complexes is their good solubility in organic solvents such as chloroform, ethanol, acetonitrile, and acetone. This facilitates their processing by spin coating. The performance of the tetrakis complex (pyH)$^+$[Eu(tta)$_4$]$^-$ in OLEDs was studied by Liang et al.[1197]

Hong et al. were able to make OLEDs emitting narrow-band blue light (482 nm) by incorporation of the [Tm(acac)$_3$(phen)] complex.[1198] Zhang et al. observed a change in emission color from green-white to red when the temperature of the compound [(Eu$_{0.1}$Gd$_{0.9}$)(tta)$_3$(tppo)$_2$] was increased from 77 to 300 K.[1199] At cryogenic temperatures, triplet emission (phosphorescence) of the organic ligand is observed, while at higher temperatures the phosphorescence is quenched by the europium(III) ion, and the typical red luminescence of Eu^{3+} is seen. An OLED based on this compound could be used for temperature-monitoring. Samarium(III) complexes give orange electroluminescence. This was illustrated by OLEDs incorporating the complexes [Sm(tta)$_3$(tppo)$_2$],[1200] [Sm(tta)$_3$(phen)],[1201] [Sm(dbm)$_3$-(bath)],[1202] or [Sm(btfac)$_3$(phen)].[1203]

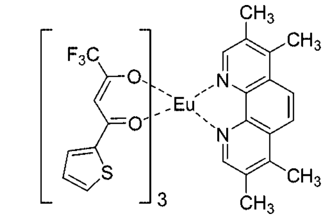

Figure 110. Europium(III) complex [Eu(tta)$_3$(tmphen)].

Several research groups have tried to develop white-light-emitting lanthanide-based OLEDs. Kido et al. made a white-emitting OLED by combining in the emissive layer [Eu(dbm)$_3$(phen)] for red emission, [Tb(dbm)$_3$(phen)] for green emission, and TPD for blue emission.[1160] TPD also has hole-transporting properties. Tris(8-hydroxyquinolinato)aluminum(III) was used as the electron-transporting layer. Zhao et al. obtained white emission from an OLED containing [Eu$_x$Tb$_{1-x}$(acac)$_3$(phen)] in the emissive layer.[1204] Pyo et al. designed a white-emitting OLED based on [Eu(tta)$_3$(phen)], [Tb(acac)$_3$(Cl-phen)], and TPD.[1205] Here, Cl-phen is a chlorine-substituted phenanthroline group. A voltage-tunable OLED was obtained by using a mixed samarium(III) and europium(III) complex, [Sm$_{0.7}$Eu$_{0.3}$(tta)$_3$-(tppo)$_2$].[1206] Raising the voltage of the device resulted in a gradual change of the red emission color to a yellowish one, due to a higher contribution of triplet emission by the 2-thenoyltrifluoroacetonate ligands. Hong et al. designed a white-light-emitting OLED, consisting of [Dy(acac)$_3$(phen)] as the emitting layer and poly(*N*-vinylcarbazole) (PVK) as the hole-transporting layer.[1207] The white emission was obtained by a superposition of a yellow emission band ($^4F_{9/2} \rightarrow {}^6H_{13/2}$ transition at 580 nm) and a blue emission band ($^4F_{9/2} \rightarrow {}^6H_{15/2}$ transition at 480 nm). The white emission was found to be independent of the drive voltage. An efficient white-emitting OLED with the red-emitting europium(III) complex [Eu(tta)$_3$(tmphen)], where tmphen is 3,4,7,8-tetramethyl-1,10-phenanthroline, was proposed (Figure 110).[1208] The OLED had a maximum brightness of 19 000 cd/m^2.

Huang et al. used the terbium complex tris-(1-phenyl-3-methyl-4-isobutyryl-5-pyrazolone)-bis(triphenyl phosphine oxide), [Tb(pmip)$_3$(tppo)$_2$], not as the emissive layer, but as the electron-transporting layer in a blue-emitting OLED.[1209] Chu et al. made a bifunctional organic diode containing [Y(acac)$_3$(phen)] for both light-to-electricity conversion (photovoltaic cell) and electricity-to-light conversion (OLED).[1210] Blue electrophosphorescent iridium(III) complexes can be used as a codopant to enhance the europium(III) luminescence.[1211]

Infrared-emitting OLEDs could be useful for application in polymer optical amplifiers. One of the first examples were OLEDs containing the erbium(III) 8-hydroxyquinolinate complex, ErQ$_3$, which emits in the infrared at 1540 nm (Figure 111).[1212−1216] Although the ErQ$_3$ complexes are often

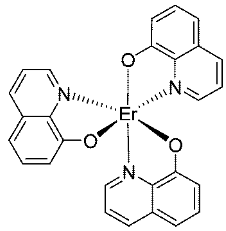

Figure 111. Erbium(III) quinolinate, ErQ_3.

considered to have a 1:3 metal-to-ligand ratio, the structural chemistry of the lanthanide quinolinates is very complicated, and complexes of different stoichiometries were found to occur.[1217,1218] Also the β-diketonate complex $Er(acac)_3$ and $[Er(acac)_3(phen)]$ have been used instead of ErQ_3 in erbium-doped OLEDs.[1219,1220] Besides erbium(III) also neodymium(III),[1221−1224] ytterbium(III),[1223,1225−1227] holmium(III),[1228] and praseodymium(III)[1229] were selected for the construction of near-infrared-emitting OLEDs.

10.5. Luminescent Chemical Sensors

Amao et al. developed an optical sensor for monitoring oxygen concentration in the gas phase based on luminescence intensity changes of $[Eu(tta)_3(phen)]$ immobilized in a poly(styrene-*co*-trifluoroethylmethacrylate) film.[1230] Later on, these authors extended the work to other europium(III) complexes, but $[Eu(tta)_3(phen)]$ was found to be the superior luminescent compound for this application.[1231] The reason for the choice of a fluorinated polymer for the supporting film is the high oxygen permeability of these materials. The luminescence intensity decreased with increasing oxygen concentration, because the luminescence is quenched by oxygen. The films showed near-linear Stern−Volmer plots. The sensor could calibrated by exposing the film to atmospheres of 100% argon (I_0) and 100% oxygen (I_{100}). The ratio I_0/I_{100} was found to be 2.40 in the case of $[Eu(tta)_3(phen)]$. Based on the same principle, Amao et al. designed an oxygen sensor based on $[Tb(acac)_3(phen)]$ absorbed on an alumina film.[1232] The films exhibited curved Stern−Volmer plots probably because of multisite quenching.

Parker and co-workers developed an oxygen sensor for monitoring the concentration of dissolved oxygen in water.[1233] They incorporated cationic macrocyclic terbium(III) complexes derived from DOTA and bearing an *N*-methylphenanthridinium chromophore in sol−gel-derived thin films (Figure 112). The films were prepared by controlled hydrolysis and condensation of ethyltriethoxysilane (ETEOS). The terbium(III) complexes were physically entrapped in the sol−gel glass matrix. The advantages of sol−gel glasses for sensors in comparison to polymer matrices is their higher and better controllable porosity, as well as a higher (photo)-chemical stability. The sensitivity of the films doped with Tb^{3+} for dissolved oxygen can be attributed to the small energy gap (900 cm^{-1}) between the $^5D_4$ excited state of Tb^{3+} and the triplet of the aromatic group. Exposure of the thin films to an aqueous solution containing dissolved oxygen led to a partial quenching of the terbium(III) luminescence. On the basis of the luminescence decay curves (measured at 547 nm), a linear calibration model could be defined over an oxygen concentration range between 0 and 0.5 mol/L. The sensor was operative over the pH range from 2 to 9. The highest sensitivity was obtained for the tetraamide complex.

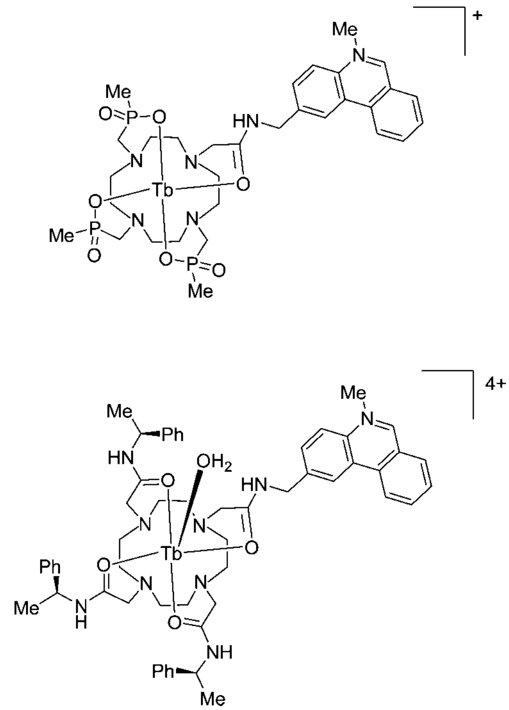

Figure 112. Tb-DOTA complexes bearing an *N*-methylphenanthridinium chromophore.[1233]

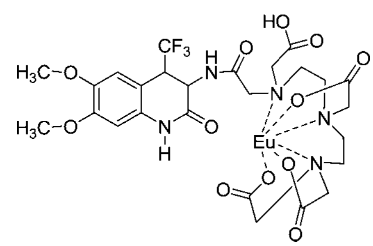

Figure 113. Europium(III) complex of a 4-trifluoromethylcarbostyril derivative of DTPA.

A pH sensor based on measurement of the luminescence lifetime of a europium(III) complex dissolved in a sol−gel glass matrix was developed.[1234−1236] The ligand for Eu^{3+} was a 4-trifluoromethylcarbostyril derivative of DTPA, which allowed near-UV to visible sensitization of the europium luminescence (350−400 nm) (Figure 113). The authors showed that excitation of the Eu^{3+} via a commercially available UV LED with an emission maximum at 370 nm was possible. The europium(III) complex was entrapped in thin films of different sol−gel matrices derived from TMOS and an organosilicon compound. The luminescence of europium(III) complex immobilized in the sol−gel matrix did not show a pH dependence in the range from pH 1 to 10, although a pH sensitivity was observed for the complex dissolved in an aqueous solution. However, pH-sensitive films could be obtained by coimmobilization of the nonfluorescent pH indicator bromothymol blue (BTB) in the hybrid matrix. This pH indicator dye has an alkaline absorption maximum close to the main emission band of Eu^{3+} at 615 nm. An increase in pH value leads to a decrease of the luminescence intensity. The sensor was based on measurement of the luminescence lifetime as a function of the pH. The luminescence lifetimes decreased with increasing pH values. The linearity of the sensor spans the pH range from 4 to 9.5, so the physiological pH range is covered. A limitation of these sensors is their high sensitivity to the ionic strength. The reader can find further information on optical

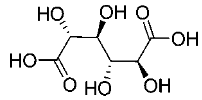

Figure 114. Mucic acid.

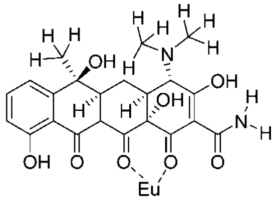

Figure 115. Europium(III) tetracycline complex.

sensors based on sol−gel materials in the available reviews.[1237,1238]

A porous terbium(III)-containing metal−organic framework derived from mucic acid (a polyhydroxydicarboxylic acid) (Figure 114) was used to sense anions in aqueous solution.[1239] The anions (F^-, Cl^-, Br^-, I^-, CN^-, NO_3^-, NO_2^-, SO_4^{2-}, CO_3^{2-}, PO_4^{3-}) interact with the Tb^{3+} ions in the pores of the network and influence their luminescence properties. The intensity of the $^5D_4 \rightarrow {}^7F_5$ transition was monitored as a function of the anion concentration. In general, an enhancement of the luminescence in the presence of anions was observed. The strongest effect was seen for the carbonate anions, whereas no significant enhancement could be measured for the sulfate and phosphate anions. A modest enhancement was observed for the nitrate ion, whereas a strong enhancement was exhibited by the nitrite ion. A europium(III)-containing hybrid material derived from a precursor obtained by reaction of 2,6-pyridinedicarboxylic acid was proposed as a sensor for Cu^{2+}.[1240] The working principle of this type of sensor is based on the quenching of the Eu^{3+} luminescence by Cu^{2+} ions.

Thin films of a europium(III) tetracycline complex dissolved in poly(vinyl alcohol) were deposited on top of a quartz surface coated with silver nanoparticles (Figure 115).[1241] It was found that the presence of the silver nanoparticles enhanced the luminescence intensity and reduced the luminescence decay time of the europium(III) tetracycline complex in the polymer film. These results indicate that metal-enhanced luminescence can be useful in the design of lanthanide-based luminescent sensors. The europium(III) tetracycline complex was proposed as a luminescent probe for hydrogen peroxide (H_2O_2), because H_2O_2 molecules strongly influence the luminescence properties of the europium(III) tetracycline complex.[1242] A recent review describes biochemical applications of luminescent europium(III) tetracycline complexes.[1243]

10.6. Luminescent Molecular Thermometers

The temperature dependence of the luminescence properties of lanthanide(III) complexes can be used in *optical sensors for temperature measurements*. The advantage of optical sensors is that they are useful for thermal mapping, that is, for visualizing the temperature distribution over a surface. Conventional temperature sensors can be applied only for one-point measurements on surfaces. There are some other conditions in which nonelectrical techniques for temperature measurements are required, for instance, in the presence of very strong electric or magnetic fields, or in cases where the attachments of thermocouples would change the temperature to be measured.[1244] The choice of the lanthanide ion for this application has mainly been restricted to Eu^{3+}, although also some studies on the use of Tb^{3+} had been reported. The luminescent lanthanide complexes can be embedded in sol−gel glasses, Langmuir−Blodgett films, and polymer films, with the latter matrix being the preferred one. Changes in temperature are reflected in changes in luminescence intensity and luminescence lifetime. Measurement of the luminescence lifetime is preferable in temperature sensor applications over measurement of luminescence intensities. Sensors based on measurement of the luminescence lifetimes (decay times) are more robust and stable because the luminescence lifetime is not affected by the intensity of the excitation source nor by the thickness of the sensor film. Khalil et al. give a detailed description of the use of europium(III) β-diketonate complexes as temperature sensors.[1245] Not all europium(III) β-diketonate complexes exhibit the same temperature sensitivity for their luminescence properties. It is often observed that tris-β-diketonate complexes show a larger temperature dependence than the tetrakis-β-diketonate complexes or the Lewis based adducts of tris complexes. It is argued that the fourth β-diketonate ligand or the Lewis base limits nonradiative deactivation processes, resulting in complexes whose luminescence is less temperature sensitive. Also the luminescence lifetimes of the tris-β-diketonate complexes are shorter than that of the tetrakis complexes. However, one should realize that pure anhydrous tris complexes are very difficult to synthesize, and compounds reported as tris complexes are in many cases hydrated tris-β-diketonate complexes. A very often used luminescent lanthanide complex for temperature-sensing applications is the europium(III) tris-2-thenoyltrifluoroacetonate complex [Eu(tta)$_3$]. The luminescence lifetime of this complex is approximately 200 μs at room temperature. Both the quantum yield and the lifetime of [Eu(tta)$_3$] are temperature sensitive. An increase in temperature decreases the luminescence intensity by 2.1% per degree Celsius. An additional advantage of [Eu(tta)$_3$] is that its luminescence properties are not very sensitive to the oxygen concentration. The study of Khalil et al. reveals that the luminescence decay time as a function of the temperature depends on three factors: (1) the type and number of ligands in the complex; (2) the type of polymer used for the matrix; (3) the concentration ratio of complex/polymer.[1245] Higher concentration ratios give shorter lifetimes and higher temperature sensitivities. It should be noted that photodegradation can cause intensity losses of the europium(III) complex of more than 15% per hour upon UV irradiation. Embedding of the europium(III) complex in a polymer matrix has a positive effect on the photostability. Different temperature sensitivities are seen for the same europium(III) complex, depending on the polymer matrix. The largest changes in temperature sensitivity and decay times for the same complexes at different dilutions in the polymer matrix are observed for poly(fluoroacrylic acid), while less drastic changes were observed for the polycarbonate poly(bisphenol A carbonate) and Teflon. Basu and Vasantharajan compared the luminescence lifetimes and temperature sensitivity of the lifetimes of Eu(tta)$_3$ in different polymer matrices: polystyrene, polyurethane, poly(methyl methacrylate), and model airplane dope.[1246] High temperature sensitivity was found for Eu(tta)$_3$ in a polystyrene matrix, in the temperature range from 10 to 60 °C.

Sol−gel glasses derived from vinyltriethoxysilane and codoped with [Eu(hfac)$_3$(tppo)$_2$] and [Tb(hfac)$_3$(ttpo)$_2$] show

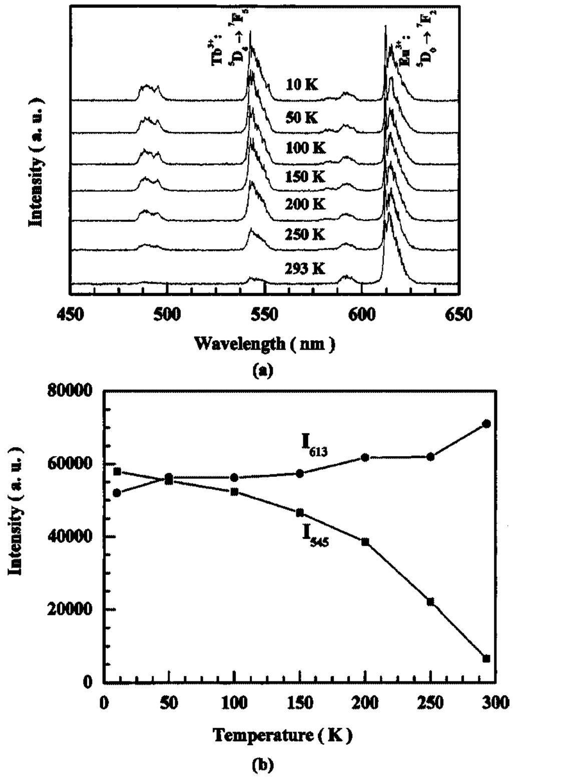

Figure 116. (a) Photoluminescence spectra of ormosils doped with $[Eu(hfac)_3(tppo)_2]$ and $[Tb(hfac)_3(ttpo)_2]$ at different temperatures between 10 and 293 K; $[Eu^{3+}] = [Tb^{3+}]$. (b) Integrated intensities of the main emission bands at 454 nm (Tb^{3+}) and 615 nm (Eu^{3+}) as a function of temperature. Reprinted with permission from ref 1247. Copyright 2005 American Institute of Physics.

a strong temperature dependence for their luminescence properties (Figure 116).[1247] In particular, the energy transfer from Tb^{3+} to Eu^{3+} strongly depends on the temperature, giving rise to temperature-dependent ratios of the luminescence intensities of the Tb^{3+} emission bands and the Eu^{3+} emission bands. The energy transfer from $Tb^{3+}$to Eu^{3+} can be explained by the Förster mechanism. Therefore the samples exhibit different emission colors at different temperatures. The luminescence color was found to change from orange at 10 K to red at 293 K. It was proposed to develop an optical fiber sensor for temperature measurements based on this system. The temperature-dependent luminescence intensity of a silica sol−gel glass fiber doped with $Eu(NO_3)_3$ has been used to monitor temperatures between 80 and 500 °C.[1248] A simple UV-LED was used as the excitation source. Optical temperature sensors excitable by blue LEDs (operating at wavelengths of 425, 435, or 450 nm) were obtained by doping a europium(III) β-diketonate complex with a 4-(4,6-di(1*H*-indazol-1-yl)-1,3,5-triazin-2-yl)-*N*,*N*-diethylbenzenamine (DEADIT) coligand in a polymer film (Figure 117).[1249] The DEADIT ligand contains the anilinetriazine push−pull chromophore, which allows visible light sensitization of the Eu^{3+} ion. For the preparation of the europium(III) polymer films, a solvent had to be found in which the europium(III) complex did not dissociate. The complexes did not dissociate in chloroform and toluene but were totally destroyed in ethanol, methanol, or DMF. Partial dissociation occurred in acetone or THF, especially in dilute solutions. The inability to use DMF, in which many polymers are soluble, did limit the choice of the polymer host. The europium(III) complex was embedded in different polymers: polystyrene, poly(styrene-*co*-acrylonitrile), polysulfone, poly-

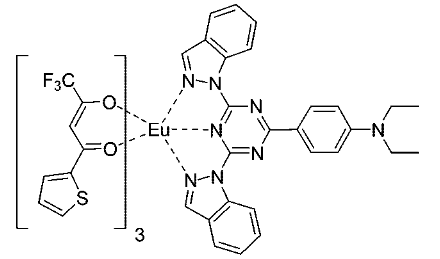

Figure 117. Adduct of $Eu(tta)_3$ with 4-(4,6-di(1*H*-indazol-1-yl)-1,3,5-triazin-2-yl)-*N*,*N*-diethylbenzenamine.

(vinylidene chloride-*co*-acrylonitrile), polymethacrylonitrile, and ethylcellulose. The complex was also immobilized on reverse phase silica beads and in an ormosil matrix. Both the luminescence intensity and the luminescence decay time were found to be temperature sensitive, but the temperature dependence of the luminescence decay time was used for temperature measurements. The highest temperature sensitivity was observed for the complex in poly(vinylidene chloride-*co*-acrylonitrile). This matrix also protects the complex from interaction with oxygen (which also affects the luminescence intensities) and has a beneficial effect on the photostability of the europium(III) complex. The sensors are attractive for temperature monitoring at physiological conditions.

The use of polymer Langmuir−Blodgett films containing a europium(III) complex as optical temperature sensor was reported.[1250] The LB films consisted of a mixture of poly(*N*-dodecylacrylamide) (pDDA) and $[Eu(tta)_3(phen)]$ sandwiched between poly(*N*-dodecylacrylamide) layers. The poly(*N*-dodecylacrylamide) layers were used to minimize the influence of molecular oxygen. The authors mention that the luminescence decay time of $[Eu(tta)_3(phen)]$ in the LB films is longer than that in cast films because of a more uniform distribution of the complex in the LB films. The intensity of the $^5D_0 \rightarrow {}^7F_2$ transition at 613 nm decreases linearly with temperature between 320 and 370 K. The LB films gave a sufficient intensity contrast at different temperatures to make the temperature differences visible by a CCD camera. The luminescence decay times of europium(III) β-diketonate complex in a poly(vinyl methyl ketone) film and in poly(*tert*-butyl styrene) microparticles were found to be highly temperature-dependent between 0 and 70 °C, and could be used for optical sensing of temperature.[1251] A temperature sensitivity of the luminescence up to 5.6% per degree Celsius was reported for a tetranuclear europium(III) complex $[Eu_4(\mu\text{-}O)L_{10}]$, where L = 2-hydroxy-4-octyloxybenzophenone, doped in a PMMA film.[1252] The advantage of this complex is its high thermal stability,[1253] so after incorporation of the complex in thermostable polyphenylsilsesquioxane (PPSQ) a temperature-sensitive material for high-temperature applications could be developed.[1254]

An extension of the application of europium(III)-doped polymer films as temperature sensors is *fluorescent microthermal imaging* (FMI) by these materials. FMI is a hot spot-localizing technique that is complementary to *liquid crystal thermography* (LCT) with the advantage of having a high spatial resolution. FMI allows coverage of a much wider temperature range than LCT. $Eu(tta)_3$ doped in PMMA was used to measure the heating of integrated circuits with a temperature resolution of 0.01 °C and a spatial resolution of 15 μm.[1255] A film of $Eu(tta)_3$-doped PMMA was spin-coated onto the surface of an integrated circuit chip. The chip was illuminated with long-wave UV light, and the orange luminescence was imaged onto a CCD camera. The

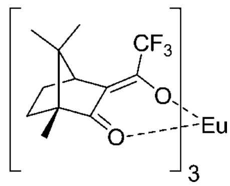

Figure 118. Structure of [Eu(facam)$_3$].

optical features of the image were removed by optical imaging processing so that a purely thermal map of the surface temperature profile was obtained. In a follow-up paper, the authors were able to improve their method to a spatial resolution of 0.7 μm.[1256] Later work showed that a temperature resolution of 6 mK can be obtained.[1257] Besides electronic failure analysis,[1257] this method has also been applied for the measurements of temperature changes in glass resin thin films during reactive etching,[1258,1259] for study of failure in solar cells, for the observation of hot spots in superconductors at temperatures down to 50 K,[1260−1262] and for heat transfer analysis.[1263] For thermal imaging at cryogenic temperatures, europium tris[3-(trifluoro-methylhydroxymethylene)-(+)-camphorate], Eu(tfc)$_3$ or Eu(facam)$_3$ (Figure 118), is often preferred over Eu(tta)$_3$.[1264,1265] The most often used polymer matrix for the europium(III) complexes is PMMA. Replacement of PMMA by deuterated PMMA improved the sensitivity of the method by a factor of 2 in comparison with PMMA.[1266] The different factors influencing the image quality and sensitivity have been systematically analyzed.[1267] Photodegradation of europium(III) β-diketonate complexes (UV bleaching) is a problem for long-term studies. Eu(tta)$_3$ in a polymer binder is used as a *temperature-sensitive paint* (TSP) for temperature mapping in aerodynamic measurements.[1268−1270] It allows visualization of the surface temperature distribution of an aerodynamic body like an airplane. The binder is a clear model airplane dope like Chromaclear (produced by DuPont) or Shellac.

11. Conclusions and Outlook

This review shows that research in the field of lanthanide-based luminescent hybrid materials is very active. A count of the number of papers published in a given year indicates that this interest is still increasing. However, an evident trend is that research is gradually shifting to more complex systems. For instance, very few studies on lanthanide complexes doped into pure silica sol−gel glasses are still appearing, whereas present work is more concentrated on lanthanide complexes in organically modified silicates and especially on complexes covalently linked to the host matrix. This shift in the choice of materials for investigation can be explained by a better understanding of how to obtain materials with improved mechanical properties, of how to avoid leaching of the lanthanide complex from the hybrid matrix, or of how to reduce luminescence quenching caused by clustering of lanthanide ions. Another trend is the increase in interest in hybrid materials based on lanthanide-doped nanoparticles. These materials deserve attention from the scientific community because they combine the excellent luminescent properties of inorganic phosphors and the processability of molecular materials.

In general, incorporation of a lanthanide complex into a inorganic hybrid matrix significantly improves its thermal and (photo)chemical stability. This can partially be explained by the shielding of the lanthanide complex from the atmosphere and especially from atmospheric oxygen and moisture. The entrapment of the lanthanide complex in the hybrid matrix often leads to a more intense photoluminescence because of light absorption by the host matrix and subsequent transfer of the excitation energy to the lanthanide complex and finally to the emitting lanthanide(III) ion. By far the most popular lanthanide(III) ion in hybrid materials is the Eu^{3+} ion with its bright red photoluminescence.

An interesting research topic would be a systematic investigation of hybrid materials doped with multiple lanthanide ions, that is, materials that contain a mixture of lanthanide ions. First of all, there is the possibility of sensitizing the luminescence of a lanthanide ion via another metal ion, being a lanthanide or a transition-metal ion. Examples are the sensitization of Tb^{3+} luminescence by Ce^{3+} or of Er^{3+} luminescence by Yb^{3+}. Second, such multiply doped systems offer the opportunity of designing materials with a tunable emission color, depending on the concentration and concentration ratio of the metal ions, the excitation wavelength, or the temperature. Finally, these hybrid materials are of interest for observing upconversion effects.

The structural characterization of the lanthanide complexes inside the hybrid host matrices remains a challenge. In some examples, it is found that incorporation of the lanthanide complex into the host matrix has only a limited influence on the fine structure of the luminescence spectra and therefore possibly also only a limited influence on the structure of the complexes; this is by no means a general observation. Interactions between the lanthanide complex and its environment are expected in the case of silica-based host matrices or in case of polymers with coordinating functional groups.

Although different applications are suggested for lanthanide-based luminescent hybrid materials, it is unlikely that these materials will enter our daily life as long as research remains focused on the lanthanide β-diketonates. Despite their good luminescence behavior, these compounds are simply too unstable for long-term use in devices. Even after incapsulation of the complexes in inert hosts, their stability remains questionable. Therefore, it is strongly recommended that scientists working in this field pay more attention to luminescent lanthanide complexes other than β-diketonate complexes. A promising class of compounds are the lanthanide salts of (aromatic) carboxylic acids, but more work needs to be invested in order to design carboxylates that can efficiently sensitize europium(III) luminescence. Complexes of ligands like pyridine-2,6-dicarboxylate (dipicolinate) are interesting luminescent compounds with an improved stability, and they are becoming more and more in favor for luminescent-based applications.[1271−1275] Other types of lanthanide complexes that have properties that make them interesting as luminescent dopants in hybrid materials are the 2-hydroxyisophthalamides,[1276−1278] cyclen derivatives,[1279] and 8-hydroxyquinolinates.[1280] Also lanthanide-doped nanoparticles could offer an alternative for the lanthanide β-diketonates.

12. List of Abbreviations and Symbols

acac	acetylacetonate
AEAPAS	*N*-2-aminoethyl-3-aminopropyltriethoxysilane
AEP	aminoethylphosphate
APTM	3-aminopropyltrimethoxysilane
APTS	3-aminopropyltriethoxysilane
bath	bathophenanthroline (4,7-diphenyl-1,10-phenanthroline)
BDC	1,4-benzenedicarboxylate

bipy	2,2′-bipyridine
$bipyO_2$	2,2′-bipyridine-*N*,*N*-dioxide
BTC	1,2,5-benzenetricarboxylate
btfac	benzoyltrifluoroacetylacetonate
bzac	benzoylacetonate
CPTM	3-chloropropyltrimethoxysilane
CTAB	cetyltrimethylammonium bromide
dam	diantipyrylmethane
dbm	dibenzoylmethanate
DEDMS	diethoxydimethylsilane
DEDPS	diethoxydiphenylsilane
DEDS	diethoxydiethylsilane
DMF	*N*,*N*-dimethylformamide
DMSO	dimethylsulfoxide
dnm	dinaphthoylmethanate
dpa	dipicolinate (pyridine-2,6-dicarboxylate)
dpm	dipivaloylmethanate
ELSA	electrostatic layer-by-layer self-assembly
ESA	electrostatic self-assembly
ET	energy transfer
ETEOS	ethyltriethoxysilane
EXAFS	extended X-ray absorption fine structure
FLN	fluorescence line narrowing
fod	6,6,7,7,8,8,8-heptafluoro-2,2-dimethyl-3,5-octadionate
fwhm	full width at half-maximum
GDLC	glass-dispersed liquid crystals
gly	monoglyme (1,2-dimethoxyethane)
GLYMO	3-glycidoxypropyltrimethoxysilane (GPTMS)
GPTMS	3-glycidoxypropyltrimethoxysilane (GLYMO)
hfac	hexafluoroacetylacetonate
HMDS	hexamethyldisilazane
HMPA	hexamethyl phosphoric triamide
ICPTES	3-isocyanatopropyltriethoxysilane
ISA	ionic self-assembly
ISC	intersystem crossing
ITO	indium tin oxide
k_r	rate constant for radiative deactivation
k_{nr}	rate constant for nonradiative deactivation
LB	Langmuir−Blodgett
LDH	layered double hydroxide
LED	light-emitting diode
MEMO	methacryloxypropyltrimethoxysilane
MOF	metal−organic framework
MPTMA	3-(trimethoxysilyl)propyl methacrylate
MTMS	methyltrimethoxysilane
n	refractive index
ntac	2-naphtoyltrifluoroacetonate
oda	oxydiacetate
OLED	organic light-emitting diode
ormosil	organically modified silicate
PE	polyethylene
PEG	poly(ethylene glycol)
PEG-200	poly(ethylene glycol) with an average molar mass of 200 g/mol
PEMA	poly(ethylmethacrylate)
PEO	poly(oxyethylene)
phen	1,10-phenanthroline
PMMA	poly(methyl methacrylate)
POM	polyoxometalate
PPSQ	polyphenylsilsesquioxane
PS	polystyrene
PSHB	persistent spectral hole burning
PVA	poly(vinyl alcohol)
PVP	poly(vinyl pyrrolidone)
S	singlet
SAXS	small-angle X-ray scattering
T	triplet
TEOS	tetraethylorthosilicate
TEPED	*N*-[(3-triethoxysilyl)propyl]ethylenediamine
TEPS	triethoxyphenylsilane
terpy	2,2′,6′,2″-terpyridine
TFTM	3,3,3-trifluoropropyltrimethoxysilane
TMA	tetramethylammonium
tmphen	3,4,7,8-tetramethyl-1,10-phenanthroline
TMOS	tetramethylorthosilicate
TMSPM	3-(trimethoxysilyl)propyl methacrylate
tppo	triphenylphosphine oxide
tta	2-thenoyltrifluoroacetonate
thd	2,2,6,6-tetramethyl-3,5-heptanedionate
5CB	4-pentyl-4′-cyanobiphenyl
Φ	luminescence quantum yield
Φ_{Ln}	intrinsic luminescence quantum yield
Φ_{tot}	overall luminescence quantum yield
Ω_λ	Judd−Ofelt intensity parameter
η_{sens}	efficiency of sensitization (efficiency of energy transfer)
τ_{obs}	observed luminescence lifetime
τ_R	radiative lifetime

13. Acknowledgments

The author acknowledges financial support by the K.U. Leuven (Project GOA 08/05) and by the FWO-Flanders (Research Project G.0508.07).

14. References

(1) Bünzli, J.-C. G. Luminescent Probes. In *Lanthanide Probes in Life, Chemical and Earth Sciences: Theory and Practice*; Bünzli, J.-C. G., Choppin, G. R., Eds.; Elsevier: Amsterdam, 1989.
(2) Kenyon, A. J. *Prog. Quantum Electron.* **2002**, *26*, 225.
(3) Blasse, G.; Grabmaier, B. C. *Luminescent Materials*; Spinger-Verlag: Berlin, 1994.
(4) Blasse, G. *Prog. Solid State Chem.* **1988**, *18*, 79.
(5) Elbanowski, M.; Makowsaka, B. J. *Photochem. Photobiol. A* **1996**, *99*, 85.
(6) Bünzli, J.-C. G. *Acc. Chem. Res.* **2006**, *39*, 53.
(7) Bünzli, J.-C. G.; Piguet, C. *Chem. Soc. Rev.* **2005**, *34*, 1048.
(8) Hasegawa, Y.; Wada, Y.; Yanagida, S. *J. Photochem. Photobiol. C* **2004**, *5*, 183.
(9) Tissue, B. M. *Chem. Mater.* **1998**, *10*, 2837.
(10) Carnall, W. T.; Beitz, J. V.; Crosswhite, H.; Rajnak, K.; Mann, J. B. Spectroscopic properties of the f-elements in compounds and solutions. In *Systematics and the Properties of Lanthanides*; Sinha, S. P., Ed.; D. Reidel Publishing Company: Dordrecht, The Netherlands, 1983; p 389.
(11) Carnall, W. T. The absorption and fluorescence spectra of rare earth ions in solution. In *Handbook on the Physics and Chemistry of Rare Earths*; Gschneidner, K. A., Jr., Eyring, L., Eds.; Elsevier: Amsterdam, 1979; Vol. 3, Chapter 24, p 171.
(12) Blasse, J. Chemistry and Physics of R-activated Phosphors. In *Handbook on the Physics and Chemistry of Rare Earths*; Gschneidner, K. A., Jr., Eyring, L., Eds.; Elsevier: Amsterdam, 1979; Vol. 4, Chapter 34, p 237.
(13) Weber, M. J. Rare Earth Lasers. In *Handbook on the Physics and Chemistry of Rare Earths*; Gschneidner, K. A., Jr., Eyring, L., Eds.; Elsevier: Amsterdam, 1979; Vol. 4, Chapter 35, p 275.
(14) Morrison, C. A.; Leavitt, R. P. Spectroscopic properties of triply ionized lanthanides in transparent host crystals. In *Handbook on the Physics and Chemistry of Rare Earths*; Gschneidner, K. A., Jr., Eyring, L., Eds.; Elsevier: Amsterdam, 1982; Vol. 5, Chapter 46, p 461.
(15) Kickelbick, G., Ed. *Hybrid Materials: Synthesis, Characterization and Applications*; Wiley-VCH: Weinheim, Germany, 2007.
(16) Gómez-Romero, P., Sanchez, C., Eds. *Functional Hybrid Materials*; Wiley-VCH: Weinheim, Germany, 2003.
(17) Judeinstein, P.; Sanchez, C. *J. Mater. Chem.* **1996**, *6*, 511.
(18) Sanchez, C.; Soler-Illia, G. J. D. A.; Ribot, F.; Lalot, T.; Mayer, C. R.; Cabuil, V. *Chem. Mater.* **2001**, *13*, 3061.
(19) Sanchez, C.; Lebeau, B.; Chaput, F.; Boilot, J. P. *Adv. Mater.* **2003**, *15*, 1969.
(20) Sanchez, C.; Julian, B.; Belleville, P.; Popall, M. *J. Mater. Chem.* **2005**, *15*, 3559.
(21) Sanchez, C.; Lebeau, B. *MRS Bull.* **2001**, *26*, 377.
(22) Lebeau, B.; Sanchez, C. *Curr. Opin. Solid State Mater. Sci.* **1999**, *4*, 11.
(23) Ribot, F.; Sanchez, C. *Comments Inorg. Chem.* **1999**, *20*, 327.
(24) Nicole, L.; Boissiere, C.; Grosso, D.; Quach, A.; Sanchez, C. *J. Mater. Chem.* **2005**, *15*, 3598.

(25) Sanchez, C.; Boissiere, C.; Grosso, D.; Laberty, C.; Nicole, L. *Chem. Mater.* **2008**, *20*, 682.
(26) Wen, J. Y.; Wilkes, G. L. *Chem. Mater.* **1996**, *8*, 1667.
(27) Gomez-Romero, P. *Adv. Mater.* **2001**, *13*, 163.
(28) Sharp, K. G. *Adv. Mater.* **1998**, *10*, 1243.
(29) Cerveau, G.; Corriu, R. J. P. *Coord. Chem. Rev.* **1998**, *178*, 1051.
(30) Kickelbick, G. *Prog. Polym. Sci.* **2003**, *28*, 83.
(31) Kickelbick, G.; Schubert, U. *Monatsh. Chem.* **2001**, *132*, 13.
(32) Hoffmann, F.; Cornelius, M.; Morell, J.; Froba, M. *Angew. Chem., Int. Ed.* **2006**, *45*, 3216.
(33) Walcarius, A. *Chem. Mater.* **2001**, *13*, 3351.
(34) Mitzi, D. B. *Chem. Mater.* **2001**, *13*, 3283.
(35) Schubert, U. *Chem. Mater.* **2001**, *13*, 3487.
(36) Escribano, P.; Julian-Lopez, B.; Planelles-Arago, J.; Cordoncillo, E.; Viana, B.; Sanchez, C. *J. Mater. Chem.* **2008**, *18*, 23.
(37) Comby, S.; Bünzli, J.-C. G Lanthanide near-infrared luminescence in molecular probes and devices. In *Handbook on the Physics and Chemistry of Rare Earths*; Gschneidner, K. A., Jr., Bünzli, J. C. G., Pescharsky, V. K., Eds.; Elsevier: Amsterdam, 2007; Vol. 37, Chapter 235, p 217.
(38) Carlos, L. D.; Ferreira, R. A. S.; de Zea Bermudez, V.; Ribeiro, S. J. L. *Adv. Mater.* **2009**, *21*, 509.
(39) Weissman, S. I. *J. Chem. Phys.* **1942**, *10*, 214.
(40) Sevchenko, A. N.; Trifimov, A. K. *J. Exp. Theor. Phys.* **1951**, *21*, 220.
(41) Whan, R. E.; Crosby, G. A. *J. Mol. Spectrosc.* **1962**, *8*, 315.
(42) Crosby, G. A.; Whan, R. E.; Alire, R. M. *J. Chem. Phys.* **1961**, *34*, 743.
(43) Crosby, G. A.; Whan, R. E.; Freeman, J. J. *J. Phys. Chem.* **1962**, *66*, 2493.
(44) Kleinerman, M. *Bull. Am. Phys. Soc.* **1964**, *9*, 265.
(45) Misra, V.; Mishra, H. *J. Chem. Phys.* **2008**, *128*, 244701.
(46) Yang, C.; Fu, L. M.; Wang, Y.; Zhang, J. P.; Wong, W. T.; Ai, X. C.; Qiao, Y. F.; Zou, B. S.; Gui, L. L. *Angew. Chem., Int. Ed.* **2004**, *43*, 5010.
(47) Hebbink, G. A.; Klink, S. I.; Grave, L.; Alink, P. G. B.O.; van Veggel, F. C. J. M. *ChemPhysChem* **2002**, *3*, 1014.
(48) Matsuda, Y.; Makishima, S.; Shionoya, S. *Bull. Chem. Soc. Jpn.* **1968**, *41*, 1513.
(49) Filipescu, N.; Sager, W. F.; Serafin, F. A. *J. Phys. Chem.* **1964**, *68*, 3324.
(50) Sato, S.; Wada, M. *Bull. Chem. Soc. Jpn.* **1970**, *43*, 1955.
(51) Tobita, S.; Arakawa, M.; Tanaka, I. *J. Phys. Chem.* **1984**, *88*, 2697.
(52) Tobita, S.; Arakawa, M.; Tanaka, I. *J. Phys. Chem.* **1985**, *89*, 5649.
(53) Bhaumik, M. L.; El-Sayed, M. A. *J. Phys. Chem.* **1965**, *69*, 275.
(54) Latva, M.; Takalo, H.; Mukkala, V. M.; Matachescu, C.; Rodriguez-Ubis, J. C.; Kankare, J. *J. Lumin.* **1997**, *75*, 149.
(55) Balzani, V.; Moggi, L.; Manfrin, M. F.; Bolletta, F. *Coord. Chem. Rev.* **1975**, *15*, 321.
(56) Wilkinson, F. *Pure Appl. Chem.* **1975**, *41*, 661.
(57) Petoud, S.; Bünzli, J.-C. G.; Glanzman, T.; Piguet, C.; Xiang, Q.; Thummel, R. P. *J. Lumin.* **1999**, *82*, 69.
(58) Faustino, W. M.; Malta, O. L.; de Sa, G. F. *J. Chem. Phys.* **2005**, *122*, 054109.
(59) Malta, O. L. *J. Lumin.* **1997**, *71*, 229.
(60) D'Aleo, A.; Picot, A.; Beeby, A.; Williams, J. A. G.; Le Guennic, B.; Andraud, C.; Maury, O. *Inorg. Chem.* **2008**, *47*, 10258.
(61) Fonger, W. H.; Struck, C. W. *J. Chem. Phys.* **1970**, *52*, 6364.
(62) Lazarides, T.; Sykes, D.; Faulkner, S.; Barbieri, A.; Ward, M. D. *Chem.—Eur. J.* **2008**, *14*, 9389.
(63) Ward, M. D. *Coord. Chem. Rev.* **2007**, *251*, 1663.
(64) Ronson, T. K.; Lazarides, T.; Adams, H.; Pope, S. J. A.; Sykes, D.; Faulkner, S.; Coles, S. J.; Hursthouse, M. B.; Clegg, W.; Harrington, R. W.; Ward, M. D. *Chem.—Eur. J.* **2005**, *12*, 9299.
(65) Lazarides, T.; Adams, H.; Sykes, D.; Faulkner, S.; Calogero, G.; Ward, M. D. *Dalton Trans.* **2008**, 691.
(66) Shavaleev, N. M.; Moorcraft, L. P.; Pope, S. J. A.; Bell, Z. R.; Faulkner, S.; Ward, M. D. *Chem. Commun.* **2003**, 1134.
(67) Chen, F. F.; Bian, Z. Q.; Liu, Z. W.; Nie, D. B.; Chen, Z. Q.; Huang, C. H. *Inorg. Chem.* **2008**, *47*, 2507.
(68) Imbert, D.; Cantuel, M.; Bünzli, J.-C. G.; Bernardinelli, G.; Piguet, C. *J. Am. Chem. Soc.* **2003**, *125*, 15698.
(69) Fery-Forgues, S.; Lavabre, D. *J. Chem. Educ.* **1999**, *76*, 1260.
(70) Werts, M. H. V.; Jukes, R. T. F.; Verhoeven, J. W. *Phys. Chem. Chem. Phys.* **2002**, *4*, 1542.
(71) Haas, Y.; Stein, G. *J. Phys. Chem.* **1971**, *75*, 3677.
(72) Haas, Y.; Stein, G. *J. Phys. Chem.* **1971**, *75*, 3668.
(73) Thompson, L.; Legendziewicz, J.; Cybinska, J.; Pan, L.; Brennessel, W. *J. Alloys Compd.* **2002**, *341*, 312.
(74) Görller-Walrand, C.; Binnemans, K. Spectral intensities of f-f transitions. In *Handbook on the Physics and Chemistry of Rare Earths*; Gschneidner, K. A., Jr., Eyring, L., Eds.; Elsevier: Amsterdam, 1998; Vol. 25, Chapter 167, p 101.
(75) Goldner, P.; Auzel, F. *J. Appl. Phys.* **1996**, *79*, 7972.
(76) Neto, J. A. M.; Hewak, D. W.; Tate, H. *J. Non-Cryst. Solids* **1995**, *183*, 201.
(77) Quimby, R. S.; Miniscalco, J. W. *J. Appl. Phys.* **1994**, *75*, 613.
(78) Auzel, F. *J. Alloys Compds.* **2004**, *380*, 9.
(79) Eaton, D. F. *Pure Appl. Chem.* **1998**, *60*, 1107.
(80) Nakamura, S.; Takei, S.; Akiba, K. *Anal. Sci.* **2002**, *18*, 319.
(81) Chauvin, A. S.; Gumy, F.; Imbert, D.; Bünzli, J.-C. G. *Spectrosc. Lett.* **2004**, *37*, 517 [Erratum: *Spectrosc. Lett.* **2007**, *40*, 193].
(82) Bril, A.; De Jager-Veenis, W. *J. Res. Natl. Bur. Stand.* **1976**, *80A*, 401.
(83) Bril, A.; De Jager-Veenis, W. *J. Electrochem. Soc.* **1976**, *123*, 396.
(84) de Mello Donegá, C.; Alves, S., Jr.; de Sá, G. F. *Chem. Commun.* **1996**, 1199.
(85) de Mello Donegá, C.; Ribeiro, S. J. L.; Gonçalves, R. R.; Blasse, G. *J. Phys. Chem. Solids* **1996**, *57*, 1727.
(86) Malta, O. L.; Brito, H. F.; Menezes, J. F. S.; Gonçalves e Silva, F. R.; de Mello Donegá, C *Chem. Phys. Lett.* **1998**, *282*, 233.
(87) Gudmundson, R. A.; Marsh, O. J.; Matovich, E. *J. Chem. Phys.* **1963**, *39*, 272.
(88) Carlos, L. D.; de Mello Donegá, C.; Albuquerque, R. Q.; Alves, S., Jr.; Menezes, J. F. S.; Malta, O. L. *Mol. Phys.* **2003**, *101*, 1037.
(89) Bhaumik, M. L. *J. Chem. Phys.* **1964**, *40*, 3711.
(90) Watson, M. M.; Zerger, R. P.; Yardley, J. T.; Stucky, G. D. *Inorg. Chem.* **1975**, *14*, 2675.
(91) Dieke, G. H. *Spectra and Energy Levels of Rare Earth Ions in Crystals*; Interscience Publishers: New York, 1968.
(92) Wybourne, B. G. *Spectroscopic Properties of the Rare Earths*; Wiley: New York, 1965.
(93) Judd, B. R. *Operator Techniques in Atomic Spectroscopy*; Princeton University Press: Princeton, NJ, 1988.
(94) Hüfner, S. *Optical Spectra of Transparent Rare Earths Compounds*; Academic Press: New York, 1978.
(95) Smentek, L.; Wybourne, B. G. *Optical Spectroscopy of Lanthanides: Magnetic and Hyperfine Interactions*; CRC Press: Boca Raton, FL, 2007.
(96) Newman, D. G.; Ng, B. *Crystal Field Handbook*; Cambridge University Press: Cambridge, U.K., 2000.
(97) Liu, G. K., Jacquier, B., Eds. *Spectroscopic Properties of Rare Earths in Optical Materials*; Springer: Berlin, 2005.
(98) Görller-Walrand, C.; Binnemans, K. Rationalization of Crystal Field Parametrization. In *Handbook on the Physics and Chemistry of Rare Earths*; Gschneidner, K. A., Jr., Eyring, L., Eds.; Elsevier: Amsterdam, 1996; Vol. 23, Chapter 155, p 121.
(99) Garcia, D.; Faucher, M. Crystal field in non-metallic rare earth compounds. In *Handbook on the Physics and Chemistry of Rare Earths*; Gschneidner, K. A., Jr., Eyring, L., Eds.; Elsevier: Amsterdam, 1995; Vol. 21, Chapter 144, p 263.
(100) Carnall, W. T.; Crosswhite, H.; Crosswhite, H. M. *Energy Level Structure and Transition Probabilities of the Trivalent Lanthanides in LaF_3*; Argonne National Laboratory: Argonne, IL, 1977.
(101) Carnall, W. T.; Fields, P. R.; Rajnak, K. *J. Chem. Phys.* **1968**, *49*, 4424.
(102) Carnall, W. T.; Fields, P. R.; Rajnak, K. *J. Chem. Phys.* **1968**, *49*, 4443.
(103) Carnall, W. T.; Fields, P. R.; Rajnak, K. *J. Chem. Phys.* **1968**, *49*, 4447.
(104) Carnall, W. T.; Fields, P. R.; Rajnak, K. *J. Chem. Phys.* **1968**, *49*, 4450.
(105) Judd, B. R. *Phys. Rev.* **1962**, *127*, 750.
(106) Ofelt, G. S. *J. Chem. Phys.* **1962**, *37*, 511.
(107) Axe, J. D. *J. Chem. Phys.* **1963**, *39*, 1154.
(108) Carnall, W. T.; Fields, P. R.; Wybourne, B. G. *J. Chem. Phys.* **1965**, *42*, 3797.
(109) Carnall, W. T.; Fields, P. R.; Rajnak, K. *J. Chem. Phys.* **1968**, *49*, 4412.
(110) Peacock, R. D. *Struct. Bonding (Berlin)* **1975**, *22*, 83.
(111) Henrie, D. E.; Fellows, R. L.; Choppin, G. R. *Coord. Chem. Rev.* **1976**, *18*, 199.
(112) Yatmirskii, K. B.; Davidenko, N. K. *Coord. Chem. Rev.* **1979**, *27*, 223.
(113) Walsh, B. M. Judd-Ofelt Theory: Principles and Practices. In *Advances in Spectroscopy for Lasers and Sensing*; Di Bartolo, B., Forte, O., Eds.; NATO Science Series II: Mathematics, Physics and Chemistry; Springer: Dordrecht, The Netherlands, 2006; Vol. 231, Chapter 21, p 403.
(114) Binnemans, K. Rare-Earth Beta-Diketonates. In *Handbook on the Physics and Chemistry of Rare Earths*; Gschneidner, K. A., Jr., Bünzli, J.-C. G., Pecharsky, V. K., Eds.; Elsevier: Amsterdam, 2005; Volume *35*, Chapter 225, p 107.
(115) Forsberg, J. H. *Sc, Y, La-Lu Rare Earth Elements*; Gmelin Handbook of Inorganic Chemistry (System Nr. 39), D3; Springer-Verlag: Berlin, 1981; p 65.

(116) de Sa, G. F.; Malta, O. L.; Donega, C. D.; Simas, A. M.; Longo, R. L.; Santa-Cruz, P. A.; da Silva, E. F. *Coord. Chem. Rev.* **2000**, *196*, 165.
(117) Hasegawa, Y.; Wada, Y.; Yanagida, S. *J. Photochem. Photobiol. C* **2004**, *5*, 183.
(118) Yanagida, S.; Hasegawa, Y.; Murakoshi, K.; Wada, Y.; Nakashima, N.; Yamanaka, T. *Coord. Chem. Rev.* **1998**, *171*, 461.
(119) Melby, L. R.; Rose, N. J.; Abramson, E.; Caris, J. C. *J. Am. Chem. Soc.* **1964**, *86*, 5117.
(120) Bauer, H.; Blanc, J.; Ross, D. L. *J. Am. Chem. Soc.* **1964**, *86*, 5125.
(121) Freeman, J. J.; Crosby, G. A. *J. Phys. Chem.* **1963**, *67*, 2717.
(122) Sager, W. F.; Filipescu, N.; Serafin, F. A. *J. Phys. Chem.* **1965**, *69*, 1092.
(123) Iwamuro, M.; Wada, Y.; Kitamura, T.; Nakashima, N.; Yanagida, S. *Phys. Chem. Chem. Phys.* **2000**, *2*, 2291.
(124) Yang, Y. S.; Gong, M. L.; Li, Y. Y.; Lei, H. Y.; Wu, S. L. *J. Alloys Compd.* **1994**, *207*−*208*, 112.
(125) Wu, S. L.; Yang, Y. S. *J. Alloys Compd.* **1992**, *180*, 403.
(126) Wu, S. L.; Wu, Y. L.; Yang, Y. S. *J. Alloys Compd.* **1992**, *180*, 399.
(127) Blasse, G. *Struct. Bonding (Berlin)* **1976**, *26*, 43.
(128) Napier, G. D. R.; Neilson, J. D.; Shepherd, T. M. *Chem. Phys. Lett.* **1975**, *31*, 328.
(129) Weber, M. J. *J. Non-Cryst. Solids* **1990**, *123*, 208.
(130) Marion, J. E.; Weber, M. J. *Eur. J. Solid State Inorg. Chem.* **1991**, *28*, 271.
(131) Reisfeld, R.; Jørgensen, C. K. *Lasers and Excited States of Rare Earths*; Springer Verlag: Heidelberg, Germany, 1977.
(132) Miniscalco, M. J. *J. Lightwave Technol.* **1991**, *9*, 234.
(133) Chakrabarti, S.; Sahu, J.; Chakraborty, M.; Acharya, H. N. *J. Non-Cryst. Solids* **1994**, *180*, 96.
(134) Pope, E. J. A.; MacKenzie, J. D. *J. Non-Cryst. Solids* **1988**, *106*, 236.
(135) Pope, E. J. A.; MacKenzie, J. D. *J. Am. Ceram. Soc.* **1993**, *76*, 1325.
(136) Wang, S. S.; Zhou, Y.; Lam, Y. L.; Kam, C. H.; Chan, Y. C.; Yao, X. *Mater. Res. Innovations* **1997**, *1*, 92.
(137) Sun, K.; Lee, W. H.; Risen, W. M. *J. Non-Cryst. Solids* **1987**, *92*, 145.
(138) Itoh, K.; Kamata, N.; Shimazu, T.; Satoh, C.; Tonooka, K.; Yamada, K. *J. Lumin.* **2000**, *87*−*89*, 676.
(139) Hench, L. L.; West, J. K. *Chem. Rev.* **1990**, *90*, 33.
(140) Brinker, C. J.; Scherer, G. W. *Sol-Gel Science: The Physics and Chemistry of Sol-Gel Processing*; Academic Press: San Diego, CA, 1989.
(141) Buckley, A. M.; Greenblatt, A. *J. Chem. Educ.* **1994**, *71*, 599.
(142) Collinson, M. M. In *Handbook of Advanced Electronic and Photonic Materials and Devices*; Nalwa, H. S., Ed.; Academic Press, San Diego, CA, 2001; Vol. 5, Chapter 6, p 163.
(143) Böhmer, M. R.; Balkenende, A. R.; Bernards, T. N. M.; Peeters, M. P. J.; van Bommel, M. J.; Boonekamp, E. P.; Verheijen, M. A.; Krings, L. H. M.; Vroon, Z. A. E. P. In *Handbook of Advanced Electronic and Photonic Materials and Devices*; Nalwa, H. S., Ed.; Academic Press: San Diego, CA, 2001; Volume *5*, Chapter 8, p 219.
(144) Dunn, B.; Zink, J. I. *J. Mater. Chem.* **1991**, *1*, 903.
(145) Reisfeld, R. *Opt. Mater.* **2001**, *16*, 1.
(146) Reisfeld, R. *J. Fluoresc.* **2002**, *12*, 317.
(147) Reisfeld, R. *J. Non-Cryst. Solids* **1990**, *121*, 254.
(148) Reisfeld, R.; Jørgensen, C. K. *Struct. Bonding (Berlin)* **1992**, *72*, 207.
(149) Avnir, D.; Levy, D.; Reisfeld, R. *J. Phys. Chem.* **1984**, *88*, 5956.
(150) Avnir, D.; Kaufman, V. R.; Reisfeld, R. *J. Non-Cryst. Solids* **1985**, *74*, 395.
(151) Mizuno, T.; Nagata, H.; Maanbe, S. *J. Non-Cryst. Solids* **1988**, *100*, 236.
(152) Adachi, T.; Sakka, S. *J. Non-Cryst. Solids* **1988**, *99*, 118.
(153) Thomas, I. M.; Payne, S. A.; Wilke, G. D. *J. Non-Cryst. Solids* **1992**, *151*, 183.
(154) Kawaguchi, T.; Hishikura, H.; Iura, J.; Kokubu, Y. *J. Non-Cryst. Solids* **1984**, *63*, 61.
(155) Grandi, S.; Costa, L. *J. Non-Cryst. Solids* **1998**, *225*, 141.
(156) Avnir, D. *Acc. Chem. Res.* **1995**, *28*, 328.
(157) Levy, D.; Reisfeld, R.; Avnir, D. *Chem. Phys. Lett.* **1984**, *109*, 593.
(158) Reisfeld, R.; Zigansky, E.; Gaft, M. *Mol. Phys.* **2004**, *102*, 1319.
(159) Campostrini, R.; Carturan, G.; Ferrari, M.; Montagna, M.; Pilla, O. *J. Mater. Res.* **1992**, *7*, 745.
(160) Ferrari, M.; Campostrini, R.; Carturan, G.; Montagna, M. *Philos. Mag. B* **1992**, *65*, 251.
(161) Bouajaj, A.; Ferrari, M.; Montagna, M.; Moser, E.; Piazza, A.; Campostrini, R.; Carturan, G. *Philos. Mag. B* **1995**, *71*, 633.
(162) Devlin, K.; Okelly, B.; Tang, Z. R.; McDonagh, C.; McGilp, J. F. *J. Non-Cryst. Solids* **1991**, *135*, 8.
(163) McDonagh, C.; Okelly, B.; Devlin, K.; Tang, Z. R.; McGilp, J. F. *Inst. Phys. Conf. Ser.* **1990**, *111*, 435.
(164) McDonagh, C.; Ennis, G.; Marron, P.; O'Kelly, B.; Tang, Z. R.; McGilp, J. F. *J. Non-Cryst. Solids* **1992**, *147*−*148*, 97.
(165) Wang, X. G.; Wu, H. Y.; Xie, D. T.; Weng, S. F.; Wu, J. G. *J. Rare Earths* **2002**, *20*, 172.
(166) Martin, I. R.; Mendez-Ramos, J.; Delgado, F.; Lavin, V.; Rodriguez-Mendoza, U. R.; Rodriguez, V. D.; Yanes, A. C. *J. Alloys Compd.* **2001**, *323*, 773.
(167) Jia, W. Y.; Liu, H. M.; Felofilov, S. P.; Meltzer, R.; Jiao, J. *J. Alloys Compd.* **2000**, *311*, 11.
(168) Piazza, A.; Bouajaj, A.; Ferrari, M.; Montagna, M.; Campostrini, R.; Carturan, G. *J. Phys. IV* **1994**, *4*, 569.
(169) Bouajaj, A.; Monteil, A.; Bovier, C.; Ferrari, M.; Piazza, A. *J. Phys. IV* **1994**, *4*, 579.
(170) Andrianasolo, B.; Ferrari, M.; Monteil, A.; Duval, E.; Serughetti, A.; Campostrini, R.; Carturan, G.; Montagna, M.; Rossi, F. *J. Phys. IV* **1991**, *1*, 501.
(171) Lochhead, M. J.; Bray, K. L. *J. Non-Cryst. Solids.* **1994**, *170*, 143.
(172) Krebs, J. K.; Brownstein, J. M. *J. Lumin.* **2007**, *124*, 257.
(173) Kim, T.; Yoon, Y.; Kil, D.; Hwang, Y.; Chung, H.; Kim, I. N.; Ahn, Y. *Mater. Lett.* **2001**, *47*, 290.
(174) Zupanc-Meznar, L.; Cerc-Korosec, R.; Bukovec, P.; Gomilsek, J. P. *J. Vac. Sci. Technol., B* **2000**, *18*, 1097.
(175) Rocha, L. A.; Molina, E. F.; Ciuffi, K. J.; Calefi, P. S.; Nassar, E. *J. Mater. Chem. Phys.* **2007**, *101*, 238.
(176) Ribeiro, S. J. L.; Hiratsuka, R. S.; Massabni, A. M. G.; Davolos, M. R.; Santilli, C. V.; Pulcinelli, S. H. *J. Non-Cryst. Solids* **1992**, *147*, 162.
(177) Driesen, K.; Binnemans, K.; Görller-Walrand, C. *Mater. Sci. Eng., C* **2001**, *18*, 255.
(178) Driesen, K.; Lenaerts, P.; Binnemans, K.; Görller-Walrand, C. *Phys. Chem. Chem. Phys.* **2002**, *4*, 552.
(179) Perry, C.; Aubonnet, S. *J. Sol-Gel Sci. Technol.* **1998**, *13*, 593.
(180) Pucker, G.; Parolin, S.; Moser, E.; Montagna, M.; Ferrari, M.; Del Longo, L. *Spectrochim. Acta A* **1998**, *54*, 2133.
(181) Rand, E. R.; Smuckler, M. B.; Eden, G.; Bradley, M. S.; Bruno, J. W. *Inorg. Chim. Acta* **1995**, *233*, 71.
(182) Assefa, Z.; Haire, R. G.; Caulder, D. L.; Shuh, D. K. *Spectrochim. Acta A* **2004**, *60*, 1873.
(183) Hreniak, D.; Jasiorski, M.; Maruszewski, K.; Kepinski, L.; Krajczyk, L.; Misiewicz, J.; Strek, W. *J. Non-Cryst. Solids* **2002**, *298*, 146.
(184) Biswas, A.; Friend, C. S.; Maciel, G. S.; Prasad, P. N. *J. Non-Cryst. Solids* **2000**, *261*, 9.
(185) Hu, X. Y.; Fan, J.; Li, T.; Zhang, D. K.; Chen, W. Z.; Bai, J. T.; Hou, X. *Opt. Mater.* **2007**, *29*, 1327.
(186) Suzuki, R.; Takei, S.; Tashiro, E.; Machida, K. *J. Alloys Compd.* **2006**, *408*, 800.
(187) Hanzawa, H.; Ueda, D.; Adachi, G.; Machida, K.; Kanematsu, Y. *J. Lumin.* **2001**, *94*, 503.
(188) Tsuboi, H.; Soga, K.; Inoue, H.; Makishima, A. *J. Am. Ceram. Soc.* **1998**, *81*, 1197.
(189) Zaitoun, M. A.; Kim, T.; Lin, C. T. *J. Phys. Chem. B* **1998**, *102*, 1122.
(190) Zaitoun, M. A.; Goken, D. M.; Bailey, L. S.; Kim, T.; Lin, C. T. *J. Phys. Chem. B.* **2000**, *104*, 189.
(191) Nogami, M. *J. Non-Cryst. Solids* **1999**, *259*, 170.
(192) Toghe, N.; Moore, G. S.; MacKenzie, J. D. *J. Non-Cryst. Solids* **1984**, *63*, 95.
(193) MacKenzie, J. D. *J. Non-Cryst. Solids* **1982**, *48*, 1.
(194) Fan, X. P.; Wang, Q. M.; Xiong, G. H. *Mater. Sci. Eng., B* **1993**, *21*, 55.
(195) Bouajaj, A.; Ferrari, M.; Montagna, M. *J. Sol-Gel Sci. Technol.* **1997**, *8*, 391.
(196) De, G.; Kundu, D.; Karmakar, B.; Ganguli, D. *Mater. Lett.* **1993**, *16*, 231.
(197) Satoh, S.; Susa, K.; Matsuyama, I.; Suganuma, T.; Matsumura, H. *J. Non-Cryst. Solids* **1997**, *217*, 22.
(198) Elmer, T. H. *J. Am. Ceram. Soc.* **1981**, *64*, 150.
(199) Uytterhoeven, J.; Naveau, H. *Bull. Soc. Chim. France* **1962**, *1*, 27.
(200) Rabinovich, E. M.; Wood, D. L.; Johnson, D. W.; Fleming, D. A.; Vincent, S. M.; MacChesney, J. B. *J. Non-Cryst. Solids* **1986**, *82*, 42.
(201) Costa, V. C.; Vasconcelos, W. L.; Bray, K. L. *Quim. Nov.* **1998**, *21*, 374.
(202) Stone, B. T.; Costa, V. C.; Bray, K. L. *Chem. Mater.* **1994**, *9*, 2703.
(203) Li, H. H.; Inoue, S.; Machida, K.; Adachi, G. *Chem. Mater.* **1999**, *11*, 3171.
(204) Bhagat, S. D.; Kim, Y. H.; Ahn, Y. S. *Appl. Surf. Sci.* **2006**, *253*, 2217.
(205) Dejneka, M.; Snitzer, E.; Riman, R. E. *J. Non-Cryst. Solids* **1996**, *202*, 23.
(206) Saad, M.; Poulain, M. *J. Non-Cryst. Solids* **1995**, *184*, 352.

(207) Vioux, A. *Chem. Mater.* **1997**, *9*, 2292.
(208) Boye, D. M.; Silversmith, A. J.; Nguyen, T. N.; Hoffman, K. R. *J. Non-Cryst. Solids.* **2007**, *353*, 2350.
(209) Patra, A.; Kundu, D.; Ganguli, D. *J. Sol-Gel Sci. Technol.* **1997**, *9*, 65.
(210) Silversmith, A. J.; Boye, D. M.; Brewer, K. S.; Gillespie, C. E.; Lu, Y.; Campbell, D. L. *J. Lumin.* **2006**, *121*, 14.
(211) Brecher, C.; Riseberg, L. A. *Phys. Rev. B* **1976**, *13*, 81.
(212) Brecher, C.; Riseberg, L. A. *Phys. Rev. B* **1980**, *21*, 2607.
(213) Weber, M. J.; Paisner, J. A.; Sussman, S. S.; Yen, W. M.; Riseberg, L. A.; Brecher, C. *J. Lumin.* **1976**, *12*, 729.
(214) Lochhead, M. J.; Bray, K. L. *Chem. Mater.* **1995**, *7*, 572.
(215) Costa, V. C.; Lochhead, M. J.; Bray, K. L. *Chem. Mater.* **1996**, *8*, 783.
(216) Nogami, M.; Abe, Y. *J. Non-Cryst. Solids* **1996**, *197*, 73.
(217) Silversmith, A. J.; Nguyen, N. T. T.; Sullivan, B. W.; Boye, D. M.; Ortiz, C.; Hoffman, K. R. *J. Lumin.* **2008**, *128*, 931.
(218) Armellini, C.; Ferrari, M.; Montagna, M.; Pucker, G.; Bernard, C.; Monteil, A. *J. Non-Cryst. Solids* **1999**, *245*, 115.
(219) Barbier, D.; Orignac, X.; Du, X. M.; Almeida, R. M. *J. Sol-Gel Sci. Technol.* **1997**, *8*, 1013.
(220) Nogami, M.; Nagakura, T.; Hayakawa, T.; Sakai, T. *Chem. Mater.* **1998**, *10*, 3991.
(221) Sahu, J.; Biswas, A.; Chakrabarti, S.; Acharya, H. N. *J. Non-Cryst. Solids* **1996**, *197*, 129.
(222) Matthews, L. R.; Knobbe, E. T. *Chem. Mater.* **1993**, *5*, 1697.
(223) Matthews, L. R.; Wang, X. J.; Knobbe, E. T. *J. Non-Cryst. Solids* **1994**, *178*, 44.
(224) Yan, B.; Zhang, H. J.; Wang, S. B.; Ni, J. Z. *Mater. Chem. Phys.* **1997**, *51*, 92.
(225) Strek, W.; Sokolnicki, J.; Legendziewicz, J.; Maruszewski, K.; Reisfeld, R.; Pavich, T. *Opt. Mater.* **1999**, *13*, 41.
(226) Sun, L.-N.; Zhang, H.-J.; Meng, Q.-G.; Liu, F.-Y.; Fu, L.-S.; Peng, C.-Y.; Yu, J.-B.; Zheng, G.-L.; Wang, S.-B. *J. Phys. Chem. B* **2005**, *109*, 6174.
(227) Tanner, P. A.; Yan, B.; Zhang, H. J. *J. Mater. Sci.* **2000**, *35*, 4325.
(228) Reisfeld, R.; Saraidarov, T.; Pietraszkiewicz, M.; Lis, S. *Chem. Phys. Lett.* **2001**, *349*, 266.
(229) Bredol, M.; Jüstel, T.; Gutzov, S. *Opt. Mater.* **2001**, *18*, 337.
(230) Wu, R. H.; Zhao, H. Z.; Su, X. D. *J. Non-Cryst. Solids* **2000**, *278*, 223.
(231) Magyar, A. P.; Silversmith, A. J.; Brewer, K. S.; Boye, D. M. *J. Lumin.* **2004**, *108*, 49.
(232) Sokolnicki, J.; Maruszewski, K.; Strek, W.; Legendziewicz, J. *J. Sol-Gel Sci. Technol.* **1998**, *13*, 611.
(233) An, B. L.; Ye, J. Q.; Gong, M. L.; Yin, X. H.; Yang, Y. S.; Zheng, X. G.; Deng, S. Z.; Xu, N. Z. *Mater. Res. Bull.* **2001**, *36*, 1335.
(234) Wang, X. G.; Wu, H. Y.; Zhao, S. Q.; Weng, S. F.; Wu, J. G. *Spectrosc. Spectral Anal.* **2006**, *26*, 805.
(235) Qian, G. D.; Wang, M. Q.; Wang, M.; Fan, X. P.; Hong, Z. L. *J. Mater. Sci. Lett.* **1997**, *16*, 322.
(236) Fan, X. P.; Wang, M. Q.; Wang, Z. Y. *J. Phys. Chem. Solids* **1999**, *60*, 53.
(237) Qian, G. D.; Wang, M. Q.; Wang, M. *J. Photochem. Photobiol. A* **1997**, *107*, 121.
(238) Wang, S. P.; Wang, R. F.; Zhang, J. J.; Liu, C. G. *J. Rare Earths* **2003**, *21*, 153.
(239) Liu, Y.; Yang, Y.; Qian, G. D.; Wang, Z. Y.; Wang, M. Q. *Mater. Sci. Eng., B* **2007**, *137*, 74.
(240) Fan, C. P.; Wang, Z. Y.; Wang, M. Q. *J. Sol-Gel Sci. Technol.* **2004**, *30*, 95.
(241) Sun, L. N.; Zhang, H. J.; Fu, L. S.; Liu, F. Y.; Meng, Q. G.; Peng, C. Y.; Yu, J. B. *Adv. Funct. Mater.* **2005**, *15*, 1041.
(242) Liu, Y.; Yang, Y.; Qian, G. D.; Wang, Z. Y.; Wang, M. Q. *Mater. Sci. Eng., B* **2007**, *137*, 74.
(243) Liu, Y.; Ye, C. F.; Qian, G. D.; Qiu, J. R.; Wang, M. Q. *J. Lumin.* **2006**, *118*, 158.
(244) Sun, L.-N.; Zhang, H.-J.; Meng, Q.-G.; Liu, F.-Y.; Fu, L.-S.; Peng, C.-Y.; Yu, J.-B.; Zheng, G.-L.; Wang, S.-B. *J. Phys. Chem. B.* **2005**, *109*, 6174.
(245) Hao, X. P.; Fan, X. P.; Wang, M. Q. *Thin Solid Films* **1999**, *353*, 223.
(246) Jin, T.; Tsutsumi, S.; Deguchi, Y.; Machida, K.; Adachi, G. *J. Alloys Compd.* **1997**, *252*, 59.
(247) Jin, T.; Tsutsumi, S.; Deguchi, Y.; Machida, K.; Adachi, G. Y. *J. Electrochem. Soc.* **1995**, *142*, L195.
(248) Jin, T.; Inoue, S.; Machida, K.; Adachi, G. Y. *J. Alloys Compd.* **1998**, *265*, 234.
(249) Li, H.; Inoue, S.; Machida, K.; Adachi, G. *J. Lumin.* **2000**, *87*−*89*, 1069.
(250) Yang, Y. T.; Zhang, S. Y. *Mater. Sci. Eng., B* **2005**, *116*, 82.
(251) Yan, B.; Zhang, H. J.; Ni, J. Z. *Mater. Sci. Eng., B* **1997**, *52*, 123.
(252) Lai, D. C.; Dunn, B.; Zink, J. I. *Inorg. Chem.* **1996**, *35*, 2152.
(253) Godlewska, P.; Macalik, L.; Hanuza, J. *J. Alloys Compd.* **2008**, *451*, 236.
(254) Schem, M.; Bredol, M. *Thin Solid Films* **2005**, *474*, 31.
(255) Bredol, M.; Schem, M. *Opt. Mater.* **2004**, *27*, 521.
(256) Schem, M.; Bredol, M. *Opt. Mater.* **2004**, *26*, 137.
(257) Sokolnicki, J.; Legendziewicz, J.; Riehl, J. P. *J. Phys. Chem. B* **2002**, *106*, 1508.
(258) Huskowska, E.; Gawryszewska, P.; Legendziewicz, J.; Maupin, C. L.; Riehl, J. P. *J. Alloys Compd.* **2000**, *303*, 325.
(259) Morita, M.; Rau, D.; Kai, T. *J. Lumin.* **2002**, *100*, 97.
(260) Gawryszewska, P. P.; Pietraszkiewicz, M.; Riehl, J. P.; Legendziewicz, J. *J. Alloys Compd.* **2000**, *300*, 283.
(261) Zaitoun, M. A.; Kim, T.; Jaradat, Q. M.; Monami, K.; Qaseer, H. A.; El-Qisairi, A. K.; Qudah, A.; Radwan, N. E. *J. Lumin.* **2008**, *128*, 227.
(262) Hnatejko, Z.; Klonkowski, A.; Lis, S.; Czarnobaj, K.; Pietraszkiewicz, M.; Elbanowski, M. *Mol. Cryst. Liq. Cryst.* **2000**, *354*, 795.
(263) Czarnobaj, K.; Elbanowski, M.; Hnatejko, Z.; Klonkowski, A. M.; Lis, S.; Pietraszkiewicz, M. *Spectrochim. Acta A* **1998**, *54*, 2183.
(264) Klonkowski, A. M.; Szalkowska, I.; Lis, S.; Pietraszkiewicz, M.; Hnatejko, Z. *J. Lumin.* **2005**, *115*, 122.
(265) Reisfeld, R.; Saraidarov, T.; Gaft, M.; Pietraszkiewicz, M.; Pietraszkiewicz, O.; Bianketti, S. *Opt. Mater.* **2003**, *24*, 1.
(266) Reisfeld, R.; Saraidarov, T.; Ziganski, E.; Gaft, M.; Lis, S.; Pietraszkiewicz, M. *J. Lumin.* **2003**, *102*, 243.
(267) Klonkowski, A. M.; Szalkowska, I.; Pietraszkiewicz, M.; Hnatejko, Z.; Lis, S.; Klukowska, A.; Posset, U. *J. Non-Cryst. Solids* **2005**, *351*, 2047.
(268) Reisfeld, R. *Struct. Bonding (Berlin)* **2004**, *106*, 209.
(269) Saraidarov, T.; Reisfeld, R.; Pietraszkiewicz, M. *Chem. Phys. Lett.* **2000**, *330*, 515.
(270) Yan, Z. Z.; Tang, Y.; Liu, W. S.; Tan, M. Y. *Solid State Sci.* **2008**, *10*, 332.
(271) Dargiewicz-Nowicka, J.; Makarska, M.; Villegas, M. A.; Legendziewicz, J.; Radzki, S. *J. Alloys Compd.* **2004**, *380*, 380.
(272) Li, X. Q.; Qiu, J. L.; Zhang, L.; Mu, J. *J. Dispersion Sci. Technol.* **2007**, *28*, 1081.
(273) Cervantes, M.; Clark, A.; Terpugov, V.; Medrano, F. *J. Opt. Technol.* **2002**, *69*, 61.
(274) Serra, O. A.; Nassar, E. J.; Zapparolli, G.; Rosa, I. L. V. *J. Alloys Compd.* **1994**, *207*, 454.
(275) Gutzov, S.; Bredol, M. *J. Mater. Sci.* **2006**, *41*, 1835.
(276) Malashkevich, G. E.; Semkova, G. I.; Stupak, A. P.; Sukhodolov, A. V. *Phys. Solid State* **2004**, *46*, 1425.
(277) Ronda, C. R.; Jüstel, T.; Nikol, H. *J. Alloys Compd.* **1988**, *275*, 669.
(278) Feldmann, C.; Jüstel, T.; Ronda, C. R.; Schmidt, P. J. *Adv. Funct. Mater.* **2003**, *13*, 511.
(279) Hong, J. H.; Zhang, Z. G.; Cong, C. J.; Zhang, K. L. *J. Non-Cryst. Solids* **2007**, *353*, 2431.
(280) Garcia, J.; Mondragon, M. A.; Maya, O.; Campero, A. *J. Alloys Compd.* **1998**, *275*, 273.
(281) Grobelna, B.; Lipowska, B.; Klonkowski, A. M. *J. Alloys Compd.* **2006**, *419*, 191.
(282) Grobelna, B.; Szabelski, M.; Kledzik, K.; Klonkowski, A. M. *J. Non-Cryst. Solids* **2007**, *353*, 2861.
(283) Bredol, M.; Gutzov, S. *Opt. Mater.* **2002**, *20*, 233.
(284) Bredol, M.; Gutzov, S.; Jüstel, T. *J. Non-Cryst. Solids* **2003**, *321*, 225.
(285) Ciuffi, K. J.; de Lima, O. J.; Sacco, H. C.; Nassar, E. J. *J. Non-Cryst. Solids* **2002**, *304*, 126.
(286) Kurokawa, Y.; Ishizaka, T.; Ikoma, T.; Tero-Kubota, S. *Chem. Phys. Lett.* **1998**, *287*, 737.
(287) Kobayashi, Y.; Ishizaka, T.; Kurokawa, Y. *J. Mater. Sci.* **2005**, *40*, 263.
(288) Ishizaka, T.; Kurokawa, Y.; Makino, T.; Segawa, Y. *Opt. Mater.* **2001**, *15*, 293.
(289) Ishizaka, T.; Kurokawa, Y. *J. Appl. Phys.* **2001**, *90*, 243.
(290) Lecomte, M.; Viana, B.; Sanchez, C. *J. Chim. Phys.* **1991**, *88*, 39.
(291) Kiisk, V.; Sildos, I.; Lange, S.; Reedo, V.; Tatte, T.; Kirm, M.; Aarik, J. *Appl. Surf. Sci.* **2005**, *247*, 412.
(292) Gaponenko, N. V.; Sergeev, O. V.; Stepanova, E. A.; Parkun, V. M.; Mudryi, A. V.; Gnaser, H.; Misiewicz, J.; Heiderhoff, R.; Balk, L. J.; Thompson, G. E. *J. Electrochem. Soc.* **2001**, *148*, H13.
(293) Palomino-Merino, R.; Conde-Gallardo, A.; Garcia-Rocha, M.; Hernandez-Calderon, I.; Castano, V.; Rodriguez, R. *Thin Solid Films* **2001**, *401*, 118.
(294) Conde-Gallardo, A.; Garcia-Rocha, M.; Palomino-Merino, R.; Velasquez-Quesada, M. P.; Hernandez-Calderon, I. *Appl. Surf. Sci.* **2003**, *212*, 583.
(295) Jia, C. W.; Xie, E. Q.; Peng, A. H.; Jiang, R.; Ye, F.; Lin, H. F.; Xu, T. *Thin Solid Films* **2006**, *496*, 555.

(296) Jia, C. W.; Xie, E. Q.; Zhao, J. G.; Sun, Z. W.; Peng, A. H. *J. Appl. Phys.* **2006**, *100*, 023529.
(297) Stathatos, E.; Lianos, P. *Chem. Phys. Lett.* **2006**, *417*, 406.
(298) Bucella, S.; Riello, P.; Scremin, B. F.; Calvelli, P.; Polloni, R.; Speghini, A.; Bettinelli, M.; Benedetti, A. *Opt. Mater.* **2004**, *27*, 249.
(299) Li, H. H.; Ueda, D.; Inoue, S.; Machida, K.; Adachi, G. *Bull. Chem. Soc. Jpn.* **2002**, *75*, 161.
(300) Reisfeld, R.; Zelner, M.; Patra, A. *J. Alloys Compd.* **2000**, *300*, 147.
(301) Pereyra-Perea, E.; Estrada-Yanez, M. R.; Garcia, M. *J. Phys. D* **1998**, *31*, L7.
(302) Koslova, N. I.; Viana, B.; Sanchez, C. *J. Mater. Chem.* **1993**, *3*, 111.
(303) Chacon-Roa, C.; Guzman-Mendoza, J.; Aguilar-Frutis, M.; Garcia-Hipolito, M.; Alvarez-Fragoso, O.; Falcony, C. *J. Phys. D* **2008**, *41*, 015104.
(304) Villanueva-Ibanez, M.; Le Luyer, C.; Marty, O.; Mugnier, J. *Opt. Mater.* **2003**, *24*, 51.
(305) Kojima, K.; Tsuchiya, K.; Wada, N. *J. Sol-Gel Sci. Technol.* **2000**, *19*, 511.
(306) Koslova, N. I.; Viana, B.; Sanchez, C. *J. Mater. Chem.* **1993**, *3*, 111.
(307) Zareba-Groz, I.; Pazik, R.; Tylus, W.; Mielcarek, W.; Hermanowicz, K.; Strek, W.; Maruszewski, K. *Opt. Mater.* **2007**, *29*, 1103.
(308) Ismail, A. A.; Abboudi, M.; Holloway, P.; El-Shall, H. *Mater. Res. Bull.* **2007**, *42*, 137.
(309) Hernandez, I.; Cordoba, G.; Padilla, J.; Mendez-Vivar, J.; Arroyo, R. *Mater. Lett.* **2008**, *62*, 1945.
(310) Martucci, A.; Brusatin, G.; Guglielmi, M.; Strohhofer, C.; Fick, J.; Pelli, S.; Righini, G. C. *J. Sol-Gel Sci. Technol.* **1998**, *13*, 535.
(311) Sigoli, F. A.; Messaddeq, Y.; Ribeiro, S. J. L. *J. Sol-Gel Sci. Technol.* **2008**, *45*, 179.
(312) Zhang, L.; Yao, Y.; Ye, X.; Wu, Q. *J. Phys. Chem. B.* **2007**, *111*, 335.
(313) Coutier, C.; Audier, M.; Fick, J.; Rimet, R.; Langlet, M. *Thin Solid Films* **2000**, *372*, 177.
(314) Strohhofer, C.; Fick, J.; Vasconcelos, H. C.; Almeida, R. M. *J. Non-Cryst. Solids* **1998**, *226*, 182.
(315) Zevin, M.; Reisfeld, R. *Chem. Mater.* **1997**, *8*, 37.
(316) Goncalves, R. R.; Carturan, G.; Montagna, M.; Ferrari, M.; Zampedri, L.; Pelli, S.; Righini, G. C.; Ribeiro, S. J. L.; Messaddeq, Y. *Opt. Mater.* **2004**, *25*, 131.
(317) Hirano, S.; Yogo, T.; Kikuta, K.; Sakamoto, W.; Koganei, H. *J. Am. Ceram. Soc.* **1996**, *79*, 3041.
(318) Nedelec, J. M.; Avignant, D.; Mahiou, R. *Chem. Mater.* **2002**, *14*, 651.
(319) Rao, R. P. *J. Electrochem. Soc.* **1996**, *143*, 189.
(320) Daniele, S.; Hubert-Pfalzgraf, L. G. *Mater. Lett.* **2004**, *58*, 1989.
(321) Mansuy, C.; Nedelec, J. M.; Dujardin, C.; Mahiou, R. *J. Sol-Gel Sci. Technol.* **2006**, *38*, 97.
(322) Mansuy, C.; Nedelec, J. M.; Dujardin, C.; Mahiou, R. *Opt. Mater.* **2007**, *29*, 697.
(323) Potdevin, A.; Chadeyron, G.; Boyer, D.; Mahiou, R. *J. Non-Cryst. Solids* **2006**, *352*, 2510.
(324) Hreniak, D.; Strek, W.; Mazur, P.; Pazik, R.; Zabkowska-Waclawek, M. *Opt. Mater.* **2004**, *26*, 117.
(325) Kim, H.; Kim, Y. T.; Chae, H. K. *J. Sol-Gel Sci. Technol.* **2005**, *33*, 75.
(326) Nedelec, J. M. *J. Nanomater.* **2007**, 36392 Spec. Issue 2.
(327) Mehta, S. M.; Parmar, M. U.; Prasad, M. *J. Indian Chem. Soc.* **1936**, *13*, 128.
(328) Brandel, V.; Iroulart, G.; Simoni, E.; Genet, M.; Audiere, J. P. *New J. Chem.* **1990**, *14*, 113.
(329) Brandel, V.; Iroulart, G.; Simoni, E.; Genet, M.; Audiere, J. P. *New J. Chem.* **1991**, *15*, 247.
(330) Genet, M.; Brandel, V.; Lahalle, M. P.; Simoni, E. *Proc. SPIE* **1990**, *1328*, 194.
(331) Genet, M.; Brandel, V.; Lahalle, M. P.; Simoni, E. *C. R. Acad. Sci. II* **1990**, *311*, 1321.
(332) Lou, L.; Mugnier, J.; Bahtat, M.; Simoni, E.; Brandel, V.; Genet, M. *J. Non-Cryst. Solids* **1994**, *171*, 115.
(333) Reisfeld, R.; Minti, H.; Patra, A.; Ganguli, D.; Gaft, M. *Spectrochim. Acta A* **1998**, *54*, 2143.
(334) Sekine, N.; Ueda, T.; Matsui, K. *Jpn. J. Appl. Phys.* **1998**, *37*, 78.
(335) Biswas, A.; Chakrabarti, S.; Acharya, H. N. *Mater. Sci. Eng., B* **1997**, *49*, 191.
(336) Biswas, A.; Sahu, J.; Acharya, H. N. *Mater. Sci. Eng., B* **1996**, *41*, 329.
(337) Armellini, C.; Del Longo, L.; Ferrari, M.; Montagna, M.; Pucker, G.; Sagoo, P. *J. Sol-Gel Sci. Technol.* **1998**, *13*, 599.
(338) Biswas, A.; Acharya, H. N. *Mater. Res. Bull.* **1997**, *32*, 1551.
(339) Sahu, J.; Biswas, A.; Acharya, H. N. *Mater. Lett.* **1995**, *24*, 31.
(340) Moreshead, W. V.; Nogues, J. L. R.; Krabill, R. H. *J. Non-Cryst. Solids* **1990**, *121*, 267.
(341) Fujiyama, T.; Hori, M.; Sasaki, M. *J. Non-Cryst. Solids* **1990**, *121*, 273.
(342) Fujiyama, T.; Yokoyama, T.; Hori, M.; Sasaki, M. *J. Non-Cryst. Solids* **1991**, *135*, 198.
(343) Orignac, X.; Barbier, D.; Du, X. M.; Almeida, R. M. *Appl. Phys. Lett.* **1996**, *69*, 895.
(344) Langlet, M.; Coutier, C.; Meffre, W.; Audier, M.; Fick, J.; Rimet, R.; Jacquier, B. *J. Lumin.* **2002**, *96*, 295.
(345) Costa, V. C.; Shen, Y. R.; Santos, A. M. M.; Bray, K. L. *J. Non-Cryst. Solids* **2002**, *304*, 238.
(346) Pivin, J. C.; Sendova-Vassileva, M.; Lagarde, G.; Singh, F.; Podhorodecki, A.; Misiewicz, J. J. *Optoelectron. Adv. Mater.* **2007**, *9*, 1872.
(347) Ishizaka, T.; Kurokawa, Y. *J. Lumin.* **2001**, *92*, 57.
(348) Reisfeld, R.; Panczer, G.; Patra, A.; Gaft, M. *Mater. Lett.* **1999**, *38*, 413.
(349) Gutzov, S.; Ahmed, G.; Petkova, N.; Fueglein, E.; Petkov, I. *J. Non-Cryst. Solids* **2008**, *354*, 3438.
(350) Stone, B. T.; Bray, K. L. *J. Non-Cryst. Solids* **1996**, *197*, 136.
(351) Lee, L. L.; Tsai, D. S. *J. Mater. Sci. Lett.* **1994**, *13*, 615.
(352) Chen, S. Y.; Ting, C. C.; Li, C. H. *J. Mater. Chem.* **2002**, *12*, 1118.
(353) Ryu, C. K.; Choi, H.; Kim, K. *Appl. Phys. Lett.* **1995**, *66*, 2496.
(354) Zhou, Y.; Lam, Y. L.; Wang, S. S.; Liu, H. L.; Kam, C. H.; Chan, Y. C. *Appl. Phys. Lett.* **1997**, *71*, 587.
(355) Biswas, A.; Acharya, H. N. *Indian J. Pure Appl. Phys.* **1997**, *35*, 532.
(356) Duverger, C.; Montagna, M.; Rolli, R.; Ronchin, S.; Zampedri, L.; Fossi, M.; Pelli, S.; Righini, G. C.; Monteil, A.; Armellini, C.; Ferrari, M. *J. Non-Cryst. Solids* **2001**, *280*, 261.
(357) Nga, P. T.; Barthou, C.; Benalloul, P.; Thang, P. N.; Chung, L. N.; Hoi, P. V.; Luat, P. V.; Cuong, P. T. *J. Non-Cryst. Solids* **2006**, *352*, 2385.
(358) Yeatman, E. M.; Ahmad, M. M.; McCarthy, O.; Vannucci, A.; Gastaldo, P.; Barbier, D.; Mongardien, D.; Moronvalle, C. *Opt. Commun.* **1999**, *164*, 19.
(359) Slooff, L. H.; de Dood, M. J. A.; van Blaaderen, A.; Polman, A. *J. Non-Cryst. Solids* **2001**, *296*, 158.
(360) Biswas, A.; Maciel, G. S.; Kapoor, R.; Friend, C. S.; Prasad, P. N. *Appl. Phys. Lett.* **2003**, *82*, 2389.
(361) Marques, A. C.; Almeida, R. M.; Chiasera, A.; Ferrari, M. *J. Non-Cryst. Solids* **2003**, *322*, 272.
(362) Ferrari, M.; Armellini, C.; Ronchin, S.; Rolli, R.; Duverger, C.; Monteil, A.; Balu, N.; Innocenzi, P. *J. Sol-Gel Sci. Technol.* **2000**, *19*, 569.
(363) Duverger, C.; Montagna, M.; Rolli, R.; Ronchin, S.; Zampedri, L.; Fossi, M.; Pelli, S.; Righini, G. C.; Monteil, A.; Armellini, C.; Ferrari, M. *J. Non-Cryst. Solids* **2001**, *280*, 261.
(364) Pedrazza, U.; Romano, V.; Luthy, W. *Opt. Mater.* **2007**, *29*, 905.
(365) Comby, S.; Gumy, F.; Bünzli, J.-C. G.; Saraidarov, T.; Reisfeld, R. *Chem. Phys. Lett.* **2006**, *432*, 128.
(366) Orignac, X.; Barbier, D.; Du, X. M.; Almeida, R. M.; McCarthy, O.; Yeatman, E. *Opt. Mater.* **1999**, *12*, 1.
(367) Buddhudu, S.; Morita, M.; Murakami, S.; Rau, D. *J. Lumin.* **1999**, *83*−*84*, 199.
(368) Morita, M.; Buddhudu, S.; Rau, D.; Murakami, S. *Struct. Bonding (Berlin)* **2004**, *107*, 115.
(369) Dai, S.; Xu, W.; Metcalf, D. H.; Toth, L. M. *Chem. Phys. Lett.* **1996**, *262*, 315.
(370) Wang, M. Q.; Qian, G. D.; Lu, S. Z. *Mater. Sci. Eng., B* **1998**, *55*, 119.
(371) Song, C. F.; Lu, M. K.; Yang, P.; Xu, D.; Yuan, D. R.; Zhou, G. J.; Gu, F. *Mater. Sci. Eng., B* **2003**, *97*, 64.
(372) Gan, F. X. *Optical and Spectroscopic Properties of Glass*; Springer Verlag: Berlin, 1992.
(373) Reisfeld, R.; Jørgensen, C. K. *Struct. Bond. (Berlin)* **1982**, *49*, 1.
(374) Strek, W.; Legendziewicz, J.; Lukowiak, E.; Maruszewski, K.; Sokolnicki, J.; Boiko, A. A.; Borzechowska, M. *Spectrochim. Acta A* **1998**, *54*, 2215.
(375) Patra, A.; Ganguli, D. *J. Mater. Sci. Lett.* **1993**, *12*, 116.
(376) De, G.; Licciulli, A.; Nacucchi, M. *J. Non-Cryst. Solids* **1996**, *201*, 153.
(377) Armellini, C.; Del Longo, L.; Ferrari, M.; Montagna, M.; Pucker, G.; Sagoo, P. *J. Sol-Gel Sci. Technol.* **1998**, *13*, 599.
(378) Patra, A.; Reisfeld, R.; Minti, H. *Mater. Lett.* **1998**, *37*, 325.
(379) Moretti, F.; Chiodini, N.; Fasoli, M.; Griguta, L.; Vedda, A. *J. Lumin.* **2007**, *126*, 759.
(380) Gutzov, S.; Berger, C.; Bredol, M.; Lengauer, C. L. *J. Mater. Sci. Lett.* **2002**, *21*, 1105.
(381) Moutonnet, D.; Chaplain, R.; Gauneau, M.; Pelous, Y.; Rehspringer, J. L. *Mater. Sci. Eng., B* **1991**, *9*, 455.

(382) Malashkevich, G. E.; Semkova, G. I.; Strek, W. *J. Alloys Compd.* **2002**, *341*, 244.
(383) Hazenkamp, M. F.; Blasse, G. *Chem. Mater.* **1990**, *2*, 105.
(384) Mack, H.; Resifeld, R.; Avnir, D. *Chem. Phys. Lett.* **1983**, *99*, 238.
(385) Gerasimova, V. I.; Zavorotnyi, Y. S.; Rybaltovskii, A. O.; Lemenovskii, D. A.; Timofeeva, V. A. *Quantum Electron.* **2006**, *36*, 791.
(386) Bredol, M.; Kynast, U.; Boldhaus, M.; Lau, C. *Ber. Bunsen-Ges.* **1998**, *102*, 1557.
(387) Dang, S.; Sun, L.-N.; Zhang, H.-J.; Guo, X.-M.; Li, Z.-F.; Feng, J.; Guo, H.-D.; Guo, Z.-Y. *J. Phys. Chem. C* **2008**, *112*, 13240.
(388) Auzel, F. *J. Lumin.* **1990**, *45*, 341.
(389) Auzel, F. *C. R. Sceances Acad. Sci., Ser. B* **1966**, *262*, 1016.
(390) Auzel, F. *Chem. Rev.* **2004**, *104*, 139.
(391) Martin, I. R.; Yanes, A. C.; Mendez-Ramos, J.; Torres, M. E.; Rodriguez, V. D. *J. Appl. Phys.* **2001**, *89*, 2520.
(392) Maciel, G. S.; Biswas, A.; Prasad, P. N. *Opt. Commun.* **2000**, *178*, 65.
(393) Maciel, G. S.; Biswas, A.; Kapoor, R.; Prasad, P. N. *Appl. Phys. Lett.* **2000**, *76*, 1978.
(394) Xu, W.; Dai, S.; Toth, L. M.; Delcul, G. D.; Peterson, J. R. *J. Phys. Chem.* **1995**, *99*, 4447.
(395) Otto, A. P.; Brewer, K. S.; Silversmith, A. J. *J. Non-Cryst. Solids* **2000**, *265*, 176.
(396) Sanchez, C.; Ribot, F. *New J. Chem.* **1994**, *18*, 1007.
(397) Sanchez, C.; Ribot, F.; Lebeau, B. *J. Mater. Chem.* **1999**, *9*, 35.
(398) Bekiari, V.; Lianos, P. *Adv. Mater.* **1998**, *10*, 1455.
(399) Bekiari, V.; Pistolis, G.; Lianos, P. *J. Non-Cryst. Solids* **1998**, *226*, 200.
(400) Bekiari, V.; Pistolis, G.; Lianos, P. *Chem. Mater.* **1999**, *11*, 3189.
(401) Molina, C.; Dahmouche, K.; Santilli, C. V.; Craievich, A. F.; Ribeiro, S. J. L. *Chem. Mater.* **2001**, *13*, 2818.
(402) Bekiari, V.; Lianos, P. *J. Lumin.* **2003**, *101*, 135.
(403) Chuai, X. H.; Zhang, H. J.; Li, F. S.; Wang, S. B.; Zhou, G. Z. *Mater. Lett.* **2000**, *46*, 244.
(404) Driesen, K.; Fourier, S.; Gorller-Walrand, C.; Binnemans, K. *Phys. Chem. Chem. Phys.* **2003**, *5*, 198.
(405) Driesen, K.; Van Deun, R.; Gorller-Walrand, C.; Binnemans, K. *Chem. Mater.* **2004**, *16*, 1531.
(406) Welton, T. *Chem. Rev.* **1999**, *99*, 2071.
(407) Greaves, T. L.; Drummond, C. J. *Chem. Rev.* **2008**, *108*, 206.
(408) Dupont, J.; de Souza, R. F.; Suarez, P. A. Z. *Chem. Rev.* **2002**, *102*, 3667.
(409) Parvulescu, V. I.; Hardacre, C. *Chem. Rev.* **2007**, *107*, 2615.
(410) Driesen, K.; Nockemann, P.; Binnemans, K. *Chem. Phys. Lett.* **2004**, *395*, 306.
(411) Arenz, S.; Babai, A.; Binnemans, K.; Driesen, K.; Giernoth, R.; Mudring, A. V.; Nockemann, P. *Chem. Phys. Lett.* **2005**, *402*, 75.
(412) Nockemann, P.; Beurer, E.; Driesen, K.; Van Deun, R.; Van Hecke, K.; Van Meervelt, L.; Binnemans, K. *Chem. Commun.* **2005**, 4354.
(413) Binnemans, K. *Chem. Rev.* **2007**, *107*, 2592.
(414) Nockemann, P.; Binnemans, K.; Driesen, K. *Chem. Phys. Lett.* **2005**, *415*, 131.
(415) Earle, M. J.; Gordon, C. M.; Plechkova, N. V.; Seddon, K. R.; Welton, T. *Anal. Chem.* **2007**, *79*, 758.
(416) Lunstroot, K.; Driesen, K.; Nockemann, P.; Gorller-Walrand, C.; Binnemans, K.; Bellayer, S.; Le Bideau, J.; Vioux, A. *Chem. Mater.* **2006**, *18*, 5711.
(417) Néouze, M. A.; Le Bideau, J.; Leroux, F.; Vioux, A. *Chem. Commun.* **2005**, 1082.
(418) Vioux, A.; Le Bideau, J.; Néouze, M. A.; Leroux, F. Ionic conducting gels, their preparation process, and their uses, Patent 2005/007746, 19 pp., World Patent WO2857004, 2005.
(419) Néouze, M. A.; Le Bideau, J.; Vioux, A. *Prog. Solid State Chem.* **2005**, *33*, 217.
(420) Néouze, M. A.; Le Bideau, J.; Gaveau, P.; Bellayer, S.; Vioux, A. *Chem. Mater.* **2006**, *18*, 3931.
(421) Le Bideau, J.; Gaveau, P.; Bellayer, S.; Néouze, M.-A.; Vioux, A. *Phys. Chem. Chem. Phys.* **2007**, *9*, 5419.
(422) Lunstroot, K.; Driesen, K.; Nockemann, P.; Van Hecke, K.; Van Meervelt, L.; Görller-Walrand, C.; Binnemans, K.; Bellayer, S.; Viau, L.; Le Bideau, J.; Vioux, A. *Dalton Trans.* **2009**, 298.
(423) Oton, J. M.; Serrano, O.; Serna, C. J.; Levy, D. *Liq. Cryst.* **1991**, *10*, 733.
(424) Levy, D.; Pena, J. M. S.; Serna, C. J.; Oton, J. M. *J. Non-Cryst. Solids* **1992**, *147*, 646.
(425) Levy, D.; Esquivias, L. *Adv. Mater.* **1995**, *7*, 120.
(426) Driesen, K.; Binnemans, K. *Liq. Cryst.* **2004**, *31*, 601.
(427) Escribano, P.; Julian-Lopez, B.; Planelles-Arago, J.; Cordoncillo, E.; Viana, B.; Sanchez, C. *J. Mater. Chem.* **2008**, *18*, 23.
(428) Sanchez, C.; Lebeau, B. *MRS Bull.* **2001**, *26*, 377.
(429) Schmidt, H. *J. Non-Cryst. Solids* **1985**, *73*, 681.
(430) Schmidt, H.; Wolter, H. *J. Non-Cryst. Solids* **1990**, *121*, 428.
(431) Schmidt, H. *J. Non-Cryst. Solids* **1989**, *112*, 419.
(432) Xiao, J.; Liu, H. X.; Ouyang, S. X. *Acta Chim. Sin.* **2007**, *65*, 2063.
(433) Klonkowski, A. M.; Szalkowska, I.; Pietraszkiewicz, M.; Hnatejko, Z.; Lis, S.; Klukowska, A.; Posset, U. *J. Non-Cryst. Solids* **2005**, *351*, 2047.
(434) Moreno, E. M.; Levy, D. *Chem. Mater.* **2000**, *12*, 2334.
(435) Rottman, C.; Grader, G.; Avnir, D. *Chem. Mater.* **2001**, *13*, 3631.
(436) Iwasaki, M.; Kuraki, J.; Ito, S. *J. Sol-Gel Sci. Technol.* **1998**, *13*, 587.
(437) Jin, T.; Tsutsumi, S.; Deguchi, Y.; Machida, K.; Adachi, G. *J. Electrochem. Soc.* **1996**, *143*, 3333.
(438) Jin, T.; Inoue, S.; Tsutsumi, S.; Machida, K.; Adachi, G. Y. *J. Non-Cryst. Solids* **1998**, *223*, 123.
(439) Jin, T.; Inoue, S.; Machida, K.; Adachi, G. Y. *J. Alloys Compd.* **1998**, *265*, 234.
(440) Li, H. H.; Inoue, S.; Ueda, D.; Machida, K.; Adachi, G. *Bull. Chem. Soc. Jpn.* **2000**, *73*, 251.
(441) Machida, K.; Li, H.; Ueda, D.; Inoue, S.; Adachi, G. *J. Lumin.* **2000**, *87*–*89*, 1257.
(442) Hao, X. P.; Fan, X. P.; Wang, M. Q. *Thin Solid Films* **1999**, *353*, 223.
(443) Xiao, J.; Liu, H. X.; Ouyang, S. X. *Acta Chim. Sin.* **2006**, *64*, 943.
(444) Guo, J. F.; Fu, L. S.; Li, H. R.; Zheng, Y. X.; Meng, Q. G.; Wang, S. B.; Liu, F. Y.; Wang, J.; Zhang, H. J. *Mater. Lett.* **2003**, *57*, 3899.
(445) Fan, X. P.; Li, W.; Wang, F.; Wang, M. Q. *Mater. Sci. Eng., B* **2003**, *100*, 147.
(446) de Souza, J. M.; de Sa, G. F.; de Azevedo, W. M.; Alves, S.; de Farias, R. F. *Opt. Mater.* **2005**, *27*, 1187.
(447) Qian, G. D.; Wang, M. Q.; Yang, Z. *J. Non-Cryst. Solids* **2001**, *286*, 235.
(448) Qian, G. D.; Wang, M. Q.; Yang, Z. *J. Phys. Chem. Solids* **2002**, *63*, 1829.
(449) Qian, G. D.; Yang, Z.; Wang, M. Q. *J. Non-Cryst. Solids* **2002**, *96*, 211.
(450) Wang, H. S.; Qian, G. D.; Zhang, J. H.; Luo, Y. S.; Wang, Z. Y.; Wang, M. Q. *J. Alloys Compd.* **2005**, *479*, 216.
(451) Qian, G. D.; Wang, M. Q. *J. Am. Ceram. Soc.* **2000**, *83*, 703.
(452) Qian, G. D.; Wang, M. Q. *Mater. Res. Bull.* **2001**, *36*, 2289.
(453) Guo, J. F.; Fu, L. S.; Li, H. R.; Zheng, Y. X.; Meng, Q. G.; Wang, S. B.; Liu, F. Y.; Wang, J.; Zhang, H. J. *Mater. Lett.* **2003**, *57*, 3899.
(454) de Farias, R. F.; Alves, S.; Belian, M. F.; de Sa, G. F. *Opt. Mater.* **2002**, *18*, 431.
(455) Fan, X. P.; Wang, Z. Y.; Wang, M. Q. *J. Lumin.* **2002**, *99*, 247.
(456) Klonkowski, A. M.; Grobelna, B.; But, S.; Lis, S. *J. Non-Cryst. Solids* **2006**, *352*, 2213.
(457) Klonkowski, A. M.; Lis, S.; Hnatejko, Z.; Czarnobaj, K.; Pietraszkiewicz, M.; Elbanowski, M. *J. Alloys Compd.* **2000**, *300*, 55.
(458) Julian, B.; Corberan, R.; Cordoncillo, E.; Escribano, P.; Viana, B.; Sanchez, C. *J. Mater. Chem.* **2004**, *14*, 3337.
(459) Yuh, S. K.; Bescher, E. P.; Babonneau, F.; Mackenzie, J. D. *Mater. Res. Soc. Symp. Proc.* **1994**, *346*, 803.
(460) Yuh, S. K.; Bescher, E. P.; Mackenzie, J. D. *Proc. SPIE* **1994**, *2288*, 248.
(461) Park, O. H.; Pinot, J.; Bae, B. S. *J. Sol-Gel Sci. Technol.* **2004**, *32*, 273.
(462) Charbuillot, Y.; Ravaine, D.; Armand, M.; Poinsignon, C. *J. Non-Cryst. Solids* **1988**, *103*, 325.
(463) Rousseau, F.; Poinsignon, C.; Garcia, J.; Popall, M. *Chem. Mater.* **1995**, *7*, 828.
(464) Stathatos, E.; Lianos, P. *Appl. Phys. Lett.* **2007**, *90*, 061110.
(465) Bekiari, V.; Lianos, P. *Chem. Mater.* **1998**, *10*, 3777.
(466) Bekiari, V.; Lianos, P. *J. Nanosci. Nanotechnol.* **2006**, *6*, 372.
(467) Carlos, L. D.; Sa Ferreira, R. A.; Goncalves, M. C.; de Zea Bermudez, V. *J. Alloys Compd.* **2004**, *374*, 50.
(468) Dahmouche, K.; Santilli, C. V.; Pulcinelli, S. H.; Sa Ferreira, R. A.; Carlos, L. D.; Bermudez, V. D.; Craievich, A. F. *J. Sol-Gel Sci. Technol.* **2006**, *37*, 99.
(469) Yan, B.; Sui, Y. L. *Opt. Mater.* **2006**, *28*, 1216.
(470) Zhao, L. M.; Yan, B. *J. Lumin.* **2006**, *118*, 317.
(471) Yan, B.; Zhao, L. M. *Mater. Lett.* **2005**, *59*, 795.
(472) Wang, F. F.; Yan, B. *J. Fluoresc.* **2007**, *17*, 418.
(473) Wang, Q. M.; Yan, B. *J. Mater. Res.* **2005**, *20*, 592.
(474) Yan, B.; Ma, D. J.; Wang, Q. M. *J. Rare Earths* **2005**, *23* (Suppl. S), 13.
(475) Wang, Q. M.; Yan, B. *Cryst. Growth Des.* **2005**, *5*, 497.
(476) Wang, Q. M.; Yan, B. *J. Photochem. Photobiol. A* **2005**, *175*, 159.
(477) Wang, Q. M.; Yan, B.; Zhang, X. H. *J. Non-Cryst. Solids* **2006**, *352*, 4136.
(478) Wang, F. F.; Yan, B. *J. Photochem. Photobiol. A* **2008**, *194*, 238.
(479) Sui, Y. L.; Yan, B. *Inorg. Mater.* **2006**, *42*, 144.
(480) Sui, Y. L.; Yan, B. *Appl. Surf. Sci.* **2006**, *252*, 4306.
(481) Zhao, L. M.; Yan, B. *Colloids Surf. A* **2006**, *275*, 64.

(482) Zhao, L. M.; Yan, B. *Mater. Res. Bull.* **2006**, *41*, 1.
(483) Sui, S. L.; Yan, B.; Wang, Q. M. *Mol. Cryst. Liq. Cryst.* **2006**, *457*, 193.
(484) Yan, B.; Xu, S.; Lu, H. F. *J. Fluoresc.* **2007**, *17*, 155.
(485) Lu, H. F.; Yan, B. *J. Non-Cryst. Solids* **2006**, *352*, 5331.
(486) Liu, F. Y.; Fu, L. S.; Wang, J.; Liu, Z.; Li, H. R.; Zhang, H. J. *Thin Solid Films* **2002**, *419*, 178.
(487) Wang, Q. M.; Yan, B. *Mater. Lett.* **2006**, *60*, 3420.
(488) Yan, B.; Yao, R. F.; Wang, Q. M. *Mater. Lett.* **2006**, *60*, 3063.
(489) Wang, Q. M.; Yan, B. *J. Organomet. Chem.* **2006**, *691*, 3567.
(490) Wang, Q. M.; Yan, B. *J. Organomet. Chem.* **2006**, *691*, 545.
(491) Yan, B.; Zhou, B.; Wang, Q. M. *J. Lumin.* **2007**, *126*, 556.
(492) Cordoncillo, E.; Viana, B.; Escribano, P.; Sanchez, C. *J. Mater. Chem.* **1998**, *8*, 507.
(493) Cordoncillo, E.; Guaita, F. J.; Escribano, P.; Philippe, C.; Viana, B.; Sanchez, C. *Opt. Mater.* **2001**, *18*, 309.
(494) Iwasaki, M.; Sato, N.; Kuraki, J.; Ito, S. *J. Sol-Gel Sci. Technol.* **2000**, *19*, 357.
(495) Sorek, Y.; Zevin, M.; Reisfeld, R.; Hurvits, T.; Ruschin, S. *Chem. Mater.* **1997**, *9*, 670.
(496) Cybinska, J.; Legendziewicz, J.; Trush, V.; Reisfeld, R.; Saraidarov, T. *J. Alloys Compd.* **2008**, *451*, 94.
(497) Reisfeld, R.; Saraidarov, T.; Gaft, M.; Pietraskiewicz, M. *Opt. Mater.* **2007**, *29*, 521.
(498) Trejo-Valdez, M.; Jenouvrier, P.; Langlet, M. *J. Non-Cryst. Solids.* **2004**, *345*, 628.
(499) Nassar, E. J.; Goncalves, R. R.; Ferrari, M.; Messaddeq, Y.; Ribeiro, S. J. L. *J. Alloys Compd.* **2002**, *334*, 221.
(500) de Farias, R. F.; Alves, S.; Belian, M. F.; de Sa, G. F. *J. Colloid Interface Sci.* **2001**, *243*, 523.
(501) Xue, W. X.; Hu, X. *Chem. Phys. Lett.* **2004**, *397*, 227.
(502) Dias, F. A.; Ribeiro, S. J. L.; Goncalves, R. R.; Messaddeq, Y.; Carlos, L. D.; de Zea Bermudez, V.; Rocha, J. *J. Alloys Compd.* **2004**, *374*, 74.
(503) Julian, B.; Gervais, C.; Cordoncillo, E.; Escribano, P.; Babonneau, F.; Sanchez, C. *Chem. Mater.* **2003**, *15*, 3026.
(504) Julian, B.; Gervais, C.; Rager, M. N.; Maquet, J.; Cordoncillo, E.; Escribano, P.; Babonneau, F.; Sanchez, C. *Chem. Mater.* **2004**, *16*, 521.
(505) Julian, B.; Beltran, H.; Cordoncillo, E.; Escribano, P.; Viana, B.; Sanchez, C. *J. Sol-Gel Sci. Technol.* **2003**, *26*, 977.
(506) Koslova, N. I.; Viana, B.; Sanchez, C. *J. Mater. Chem.* **1993**, *3*, 111.
(507) Cordoncillo, E.; Escribano, P.; Guaita, F. J.; Philippe, C.; Viana, B.; Sanchez, C. *J. Sol-Gel Sci. Technol.* **2002**, *24*, 155.
(508) Viana, B.; Koslova, N.; Aschehough, P.; Sanchez, C. *J. Mater. Chem.* **1995**, *5*, 719.
(509) Viana, B.; Cordoncillo, E.; Philippe, C.; Sanchez, C.; Guaita, F. J.; Escribano, P. *Proc. SPIE* **2000**, *3943*, 328.
(510) Thompson, L. C.; Marvin, J. R.; Bettenberg, N. C. *J. Alloys Compd.* **1992**, *180*, 229.
(511) Shea, K. J.; Loy, D. A.; Webster, O. *J. Am. Chem. Soc.* **1992**, *114*, 6700.
(512) Shea, K. J.; Loy, D. A. *Chem. Mater.* **2001**, *13*, 3306.
(513) Shea, K. J.; Loy, D. A. *MRS Bull.* **2001**, *26*, 368.
(514) Loy, D. A.; Shea, K. J. *Chem. Rev.* **1995**, *95*, 1431.
(515) Fujita, S.; Inagaki, S. *Chem. Mater.* **2008**, *20*, 891.
(516) de Zea Bermudez, V.; Carlos, L. D.; Alcacer, L. *Chem. Mater.* **1999**, *11*, 569.
(517) de Zea Bermudez, V.; Alcacer, L.; Acosta, J. L.; Morales, E. *Solid State Ionics* **1999**, *116*, 197.
(518) Carlos, L. D.; de Zea Bermudez, V.; Sa Ferreira, R. A.; Marques, L.; Assuncao, M. *Chem. Mater.* **1999**, *11*, 581.
(519) Carlos, L. D.; Sa Ferreira, R. A.; de Zea Bermudez, V.; Ribeiro, S. J. L. *Adv. Funct. Mater.* **2001**, *11*, 111.
(520) Bekiari, V.; Lianos, P.; Stangar, U. L.; Orel, B.; Judeinstein, P. *Chem. Mater.* **2000**, *12*, 3095.
(521) de Zea Bermudez, V.; Carlos, L. D.; Duarte, M. C.; Silva, M. M.; Silva, C. J. R.; Smith, M. J.; Assuncao, M.; Alcacer, L. *J. Alloys Compd.* **1998**, *275*, 21.
(522) Dahmouche, K.; Carlos, L. D.; de Zea Bermudez, V.; Sa Ferreira, R. A.; Santilli, C. V.; Craievich, A. F. *J. Mater. Chem.* **2001**, *11*, 3249.
(523) Silva, M. M.; de Zea Bermudez, V.; Carlos, L. D.; Passos de Almeida, A. P.; Smith, M. J. *J. Mater. Chem.* **1999**, *9*, 1735.
(524) Dahmouche, K.; Goncalves, M. C.; Santilli, C. V.; de Zea Bermudez, V.; Carlos, L. D.; Craievich, A. F. *Nucl. Instrum. Methods Phys. Res., Sect. B* **2003**, *199*, 117.
(525) Carlos, L. D.; Sa Ferreira, R. A.; de Zea Bermudez, V.; Molina, C.; Bueno, L. A.; Ribeiro, S. J. L. *Phys. Rev. B* **1999**, *60*, 10042.
(526) Goncalves, M. C.; de Zea Bermudez, V.; Sa Ferreira, R. A.; Carlos, L. D.; Ostrovskii, D.; Rocha, J. *Chem. Mater.* **2004**, *16*, 2530.
(527) Carlos, L. D.; Massaddeq, Y.; Brito, H. F.; Sa Ferreira, R. A.; de Zea Bermudez, V.; Ribeiro, S. J. L. *Adv. Mater.* **2000**, *12*, 594.
(528) Nobre, S. S.; Brites, C. D. S.; Sa Ferreira, R. A.; de Zea Bermudez, V.; Carcel, C.; Moreau, J. J. R.; Rocha, J.; Man, M. W. C.; Carlos, L. D. *J. Mater. Chem.* **2008**, *18*, 4172.
(529) Carlos, L. D.; Sa Ferreira, R. A. S.; Orion, I.; de Zea Bermudez, V.; Rocha, J. *J. Lumin.* **2000**, *87*−*89*, 702.
(530) Sa Ferreira, R. A.; Carlos, L. D.; Goncalves, R. R.; Ribeiro, S. J. L.; de Zea Bermudez, V. *Chem. Mater.* **2001**, *13*, 2991.
(531) de Zea Bermudez, V.; Sa Ferreira, R. A.; Carlos, L. D.; Molina, C.; Dahmouche, K.; Ribeiro, S. J. L. *J. Phys. Chem. B* **2001**, *105*, 3378.
(532) Pecoraro, E.; Sa Ferreira, R. A.; Molina, C.; Ribeiro, S. J. L.; Messaddeq, Y.; Carlos, L. D. *J. Alloys Compd.* **2008**, *451*, 136.
(533) Carlos, L. D.; Sa Ferreira, R. A.; de Zea Bermudez, V. *Electrochim. Acta* **2000**, *45*, 1555.
(534) Goncalves, M. C.; Silva, N. J. O.; de Zea Bermudez, V.; Sa Ferreira, R. A.; Carlos, L. D.; Dahmouche, K.; Santilli, C. V.; Ostrovskii, D.; Correia Vilela, I. C.; Craievich, A. F. *J. Phys. Chem. B* **2005**, *109*, 20093.
(535) Bekiari, V.; Lianos, P.; Judeinstein, P. *Chem. Phys. Lett.* **1999**, *307*, 310.
(536) Carlos, L. D.; Sa Ferreira, R. A.; Rainho, J. P.; de Zea Bermudez, V. *Adv. Funct. Mater.* **2002**, *12*, 819.
(537) Molina, C.; Dahmouche, K.; Messaddeq, Y.; Ribeiro, S. J. L.; Silva, M. A. P.; de Zea Bermudez, V.; Carlos, L. D. *J. Lumin.* **2003**, *104*, 93.
(538) Fernandes, M.; Goncalves, M. C.; de Zea Bermudez, V.; Sa Ferreira, R. A.; Carlos, L. D.; Charas, A.; Morgado, J. *J. Alloys Compd.* **2008**, *451*, 201.
(539) Fu, L. S.; Sa Ferreira, R. A.; Silva, N. J. O.; Fernandes, A. J.; Ribeiro-Claro, P.; Goncalves, I. S.; de Zea Bermudez, V.; Carlos, L. D. *J. Mater. Chem.* **2005**, *15*, 3117.
(540) Moleski, R.; Stathatos, E.; Bekiari, V.; Lianos, P. *Thin Solid Films* **2002**, *416*, 279.
(541) Lima, P. P.; Nobre, S. S.; Freire, R. O.; Junior, S. A.; Sa Ferreira, R. A.; Pischel, U.; Malta, O. L.; Carlos, L. D. *J. Phys. Chem. C* **2007**, *111*, 17627.
(542) Lima, P. P.; Sa Ferreira, R. A.; Freire, R. O.; Paz, F. A. A.; Fu, L. S.; Alves, S.; Carlos, L. D.; Malta, O. L. *ChemPhysChem* **2006**, *7*, 735.
(543) de Zea Bermudez, V.; Ostrovskii, D.; Goncalves, M. C.; Lavoryk, S.; Carlos, L. D.; Sa Ferreira, R. A. *J. Phys. Chem. B* **2005**, *109*, 7110.
(544) de Zea Bermudez, V.; Ostrovskii, D.; Goncalves, M. C.; Carlos, L. D.; Sa Ferreira, R. A.; Reis, L.; Jacobsson, P. *Phys. Chem. Chem. Phys.* **2004**, *6*, 638.
(545) de Zea Bermudez, V.; Ostrovskii, D.; Lavoryk, S.; Goncalves, M. C.; Carlos, L. D. *Phys. Chem. Chem. Phys.* **2004**, *6*, 649.
(546) Goncalves, M. C.; de Zea Bermudez, V.; Ostrovskii, D.; Carlos, L. D. *J. Mol. Struct.* **2002**, *611*, 83.
(547) Guo, X. M.; Fu, L. S.; Zhang, H. J.; Gao, S. Y.; Ju, J. B. *J. Lumin.* **2007**, *122*−*123*, 892.
(548) Fernandes, M.; de Zea Bermudez, V.; Sa Ferreira, R. A.; Carlos, L. D.; Martins, N. V. *J. Lumin.* **2008**, *128*, 205.
(549) Fernandes, M.; de Zea Bermudez, V.; Sa Ferreira, R. A.; Carlos, L. D.; Charas, A.; Morgado, J.; Silva, M. M.; Smith, M. J. *Chem. Mater.* **2007**, *19*, 3892.
(550) Yan, B.; Wang, F. F. *J. Organomet. Chem.* **2007**, *692*, 2395.
(551) Han, Y. H.; Lin, J. *J. Solid State Chem.* **2003**, *171*, 396.
(552) Yan, B.; Wang, Q. M.; Ma, D. J. *Inorg. Chem.* **2009**, *48*, 36.
(553) Nunes, S. C.; de Zea Bermudez, V.; Cybinska, J.; Sa Ferreira, R. A.; Legendziewicz, J.; Carlos, L. D.; Silva, M. M.; Smith, M. J.; Ostrovskii, D.; Rocha, J. *J. Mater. Chem.* **2005**, *15*, 3876.
(554) Nunes, S. C.; de Zea Bermudez, V.; Cybinska, J.; Sa Ferreira, R. A.; Carlos, L. D.; Legendziewicz, J.; Silva, M. M.; Smith, M. J.; Ostrovskii, D. *J. Alloys Compd.* **2008**, *451*, 510.
(555) Han, Y. H.; Taylor, A.; Mantle, M. D.; Knowles, K. M. *J. Non-Cryst. Solids* **2007**, *353*, 313.
(556) Li, H. R; Zhang, H. J.; Lin, J.; Wang, S. B.; Yang, K. Y. *J. Non-Cryst. Solids* **2000**, *278*, 218.
(557) Li, Y. H.; Zhang, H. J.; Wang, S. B.; Meng, Q. G.; Li, H. R.; Chuai, X. H. *Thin Solid Films* **2001**, *385*, 205.
(558) Yan, B. *Mater. Lett.* **2003**, *57*, 2535.
(559) Yan, B.; You, J. Y. *J. Rare Earths* **2002**, *20*, 404.
(560) Fan, X. P.; Wang, M. Q.; Wang, Z. Y. J. *J. Phys. Chem. Solids* **1999**, *60*, 53.
(561) Qian, G. D.; Wang, M. Q. *Mater. Res. Bull.* **2001**, *36*, 2289.
(562) Krug, H.; Schmidt, H. *New J. Chem.* **1994**, *18*, 1125.
(563) Xu, J.; Aubonnet, S.; Barry, H. F.; MacCraith, B. D. *Mater. Lett.* **2003**, *57*, 4276.
(564) Bian, L. J.; Qian, X. F.; Yin, J.; Zhu, Z. K.; Lu, Q. H. *Mater. Sci. Eng., B* **2003**, *100*, 53.

(565) Fu, L. S.; Zhang, H. J.; Wang, S. B.; Meng, Q. G.; Yang, K. Y.; Ni, J. Z. *Chem. Res. Chin. Univ.* **1999**, *15*, 100.
(566) Franville, A. C.; Zambon, D.; Mahiou, R.; Chou, S.; Troin, Y.; Cousseins, J. C. *J. Alloys Compd.* **1998**, *275*, 831.
(567) Franville, A. C.; Zambon, D.; Mahiou, R.; Troin, Y. *Chem. Mater.* **2000**, *12*, 428.
(568) Franville, A. C.; Mahiou, R.; Zambon, D.; Cousseins, J. C. *Solid State Sci.* **2001**, *3*, 211.
(569) Zhao, L. M.; Yan, B.; Wang, Q. M. *Monatsh. Chem.* **2005**, *136*, 1545.
(570) Liu, F. Y.; Fu, L. S.; Wang, J.; Meng, Q. G.; Li, H. R.; Guo, J. F.; Zhang, H. J. *New J. Chem.* **2003**, *27*, 233.
(571) Lin, N. N.; Li, H. R.; Wang, Y. G.; Feng, Y.; Qin, D. S.; Gan, Q. Y.; Chen, S. D. *Eur. J. Inorg. Chem.* **2008**, 4781.
(572) Li, H. R.; Yu, J. B.; Liu, F. Y.; Zhang, H. J.; Fu, L. S.; Meng, Q. G.; Peng, C. Y.; Lin, J. *New J. Chem.* **2004**, *28*, 1137.
(573) Cousinie, S.; Gressier, M.; Reber, C.; Dexpert-Ghys, J.; Menu, M. J. *Langmuir* **2008**, *24*, 6208.
(574) Tong, B. H.; Wang, S. J.; Hao, H.; Ling, F. R.; Meng, Y. Z.; Wang, B. *J. Photochem. Photobiol. A* **2007**, *191*, 74.
(575) Tong, B. H.; Wang, S. J.; Meng, Y. Z.; Wang, B. *Photochem. Photobiol. Sci.* **2007**, *6*, 519.
(576) Kloster, G. M.; Taylor, C. M.; Watton, S. P. *Inorg. Chem.* **1999**, *38*, 3954.
(577) Kloster, G. M.; Watton, S. P. *Inorg. Chim. Acta* **2000**, *297*, 156.
(578) Li, H. R.; Lin, J.; Zhang, H. J.; Fu, L. S.; Meng, Q. G.; Wang, S. B. *Chem. Mater.* **2002**, *14*, 3651.
(579) Li, H. R.; Fu, L. S.; Liu, F. Y.; Wang, S. B.; Zhang, H. J. *New J. Chem.* **2002**, *26*, 674.
(580) Li, H. R.; Fu, L. S.; Lin, J.; Zhang, H. J. *Thin Solid Films* **2002**, *416*, 197.
(581) Binnemans, K.; Lenaerts, P.; Driesen, K.; Gorller-Walrand, C. *J. Mater. Chem.* **2004**, *14*, 191.
(582) Lenaerts, P.; Ryckebosch, E.; Driesen, K.; Van Deun, R.; Nockemann, P.; Gorller-Walrand, C.; Binnemans, K. *J. Lumin.* **2005**, *114*, 77.
(583) Sun, L. N.; Zhang, H. H.; Yu, H. B.; Meng, Q. G.; Liu, F. Y.; Peng, C. Y. *J. Photochem. Photobiol. A* **2008**, *193*, 153.
(584) Lenaerts, P.; Storms, A.; Mullens, J.; D'Haen, J.; Gorller-Walrand, C.; Binnemans, K.; Driesen, K. *Chem. Mater.* **2005**, *17*, 5194.
(585) Lenaerts, P.; Gorller-Walrand, C.; Binnemans, K. *J. Lumin.* **2006**, *117*, 163.
(586) Luo, Y.; Han, Y. H.; Lin, J. *J. Lumin.* **2007**, *122*−*123*, 83.
(587) Liu, J. L.; Yan, B. *J. Phys. Chem. B* **2008**, *112*, 10898.
(588) Wang, Q. M.; Yan, B. *Inorg. Chem. Commun.* **2004**, *7*, 747.
(589) Wang, Q. M.; Yan, B. *J. Mater. Chem.* **2004**, *14*, 2450.
(590) Wang, Q. M.; Yan, B. *Mater. Lett.* **2006**, *60*, 3420.
(591) Yan, B.; Sui, Y. L. *Mater. Lett.* **2007**, *61*, 3715.
(592) Sui, Y. L.; Yan, B. *J. Photochem. Photobiol. A* **2006**, *182*, 1.
(593) Liu, J. L.; Yan, B. *J. Phys. Chem. C* **2008**, *112*, 14168.
(594) Dong, D. W.; Jiang, S. C.; Men, Y. F.; Ji, X. L.; Jiang, B. Z. *Adv. Mater.* **2000**, *12*, 646.
(595) Dong, D. W.; Men, Y. F.; Jiang, S. C.; Ji, X. L.; Jiang, B. Z. *Mater. Chem. Phys.* **2001**, *70*, 249.
(596) Dong, D. W.; Jiang, B. Z. *Mater. Chem. Phys.* **2003**, *78*, 501.
(597) Dong, D. W.; Yang, Y. S.; Jiang, B. Z. *Mater. Chem. Phys.* **2006**, *95*, 89.
(598) Bourg, S.; Broudic, J.-C.; Conocar, O.; Moreau, J. J. E.; Meyer, D.; Wong Chi Man, M. *Chem. Mater.* **2001**, *13*, 491.
(599) Nassar, E. J.; Serra, O. A.; Rosa, I. L. V. *J. Alloys Compd.* **1997**, *250*, 380.
(600) de Farias, R. F.; de Freiats, A. P. F.; Belian, M. F.; Malta, O. L.; de Sa, G. F.; Alves, S., Jr. *J. Alloys Compd.* **2008**, *459*, 543.
(601) Guo, X. M.; Guo, H. D.; Fu, L. S.; Zhang, H. J.; Carlos, L. D.; Deng, R. P.; Yu, J. B. *J. Photochem. Photobiol. A* **2008**, *200*, 318.
(602) Lu, H. F.; Yan, B.; Liu, J. L. *Inorg. Chem.* **2009**, *48*, 3966.
(603) Yan, B.; Wang, Q. M.; Ma, D. J. *Inorg. Chem.* **2009**, *48*, 36.
(604) Embert, F.; Mehdi, A.; Reye, C.; Corriu, R. J. P. *Chem. Mater.* **2001**, *13*, 4542.
(605) Corriu, R. J. P.; Embert, F.; Guari, Y.; Mehi, A.; Reyé, C. *Chem. Commun.* **2001**, 1116.
(606) Besson, E.; Mehdi, A.; Reye, C.; Corriu, R. J. P. *J. Mater. Chem.* **2006**, *16*, 246.
(607) Khimich, N. N.; Zub, Y. L.; Koptelova, L. A.; Mashchenko, T. S.; Troshina, E. P.; Voronkov, M. G. *Russian J. Appl. Chem.* **2006**, *79*, 1769 [*Prikl. Khim.* **2006**, *79*, 1789].
(608) Corriu, R. J. P.; Embert, F.; Guari, Y.; Reye, C.; Guilard, R. *Chem.*—*Eur. J.* **2002**, *8*, 5732.
(609) Quici, S.; Cavazzini, M.; Raffo, M. C.; Armelao, L.; Bottaro, G.; Accorsi, G.; Sabatini, C.; Barigelletti, F. *J. Mater. Chem.* **2006**, *16*, 741.
(610) Armelao, L.; Bottaro, G.; Quici, S.; Cavazzini, M.; Raffo, M. C.; Barigelletti, F.; Accorsi, G. *Chem. Commun.* **2007**, 2911.
(611) Raehm, L.; Mehdi, A.; Wickleder, C.; Reye, C.; Corriu, R. J. P. *J. Am. Chem. Soc.* **2007**, *129*, 12636.
(612) Qiao, X. F.; Yan, B. *Inorg. Chem.* **2009**, *48*, 4714.
(613) Li, H. R.; Liu, P.; Wang, Y. G.; Zhang, L.; Yu, J. B.; Zhang, H. J.; Liu, B. Y.; Schubert, U. *J. Phys. Chem. C* **2009**, *113*, 3945.
(614) Breck, D. W. *Zeolite Molecular Sieves: Structure, Chemistry and Use*; Wiley: New York, 1974.
(615) Barrer, R. M. *Zeolites and Clays as Sorbents and Molecular Sieves*; Academic Press: London, 1978.
(616) van Bekkum, H., Flanigen, E. M., Jansen, J. C., Eds. *Introduction to Zeolite Science and Practice*; Elsevier: Amsterdam, 1991.
(617) Milton, R. M. U.S. Patent 2,882,244, 1959.
(618) Olson, D. H. *J. Phys. Chem.* **1970**, *74*, 2758.
(619) Breck, D. W. U.S. Patent 3,130,007, 1964.
(620) Costenoble, M. L.; Mortier, W. J.; Uytterhoeven, J. B. *J. Chem. Soc., Faraday Trans. I* **1976**, *72*, 1877.
(621) Breck, D. W. *J. Chem. Educ.* **1964**, *41*, 678.
(622) Huang, Y. Y. *J. Chem. Educ.* **1980**, *57*, 112.
(623) Jüstel, T.; Wiechert, D. U.; Lau, C.; Sendor, D.; Kynast, U. *Adv. Funct. Mater.* **2001**, *11*, 105.
(624) Nassar, E. J.; Serra, O. A. *Mater. Chem. Phys.* **2002**, *74*, 19.
(625) Nassar, E. J.; Serra, O. A.; Souza-Aguiar, E. F. *Quim. Nov.* **1998**, *21*, 121.
(626) Suib, S. L.; Zerger, R. P.; Stucky, G. D.; Morrison, T. I.; Shenoy, G. K. *J. Chem. Phys.* **1984**, *80*, 2203.
(627) Hazenkamp, M. F.; Vanderveen, A. M. H.; Feiken, N.; Blasse, G. *J. Chem. Soc., Faraday Trans.* **1991**, *88*, 141.
(628) Berry, F. J.; Carbucicchio, M.; Chiari, A.; Johnson, C.; Moore, E. A.; Mortimer, M.; Vetel, F. F. F. *J. Mater. Chem.* **2000**, *10*, 2131.
(629) Baker, M. D.; Olken, M. M.; Ozin, G. A. *J. Am. Chem. Soc.* **1988**, *110*, 5709.
(630) Lee, S. B.; Hwang, H. S.; Kim, P. S.; Jang, D. J. *Catal. Lett.* **1999**, *57*, 221.
(631) Hwang, H.; Lee, S.; Jang, D. J. *Bull. Korean Chem. Soc.* **1998**, *19*, 471.
(632) Firor, R. L.; Seff, K. *J. Am. Chem. Soc.* **1978**, *100*, 976.
(633) Firor, R. L.; Seff, K. *J. Am. Chem. Soc.* **1978**, *100*, 978.
(634) Suib, S. L.; Zerger, R. P.; Stucky, G. D.; Emberson, R. M.; Debrunner, P. G.; Iton, L. E. *Inorg. Chem.* **1980**, *19*, 1858.
(635) Jørgensen, C. K. *J. Am. Chem. Soc.* **1978**, *100*, 5968.
(636) Hazenkamp, L. F.; Van der Veen, A. M. H.; Blasse, G. *J. Chem. Soc., Faraday Trans.* **1992**, *88*, 133.
(637) Hong, S. B.; Shin, E. W.; Moon, S. H.; Pyun, C. H.; Kim, C. H.; Uh, Y. S. *J. Phys. Chem.* **1995**, *99*, 12274.
(638) Hong, S. B.; Seo, J. S.; Pyun, C. H.; Kim, C. H.; Uh, Y. S. *Catal. Lett.* **1995**, *30*, 87.
(639) Hong, S. B.; Shin, E. W.; Moon, S. H.; Pyun, C. H.; Kim, C. H.; Uh, Y. S. *J. Phys. Chem.* **1995**, *99*, 12278.
(640) Tiseanu, C.; Frunza, L.; Kumke, M. *Phys. B* **2004**, *352*, 358.
(641) Tiseanu, C.; Gessner, A.; Kumke, M. U. *J. Non-Cryst. Solids* **2008**, *354*, 1969.
(642) Tiseanu, C.; Kumke, M. U.; Parvulescu, V. I.; Gessner, A.; Gagea, B. C.; Martens, J. A. *J. Phys. Chem. B.* **2006**, *110*, 25707.
(643) Hong, S. B. *J. Phys. Chem. B* **2001**, *105*, 11961.
(644) Kynast, U.; Weiler, V. *Adv. Mater.* **1994**, *6*, 937.
(645) Jüstel, T.; Wiechert, D. U.; Lau, C.; Sendor, D.; Kynast, U. *Adv. Funct. Mater.* **2001**, *11*, 105.
(646) Serra, O. A.; Nassar, E. J.; Zapparolli, G.; Rosa, I. L. V. *J. Alloys Compd.* **1995**, *225*, 63.
(647) Sendor, D.; Kynast, U. *Adv. Mater.* **2002**, *14*, 1570.
(648) Rosa, I. L. V.; Serra, O. A.; Nassar, E. J. *J. Lumin.* **1997**, *72*−*74*, 532.
(649) Alvaro, M.; Fornes, V.; Garcia, S.; Garcia, H.; Scaiano, J. C. *J. Phys. Chem. B* **1998**, *102*, 8744.
(650) Dexpert-Ghys, J.; Picard, C.; Taurines, A. *J. Inclusion Phenom. Macrocycl. Chem.* **2001**, *39*, 261.
(651) Bredol, M.; Kynast, U.; Ronda, C.; Welker, T. European Patent EP522627 1993.
(652) Bel'tyukova,S. V.; Tselik, E. I.; Egorova, A. V.; Tesluyk, O. I. *J. Appl. Spectrosc.* **2003**, *70*, 307 (*Zh. Prikl. Spectrosc.* **2003**, *70*, 272).
(653) Bel'tyukova, S. V.; Tselik, E. I.; Egorova, A. V.; Efryushina, N. P. *J. Appl. Spectrosc.* **2001**, *68*, 598 (*Zh. Prikl. Spectrosc.* **2001**, *68*, 459).
(654) Liu, H. H.; Song, H. W.; Li, S. W.; Ren, X. G.; Lu, S. Z.; Yu, H. Q.; Pan, G. H.; Zhang, H.; Hu, L. Y.; Dai, Q. L.; Qin, R. F.; Yu, J. H.; Wang, G. M.; Jiang, J. X. *J. Nanosci. Nanotechnol.* **2008**, *8*, 3959.
(655) Lezhina, M. M.; Kynast, U. H. *Phys. Solid State* **2005**, *47*, 1485.
(656) Rocha, J.; Carlos, L. D.; Rainho, J. P.; Lin, Z.; Ferreira, P.; Almeida, R. M. *J. Mater. Chem.* **2000**, *10*, 1371.
(657) Wada, Y.; Okubo, T.; Ryo, M.; Nakazawa, T.; Hasegawa, Y.; Yanagida, S. *J. Am. Chem. Soc.* **2000**, *122*, 8583.

(658) Ryo, M.; Wada, Y.; Okubo, T.; Nakazawa, T.; Hasegawa, Y.; Yanagida, S. *J. Mater. Chem.* **2002**, *12*, 1748.
(659) Ryo, M.; Wada, Y.; Okubo, T.; Hasegawa, Y.; Yanagida, S. *J. Phys. Chem. B* **2003**, *107*, 11302.
(660) Ryo, M.; Wada, Y.; Okubo, T.; Yanagida, S. *Res. Chem. Intermed.* **2004**, *30*, 191.
(661) Chen, W.; Sammynaiken, R.; Huang, Y. *J. Appl. Phys.* **2000**, *88*, 1424.
(662) Wada, Y.; Sato, M.; Tsukahara, Y. *Angew. Chem., Int. Ed.* **2006**, *45*, 1925.
(663) Tsukahara, Y.; Sato, M.; Katagiri, S.; Honda, T.; Nakamura, K.; Wada, Y. *J. Alloys Compd.* **2008**, *451*, 194.
(664) Kresge, C. T.; Leonowicz, M. E.; Roth, W. J.; Vartuli, J. C.; Beck, J. S. *Nature* **1992**, *359*, 710.
(665) Beck, J. S.; Vartuli, J. C.; Roth, W. J.; Leonowicz, M. E.; Kresge, C. T.; Schmitt, K. D.; Chu, C. T. W.; Olson, D. H.; Sheppard, E. W.; McCullen, S. B.; Higgins, J. B.; Schlenker, J. L. *J. Am. Chem. Soc.* **1992**, *114*, 10834.
(666) Barton, T. J.; Bull, L. M.; Klemperer, W. G.; Loy, D. A.; McEnaney, B.; Misono, M.; Monson, P. A.; Pez, G.; Scherer, G. W.; Vartuli, J. C.; Yaghi, O. M. *Chem. Mater.* **1999**, *11*, 2633.
(667) Zhao, D.; Huo, Q.; Feng, J.; Chmelka, B. F.; Stucky, G. D. *J. Am. Chem. Soc.* **1998**, *120*, 6024.
(668) Chen, Y.; Chen, Q.; Song, L.; Li, H. P.; Hou, F. Z. *Microporous Mesoporous Mater.* **2009**, *122*, 7.
(669) Nicole, L.; Boissiere, C.; Grosso, D.; Quach, A.; Sanchez, C. *J. Mater. Chem.* **2005**, *15*, 3598.
(670) Scott, B. J.; Wirnsberger, G.; Stucky, G. D. *Chem. Mater.* **2001**, *13*, 3140.
(671) Xu, Q. H.; Li, L. S.; Li, B.; Yu, J. H.; Xu, R. R. *Microporous Mesoporous Mater.* **2000**, *38*, 351.
(672) Xu, Q. H.; Li, L. S.; Li, B.; Yu, J. H.; Xu, R. R. *J. Mater. Sci. Technol.* **2001**, *17*, 290.
(673) Xu, Q. H.; Dong, W. J.; Li, H. W.; Li, L. S.; Feng, S. H.; Xu, R. R. *Solid State Sci.* **2003**, *5*, 777.
(674) Fu, L. S.; Xu, Q. H.; Zhang, H. J.; Li, L. S.; Meng, Q. G.; Xu, R. R. *Mater. Sci. Eng., B* **2002**, *88*, 68.
(675) Fu, L. S.; Zhang, H. J.; Boutinaud, P. *J. Mater. Sci. Technol.* **2001**, *17*, 293.
(676) Yao, Y. F.; Zhang, M. S.; Shi, J. X.; Gong, M. L.; Zhang, H. J.; Yang, Y. S. *J. Rare Earths* **2000**, *18*, 186.
(677) Meng, Q. G.; Boutinaud, P.; Franville, A. C.; Zhang, H. J.; Mahiou, R. *Microporous Mesoporous Mater.* **2003**, *65*, 127.
(678) Fernandes, A.; Dexpert-Ghys, J.; Brouca-Cabarrecq, C.; Philippot, E.; Gleizes, A.; Galarneau, A.; Brunel, D. *Stud. Surf. Sci. Catal.* **2002**, *142*, 1371.
(679) Fernandes, A.; Dexpert-Ghys, J.; Gleizes, A.; Galarneau, A.; Brunel, D. *Microporous Mesoporous Mater.* **2005**, *83*, 35.
(680) Yin, W.; Zhang, M. S.; Kang, B. S. *J. Rare Earths* **2003**, *21* (Suppl. S), 41.
(681) Meng, Q. G.; Boutinaud, P.; Zhang, H. J.; Mahiou, R. *J. Lumin.* **2007**, *124*, 15.
(682) Gu, C. W.; Chia, P. A.; Zhao, X. S. *Appl. Surf. Sci.* **2004**, *237*, 387.
(683) Guo, X. M.; Fu, L. S.; Zhang, H. J.; Carlos, L. D.; Peng, C. Y.; Guo, J. F.; Yu, J. B.; Deng, R. P.; Sun, L. N. *New J. Chem.* **2005**, *29*, 1351.
(684) Yuan, Y. B.; Nie, J.; Zhang, Z. B.; Wang, S. J. *Appl. Catal., A* **2005**, *295*, 170.
(685) Mantri, K.; Komura, K.; Kubota, Y.; Sugi, Y. *J. Mol. Catal.* **2005**, *236*, 168.
(686) Sea, S. J.; Zhao, D.; Suh, K.; Shin, J. H.; Bae, B. S. *J. Lumin.* **2008**, *128*, 565.
(687) Aquino, J. M. F. B.; Araujo, A. S.; Melo, D. M. A.; Silva, J. E. C.; Souza, M. J. B.; Silva, A. O. S. *J. Alloys Compd.* **2004**, *374*, 101.
(688) Li, S. W.; Song, H. W.; Li, W. L.; Lu, S. Z.; Ren, X. G. *J. Nanosci. Nanotechnol.* **2008**, *8*, 1272.
(689) Zhao, D.; Seo, S. J.; Bae, B. S. *Adv. Mater.* **2007**, *19*, 3473.
(690) Tiseanu, C.; Parvulescu, V. I.; Kumke, M. U.; Dobroiu, S.; Gessner, A.; Simon, S. *J. Phys. Chem. C* **2009**, *113*, 5784.
(691) Bartl, M. H.; Scott, B. J.; Huang, H. C.; Wirnsberger, G.; Popitsch, A.; Chmelka, B. F.; Stucky, G. D. *Chem. Commun.* **2002**, 2474.
(692) Minoofar, P.; Hernandez, R.; Franville, A. C.; Chia, S. Y.; Dunn, B.; Zink, J. I. *J. Sol-Gel Sci. Technol.* **2003**, *26*, 571.
(693) Minoofar, P. N.; Dunn, B. S.; Zink, J. I. *J. Am. Chem. Soc.* **2005**, *127*, 2656.
(694) Minoofar, P. N.; Hernandez, R.; Chia, S.; Dunn, B.; Zink, J. I.; Franville, A. C. *J. Am. Chem. Soc.* **2002**, *124*, 14388.
(695) Hernandez, R.; Franville, A. C.; Minoofar, P.; Dunn, B.; Zink, J. I. *J. Am. Chem. Soc.* **2001**, *123*, 1248.
(696) Fernandes, A.; Dexpert-Ghys, J.; Brouca-Cabarrecq, C.; Philippot, E.; Gleizes, A.; Galarneau, A.; Brunel, D. *Stud. Surf. Sci. Catal.* **2002**, *142*, 1371.
(697) Gleizes, A. N.; Fernandes, A.; Dexpert-Ghys, J. *J. Alloys Compd.* **2004**, *374*, 303.
(698) Fernandes, A.; Dexpert-Ghys, J.; Gleizes, A.; Galarneau, A.; Brunel, D. *Microporous Mesoporous Mater.* **2005**, *83*, 35.
(699) Li, H. R.; Lin, J.; Fu, L. S.; Guo, J. F.; Meng, Q. G.; Liu, F. Y.; Zhang, H. J. *Microporous Mesoporous Mater.* **2002**, *55*, 103.
(700) Peng, C. Y.; Zhang, H. J.; Meng, Q. G.; Li, H. R.; Yu, J. B.; Guo, J. F.; Sun, L. N. *Inorg. Chem. Commun.* **2005**, *8*, 440.
(701) Peng, C. Y.; Zhang, H.; Yu, J.; Meng, Q.; Fu, L.; Li, H.; Sun, L.; Guo, X. *J. Phys. Chem. B* **2005**, *109*, 15278.
(702) Sun, L. N.; Yu, J. B.; Zhang, H. J.; Meng, Q. G.; Ma, E.; Peng, C. Y.; Yang, K. *Microporous Mesoporous Mater.* **2007**, *98*, 156.
(703) Feng, J.; Song, S. Y.; Xing, Y.; Zhang, H. J.; Li, Z. F.; Sun, L. N.; Guo, X. M.; Fan, W. Q. *J. Solid State Chem.* **2009**, *182*, 435.
(704) Sun, L.-N.; Zhang, H.-J.; Peng, C.-Y.; Yu, J.-B.; Meng, Q.-G.; Fu, L.-S.; Liu, F.-Y.; Guo, X.-M. *J. Phys. Chem. B* **2006**, *110*, 7249.
(705) Guo, X. M.; Guo, H. D.; Fu, L. S.; Deng, R. P.; Chen, W.; Feng, J.; Dang, S.; Zhang, H. J. *J. Phys. Chem. C* **2009**, *113*, 2603.
(706) Li, Y.; Yan, B.; Yang, H. *J. Phys. Chem. C* **2008**, *112*, 3959.
(707) Yan, B.; Zhou, B. *J. Photochem. Photobiol. A* **2008**, *195*, 314.
(708) DeOliveira, E.; Neri, C. R.; Serra, O. A.; Prado, A. G. S. *Chem. Mater.* **2007**, *19*, 5437.
(709) Yan, B.; Li, Y.; Zhou, B. *Microporous Mesoporous Mater.* **2009**, *120*, 317.
(710) Kong, L. L.; Yan, B.; Li, Y. *J. Alloys Compd.* **2009**, *481*, 549.
(711) Li, Y.; Yan, B. *J. Solid State Chem.* **2008**, *181*, 1032.
(712) Guo, X. M.; Guo, H. D.; Fu, L. S.; Zhang, H. J.; Deng, R. P.; Sun, L. N.; Feng, J.; Dang, S. *Microporous Mesoporous Mater.* **2009**, *119*, 252.
(713) Gago, S.; Fernandes, J. A.; Rainho, J. P.; Sa Ferreira, R. A.; Pillinger, M.; Valente, A. A.; Santos, T. M.; Carlos, L. D.; Ribeiro-Claro, P. J. A.; Goncalves, I. S. *Chem. Mater.* **2005**, *17*, 5077.
(714) Van Deun, R.; Fias, P.; Nockemann, P.; Schepers, A.; Parac-Vogt, T. N.; Van Hecke, K.; Van Meervelt, L.; Binnemans, K. *Inorg. Chem.* **2004**, *43*, 8461.
(715) Sun, L.-N.; Zhang, H.-J.; Yu, J.-B.; Yu, S.-Y.; Peng, C.-Y.; Dang, S.; Guo, X.-M.; Feng, J. *Langmuir* **2008**, *24*, 5500.
(716) Bruno, S. M.; Coelho, A. C.; Ferreira, R. A. S.; Carlos, L. D.; Pillinger, M.; Valente, A. A.; Ribeiro-Claro, P.; Goncalves, I. S. *Eur. J. Inorg. Chem.* **2008**, 3786.
(717) Cao, Q. Y.; Chen, Y. H.; Liu, J. H.; Gao, X. C. *Inorg. Chem. Commun.* **2009**, *12*, 48.
(718) Corriu, R. J. P.; Mehdi, A.; Reye, C.; Thieuleux, C.; Frenkel, A.; Gibaud, A. *New J. Chem.* **2004**, *28*, 156.
(719) Quach, A.; Escax, V.; Nicole, L.; Goldner, P.; Guiloot-Noel, O.; Ascheboug, P.; Hesemann, P.; Moreau, J.; Gourier, D.; Sanchez, C. *J. Mater. Chem.* **2007**, *17*, 2552.
(720) Brun, B.; Julian-Lopze, B.; Hesemann, P.; Laurent, G.; Deleuze, H.; Sanchez, C.; Achard, M. F.; Backov, R. *Chem. Mater.* **2008**, *2*, 7117.
(721) Carn, F.; Colin, A.; Achard, M. F.; Deleuze, H.; Sellier, E.; Birot, M.; Backov, R. *J.Mater. Chem.* **2004**, *14*, 1370.
(722) Newman, S. P.; Jones, W. *New J. Chem.* **1998**, *22*, 105.
(723) Rives, V.; Ulibarri, M. A. *Coord. Chem. Rev.* **1999**, *181*, 61.
(724) Brunet, E.; de la Mata, M. J.; Juanes, O.; Rodriguez-Ubis, J. C. *Chem. Mater.* **2004**, *16*, 1517.
(725) Fu, L. S.; Xu, Q. H.; Zhang, H. J.; Li, L. S.; Ni, J. Z.; Xu, R. R. *Chin. Chem. Lett.* **2000**, *11*, 171.
(726) Xu, Q. H.; Fu, L. S.; Li, L. S.; Zhang, H. J.; Xu, R. R. *J. Mater. Chem.* **2000**, *10*, 2532.
(727) Ferreira, R.; Pires, P.; de Castro, B.; Ferreira, R. A. S.; Carlos, L. D.; Pischel, U. *New J. Chem.* **2004**, *28*, 1506.
(728) Kumar, C. V.; Chaudhary, A. *Microporous Mesoporous Mater.* **1999**, *32*, 75.
(729) Ngo, H. L.; Lin, W. *J. Am. Chem. Soc.* **2002**, *124*, 14298.
(730) Xin, H.; Ebina, Y.; Ma, R. Z.; Takada, K.; Sasaki, T. *J. Phys. Chem. B* **2006**, *110*, 9863.
(731) Song, K.; Kauzlarich, S. M. *Chem. Mater.* **2004**, *6*, 386.
(732) Karmaoui, M.; Sa Ferreira, R. A.; Mane, A. T.; Carlos, L. D.; Pinna, N. *Chem. Mater.* **2006**, *18*, 4493.
(733) Karmaoui, M.; Sa Ferreira, R. A.; Carlos, L. D.; Pinna, N. *Mater. Sci. Eng., C* **2007**, *27*, 1368.
(734) Pinna, N.; Garnweitner, G.; Beato, P.; Niederberger, M.; Antonietti, M. *Small* **2005**, *1*, 112.
(735) Sa Ferreira, R. A.; Karmaoui, M.; Nobre, S. S.; Carlos, L. D.; Pinna, N. *ChemPhysChem* **2006**, *7*, 2215.
(736) Pinna, N. *J. Mater. Chem.* **2007**, *17*, 2769.
(737) Karmaoui, M.; Mafra, L.; Sa Ferreira, R. A.; Rocha, J.; Carlos, L. D.; Pinna, N. *J. Phys. Chem. C* **2007**, *111*, 2539.
(738) Sousa, F. L.; Pillinger, M.; Sa Ferreira, R. A.; Granadeiro, C. M.; Cavaleiro, A. M. V.; Rocha, J.; Carlos, L. D.; Trindade, T.; Nogueira, H. I. S. *Eur. J. Inorg. Chem.* **2006**, 726.

(739) Li, C.; Wang, G.; Evans, D. G.; Duan, X. *J. Solid State Chem.* **2004**, *177*, 4569.
(740) Zhuravleva, N. G.; Eliseev, A. A.; Lukashin, A. V.; Kynast, U.; Tret'yakov, Y. D. *Dokl. Chem.* **2004**, *396*, 87.
(741) Zhuravleva, N. G.; Eliseev, A. A.; Lukashin, A. V.; Kynast, U.; Tretyakov, Y. D. *Mendeleev Commun.* **2004**, *4*, 176.
(742) Gago, S.; Pillinger, M.; Ferreira, R. A. S.; Carlos, L. D.; Santos, T. M.; Goncalves, I. S. *Chem. Mater.* **2005**, *17*, 5803.
(743) Li, C.; Wang, L. Y.; Evans, D. G.; Duan, X. *Ind. Eng. Chem. Res.* **2009**, *48*, 2162.
(744) Jiang, W.; Tang, Y.; Liu, W. S.; Tan, M. Y. *Chin. J. Inorg. Chem.* **2006**, *22*, 2235.
(745) Lezhnina, M.; Benavente, E.; Bentlage, M.; Echevarria, Y.; Klumpp, E.; Kynast, U. *Chem. Mater.* **2007**, *19*, 1098.
(746) Sanchez, A.; Echeverria, Y.; Torres, C. M.S.; Gonzalez, G.; Benavente, E. *Mater. Res. Bull.* **2006**, *41*, 1185.
(747) Celedon, S.; Quiroz, C.; Gonzalez, G.; Sotomayor Torres, C. M.; Benavente, E. *Mater. Res. Bull.* **2009**, *44*, 1191.
(748) Pope, M. T. *Heteropoly and Isopoly Oxometalates*; Springer Verlag: New York, 1983.
(749) Hill, C. L. *Chem. Rev.* **1998**, *98*, 1.
(750) Pope, M. T.; Müller, A. *Angew. Chem., Int. Ed.* **1991**, *30*, 34.
(751) Coronado, E.; Gomez-Garcia, C. J. *Chem. Rev.* **1998**, *98*, 273.
(752) Long, D. L.; Burkholder, E.; Cronin, L. *Chem. Soc. Rev.* **2007**, *36*, 105.
(753) Katsoulis, D. E. *Chem. Rev.* **1998**, *98*, 359.
(754) Rhule, J. T.; Hill, C. L.; Judd, D. A.; Schinazi, R. F. *Chem. Rev.* **1998**, *98*, 327.
(755) Sadakane, M.; Steckhan, E. *Chem. Rev.* **1998**, *98*, 219.
(756) Kozhevnikov, I. V. *Chem. Rev.* **1998**, *98*, 171.
(757) Yusov, A. B.; Shilov, V. P. *Radiochemistry* **1999**, *41*, 1.
(758) Yamase, T. *Chem. Rev.* **1998**, *98*, 307.
(759) Lis, S. *J. Alloys Compd.* **2000**, *300*−*301*, 88.
(760) Pople, M. T. Polyoxometallates. In *Handbook on the Physics and Chemistry of Rare Earths*; Gschneidner, K. A., Jr., Bünzli, J.-C., Pescharsky, V., Eds.; Elsevier: Amsterdam, 2008; Vol. 38, Chapter 240.
(761) Yamase, T. Luminescence of Polyoxometallolanthanates. In *Handbook on the Physics and Chemistry of Rare Earths*; Gschneidner, K. A., Jr., Bünzli, J.-C., Pescharsky, V., Eds.; Elsevier: Amsterdam, 2009; Vol. 39, Chapter 243.
(762) Peacock, R. D.; Weakley, T. J. R. *J. Chem. Soc. A* **1971**, 1836.
(763) Iball, J.; Low, J. N.; Weakley, T. J. R. *J. Chem. Soc., Dalton Trans.* **1974**, 2021.
(764) Sugeta, M.; Yamase, T. *Bull. Chem. Soc. Jpn.* **1993**, *66*, 444.
(765) Stillman, M. J.; Thompson, A. J. *J. Chem. Soc., Dalton Trans.* **1976**, 1138.
(766) Blasse, G.; Dirksen, G. J.; Zonnevijlle, F. *Chem. Phys. Lett.* **1981**, *83*, 449.
(767) Blasse, G.; Dirksen, G. J.; Zonnevijlle, F. *J. Inorg. Nucl. Chem.* **1981**, *43*, 2847.
(768) Ballardini, R.; Mulazzani, Q. G.; Venturi, M.; Bolletta, F.; Balzani, V. *Inorg. Chem.* **1984**, *23*, 300.
(769) Yamase, T.; Kobayashi, T.; Sugeta, M.; Naruke, H. *J. Phys. Chem. A* **1997**, *101*, 5046.
(770) Lis, S.; But, S. *Mater. Sci. Forum* **1999**, *315*−*317*, 431.
(771) Blasse, G. *Eur. J. Solid State Inorg. Chem.* **1991**, *28*, 719.
(772) But, S.; Lis, S.; Van Deun, R.; Parac-Vogt, T. N.; Görller-Walrand, C.; Binnemans, K. *Spectrochim. Acta A* **2005**, *62*, 478.
(773) Lis, S.; But, S.; Klonkowski, A. M.; Grobelna, B. *Int. J. Photoenergy* **2003**, *5*, 233.
(774) Lis, S.; But, S.; Meinrath, G. *J. Alloys Compd.* **2004**, *374*, 366.
(775) Bartis, J.; Dankova, M.; Lessmann, J. J.; Luo, Q.-H.; Horrocks, W. D., Jr.; Francesconi, L. C. *Inorg. Chem.* **1999**, *38*, 1042.
(776) Blasse, G.; Zonnevijlle, F. *Rec. Trav. Chim. Pays-Bas* **1982**, *101*, 434.
(777) Lis, S.; But, S.; Meinrath, G. *J. Alloys Compd.* **2006**, *408*, 958.
(778) Boglio, C.; Lenoble, G.; Duhayon, C.; Hasenknopf, B.; Thouvenot, R.; Zhang, C.; Howell, R. C.; Burton-Pye, B. P.; Francesconi, L. C.; Lacote, E.; Thorimbert, S.; Malacria, M.; Afonso, C.; Tabet, J.-C. *Inorg. Chem.* **2006**, *45*, 1389.
(779) Li, W.; Yi, S.; Wu, Y.; Wu, L. *J. Phys. Chem. B* **2006**, *110*, 16961.
(780) Sun, H.; Li, H.; Bu, W.; Xu, M.; Wu, L. *J. Phys. Chem. B* **2006**, *110*, 24847.
(781) Bu, W.; Li, H.; Li, W.; Zhai, C.; Wu, L.; Wu, Y. *J. Phys. Chem. B* **2004**, *108*, 12776.
(782) Zhang, T. R.; Spitz, C.; Antonietti, M.; Faul, C. F. J. *Chem.*−*Eur. J.* **2005**, *11*, 1001.
(783) Li, W.; Bu, W. F.; Li, H. L.; Wu, L. X.; Li, M. *Chem. Commun.* **2005**, *30*, 3785.
(784) Zhang, H.; Lin, X. K.; Yan, Y.; Wu, L. X. *Chem. Commun.* **2006**, 4575.
(785) Hao, D. T. M.; Kim, H. S.; Lee, B. J.; Park, D. H.; Kwon, Y. S. *Curr. Appl. Phys.* **2006**, *6*, 605.
(786) Hoa, D. T. M.; Kim, H. S.; Lee, B. J.; Kwon, Y. S. *Mol. Cryst. Liq. Cryst.* **2006**, *444*, 113.
(787) Yin, S. Y.; Sun, H.; Yan, Y.; Li, W.; Wu, L. X. *J. Phys. Chem. B* **2009**, *113*, 2355.
(788) Balzani, V.; Credi, A.; Venturi, M. *ChemPhysChem* **2003**, *4*, 49.
(789) de Silva, A. P.; Uchiyama, S. *Nat. Nanotechnol.* **2007**, *2*, 399.
(790) Magri, D. C.; Vance, T. P.; de Silva, A. P. *Inorg. Chim. Acta* **2007**, *360*, 751.
(791) Clemente-Leon, M.; Coronado, E.; Soriano-Portillo, A.; Mingotaud, C.; Dominguez-Vera, J. M. *Adv. Colloid Interface Sci.* **2005**, *116*, 193.
(792) Sousa, F. L.; Ferreira, A. S.; Sa Ferreira, R. A.; Cavaleiro, A. M. V.; Carlos, L. D.; Nogueira, H. I. S.; Trindade, T. *J. Alloys Compd.* **2004**, *374*, 371.
(793) Ito, T.; Yashiro, H.; Yamase, T. *J. Cluster Sci.* **2006**, *17*, 375.
(794) Ito, T.; Yamase, T. *J. Alloys Compd.* **2006**, *408*, 813.
(795) Jiang, M.; Liu, M. H. *J. Colloid Interface Sci.* **2007**, *316*, 100.
(796) Jiang, M.; Zhai, X. D.; Liu, M. H. *Langmuir* **2005**, *21*, 11128.
(797) Wang, J.; Wang, H. S.; Fu, L. S.; Liu, F. Y.; Zhang, H. J. *Thin Solid Films* **2002**, *415*, 242.
(798) Wang, J.; Wang, H. S.; Fu, L. S.; Liu, F. Y.; Zhang, H. J. *Thin Solid Films* **2002**, *414*, 256.
(799) Wang, J.; Wang, H. S.; Wang, Z.; Yin, Y. D.; Liu, F. Y.; Li, H. R.; Fu, L. S.; Zhang, H. J. *J. Alloys Compd.* **2004**, *365*, 102.
(800) Wang, J.; Wang, H. S.; Liu, F. Y.; Fu, L. S.; Zhang, H. J. *J. Lumin.* **2003**, *101*, 63.
(801) Tuong, N. M.; Kim, H. S.; Hoa, D. T. M.; Lee, B. J.; Park, D. H.; Lee, N. S.; Kwon, Y. S. *Colloids Surf. A* **2006**, *284*−*285*, 198.
(802) Li, W.; Li, H. L.; Wu, L. X. *Colloids Surf. A* **2006**, *272*, 176.
(803) Decher, G. *Science* **1997**, *277*, 1232.
(804) Decher, G.; Eckle, M.; Schmitt, J.; Struth, B. *Curr. Opin. Colloid Interface Sci.* **1998**, *3*, 32.
(805) Quinn, J. F.; Johnston, A. P. R.; Such, G. K.; Zelikin, A. N.; Caruso, F. *Chem. Soc. Rev.* **2007**, *36*, 707.
(806) Liu, S. Q.; Kurth, D. G.; Bredenkötter, B.; Volkmer, D. *J. Am. Chem. Soc.* **2002**, *124*, 12279.
(807) Tien, J.; Terfort, A.; Whitesides, G. M. *Langmuir* **1997**, *13*, 5349.
(808) Faul, C. F. J.; Antonietti, M. *Adv. Mater.* **2003**, *15*, 673.
(809) Liu, S. Q.; Kurth, D. G.; Möhwald, H.; Volkmer, D. *Adv. Mater.* **2002**, *14*, 225.
(810) Dong, T.; Ma, H. Y.; Zhang, W.; Gong, L. H.; Wang, F. P.; Li, C. X. *J. Colloid Interface Sci.* **2007**, *311*, 523.
(811) Zhai, S. Y.; Chen, Y. G.; Wang, S. B.; Jiang, J. G.; Dong, S. J.; Li, J. H. *Talanta* **2004**, *63*, 927.
(812) Wang, J.; Wang, Z.; Wang, H. H.; Liu, F. Y.; Fu, L. S.; Zhang, H. J. *J. Alloys Compd.* **2004**, *376*, 68.
(813) Bu, W. F.; Li, W.; Li, H. L.; Wu, L. X.; Tang, A. C. *J. Collid Interface Sci.* **2004**, *274*, 200.
(814) Zhang, T. R.; Lu, R.; Zhang, H. Y.; Xue, P. C.; Feng, W.; Liu, X. L.; Zhao, B.; Zhao, Y. Y.; Li, T. J.; Yao, J. N. *J. Mater. Chem.* **2003**, *13*, 580.
(815) Polarz, S.; Smarsly, B.; Goltner, C.; Antonietti, M. *Adv. Mater.* **2000**, *12*, 1503.
(816) Klonkowski, A. M.; Grobelna, B.; Lis, S.; But, S. *J. Alloys Compd.* **2004**, *380*, 205.
(817) Hungerford, G.; Green, M.; Suhling, K. *Phys. Chem. Chem. Phys.* **2007**, *9*, 6012.
(818) Qi, W.; Li, H. L.; Wu, L. X. *Adv. Mater.* **2007**, *19*, 1983.
(819) Wang, J.; Liu, F. Y.; Fu, L. S.; Zhang, H. J. *Mater. Lett.* **2002**, *56*, 300.
(820) Wang, Z.; Wang, J.; Zhang, H. *J. Mater. Chem. Phys.* **2004**, *87*, 44.
(821) Xu, W.; Luo, Q. H.; Wang, H.; Francesconi, L. C.; Stark, R. E.; Akins, D. L. *J. Phys. Chem. B* **2003**, *107*, 497.
(822) Zhang, X.; Zhang, C.; Guo, H.; Huang, W.; Polenova, T.; Francesconi, L. C.; Akins, D. L. *J. Phys. Chem. B* **2005**, *109*, 19156.
(823) Li, H. L.; Qi, W.; Li, W.; Sun, H.; Bu, W. F.; Wu, L. X. *Adv. Mater.* **2005**, *17*, 2688.
(824) Li, H. L.; Li, P.; Qi, W.; Sun, H.; Wu, L. X. *Macromol. Rapid Commun.* **2008**, *29*, 431.
(825) Xu, M.; Liu, C. L.; Li, H. L.; Li, W.; Wu, L. X. *J. Colloid Interface Sci.* **2008**, *323*, 176.
(826) Lu, X. F.; Liu, X. C.; Wang, L. F.; Zhang, W. J.; Wang, C. *Nanotechnology* **2006**, *17*, 3048.
(827) Sanchez, C.; Soler-Illia, G. J. A. A.; Ribot, F.; Lalot, T.; Mayer, C. R.; Cabuil, V. *Chem. Mater.* **2001**, *13*, 3061.
(828) Proust, A.; Thouvenot, R.; Gouzerh, P. *Chem. Commun.* **2008**, 1837.
(829) Rodrigues, M. J. E.; Almeide Paz, F. A.; Sa Ferreira, R. A.; Carlos, L. D.; Nogueira, H. I. S. *Mater. Sci. Forum* **2006**, *514*−*516*, 1305.
(830) Granadeiro, C. M.; Sa Ferreira, R. A.; Soares-Santos, P. C. R.; Carlos, L. D.; Nogueira, H. I. S. *J. Alloys Compd.* **2008**, *451*, 422.

(831) But, S.; Lis, S. *J. Alloys Compd.* **2008**, *451*, 384.
(832) Wolff, N. E.; Pressley, R. *J. Appl. Phys. Lett.* **1963**, *2*, 152.
(833) Huffman, E. H. *Phys. Lett.* **1963**, *7*, 237.
(834) Huffman, E. H. *Nature* **1963**, *200*, 158.
(835) Kuriki, K.; Koike, Y.; Okamoto, Y. *Chem. Rev.* **2002**, *102*, 2347.
(836) Banks, E.; Okamoto, Y.; Ueba, Y. *J. Appl. Polym. Sci.* **1980**, *25*, 359.
(837) Ueba, Y.; Zhu, K. J.; Banks, E.; Okamoto, Y. *J. Polym. Sci.* **1982**, *20*, 1271.
(838) Nishide, H.; Izushi, T.; Yoshioka, N.; Tsuchida, E. *Polym. Bull.* **1985**, *14*, 387.
(839) Okamoto, Y.; Ueba, Y.; Nagata, I.; Banks, E. *Macromolecules* **1981**, *14*, 807.
(840) Okamoto, Y.; Ueba, Y.; Dzhanibekov, N. F.; Banks, E. *Macromolecules* **1981**, *14*, 17.
(841) Li, W.; Mishima, T.; Adachi, G. Y.; Shiokawa, J. *Inorg. Chim. Acta* **1986**, *121*, 97.
(842) Xu, W. Y.; Wang, Y. S.; Zheng, D. G.; Xia, S. L. *J. Macromol. Sci. A* **1988**, *25*, 1397.
(843) Zhang, Q. J.; Ming, H.; Zhai, Y. *J. Appl. Polym. Sci.* **1996**, *62*, 887.
(844) Zhang, Q. J.; Ming, H.; Zhai, Y. *Polym. Int.* **1996**, *41*, 413.
(845) Zhang, Q. J.; Wang, P.; Sun, X. F.; Zhai, Y.; Dai, P.; Yang, B.; Hai, M.; Xie, J. P. *Appl. Phys. Lett.* **1998**, *72*, 407.
(846) Zhang, Q. J.; Wang, P.; Zhai, Y. *J. Appl. Polym. Sci.* **1998**, *67*, 1431.
(847) Xu, X. S.; Ming, H.; Zhang, Q. J. *Opt. Commun.* **2001**, *199*, 369.
(848) Zhao, H.; Chen, B.; Cao, Y. P.; Zhang, Q. J.; Yang, B.; Ming, H.; Xie, J. P. *J. Appl. Polym. Sci.* **2002**, *86*, 2033.
(849) Zhang, Q. J.; Wang, P. *J. Mol. Struct.* **1998**, *440*, 35.
(850) Yang, B.; Ming, H.; Zhang, Q. J.; Xie, J. P. *J. Appl. Polym. Sci.* **2003**, *89*, 1124.
(851) Guo, Y.; Bai, M.; Tang, L.; Ming, H. *Chin. Phys. Lett.* **2002**, *19*, 1369.
(852) Zhao, H.; Hu, J.; Zhang, Q. J.; Bao, J.; Liu, W. H.; Gao, C.; Lu, Y. H. *J. Appl. Polym. Sci.* **2006**, *100*, 1294.
(853) Liu, H. G.; Park, S.; Jang, K.; Zhang, W. S.; Seo, H. J.; Lee, Y. I. *Mater. Chem. Phys.* **2003**, *82*, 84.
(854) Liang, H.; Zheng, Z. Q.; Li, Z. C.; Xu, J.; Chen, B.; Zhao, H.; Zhang, Q. J.; Ming, H. *Opt. Quantum Electron.* **2004**, *36*, 1313.
(855) Liu, H. G.; Lee, Y. I.; Park, S.; Jang, K.; Kim, S. S. *J. Lumin.* **2004**, *110*, 11.
(856) Kobayashi, T.; Kuriki, K.; Imai, N.; Tamura, T.; Sasaki, K.; Koike, Y.; Okamoto, Y. *Proc. SPIE* **1999**, *3623*, 206.
(857) Bonzanini, R.; Girotto, E. M.; Goncalves, M. C.; Radovanovic, E.; Muniz, E. C.; Rubira, A. F. *Polymer* **2005**, *46*, 253.
(858) Bonzanini, R.; Dias, D. T.; Girotto, E. M.; Muniz, E. C.; Baesso, M. L.; Caiut, J. M. A.; Messaddeq, Y.; Ribeiro, S. J. L.; Bento, A. C.; Rubira, A. F. *J. Lumin.* **2006**, *117*, 61.
(859) Chen, B.; Dong, N.; Zhang, Q. J.; Yin, M.; Xu, J.; Liang, H.; Zhao, H. *J. Non-Cryst. Solids* **2004**, *341*, 53.
(860) Chen, B.; Xu, J.; Dong, N.; Liang, H.; Zhang, Q. J.; Yin, M. *Spectrochim. Acta A* **2004**, *60*, 3113.
(861) Lu, J. B.; Yu, K. H.; Wang, H. Y.; He, J. F.; Cheng, G. H.; Qin, C. Y.; Lin, J. M.; Wei, W.; Peng, B. *Opt. Mater.* **2008**, *30*, 1531.
(862) Zheng, Z. Q.; Liang, H.; Ming, H.; Zhang, Q. J.; Xie, J. P. *Opt. Commun.* **2004**, *233*, 149.
(863) Dong, N.; Chen, B.; Yin, M.; Ning, L. X.; Zhang, Q. J.; Xia, S. D. *J. Rare Earths* **2004**, *22*, 31.
(864) Gordon, J.; Ballato, J.; Jin, J. Y.; Smith, D. W. *J. Polym. Sci. B* **2006**, *44*, 1592.
(865) Hasegawa, Y.; Yamamuro, M.; Wada, Y.; Kanehisa, N.; Kai, Y.; Yanagida, S. *J. Phys. Chem. A* **2003**, *107*, 1697.
(866) Sharma, P. K.; Van Doorn, A. R.; Staring, A. G. J. US Patent 5,490,010, 1996.
(867) Ding, J. J.; Jiu, H. F.; Bao, J.; Lu, J. C.; Gui, W. R.; Zhang, Q. J.; Gao, C. *J. Comb. Chem.* **2005**, *7*, 69.
(868) Luo, Y. H.; Yan, Q.; Wu, S.; Wu, W. X.; Zhang, Q. J. *J. Photochem. Photobiol. A* **2007**, *191*, 91.
(869) Cho, Y.; Choi, Y. K.; Sohn, S. H. *Appl. Phys. Lett.* **2006**, *89*, 051102.
(870) Liu, H. G.; Lee, Y. I.; Qin, W. P.; Jang, K. W.; Feng, X. S. *Mater. Lett.* **2004**, *58*, 1677.
(871) Liu, H. G.; Lee, Y. I.; Qin, W. P.; Jang, K. W.; Kim, S. S.; Feng, X. S. *J. Appl. Polym. Sci.* **2004**, *92*, 3524.
(872) Liu, H. G.; Lee, Y. I.; Feng, X. S.; Xiao, F.; Zhang, L.; Chen, X.; Jang, K. W.; Seo, H. J. *Colloids Surf. A* **2005**, *257*−*258*, 301.
(873) Liu, H. G.; Feng, X. S.; Jang, K.; Kim, S.; Won, T. J.; Cui, S.; Lee, Y. I. *J. Lumin.* **2007**, *127*, 307.
(874) Liu, H. G.; Xiao, F.; Zhang, W. S.; Chung, Y. H.; Seo, H. J.; Jang, K.; Lee, Y. I. *J. Lumin.* **2005**, *114*, 187.
(875) Pagnot, T.; Audebert, P.; Tribillon, G. *Chem. Phys. Lett.* **2000**, *322*, 572.
(876) de Souza, J. M.; Alves, S.; De Sa, G. F.; de Azevedo, W. M. *J. Alloys Compd.* **2002**, *344*, 320.
(877) Kai, J.; Parra, D. F.; Brito, H. F. *J. Mater. Chem.* **2008**, *18*, 4549.
(878) O'Riordan, A.; O'Connor, E.; Moynihan, S.; Llinares, X.; Van Deun, R.; Fias, P.; Nockemann, P.; Binnemans, K.; Redmond, G. *Thin Solid Films* **2005**, *491*, 264.
(879) Parra, D. F.; Brito, H. F.; Do Rosario Matos, J.; Dias, L. C. *J. Appl. Polym. Sci* **2002**, *83*, 2716.
(880) Lin, S.; Feuerstein, R. J.; Mickelson, A. *J. Appl. Phys.* **1996**, *79*, 2868.
(881) Manseki, K.; Yanagida, S. *Phys. Status Solidi A* **2008**, *205*, 23.
(882) Manseki, K.; Hasegawa, Y.; Wada, Y.; Ichida, H.; Kanematsu, Y.; Kushida, T. *J. Lumin.* **2007**, *122*, 262.
(883) Manseki, K.; Yanagida, S. *Chem. Commun.* **2007**, 1242.
(884) Gao, R.; Koeppen, C.; Zheng, G. Q.; Garito, A. F. *Appl. Opt.* **1998**, *37*, 7100.
(885) Srdanov, V. I.; Robinson, M. R.; Bartl, M. H.; Bu, X.; Bazan, G. C. *Appl. Phys. Lett.* **2002**, *80*, 3042.
(886) Yang, C. Y.; Srdanov, V.; Robinson, M. R.; Bazan, G. C.; Heeger, A. J. *Adv. Mater.* **2002**, *14*, 980.
(887) Wu, S.; Yu, X. O.; Huang, J. T.; Shen, J.; Yan, Q.; Wang, X.; Wu, W. X.; Luo, Y. H.; Wang, K. Y.; Zhang, Q. J. *J. Mater. Chem.* **2008**, *18*, 3223.
(888) Yanagida, S.; Hasegawa, Y.; Murakoshi, K.; Wada, Y.; Nakashima, N.; Yamanaka, T. *Coord. Chem. Rev.* **1998**, *171*, 461.
(889) Hasegawa, Y.; Murakoshi, K.; Wada, Y.; Yanagida, S.; Kim, J. H.; Nakashima, N.; Yamanaka, T. *Chem. Phys. Lett.* **1996**, *248*, 8.
(890) Hasegawa, Y.; Kimura, Y.; Murakoshi, K.; Wada, Y.; Kim, J. H.; Nakashima, N.; Yamanaka, T.; Yanagida, S. *J. Phys. Chem.* **1996**, *100*, 10201.
(891) Hasegawa, Y.; Murakoshi, K.; Wada, Y.; Kim, J. H.; Nakashima, N.; Yamanaka, T.; Yanagida, S. *Chem. Phys. Lett.* **1996**, *260*, 173.
(892) Hasegawa, Y.; Sogabe, K.; Wada, Y.; Kitamura, T.; Nakashima, N.; Yanagida, S. *Chem. Lett.* **1999**, 35.
(893) Kuriki, K.; Kobayashi, T.; Imai, N.; Tamura, T.; Tagaya, A.; Koike, Y.; Okamoto, Y. *Proc. SPIE* **2000**, *3939*, 28.
(894) Le Quang, A. Q.; Besson, E.; Hierle, R.; Mehdi, A.; Reye, C.; Corriu, R.; Ledoux-Rak, I. *Opt. Mater.* **2007**, *29*, 941.
(895) Lenaerts, P.; Driesen, K.; Van Deun, R.; Binnemans, K. *Chem. Mater.* **2005**, *17*, 2148.
(896) Ueba, Y.; Banks, E.; Okamoto, Y. *J. Appl. Polym. Sci.* **1980**, *25*, 2007.
(897) Froidevaux, P.; Happel, S.; Chauvin, A. S. *Chimia* **2006**, *60*, 203.
(898) Chauvin, A. S.; Bünzli, J.-C. G.; Bochud, F.; Scopelliti, R.; Froidevaux, P. *Chem.*−*Eur. J.* **2006**, *12*, 6852.
(899) Tang, B.; Jin, L. P.; Zheng, X. J.; Zhu, L. Y. *Spectrochim. Acta A* **1999**, *55*, 1731.
(900) Tang, B.; Jin, L. P.; Zheng, X. J.; Yang, M. S. *J. Appl. Polym. Sci.* **1999**, *74*, 2588.
(901) Wang, D. M.; Zhang, J. H.; Lin, Q.; Fu, L. S.; Zhang, H. J.; Yang, B. *J. Mater. Chem.* **2003**, *13*, 2279.
(902) Wang, L. H.; Wang, W.; Zhang, W.-G.; Kang, E. T.; Huang, W. *Chem. Mater.* **2000**, *12*, 2212.
(903) Pei, J.; Liu, X. L.; Yu, W. L.; Lai, Y. H.; Niu, Y. H.; Cao, Y. *Macromolecules* **2002**, *35*, 7274.
(904) Feng, H. Y.; Jian, S. H.; Jian, Y. P.; Lei, Z. Q.; Wang, R. M. *J. Appl. Polym. Sci.* **1998**, *68*, 1605.
(905) Bender, J. L.; Corbin, P. S.; Fraser, C. L.; Metcalf, D. H.; Richardson, F. S.; Thomas, E. L.; Urbas, A. M. *J. Am. Chem. Soc.* **2002**, *124*, 8526.
(906) Wu, Q.; Zhong, C. F.; Guo, R. F.; He, A. H.; Huang, H. L. *J. Rare Earths* **2007**, *25*, 562.
(907) Ling, Q. D.; Yang, M. J.; Wu, Z. F.; Zhang, X. M.; Wang, L. H.; Zhang, W. G. *Polymer* **2001**, *42*, 4605.
(908) Ling, Q. D.; Yang, M. J.; Zhang, W. G.; Lin, H. Z.; Yu, G.; Bai, F. L. *Thin Solid Films* **2002**, *417*, 127.
(909) Ling, Q. D.; Kang, E. T.; Neoh, K. G.; Huang, W. *Macromolecules* **2003**, *36*, 6995.
(910) Ling, Q. D.; Cai, Q. J.; Kang, E. T.; Neoh, K. G.; Zhu, F. R.; Huang, W. *J. Mater. Chem.* **2004**, *1364*, 2741.
(911) Ling, Q. D.; Song, Y.; Ding, S. J.; Zhu, C. X.; Chan, D. S. H.; Kwong, D. L.; Kang, E. T.; Neoh, K. G. *Adv. Mater.* **2005**, *17*, 455.
(912) Song, Y.; Ling, Q. D.; Zhu, C.; Kang, E. T.; Chan, D. S. H.; Wang, Y. H.; Kwong, D. L. *IEEE Electron Device Lett.* **2006**, *27*, 154.
(913) Pizzoferrato, R.; Ziller, T.; Paolesse, R.; Mandoj, F.; Micozzi, A.; Ricci, A.; Lo Sterzo, C. *Chem. Phys. Lett.* **2006**, *426*, 124.
(914) Kawa, M.; Fréchet, J. M. J. *Chem. Mater.* **1998**, *10*, 286.
(915) Kawa, M.; Fréchet, J. M. J. *Thin Solid Films* **1998**, *331*, 259.
(916) Kawa, M.; Takahagi, T. *Chem. Mater.* **2004**, *16*, 2282.
(917) Stone, D. L.; Dykes, G. M.; Smith, D. K. *Dalton Trans.* **2004**, 3902.
(918) Pitois, C.; Vestberg, R.; Rodlert, M.; Malmstrom, E.; Hult, A.; Lindgren, M. *Opt. Mater.* **2003**, *21*, 499.

(919) Pitois, C.; Hult, A.; Lindgren, M. *J. Lumin.* **2005**, *111*, 265.
(920) Glomm, W. R.; Ese, M. H. G.; Volden, S.; Pitois, C.; Hult, A.; Sjoblom, J. *Colloids Surf. A* **2007**, *299*, 186.
(921) Zhu, L. Y.; Toug, X. F.; Li, M. Z.; Wang, E. *J. Phys. Chem. B* **2001**, *105*, 2461.
(922) Vicinelli, V.; Ceroni, P.; Maestri, M.; Balzani, V.; Gorka, M.; Vogtle, F. *J. Am. Chem. Soc.* **2002**, *124*, 6461.
(923) Vogtle, F.; Gorka, M.; Vicinelli, V.; Ceroni, P.; Maestri, M.; Balzani, V. *ChemPhysChem* **2001**, *2*, 769.
(924) Saudan, C.; Ceroni, P.; Vicinelli, V.; Maestri, M.; Balzani, V.; Gorka, M.; Lee, S. K.; van Heyst, J.; Vogtle, F. *Dalton Trans.* **2004**, 1597.
(925) Giansante, C.; Ceroni, P.; Balzani, V.; Vogtle, F. *Angew. Chem., Int. Ed.* **2008**, *47*, 5422.
(926) Branchi, B.; Ceroni, P.; Bergamini, G.; Balzani, V.; Maestri, M.; van Heyst, J.; Lee, S. K.; Luppertz, F.; Vogtle, F. *Chem.—Eur. J.* **2006**, *12*, 8926.
(927) Cross, J. P.; Lauz, M.; Badger, P. D.; Petoud, S. *J. Am. Chem. Soc.* **2004**, *126*, 16278.
(928) Antoni, P.; Malkoch, M.; Vamvounis, G.; Nystrom, D.; Nystrom, A.; Lindgren, M.; Hult, A. *J. Mater. Chem.* **2008**, *18*, 2545.
(929) Kim, H. K.; Baek, N. S.; Oh, J. B.; Ka, J. W.; Roh, S. G.; Kim, Y. H.; Nah, M. K.; Hong, K. S.; Song, B. J.; Zhou, G. J. *J. Nonlinear Opt. Phys. Mater.* **2005**, *14*, 555.
(930) Oh, J. B.; Nah, M. K.; Kim, Y. H.; Kang, M. S.; Ka, J. W.; Kom, H. K. *Adv. Funct. Mater.* **2007**, *17*, 413.
(931) Kim, H. K.; Oh, J. B.; Baek, N. S.; Roh, S. G.; Nah, M. K.; Kim, Y. H. *Bull. Korean Chem. Soc.* **2005**, *26*, 201.
(932) Oh, J. B.; Paik, K. L.; Ka, J. W.; Roh, S. G.; Nah, M. K.; Kim, H. K. *Mater. Sci. Eng., C* **2004**, *24*, 257.
(933) Kim, Y. H.; Baek, N. S.; Oh, J. B.; Nah, M. K.; Roh, S. G.; Song, B. J.; Kim, H. K. *Macromol. Res.* **2007**, *15*, 272.
(934) Oh, J. B.; Kim, Y. H.; Nah, M. K.; Kim, H. K. *J. Lumin.* **2005**, *111*, 255.
(935) Nah, M. K.; Oh, J. B.; Kim, H. K.; Choi, K. H.; Kim, Y.-R.; Kang, J. G. *J. Phys. Chem. A* **2007**, *111*, 6157.
(936) Kim, H. K.; Roh, S. G.; Hong, K. S.; Ka, J. W.; Baek, N. S.; Oh, J. B.; Nah, M. K.; Cha, Y. H.; Ko, J. *Macromol. Res.* **2003**, *11*, 133.
(937) Kim, H. K.; Oh, J. B.; Baek, N. S.; Roh, S. G.; Nah, M. K.; Kim, Y. H. *Bull. Chem. Soc. Jpn.* **2005**, *26*, 201.
(938) Baek, N. S.; Kim, Y. H.; Kim, H. K. *J. Nonlinear Opt. Phys. Mater.* **2006**, *15*, 369.
(939) Cao, R.; Sun, D. F.; Liang, Y. C.; Hong, M. C.; Tatsumi, K.; Shi, Q. *Inorg. Chem.* **2002**, *41*, 2087.
(940) Pan, L.; Huang, X. Y.; Li, J.; Wu, Y. G.; Zheng, N. W. *Angew. Chem., Int. Ed.* **2000**, *39*, 527.
(941) Pan, L.; Adams, K. M.; Hernandez, H. E.; Wang, X. T.; Zheng, C.; Hattori, Y.; Kaneko, K. *J. Am. Chem. Soc.* **2003**, *125*, 3062.
(942) Long, D. L.; Blake, A. J.; Champness, N. R.; Schroder, M. *Chem. Commun.* **2000**, 1369.
(943) Guillou, O.; Daiguebonne, C. Lanthanide-containing coordination polymers. In *Handbook on the Physics and Chemistry of Rare Earths*; Gschneidner, K. A., Jr., Bünzli, J.-C., Pescharsky, V., Eds.; Elsevier: Amsterdam, 2004; Vol. 34, Chapter 221, 359.
(944) Rocha, J.; Carlos, L. D. *Curr. Opin. Solid State Mater. Sci.* **2003**, *7*, 199.
(945) Allendorf, M. D.; Bauer, C. A.; Bhakta, R. K.; Houk, R. J. T. *Chem. Soc. Rev.* **2009**, *38*, 1330.
(946) Férey, G. *Chem. Soc. Rev.* **2008**, *37*, 191.
(947) Eddaoudi, M.; Moler, D. B.; Li, H. L.; Chen, B. L.; Reineke, T. M.; O'Keeffe, M.; Yaghi, O. M. *Acc. Chem. Res.* **2001**, *34*, 319.
(948) Cheetham, A. K.; Rao, C. N. R.; Feller, R. K. *Chem. Commun.* **2006**, 4780.
(949) Daiguebonne, C.; Kerbellec, N.; Bernot, K.; Gerault, Y.; Deluzet, A.; Guillou, O. *Inorg. Chem.* **2006**, *45*, 5399.
(950) Guo, X.; Zhu, G.; Sun, F.; Li, Z.; Zhao, X.; Li, X.; Wang, H.; Qiu, S. *Inorg. Chem.* **2006**, *45*, 2581.
(951) Pan, L.; Zheng, N.; Wu, Y.; Han, S.; Yang, R.; Huang, X.; Li, J. *Inorg. Chem.* **2001**, *40*, 828.
(952) Yang, X. P.; Jones, R. A.; Rivers, J. H.; Lai, R. P. J. *Dalton Trans.* **2007**, 3936.
(953) Wan, Y. H.; Jin, L. P.; Wang, K. Z.; Zhang, L. P.; Zheng, X. J.; Lu, S. Z. *New J. Chem.* **2002**, *26*, 1590.
(954) Qu, Y. L.; Ke, Y. X.; Lu, S. M.; Fan, R.; Pan, G. Q.; Li, J. M. *J. Mol. Struct.* **2005**, *734*, 7.
(955) de Bettencourt-Dias, A. *Inorg. Chem.* **2005**, *44*, 2734.
(956) Yan, H.; Yan, B.; Shao, M. *J. Solid State Chem.* **2009**, *182*, 657.
(957) Serre, C.; Ferey, C. *J. Mater. Chem.* **2002**, *12*, 3053.
(958) Deluzet, A.; Maudez, W.; Daiguebonne, C.; Guillou, O. *Cryst. Growth Des.* **2003**, *3*, 475.
(959) Wang, Z.; Jin, C. M.; Shao, T.; Li, Y. Z.; Zhang, K. L.; Zhang, H. T.; You, X. Z. *Inorg. Chem. Commun.* **2002**, *5*, 642.
(960) Zheng, X. J.; Jin, L. P.; Gao, S.; Lu, S. Z. *New J. Chem.* **2005**, *29*, 798.
(961) Kerbellec, N.; Daiguebonne, C.; Bernot, K.; Guillou, O.; Le Guillou, *J. Alloys Compd.* **2008**, *451*, 377.
(962) Rodrigues, M. O.; da Costa Junior, N. B.; de Simone, C. A.; Araujo, A. A. S.; Brito-Silva, A. M.; Paz, F. A. A.; de Mesquita, M. E.; Junior, S. A.; Freire, R. O. *J. Phys. Chem. B* **2008**, *112*, 4204.
(963) Soares-Santos, P. C. R.; Cunha-Silva, L.; Paz, F. A. A.; Ferreira, R. A. S.; Rocha, J.; Trindade, T.; Carlos, L. D.; Nogueira, H. I. S. *Cryst. Growth Des.* **2008**, *8*, 2505.
(964) Huang, W.; Wu, D. Y.; Zhou, P.; Yan, W. B.; Guo, D.; Duan, C. Y.; Meng, Q. J. *Cryst. Growth Des.* **2009**, *9*, 1361.
(965) Sun, Y. Q.; Yang, G. Y. *Dalton Trans.* **2007**, 3771.
(966) Wu, J.-Y.; Yeh, T.-T.; Wen, Y.-S.; Twu, J.; Lu, K.-L. *Cryst. Growth Des.* **2006**, *6*, 467.
(967) Surble, S.; Serre, C.; Millange, F.; Pelle, F.; Ferey, G. *Solid State Sci.* **2007**, *9*, 131.
(968) de Lill, D. T.; Cahill, C. L. *Chem. Commun.* **2006**, 4946.
(969) Millange, F.; Serre, C.; Marrot, J.; Gardant, N.; Pelle, F.; Ferey, G. *J. Mater. Chem.* **2004**, *14*, 642.
(970) Lill, D. T. d.; Cahill, C. L. *Cryst. Growth Des.* **2007**, *7*, 2390.
(971) de Lill, D. T.; Gunning, N. S.; Cahill, C. L. *Inorg. Chem.* **2005**, *44*, 258.
(972) de Lill, D. T.; de Bettencourt-Dias, A.; Cahill, C. L. *Inorg. Chem.* **2007**, *46*, 3960.
(973) Kim, Y.; Suh, M.; Jung, D. Y. *Inorg. Chem.* **2004**, *43*, 245.
(974) Dimos, A.; Tsaousis, D.; Michaelides, A.; Skoulika, S.; Golhen, S.; Ouahab, L.; Didierjean, C.; Aubry, A. *Chem. Mater.* **2002**, *14*, 2616.
(975) Liu, W.; Jiao, T.; Li, Y.; Liu, Q.; Tan, M.; Wang, H.; Wang, L. *J. Am. Chem. Soc.* **2004**, *126*, 2280.
(976) Gu, X. J.; Xue, D. F. *Cryst. Growth Des.* **2006**, *6*, 2551.
(977) Zhao, B.; Chen, X.-Y.; Cheng, P.; Liao, D.-Z.; Yan, S.-P.; Jiang, Z.-H. *J. Am. Chem. Soc.* **2004**, *126*, 15394.
(978) Zhu, X.; Lu, J.; Li, X.; Gao, S.; Li, G.; Xiao, F.; Cao, R. *Cryst. Growth Des.* **2008**, *8*, 1897.
(979) Chandler, B. D.; Cramb, D. T.; Shimizu, G. K. H. *J. Am. Chem. Soc.* **2006**, *128*, 10403.
(980) Sun, W. B.; Yan, P. F.; Li, G. M.; Xu, H.; Zhang, J. W. *J. Solid State Chem.* **2009**, *182*, 381.
(981) Kerbellec, N.; Kustaryono, D.; Haquin, V.; Etienne, M.; Daiguebonne, C.; Guillou, O. *Inorg. Chem.* **2009**, *48*, 2837.
(982) Chen, B. L.; Yang, Y.; Zapata, F.; Lin, G. N.; Qian, G. D.; Lobkovsky, E. B. *Adv. Mater.* **2007**, *19*, 1693.
(983) Chen, B.; Wang, L.; Zapata, F.; Qian, G.; Lobkovsky, E. B. *J. Am. Chem. Soc.* **2008**, *130*, 6718.
(984) Xu, H.; Jin, R. Z.; Wu, C. Y.; Yang, Y.; Qian, G. D. *Spectrosc. Spectral Anal.* **2008**, *28*, 1734.
(985) Chen, B.; Yang, Y.; Zapata, F.; Qian, G.; Luo, Y.; Zhang, J.; Lobkovsky, E. B. *Inorg. Chem.* **2006**, *45*, 8882.
(986) Müller-Buschbaum, K.; Gomez-Torres, S.; Larsen, P.; Wickleder, C. *Chem. Mater.* **2007**, *19*, 655.
(987) Fiedler, T.; Hilder, M.; Junk, P. C.; Kynast, U. H.; Lezhnina, M. M.; Warzala, M. *Eur. J. Inorg. Chem.* **2007**, 291.
(988) Sangeetha, N. M.; Maitra, U. *Chem. Soc. Rev.* **2005**, *34*, 821.
(989) Estroff, L. A.; Hamilton, A. D. *Chem. Rev.* **2004**, *104*, 1201.
(990) Kramarenko, E. Y.; Philippova, O. E.; Khokhlov, A. R. *Polym. Sci., Ser. C* **2006**, *48*, 1.
(991) De Paoli, G.; Dzolic, Z.; Rizzo, F.; De Cola, L.; Vögtle, F.; M̈; uller, W. M.; Richardt, G.; Zinic, M. *Adv. Funct. Mater.* **2007**, *17*, 821.
(992) Wang, Q. M.; Ogawa, K.; Toma, K.; Tamiaka, H. *Chem. Lett.* **2008**, *37*, 430.
(993) Smirnov, V. A.; Philippova, O. E.; Sukhadolski, G. A.; Khokhlov, A. R. *Macromolecules* **1998**, *31*, 1162.
(994) Smirnov, V. A.; Sukhadolski, G. A.; Philippova, O. E.; Khokhlov, A. R. *J. Phys. Chem. B* **1999**, *103*, 7621.
(995) Lis, S.; Wang, Z. M.; Choppin, G. R. *Inorg. Chim. Acta* **1995**, *239*, 139.
(996) Bekiari, V.; Lianos, P. *Langmuir* **2006**, *22*, 8602.
(997) Zhang, N.; Tang, S. H.; Liu, Y. *Spectrochim. Acta A* **2003**, *59*, 1107.
(998) McCoy, C. P.; Stomeo, F.; Plush, S. E.; Gunnlaugsson, T. *Chem. Mater.* **2006**, *18*, 4336.
(999) Gunnlaugsson, T.; McCoy, C. P.; Stomeo, F. *Tetrahedron Lett.* **2004**, *45*, 8403.
(1000) Winkleman, A.; Bracher, P. J.; Gitlin, I.; Whitesides, G. M. *Chem. Mater.* **2007**, *19*, 1362.
(1001) Yan, C. H.; Jiao, L. L.; Guo, C. F.; Zhang, M.; Qiu, G. M. *J. Rare Earths* **2008**, *26*, 660.
(1002) Vetrone, F.; Capobianco, J. A. *Int. J. Nanotechnol.* **2008**, *5*, 1306.
(1003) Dosev, D.; Nichkova, M.; Kennedy, I. M. *J. Nanosci. Nanotechnol.* **2008**, *8*, 1052.

(1004) Liu, G. K.; Chen, X. Y. Spectroscopic Properties of Lanthanides in Nano-materials. In *Handbook on the Physics and Chemistry of Rare Earths*; Gschneidner, K. A., Jr., Bünzli, J. C. G., Pescharsky, V. K., Eds.; Elsevier: Amsterdam, 2007; Vol. 37, Chapter 233, p 99.
(1005) Shen, J.; Sun, L. D.; Yan, C. H. *Dalton Trans.* **2008**, 5687.
(1006) Wang, F.; Liu, X. G. *Chem. Soc. Rev.* **2009**, *38*, 976.
(1007) Wang, L. Y.; Li, Y. D. *Chem.—Eur. J.* **2007**, *13*, 4203.
(1008) Wang, F.; Zhang, Y.; Fan, X. P.; Wang, M. Q. *Nanotechnology* **2006**, *17*, 1527.
(1009) Charbonniere, L. J.; Rehspringer, J. L.; Ziessel, R.; Zimmermann, Y. *New J. Chem.* **2008**, *32*, 1055.
(1010) Wong, K. L.; Law, G. L.; Murphy, M. B.; Tanner, P. A.; Wong, W. T.; Lam, P. K. S.; Lam, M. H. W. *Inorg. Chem.* **2008**, *47*, 5190.
(1011) Tamaki, K.; Yabu, H.; Isoshima, T.; Hara, M.; Shimomura, M. *Colloids Surf. A* **2006**, *284−285*, 355.
(1012) Harma, H.; Soukka, T.; Lonnberg, S.; Paukkunen, J.; Tarkkinen, P.; Lovgren, T. *Luminescence* **2000**, *15*, 351.
(1013) Soukka, T.; Harma, H.; Paukkunen, J.; Lovgren, T. *Anal. Chem.* **2001**, *73*, 2254.
(1014) Soukka, T.; Paukkunen, J.; Harma, H.; Lonnberg, S.; Lindroos, H.; Lovgren, T. *Clin. Chem.* **2001**, *47*, 1269.
(1015) Kokko, L.; Sandberg, K.; Lovgren, T.; Soukka, T. *Anal. Chim. Acta* **2004**, *503*, 155.
(1016) Tan, M. Q.; Wang, G. L.; Hai, X. D.; Ye, Z. Q.; Yuan, J. L. *J. Mater. Chem.* **2004**, *14*, 2896.
(1017) Wu, J.; Ye, Z. Q.; Wang, G. L.; Yuan, J. L. *Talanta* **2007**, *72*, 1693.
(1018) Sivakumar, S.; Diamente, P. R.; van Veggel, F. C. J. M. *Chem.—Eur. J.* **2006**, *12*, 5878.
(1019) Diamente, P. R.; Burke, R. D.; van Veggel, F. C. J. M. *Langmuir* **2006**, *22*, 1782.
(1020) Lu, H. C.; Yi, G. S.; Zhao, S. Y.; Chen, D. P.; Guo, L. H.; Cheng, J. *J. Mater. Chem.* **2004**, *14*, 1336.
(1021) Choi, J. K.; Kim, J. C.; Lee, Y. K.; Kim, I. S.; Park, Y. K.; Hur, N. H. *Chem. Commun.* **2007**, 1644.
(1022) Corr, S. A.; Rakovich, Y. P.; Gun'ko, Y. K. *Nanoscale Res. Lett.* **2008**, *3*, 87.
(1023) Son, A.; Dhirapong, A.; Dosev, D. K.; Kennedy, I. M.; Weiss, R. M.; Hristova, K. R. *Anal. Bioanal. Chem.* **2008**, *390*, 1829.
(1024) Son, A.; Dosev, D.; Nichkova, M.; Ma, Z.; Kennedy, I. M.; Scow, K. M.; Hristova, K. R. *Anal. Biochem.* **2007**, *370*, 186.
(1025) Lewis, D. J.; Day, T. M.; MacPherson, J. V.; Pikramenou, Z. *Chem. Commun.* **2006**, 1433.
(1026) Ipe, B. I.; Yoosaf, K.; Thomas, K. G. *J. Am. Chem. Soc.* **2006**, *128*, 1907.
(1027) Massue, J.; Quinn, S. J.; Gunnlaugsson, T. *J. Am. Chem. Soc.* **2008**, *130*, 6900.
(1028) Reisfeld, R.; Gaft, M.; Saridarov, T.; Panczer, G.; Zelner, M. *Mater. Lett.* **2000**, *45*, 154.
(1029) Bol, A. A.; van Beek, R.; Meijerink, A. *Chem. Mater.* **2002**, *14*, 1121.
(1030) Julian, B.; Planelles, J.; Cordoncillo, E.; Escribano, P.; Aschehoug, P.; Sanchez, C.; Viana, B.; Pelle, F. *J. Mater. Chem.* **2006**, *16*, 4612.
(1031) Hayakawa, T.; Selvan, S. T.; Nogami, M. *J. Lumin.* **2000**, *87−89*, 532.
(1032) Selvan, S. T.; Hayakawa, T.; Nogami, M. *J. Non-Cryst. Solids* **2001**, *291*, 137.
(1033) Zalewska, M.; Klonkowski, A. M. *Phys. Chem. Glasses* **2007**, *48*, 117.
(1034) Planelles-Arago, J.; Julian-Lopez, B.; Cordoncillo, E.; Escribano, P.; Pellé, F.; Viana, B.; Sanchez, C. *J. Mater. Chem.* **2008**, *18*, 5193.
(1035) Ehrhart, G.; Capoen, B.; Robbe, O.; Beclin, F.; Boy, P.; Turrell, S.; Bouazaoui, M. *Opt. Mater.* **2008**, *30*, 1595.
(1036) Morita, M.; Rau, D.; Fujii, H.; Minami, Y.; Murakami, S.; Baba, M.; Yoshita, M.; Akiyama, H. *J. Lumin.* **2000**, *87−89*, 478.
(1037) Hayakawa, T.; Selvan, S. T.; Nogami, M. *J. Sol-Gel Sci. Technol.* **2000**, *19*, 779.
(1038) Jose, G.; Jose, G.; Thomas, V.; Joseph, C.; Iyyyachen, M. A.; Unnikrishnan, N. V. *J. Fluoresc.* **2004**, *14*, 733.
(1039) Jose, G.; Thomas, V.; Fernandez, T. T.; Adiyodi, A. K.; Joseph, C.; Ittyachen, M. A.; Unnikrishnan, N. V. *Physica B* **2005**, *357*, 270.
(1040) Jose, G.; Joseph, C.; Ittyachen, M. A.; Unnikrishnan, N. V. *Opt. Mater.* **2007**, *29*, 1495.
(1041) Mathew, S.; Rejikumar, P. R.; Joseph, X.; Unnikrishnan, N. V. *Opt. Mater.* **2007**, *29*, 1689.
(1042) Selvan, S. T.; Hayakawa, T.; Nogami, M. *J. Non-Cryst. Sol.* **2001**, *291*, 137.
(1043) Mu, J.; Liu, L.; Kang, S. Z. *Nanoscale Res. Lett.* **2007**, *2*, 100.
(1044) Liu, L. Y.; Zhang, Z. Q.; Kang, S. Z.; Mu, J. *J. Dispersion Sci. Technol.* **2007**, *28*, 769.
(1045) Klonkowski, A. M.; Zalewska, M.; Koscielska, B. *J. Non-Cryst. Sol.* **2006**, *352*, 4183.
(1046) Zalewska, M.; Klonkowski, A. *Opt. Mater.* **2008**, *30*, 725.
(1047) Fukushima, M.; Managaki, N.; Fujii, M.; Yanagi, H.; Hayashi, S. *J. Appl. Phys.* **2005**, *98*, 024316.
(1048) Hayakawa, T.; Furuhashi, K.; Nogami, M. *J. Phys. Chem. B* **2004**, *118*, 11301.
(1049) Hayakawa, T.; Selvan, S. T.; Nogami, M. *Appl. Phys. Lett.* **1999**, *74*, 1513.
(1050) Selvan, S. T.; Hayakawa, T.; Nogami, M. *J. Phys. Chem. B* **1999**, *103*, 7064.
(1051) Almeida, R. M.; Marques, A. C.; Ferrari, M. *J. Sol-Gel Sci. Technol.* **2003**, *26*, 891.
(1052) Marques, A. C.; Ramos, A. R.; Alves, E.; Almeida, R. M. *Nucl. Instrum. Methods Phys. Res. B* **2004**, *219*, 923.
(1053) Marques, A. C.; Almeida, R. M. *J. Non-Cryst. Solids* **2007**, *353*, 2613.
(1054) Reisfeld, R.; Saraidarov, T.; Levchenko, V. *J. Sol-Gel Sci. Technol.* **2009**, *50*, 194.
(1055) Geddes, C. D.; Lakowicz, J. R. *J. Fluoresc.* **2002**, *12*, 121.
(1056) Mertens, H.; Koenderink, A. F.; Polman, A. *Phys. Rev. B* **2007**, *76*, 115123.
(1057) Mertens, H.; Polman, A. *Appl. Phys. Lett.* **2006**, *89*, 211107.
(1058) Sudarsan, V.; Sivakumar, S.; van Veggel, F. C. J. M.; Raudsepp, M. *Chem. Mater.* **2005**, *17*, 4736.
(1059) Sivakumar, S.; van Veggel, F. C. J. M.; Raudsepp, M. *ChemPhysChem* **2007**, *8*, 1677.
(1060) Stouwdam, J. W.; van Veggel, F. C. J. M. *Langmuir* **2004**, *20*, 11763.
(1061) Sivakumar, S.; van Veggel, F. C. J. M.; Raudsepp, M. *J. Am. Chem. Soc.* **2005**, *127*, 12464.
(1062) Bo, S.; Wang, J.; Zhao, H.; Ren, H.; Wang, Q.; Xu, G.; Zhang, X.; Liu, X.; Zhen, Z. *Appl. Phys. B: Laser Opt.* **2008**, *91*, 79.
(1063) Que, W. X.; Kam, C. H.; Zhou, Y.; Lam, Y. L.; Chan, Y. C. *J. Appl. Phys.* **2001**, *90*, 4865.
(1064) Que, W. X.; Zhou, Y.; Lam, Y. L.; Zhou, J.; Chan, Y. C.; Kam, C. H.; Gan, L. H.; Deen, G. R. *J. Appl. Phys.* **2001**, *89*, 3058.
(1065) Que, W. X.; Kam, C. H. *Opt. Commun.* **2006**, *206*, 211.
(1066) Que, W. X.; Hu, X.; Uddin, A.; Liu, W. G. *Mater. Lett.* **2005**, *59*, 1614.
(1067) Schmechel, R.; Kennedy, M.; von Seggern, H.; Winkler, H.; Kolbe, M.; Fischer, R. A.; Li, X. M.; Benker, A.; Winterer, M.; Hahn, H. *J. Appl. Phys.* **2001**, *89*, 1679.
(1068) Chen, W.; Joly, A. G.; Kowalchuk, C. M.; Malm, J. O.; Huang, Y. N.; Bovin, J. O. *J. Phys. Chem. B* **2002**, *106*, 7034.
(1069) Soares-Santos, P. C. R.; Nogueira, H. I. S.; Felix, V.; Drew, M. G. B.; Sa Ferreira, R. A.; Carlos, L. D.; Trindade, T. *Chem. Mater.* **2003**, *15*, 100.
(1070) Iwu, K. O.; Soares-Santos, P. C. R.; Nogueira, H. I. S.; Carlos, L. D.; Trindade, T. *J. Phys. Chem. C* **2009**, *113*, 7567.
(1071) Lezhnina, M. M.; Kynast, U. *J. Alloys Compd.* **2008**, *451*, 545.
(1072) Althues, H.; Henle, J.; Kaskel, S. *Chem. Soc. Rev.* **2007**, *36*, 1454.
(1073) Goubard, F.; Vidal, F.; Bazzi, R.; Tillement, O.; Chevrot, C.; Teyssié, D. *J. Lumin.* **2007**, *126*, 289.
(1074) Dekker, R.; Klunder, D. J. W.; Borreman, A.; Diemeer, M. B. J.; Wörhoff, K.; Driessen, A.; Stouwdam, J. W.; van Veggel, F. C. J. M. *Appl. Phys. Lett.* **2004**, *85*, 6104.
(1075) Wang, J. S.; Hu, J.; Tang, D. H.; Liu, X. H.; Zen, Z. *J. Mater. Chem.* **2007**, *17*, 1597.
(1076) Kumar, G. A.; Chen, C. W.; Ballato, J.; Riman, R. E. *Chem. Mater.* **2007**, *19*, 1523.
(1077) Ji, J. M.; Coffer, J. L. *J. Phys. Chem. B* **2002**, *106*, 3860.
(1078) Althues, H.; Simon, P.; Kaskel, S. *J. Mater. Chem.* **2007**, *17*, 758.
(1079) Le Quang, A. Q.; Zyss, J.; Ledoux, I.; Truong, V. G.; Jurdyc, A. M.; Jacquier, B.; Le, D. H.; Gibaud, A. *Chem. Phys.* **2005**, *318*, 33.
(1080) Hui, Y. Y.; Lee, C. Y.; Lin, C. F. *Proceedings of the 7th IEEE Conference on Nanotechnology*, August 2−5, 2007 Hong Kong, P.R CHINA; IEEE: Piscataway, NJ, 2007, Vol. 1−3, p 866.
(1081) Lin, C. F.; Leey, C. Y.; Lu, W. B.; Su, W. F.; Hui, Y. Y. *Proceedings of the 7th IEEE Conference on Nanotechnology*, August 2−5, 2007 Hong Kong, P.R CHINA; IEEE: Piscataway, NJ, 2007, Vol. 1−3, 862.
(1082) Xu, C. H.; Jia, R. P.; Ouyang, C. F.; Wang, X.; Yao, G. Y. *Chin. Opt. Lett.* **2008**, *6*, 763.
(1083) Yu, H. Q.; Song, H. W.; Pan, G. H.; Fan, L. B.; Li, S. W.; Bai, X.; Lu, S. Z.; Zhao, H. F. *J. Nanosci. Nanotechnol.* **2008**, *8*, 6017.
(1084) Dong, B.; Song, H. W.; Yu, H. Q.; Zhang, H.; Qin, R. F.; Bai, X.; Pan, G. H.; Lu, S. Z.; Wang, F.; Fan, L. B.; Dai, Q. L. *J. Phys. Chem. C* **2008**, *112*, 1435.
(1085) Musikhin, S.; Bakueva, L.; Sargent, E. H.; Shik, A. *J. Appl. Phys.* **2002**, *91*, 6679.
(1086) Chen, Q. H.; Zheng, S. N.; Huang, C. H.; Zhang, W. G. *Appl. Surf. Sci.* **2008**, *254*, 5304.
(1087) Andric, Z.; Dramicanin, M. D.; Jokanovic, V.; Dramicanin, T.; Mitric, M.; Viana, B. *J. Optoelectron. Adv. Mater.* **2006**, *8*, 829.

(1088) Bühler, G.; Feldmann, C. *Appl. Phys. A: Mater. Sci. Process.* **2007**, *87*, 631.
(1089) Bühler, G.; Zharkouskaya, A.; Feldmann, C. *Solid State Sci.* **2008**, *10*, 461.
(1090) Zharkouskaya, A.; Feldmann, C.; Trampert, K.; Heering, W.; Lemmer, U. *Eur. J. Inorg. Chem.* **2008**, 873.
(1091) Bühler, G.; Feldmann, C. *Angew. Chem., Int. Ed.* **2006**, *45*, 4864.
(1092) Zhao, D.; Qin, W. P.; Zhang, J. S.; Wu, C. F.; Qin, G. S.; De, G. J.; Zhang, J. S.; Lu, S. Z. *Chem. Phys. Lett.* **2005**, *403*, 129.
(1093) Zhao, D.; Qin, W. P.; Wu, C. F.; Qin, G. S.; Zhang, J. S.; Lu, S. Z. *Chem. Phys. Lett.* **2004**, *388*, 400.
(1094) Shchukin, D. G.; Sukhorukov, G. B.; Möhwald, H. *J. Phys. Chem. B* **2004**, *108*, 19109.
(1095) Daiguebonne, C.; Kerbellec, N.; Guillou, O.; Bünzli, J. C.; Gumy, F.; Catala, L.; Mallah, T.; Audebrand, N.; Gerault, Y.; Bernot, K.; Calvez, G. *Inorg. Chem.* **2008**, *47*, 3700.
(1096) Edser, C. *Plast., Addit. Compd.* **2002**, *4* (3), 20.
(1097) Shchelokov, R. N. *Vestnik. Acad. Nauk USSR* **1986**, *10*, 50.
(1098) Raida, V. S.; Ivanitskii, A. E.; Bushkov, A. V.; Andrienko, O. S.; Tolstikov, G. A. *Atmos. Oceanic Opt.* **2003**, *16*, 1029.
(1099) Raida, V. S.; Minich, A. S.; Ivanitsky, A. E.; Tolstikov, G. A. *Proc. SPIE* **2003**, *5027*, 197.
(1100) Minich, A. S.; Minich, I. B.; Zelen'chukova, N. S.; Karnachuk, R. A.; Golovatskaya, I. F.; Efimova, M. V.; Raida, V. S. *Russian J. Plant Physiol.* **2006**, *53*, 762.
(1101) Goldburt, E. T.; Bolchoukhine, V. A.; Levonovitch, B. N.; Sochtine, N. P.; Sicinano, A.; Sandy, M.; von Gundlach, P. World Patent 2000024243, 2002.
(1102) Minich, I.; Minich, A.; Karnachuk, R.; Golovazkaja, I.; Raida, V. *Proceedings of the 5th Korea-Russia International Symposium on Science and Technology*; 2001, p 77.
(1103) Goldburt, E. T.; Bolchoukhine, V. A.; Levonovitch, B. N.; Sochtine, N. P. US Patent 6,153,665, 2000.
(1104) Yang, C.; Sun, Z. F.; Liu, L.; Zhang, L. Q. *J. Mater. Sci.* **2008**, *43*, 1681.
(1105) IkedaIkeda, M.; Yoshioka, J.; Shirasaki, S.; Kiyoyanagi, N.; Kitayama, Y. US Patent 20060145122, 2006.
(1106) Suyver, J. F.; Meijerink, A. *Chem. Weekbl.* **2002**, *98* (4), 12.
(1107) Li, H.; Inoue, S.; Ueda, D.; Machida, K.; Adachi, G. *Electrochem. Solid State Lett.* **1999**, *2*, 354.
(1108) Li, H.; Inoue, S.; Machida, K.; Adachi, G. *J. Electrochem. Soc.* **1997**, *144*, 4054.
(1109) Jin, T.; Inoue, S.; Tsutsumi, S.; Machida, K.; Adachi, G. *Chem. Lett.* **1997**, *2*, 171.
(1110) Reisfeld, R.; Zusman, R. US Patent 4,661,649, 1987.
(1111) Bell, C. D.; Howse, J. H. C. US Patent 5,435,937, 1995.
(1112) Slooff, L. H.; van Blaaderen, A.; Polman, A.; Hebbink, G. A.; Klink, S. I.; Van Veggel, F. C. J. M.; Reinhoudt, D. N.; Hofstraat, J. W. *J. Appl. Phys.* **2002**, *91*, 3955.
(1113) Kik, P. G.; Polman, A. *MRS Bull.* **1998**, *23*, 48.
(1114) Karve, G.; Bihari, B.; Chen, R. T. *Appl. Phys. Lett.* **2000**, *77*, 1253.
(1115) Kuriki, K.; Kobayashi, T.; Imai, N.; Tamura, T.; Tagaya, A.; Koike, Y.; Okamoto, Y. *Proc. SPIE* **2000**, *3939*, 28.
(1116) Slooff, L. H.; Polman, A.; Klink, S. I.; Hebbink, G. A.; Grave, L.; van Veggel, F. C. J. M.; Reinhoudt, D. N.; Hofstraat, J. W. *Opt. Mater.* **2000**, *14*, 101.
(1117) Kobayashi, T.; Nakatsuka, S.; Iwafuji, T.; Kuriki, K.; Imai, N.; Nakamoto, T.; Claude, C. D.; Sasaki, K.; Koike, Y. *Appl. Phys. Lett.* **1997**, *71*, 2421.
(1118) Mataki, H.; Tsuchii, K.; Mibuka, N.; Suzuki, A.; Taniguchi, J. S. H.; Yamashita, K.; Oe, K. *J. Photopolym. Sci. Technol.* **2007**, *20*, 67.
(1119) Moynihan, S.; Van Deun, R.; Binnemans, K.; Kruger, J.; von Pagen, G.; Kewell, A.; Craen, G.; Redmond, G. *Opt. Mater.* **2007**, *29*, 1798.
(1120) Schimitschek, E. J.; Schwarz, E. G. K. *Nature* **1962**, *196*, 832.
(1121) Whan, R. E.; Crosby, G. A. *J. Mol. Spectrosc.* **1962**, *8*, 315.
(1122) Filipescu, N.; Kagan, M. R.; McAvoy, N.; Serafin, F. A. *Nature* **1962**, *196*, 467.
(1123) Lempicki, A.; Samelson, H. *Phys. Lett.* **1963**, *4*, 133.
(1124) Samelson, H.; Lempicki, A.; Brecher, C.; Brophy, V. A. *Appl. Phys. Lett.* **1964**, *5*, 173.
(1125) Nehrich, R. B.; Schimitschek, E. J.; Trias, J. A. *Phys. Lett.* **1964**, *12*, 198.
(1126) Schimitschek, E. J.; Nehrich, R. B. *J. Appl. Phys.* **1964**, *34*, 2786.
(1127) Schimitschek, E. J.; Trias, J. A.; Nehrich, R. B. *J. Appl. Phys.* **1965**, *36*, 867.
(1128) Schimitschek, E. J.; Trias, J. A.; Nehrich, R. B. *J. Chem. Phys.* **1965**, *42*, 788.
(1129) Bhaumik, M. L.; Higa, S.; Lee, S. M.; Weinberg, M.; Fletcher, P. C.; Nugent, L. J.; Telk, C. L. *J. Phys. Chem.* **1964**, *68*, 1490.
(1130) Schimitschek, E. *J. Appl. Phys. Lett.* **1963**, *7*, 117.
(1131) Lempicki, A.; Brecher, C.; Samelson, H. *J. Chem. Phys.* **1964**, *41*, 1214.
(1132) Samelson, H.; Brophy, V. A.; Brecher, C.; Lempicki, A. *J. Chem. Phys.* **1964**, *41*, 3998.
(1133) Winston, H.; Marsh, O. J.; Telk, C. L.; Suzuki, C. K. *J. Chem. Phys.* **1963**, *39*, 267.
(1134) Brecher, C.; Samelson, H.; Lempicki, A. *J. Chem. Phys.* **1965**, *42*, 1081.
(1135) Bjorklund, S.; Kellmeyer, G.; Hurt, C. R.; McAvoy, N.; Filipescu, N. *Appl. Phys. Lett.* **1967**, *10*, 160.
(1136) Huffmann, E. H. *Phys. Lett.* **1963**, *7*, 237.
(1137) Huffmann, E. H. *Nature* **1963**, *200*, 158.
(1138) Whittaker, B. *Nature* **1970**, *228*, 157.
(1139) Ross, D. L.; Blanc, J. *Adv. Chem. Ser.* **1967**, *71*, 155.
(1140) Schimitschek, E. J.; Trias, J. A.; Nehrich, R. B. *Appl. Phys. Lett.* **1966**, *9*, 103.
(1141) Taniguchi, H.; Tomisawa, H.; Kido, J. *Appl. Phys. Lett.* **1995**, *66*, 1578.
(1142) Taniguchi, H.; Kido, J.; Nishiya, M.; Sasaki, S. *Appl. Phys. Lett.* **1995**, *67*, 1060.
(1143) Hasegawa, Y.; Wada, Y.; Yanagida, S.; Kawai, H.; Yasuda, N.; Nagamura, T. *Appl. Phys. Lett.* **2003**, *83*, 3599.
(1144) Nakamura, K.; Hasegawa, Y.; Kawai, H.; Yasuda, N.; Kanehisa, N.; Kai, Y.; Nagamura, T.; Yanagida, S.; Wada, Y. *J. Phys. Chem. A* **2007**, *111*, 3029.
(1145) Müllen, K., Scherf, U., Eds. *Organic Light Emitting Devices*; Wiley-VCH: Weinheim, Germany, 2006.
(1146) Yersin, H. *Highly Efficient OLEDs with Phosphorescent Materials*; Wiley-VCH: Weinheim, Germany, 2008.
(1147) Hung, L. S.; Chen, C. H. *Mater. Sci. Eng., R* **2002**, *39*, 143.
(1148) Tang, C. W.; Van Slyke, S. A. *Appl. Phys. Lett.* **1987**, *51*, 913.
(1149) Burroughes, J. H.; Bradley, D. D. C.; Brown, A. R.; Marks, R. N.; Mackay, K.; Friend, R. H.; Burns, P. L.; Holmes, A. B. *Nature* **1990**, *347*, 539.
(1150) Kido, J.; Okamoto, Y. *Chem. Rev.* **2002**, *102*, 2357.
(1151) Katkova, M. A.; Vitukhnovsky, A. G.; Bochkarev, M. N. *Usp. Khim.* **2005**, *74*, 1193.
(1152) de Bettencourt-Dias, A. *Dalton Trans.* **2007**, 2229.
(1153) Bian, Z. Q.; Huang, C. H. Progess in Electroluminescence Based on Lanthanide Complexes. In *Highly Efficient OLEDs with Phosphorescent Materials*; Yersin, H., Ed.; Wiley-VCH: Weinheim, Germany, 2008, Chapter 12, p 391.
(1154) Kido, J.; Nagai, K.; Ohashi, Y. *Chem. Lett.* **1990**, 657.
(1155) Kido, J.; Nagai, K.; Okamoto, Y.; Skotheim, T. *Chem. Lett.* **1991**, 1267.
(1156) Sano, T.; Fujita, M.; Fujii, T.; Hamada, Y.; Shibata, K.; Kuroki, K. *Jpn. J. Appl. Phys.* **1995**, *34*, 1883.
(1157) Kido, J.; Hayase, H.; Hongawa, K.; Nagai, K. *Appl. Phys. Lett.* **1994**, *65*, 2124.
(1158) Yu, J. B.; Zhou, L.; Zhang, H. J.; Zheng, Y. X.; Li, H. R.; Deng, R. P.; Peng, Z. P.; Li, Z. F. *Inorg. Chem.* **2005**, *44*, 1611.
(1159) Sun, P. P.; Duan, J. P.; Lih, J. J.; Cheng, C. H. *Adv. Funct. Mater.* **2003**, *13*, 683.
(1160) Kido, J.; Ikeda, W.; Kimura, M.; Nagai, K. *Jpn. J. Appl. Phys.* **1996**, *35*, L394.
(1161) Liang, C. J.; Hong, Z. R.; Liu, X. Y.; Zhao, D. X.; Zhao, D.; Li, W. L.; Peng, J. B.; Yu, J. Q.; Lee, C. S.; Lee, S. T. *Thin Solid Films* **2000**, *359*, 14.
(1162) Liang, C. J.; Zhao, D.; Hong, Z. R.; Zhao, D. X.; Li, X. Y.; Li, W. L.; Peng, J. B.; Yu, J. Q.; Lee, C. S.; Lee, S. T. *Appl. Phys. Lett.* **2000**, *76*, 67.
(1163) Male, N. A. H.; Salata, O. V.; Christou, V. *Synth. Met.* **2002**, *126*, 7.
(1164) Okada, K.; Wang, Y. F.; Chen, T. M.; Kitamura, M.; Nakaya, T.; Inoue, H. *J. Mater. Chem.* **1999**, *9*, 3023.
(1165) Adachi, C.; Baldo, M. A.; Forrest, S. R. *J. Appl. Phys.* **2000**, *87*, 8049.
(1166) Yin, K.; Xu, H.; Zhong, G. Y.; Ni, G.; Huang, W. *Appl. Phys. A: Mater. Sci. Process.* **2009**, *95*, 595.
(1167) Liu, L.; Li, W. L.; Hong, Z. R.; Peng, J. B.; Liu, X. Y.; Liang, C. J.; Liu, Z. B.; Yu, J. Q.; Zhao, D. X. *Synth. Met.* **1997**, *91*, 267.
(1168) Heil, H.; Steiger, J.; Schmechel, R.; van Seggern, H. *J. Appl. Phys.* **2001**, *90*, 5357.
(1169) Zhu, W. G.; Jiang, Q.; Lu, Z. Y.; Wei, X. Q.; Xie, M. G.; Zou, D. C.; Tsutsui, T. *Thin Solid Films* **2000**, *363*, 167.
(1170) Zhu, W. G.; Jiang, Q.; Lu, Z. Y.; Wei, X. Q.; Xie, M. G.; Zou, D. C.; Tsutsui, T. *Synth. Met.* **2000**, *111*, 445.
(1171) Zheng, Y. X.; Lin, J.; Liang, Y. J.; Zhou, Y. H.; Guo, C.; Wang, S. B.; Zhang, H. J. *J. Alloys Compd.* **2002**, *336*, 114.
(1172) Hu, W. P.; Matsumura, M.; Wang, M. Z.; Jin, L. P. *Jpn. J. Appl. Phys.* **2000**, *39*, 6445.
(1173) Lee, M. H.; Pyo, S. W.; Lee, H. S.; Choi, J. S.; Kim, J. S.; Kim, Y. K.; Lee, S. H.; Kim, W. Y.; Ju, S. H.; Lee, C. H. *J. Korean Phys. Soc.* **1999**, *35*, S436.

(1174) Yu, G.; Liu, Y. Q.; Wu, X.; Zhu, D. B.; Li, H. Y.; Jin, L. P.; Wang, M. Z. *Chem. Mater.* **2000**, *12*, 2537.
(1175) Kim, Y. K.; Pyo, S. W.; Choi, D. S.; Hue, H. S.; Lee, S. H.; Ha, Y. K.; Lee, H. S.; Kim, J. S.; Kim, W. Y. *Synth. Met.* **2000**, *111–112*, 113.
(1176) Tsaryuk, V.; Zolin, V.; Legendziewicz, J.; Sokolnicki, J.; Kudryashova, V. In *Proceedings of the 11th International Workshop on Inorganic Electroluminescence and the 2002 International Conference on the Science and Technology of Emissive Displays and Lighting*, Ghent, Belgium, 23–26 September 2002; Neyts, K., De Visschere, P. Poelman, D., Eds.; Ghent University: Belgium, 2002; p 65.
(1177) Zheng, Y. X.; Lin, J.; Liang, Y. J.; Zhou, Y. H.; Guo, C.; Wang, S. B.; Zhang, H. J. *J. Alloys Compd.* **2002**, *336*, 114.
(1178) Huang, L.; Wang, K. Z.; Huang, C. H.; Gao, D. Q.; Jin, L. P. *Synth. Met.* **2002**, *128*, 241.
(1179) Wang, K. Z.; Huang, L.; Gao, L. H.; Huang, C. H.; Jin, L. P. *Solid State Commun.* **2002**, *122*, 233.
(1180) Gao, D. Q.; Bian, Z. Q.; Wang, K. Z.; Jin, L. P.; Huang, C. H. *J. Alloys Compd.* **2003**, *358*, 188.
(1181) Sun, P. P.; Duan, J. P.; Shih, H. T.; Cheng, C. H. *Appl. Phys. Lett.* **2002**, *81*, 792.
(1182) Hu, W. P.; Matsamura, M.; Wang, M. Z.; Jin, L. P. *Appl. Phys. Lett.* **2000**, *77*, 4271.
(1183) Hu, W. P.; Matsumura, M.; Wang, M. Z.; Jin, L. P. *Jpn. J. Appl. Phys.* **2000**, *39*, 6445.
(1184) Wang, J. F.; Wang, R. Y.; Yang, J.; Zheng, Z. P.; Carducci, M. D.; Cayou, T.; Peyghambarian, N.; Jabbour, G. E. *J. Am. Chem. Soc.* **2001**, *123*, 6179.
(1185) Liang, F. S.; Zhou, Q. G.; Cheng, Y. X.; Wang, L. X.; Ma, D. G.; Jing, X. B.; Wang, F. S. *Chem. Mater.* **2003**, *15*, 1935.
(1186) Robinson, M. R.; O'Regan, M. B.; Bazan, G. C. *Chem. Commun.* **2000**, 1645.
(1187) Noto, M.; Irie, K.; Era, M. *Chem. Lett.* **2001**, 320.
(1188) Sun, M.; Xin, H.; Wang, K. Z.; Zhang, Y. A.; Jin, L. P.; Huang, C. H. *Chem. Commun.* **2003**, 702.
(1189) McGehee, M. D.; Bergstedt, T.; Zhang, C.; Saab, A. P.; O'Regan, M. B.; Bazan, G. C.; Srdanov, V. I.; Heeger, A. J. *Adv. Mater.* **1999**, *11*, 1349.
(1190) Diaz-Garcia, M. A.; Fernandez De Avila, S.; Kyzuk, M. G. *Appl. Phys. Lett.* **2002**, *81*, 3924.
(1191) Jiang, X. Z.; Jen, A. K. Y.; Huang, D. Y.; Phelan, G. D.; Londergan, T. M.; Dalton, L. R. *Synth. Met.* **2001**, *125*, 331.
(1192) Jiang, X. Z.; Jen, A. K. Y.; Phelan, G. D.; Huang, D. Y.; Londergan, T. M.; Dalton, L. R.; Register, R. A. *Thin Solid Films* **2002**, *416*, 212.
(1193) Zhao, D. X.; Li, W. L; Hong, Z.; Liang, C. J.; Zhao, D.; Peng, J. B.; Liu, X. Y. *Jpn. J. Appl. Phys.* **1999**, *38*, L46.
(1194) Ling, Q. D.; Yang, M. J.; Zhang, W. G.; Lin, H. Z.; Yu, G.; Bai, F. L. *Thin Solid Films* **2002**, *417*, 127.
(1195) Pei, J.; Liu, X. L.; Yu, W. L.; Lai, Y. H.; Niu, Y. H.; Cao, Y. *Macromolecules* **2002**, *35*, 7274.
(1196) Yu, G.; Liu, Y. Q.; Wu, X.; Zhu, D. B.; Li, H. Y.; Jin, L. P.; Wang, M. Z. *Chem. Mater.* **2000**, *12*, 2537.
(1197) Liang, C. J.; Li, W. L.; Hong, Z. R.; Liu, X. Y.; Peng, J. B.; Liu, L.; Lu, Z. Y.; Xie, M. Q.; Liu, Z. B.; Yu, J. Q.; Zhao, D. Q. *Synth. Met.* **1997**, *91*, 151.
(1198) Hong, Z. R.; Li, W. L.; Zhao, D. X.; Liang, C. J.; Liu, X. Y.; Peng, J. B.; Zhao, D. *Synth. Met.* **1999**, *104*, 165.
(1199) Zhang, X. M.; Sun, R. G.; Zheng, Q. B.; Kobayashi, T.; Li, W. L. *Appl. Phys. Lett.* **1997**, *71*, 2596.
(1200) Reyes, R.; Hering, E. N.; Cremona, M.; da Silva, C. F. B.; Brito, H. F.; Achete, C. A. *Thin Solid Films* **2002**, *420–421*, 23.
(1201) Deng, R. P.; Yu, J. B.; Zhang, H. J.; Zhou, L.; Peng, Z. P.; Li, Z. F.; Guo, Z. Y. *Chem. Phys. Lett.* **2007**, *443*, 258.
(1202) Chu, B.; Li, W. L.; Hong, Z. R.; Zang, F. X.; Wei, H. Z.; Wang, D. Y.; Li, M. T.; Lee, C. S.; Lee, S. T. *J. Phys. D* **2006**, *39*, 4549.
(1203) Stathatos, E.; Lianos, P.; Evgeniou, E.; Keramidas, A. D. *Synth. Met.* **2003**, *139*, 433.
(1204) Zhao, D.; Li, W.; Hong, Z.; Liu, X.; Liang, C.; Zhao, D. *J. Lumin.* **1999**, *82*, 105.
(1205) Pyo, S. W.; Lee, S. P.; Lee, H. S.; Kwon, O. K.; Hoe, H. S.; Lee, S. H.; Ha, Y. K.; Kim, Y. K.; Kim, J. S. *Thin Solid Films* **2000**, *363*, 232.
(1206) Reyes, R.; Cremona, M.; Teotonio, E. E. S.; Brito, H. F.; Malta, O. L. *Chem. Phys. Lett.* **2004**, *396*, 54.
(1207) Hong, Z. R.; Li, W. L.; Zhao, D. X.; Liang, C. J.; Liu, X. Y.; Peng, J. B.; Zhao, D. *Synth. Met.* **2000**, *111–112*, 43.
(1208) You, H.; Ma, D. G. *J. Phys. D* **2008**, *41*, 155113.
(1209) Huang, L.; Tian, H.; Li, F. Y.; Gao, D. Q.; Huang, Y. Y.; Huang, C. H. *J. Lumin.* **2002**, *97*, 55.
(1210) Chu, B.; Fan, D.; Li, W. L.; Hong, Z. R.; Li, R. G. *Appl. Phys. Lett.* **2002**, *81*, 10.
(1211) You, H.; Li, H. Z.; Fang, J. F.; Wang, Q.; Wang, L. X.; Ma, D. G. *J. Appl. Phys. D* **2007**, *40*, 1363.
(1212) Gillin, W. P.; Curry, R. *J. Appl. Phys. Lett.* **1999**, *74*, 798.
(1213) Curry, R. J.; Gillin, W. P. *Synth. Met.* **2000**, *111*, 35.
(1214) Curry, R. J.; Gillin, W. P.; Knights, A. P.; Gwilliam, R. *Opt. Mater.* **2001**, *17*, 161.
(1215) Magennis, S. W.; Ferguson, A. J.; Bryden, T.; Jones, T. S.; Beeby, A.; Samuel, I. D. W. *Synth. Met.* **2003**, *138*, 463.
(1216) Curry, R. J.; Gillin, W. P. *Curr. Opin. Solid State Mater. Sci.* **2001**, *5*, 481.
(1217) Van Deun, R.; Fias, P.; Nockemann, P.; Schepers, A.; Parac-Vogt, T. N.; Van Hecke, K.; Van Meervelt, L.; Binnemans, K. *Inorg. Chem.* **2004**, *43*, 8461.
(1218) Artizzu, F.; Marchio, L.; Mercuri, M. L.; Pilia, L.; Serpe, A.; Quochi, F.; Orru, R.; Cordella, F.; Saba, M.; Mura, A.; Bongiovanni, G.; Delplano, P. *Adv. Funct. Mater.* **2007**, *17*, 2365.
(1219) Zhao, W. Q.; Wang, P. F.; Ran, G. Z.; Ma, G. L.; Zhang, B. R.; Liu, W. M.; Wu, S. K.; Dai, L.; Qin, G. G. *J. Phys. D* **2006**, *39*, 2711.
(1220) Sun, R. G.; Wang, Y. Z.; Zheng, Q. B.; Zhang, H. J.; Epstein, A. J. *J. Appl. Phys.* **2000**, *87*, 7589.
(1221) O'Riordan, A.; Van Deun, R.; Mairiaux, E.; Moynihan, S.; Fias, P.; Nockemann, P.; Binnemans, K.; Redmond, G. *Thin Solid Films* **2008**, *516*, 5098.
(1222) O' Riordan, A.; O'Connor, E.; Moynihan, S.; Nockemann, P.; Fias, P.; Van Deun, R.; Cupertino, D.; Mackie, P.; Redmond, G. *Thin Solid Films* **2006**, *497*, 299.
(1223) Kawamura, Y.; Wada, Y.; Yanagida, S. *Jpn. J. Appl. Phys.* **2001**, *40*, 350.
(1224) Kawamura, Y.; Wada, Y.; Hasegawa, Y.; Iwamuro, M.; Kitamura, T.; Yanagida, S. *Appl. Phys. Lett.* **1999**, *74*, 3245.
(1225) Hong, Z. R.; Liang, C. J.; Li, R. G.; Zhao, D.; Fan, D.; Li, W. L. *Thin Solid Films* **2001**, *391*, 122.
(1226) Kawamura, Y.; Wada, Y.; Iwamuro, M.; Kitamura, T.; Yanagida, S. *Chem. Lett.* **2000**, 280.
(1227) Kang, T. S.; Harrison, B. S.; Foley, T. J.; Knefely, A. S.; Boncella, J. M.; Reynolds, J. R.; Schanze, K. S. *Adv. Mater.* **2003**, *15*, 1093.
(1228) Zang, F. X.; Li, W. L.; Hong, Z. R.; Wei, H. Z.; Li, M. T.; Sun, X. Y.; Lee, C. S. *Appl. Phys. Lett.* **2004**, *84*, 5115.
(1229) Hong, Z. R.; Liang, C. J.; Li, R. G.; Zang, F. X.; Fan, D.; Li, W. L.; Hung, L. S.; Lee, S. T. *Appl. Phys. Lett.* **2001**, *79*, 1942.
(1230) Amao, Y.; Okura, I.; Miyashita, T. *Chem. Lett.* **2000**, 934.
(1231) Amao, Y.; Okura, I.; Miyashita, T. *Bull. Chem. Soc. Jpn.* **2000**, *73*, 2663.
(1232) Amao, Y.; Okura, I.; Miyashita, T. *Chem. Lett.* **2000**, 1286.
(1233) Blair, S.; Kataky, R.; Parker, D. *New J. Chem.* **2002**, *26*, 530.
(1234) Lobnik, A.; Majcen, N.; Niederreiter, K.; Uray, G. *Sens. Actuators B* **2001**, *74*, 200.
(1235) Turel, M.; Cajlakovic, M.; Austin, E.; Dakin, J. P.; Uray, G.; Lobnik, A. *Sens. Actuators B* **2008**, *131*, 247.
(1236) Lobnik, A.; Niederreiter, K.; Uray, G. *Proc. SPIE* **1999**, *3856*, 243.
(1237) Wolfbeis, O. S. *Anal. Chem.* **2000**, *72*, 81R.
(1238) Wolfbeis, O. S. *J. Mater. Chem.* **2005**, *15*, 2657.
(1239) Wong, K. L.; Law, G. L.; Yang, Y. Y.; Wong, W. T. *Adv. Mater.* **2006**, *18*, 1051.
(1240) Barja, B. C.; Aramendia, P. F. *Photochem. Photobiol. Sci.* **2008**, *7*, 1391.
(1241) Wu, M.; Lakowicz, J. R.; Geddes, C. D. *J. Fluoresc.* **2005**, *15*, 53.
(1242) Wolfbeis, O. S.; Durkop, A.; Wu, M.; Lin, Z. H. *Angew. Chem., Int. Ed.* **2002**, *41*, 4495.
(1243) Courrol, L. C.; Samad, R. E. *Curr. Pharm. Anal.* **2008**, *4*, 238.
(1244) Wickersheim, K. A. US Patent 4,448,547, 1984.
(1245) Khalil, G. E.; Lau, K.; Phelan, G. D.; Carlson, B.; Gouterman, M.; Callis, J. B.; Dalton, L. R. *Rev. Sci. Instrum.* **2004**, *75*, 192.
(1246) Basu, B. B. J.; Vasantharajan, N. *J. Lumin.* **2008**, *128*, 1701.
(1247) Liu, Y.; Qian, G. D.; Wang, Z. Y.; Wang, M. Q. *Appl. Phys. Lett.* **2005**, *86*, 071907.
(1248) Guo, H. Q.; Tao, S. Q. *IEEE Sens. J.* **2007**, *7*, 953.
(1249) Borisov, S. M.; Klimant, I. *J. Fluoresc.* **2008**, *18*, 581.
(1250) Mitsuishi, M.; Kikuchi, S.; Miyashita, T.; Amao, Y. *J. Mater. Chem.* **2003**, *13*, 2875.
(1251) Borisov, S. M.; Wolfbeis, O. S. *Anal. Chem.* **2006**, *78*, 5094.
(1252) Katagirin, S.; Manseki, K.; Tsukahara, Y.; Mitsuo, K.; Wada, Y. *J. Alloys Compd.* **2008**, *453*, L1.
(1253) Manseki, K.; Hasegawa, Y.; Wada, Y.; Yanagida, S. *J. Lumin.* **2005**, *111*, 183.
(1254) Manseki, K.; Hasegawa, Y.; Wada, Y.; Yanagida, S. *J. Alloys Compd.* **2006**, *408*, 805.
(1255) Kolodnor, P.; Tyson, J. A. *Appl. Phys. Lett.* **1982**, *40*, 782.
(1256) Kolodner, P.; Tyson, J. A. *Appl. Phys. Lett.* **1983**, *42*, 117.
(1257) Herzum, C.; Boit, C.; Kolzer, J.; Otto, J.; Weiland, R. *Microelectron. J.* **1998**, *29*, 163.

(1258) Kolodner, P.; Katzir, A.; Hartsough, N. *Appl. Phys. Lett.* **1983**, *42*, 749.
(1259) Kolodner, P.; Katzir, A.; Hartsough, N. *J. Vac. Sci. Technol. B* **1983**, *1*, 501.
(1260) Hampel, G.; Kolodner, P.; Gammel, P. L.; Polakos, P. A.; deObaldia, E.; Mankiewich, P. M.; Anderson, A.; Slattery, R.; Zhang, D.; Liang, G. C.; Shih, C. F. *Appl. Phys. Lett.* **1996**, *69*, 571.
(1261) Haugen, O.; Johansen, T. H.; Chen, H.; Yurchenko, V.; Vase, P.; Winkler, D.; Davidson, B. A.; Testa, G.; Sarnelli, E.; Altshuler, E. *IEEE Trans. Appl. Supercond.* **2007**, *17*, 3215.
(1262) Niratisairak, S.; Haugen, O.; Johansen, T. H.; Ishibashi, T. *Physica C* **2008**, *468*, 442.
(1263) McGrath, J. J.; Lian, B. US Patent 6,648,506, 2003.
(1264) Kolodner, P. R.; Hampel, K. G.; Gammel P. L. US Patent 5,971,610, 1999.
(1265) Haugen, O.; Johansen, T. H. *J. Lumin.* **2008**, *128*, 1479.
(1266) Kolodner, P. R. US Patent 4,819,658, 1989.
(1267) Barton, D. L.; Tangyunyong, P. *Microelectron. Eng.* **1996**, *31*, 271.
(1268) Liu, T.; Sullivan, J. P. *Pressure and Temperature Sensitive Paints*; Springer Verlag: Berlin, 2005.
(1269) Liu, T.; Campbell, B. T.; Sullivan, J. P. *Exp. Therm. Fluid Sci.* **1995**, *10*, 101.
(1270) Liu, T.; Campbell, B. T.; Sullivan, J. P.; Lafferty, J.; Yanta, W. *J. Thermophys. Heat Trans.* **1995**, *9*, 605.
(1271) Brayshaw, S. A.; Harrowfield, J. M.; Soboloev, A. N. *Acta Crystallogr.* **1995**, *C51*, 1799.
(1272) Stump, N. A.; Schweitzer, G. K.; Pesterfield, L. L.; Peterson, J. R.; Murray, G. M. *Spectrosc. Lett.* **1992**, *25*, 1421.
(1273) Lima, P. P.; Malta, O. L.; Alves, S. *Quim. Nov.* **2005**, *28*, 805.
(1274) George, M. R.; Golden, C. A.; Grossel, M. C.; Curry, R. J. *Inorg. Chem.* **2006**, *45*, 1739.
(1275) Gassner, A. L.; Duhot, C.; Bünzli, J.-C. G.; Chauvin, A. S. *Inorg. Chem.* **2008**, *47*, 7802.
(1276) Petoud, S.; Cohen, S. M.; Bünzli, J.-C. G.; Raymond, K. N. *J. Am. Chem. Soc.* **2003**, *125*, 13324.
(1277) Moore, E. G.; Samuel, A. P. S.; Raymond, K. N. *Acc. Chem. Res.* **2009**, *42*, 542.
(1278) Moore, E. G.; Xu, J. D.; Jocher, J.; Castro-Rodriguez, I.; Raymond, K. N. *Inorg. Chem.* **2008**, *47*, 3105.
(1279) Zucchi, G.; Ferrand, A. C.; Scopelliti, R.; Bünzli, J.-C. G. *Inorg. Chem.* **2002**, *41*, 2459.
(1280) Comby, S.; Imbert, D.; Chauvin, A. S.; Bünzli, J.-C. G. *Inorg. Chem.* **2006**, *45*, 732.

CR8003983